Translation waves induced by high head lock systems

Juliana Canal case study

F.J. (Frank) Smorenburg
1384163
Master Thesis

ARCADIS

TU Delft Delft University of Technology

de Vries & van de Wiel
Kust & Oeverwerken

TRANSLATION WAVES INDUCED BY HIGH HEAD LOCK SYSTEMS

JULIANA CANAL CASE STUDY

by

F.J. (Frank) Smorenburg

in partial fulfillment of the requirements for the degree of

Master of Science
in Hydraulic Engineering

at the Delft University of Technology,
to be defended publicly on November 16, 2016 at 16:00.

Chairman:	Prof. ir. T. Vellinga,	TU Delft
Thesis committee:	Ir. H. J. Verhagen,	TU Delft
	Ir. H. G. Tuin,	Arcadis
	Ir. P. Quist,	TU Delft

Status: Final Report

ARCADIS TU Delft Delft University of Technology de Vries & van de Wiel Kust & Oeverwerken

ABSTRACT

The rate of transport to the hinterland over inland waterways is increasing in Europe. The vessels transporting the cargo continue to become larger. To provide the network that meets the markets demand, the dimensions of the waterways, canals and other hydraulic infrastructure, are being enlarged. To improve the European Waterways, the European Commission has granted the TenT-subsidy (Balazs, 2015 [1]). This research focusses on hydraulic infrastructure, in particular on the lock complexes. The lock complexes can be divided in low head lock systems and high head lock systems, this research covers the high head lock systems. Filling and emptying of lock systems create translation waves. In 1935, prof. Thijsse derived a theory on the propagation of translation waves in canal systems (Thijsse, 1935 [2]). This theory is used as the foundation to investigated the main goal of this research, to predict how translation waves evolve in a canal and what the consequences for the workability of water-borne construction equipment are. Accompanying processes for the construction works, such as construction inspections by divers, are included.

In this research the measures to reduce effects of translation waves are control options related to the lock complex only. Adaptations to the water-borne construction equipment or to the bathymetry of the canal are excluded from this research. Currents induced by other external factors than translation waves induced by the lock complex, are not investigated. The research is applied to a case study, the Juliana Canal.

The Juliana Canal is part of the North Sea - Mediterranean corridor and is a canal under reconstruction to meet the European regulations. In present state the Juliana Canal meets the demands of a "CEMT Va" canal and is now upgraded to comply with the regulations of the larger "CEMT Vb" vessels. Therefore it has to be widened and deepened. The construction works were granted by "Rijkswaterstaat" to "de Vries & van de Wiel", part of DEME-group. Arcadis is one of the sub-contractors, in the role of design support. These activities started in 2013 and are expected to be completed in 2018. The construction works are performed from the banks of the canal and with water-borne construction equipment.

The propagation and effects of translation waves in the intensively used Juliana Canal are investigated. The canal has to be attainable for shipping during construction works. The area of interest in this research is limited to the upstream section of Born, up to the bend upstream of the port of Stein in the Juliana Canal. The Middle lock chamber of the lock complex near the village of Born has already been enlarged to class "CEMT Vb". Larger lock chambers give larger translation waves, but no construction works to reduce the effects of the larger waves have been done so far to the canal itself. The combination of high shipping intensity and already large translation waves as a result of overdue construction works, create highly undesirable working conditions which reduce the workability for the water-borne construction equipment.

First step to achieve the main research goal is the development of a model to analyse how a translation wave propagates through a canal. Then the limit states of the water-borne construction equipment are determined. After that, the adaptation possibilities of a high head lock system are investigated and expressed in different scenarios. Finally, the scenarios are implemented in the model. The currents and water level changes under different conditions are analysed and advise is given on the different scenarios.

To predict the adaptations of water level changes and currents due to translation waves a 1D-model is developed. In the model, theory from Thijsse (Thijsse, 1935 [2]) on the development of a translation wave is applied and extended on more complex discharge extractions from the canal. Where the theory is limited to the changes of a single pulse, the total discharge-time relation of filling the lock chamber is implemented in the model. The discharge relation is divided in subsequent pulses of one second. The propagating and reflecting of each pulse through the canal is calculated, subsequently the pulses are placed after each other resulting in the total translation wave. The bathymetry of the canal-system determines the transition points and reflections, a schematization of the modelled canal section is given in figure 1. The modelled locations are presented in the figure as well. To obtain a good representation of the translation wave in this canal, a set of 42 reflections were included in this model.

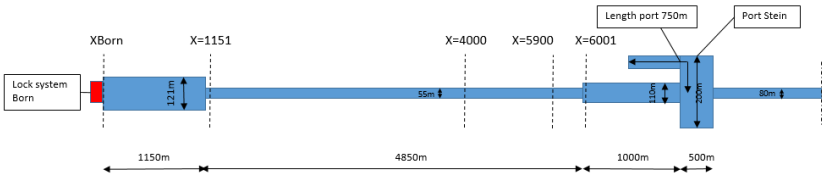

Figure 1: Scheme of the bathymetry in modelled canal section.

If the currents in the canal become too large, unworkable construction situations arise. The current at which construction works or accompanying processes can no longer continue, is defined as the limit state. The decisive process that determines the maximum allowable current by translation waves in this case study, is the inspection by divers. The maximum current towards the north is determined at $u_{min} = -0.13 m/s$, to the south at $u_{max} = +0.30 m/s$. Other limit states or limit states for future projects can easily be implemented in the model. The measures taken to reduce the impact of translation waves in the canal are limited to adaptations in control of the lock complex. Two control options can be done at the locks. The first option is regulating the magnitude of the discharge to fill the lock chamber. This is normally done by defining the number of culverts used during filling. The second option is to vary the time between sequent fillings. The scenarios modelled first, are filling with 1 culvert, 2 culverts which is the present situation, 4 culverts which is a theoretical case and filling two chambers simultaneously. The scenarios for the second option are filling the East lock chamber 5, 10 and 15 minutes after the Middle chamber. This is performed for fillings with 2 culverts and with 1 culvert.

In the present situation, the currents exceed the defined limit state due to translation waves. None of the investigated scenarios result in no downtime but the downtime can be reduced significantly. The most favourable scenario from the first group of control options, vary between 1, 2 and 4 culverts, depending on the location. Simultaneous filling is at none of the locations the best scenario and should be avoided. In the second group of control options, the scenario where the lock chamber is filled with one culvert and 15 minutes between sequent waves, results at 4 of the 5 locations in the least downtime. At the other location the best option is the scenario where the chamber is filled with 2 culverts and also 15 minutes between the waves. There is not a scenario that is the best scenario for all locations along the canal. The resulting water level change and current are the summation of the original wave and reflection waves. The reflection waves are created by e.g. reflections at a port or changes in the width of the canal. The distance of the construction location to these transition points determine which reflections, and with what magnitude, are at that specific location. This makes the net water level change and net current very location dependent. For each location the model has to be run with different scenarios. This can be seen in figure 2, where the resulting currents of the same 3 scenarios with 2 subsequent waves are modelled. The effects of different time periods between subsequent waves have contrary results for the maximum currents of the second wave.

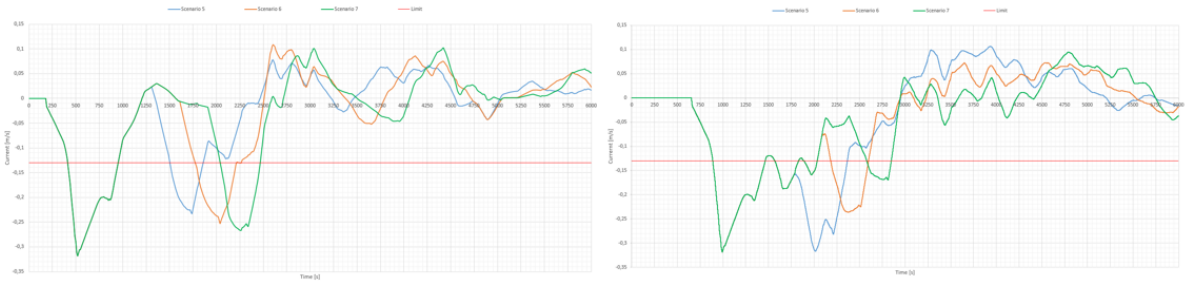

Figure 2: Results of 3 scenarios modelled at X1151 and X4000

Concluding, the model gives a good representation of the situation in reality, for the modelled locations in canal. For future projects, the model can relatively easy be adapted to another canal-system by changing the bathymetry, lock discharges and transition points. The model is applicable to gain insights of a system for designs. It can be used as a decision tool during construction works as well due to the short calculation period. The use of this model can forecast the working conditions and limit the downtime.

PREFACE

This report is the results of the thesis research conducted as part of the Master Hydraulic Engineering at the faculty Civil Engineering and Geosciences of Delft University of Technology. The research was developed in cooperation with Arcadis and conducted for the construction works of de Vries & van de Wiel. The focus of the thesis is on translation waves induced by high head lock systems.

The project would not have been possible without the help of the colleagues at Arcadis. They were always available for questions or to help out when problems occurred. I would like to give special thanks to Henry Tuin for his daily guidance, discussions on proceeding to next steps, your critical notes on reports and being member of the graduation committee for Arcadis. Your enthusiasm on the topic kept me motivated and interested during the whole graduation period. I would also give thanks to the people at de Vries & van de Wiel at the construction site in Stein and on the construction pontoon *Mattedoor* for collaborating in the research and providing the data used in the investigation.

I would like to thank the other members of the graduation committee prof. ir. Tiedo Vellinga as chairman of the committee and ir. Henk Jan Verhagen and ir. Peter Quist for their guidance, discussions and feedback during the meetings. Last but not least I would like to thank my friends and family for their unconditional support during my entire study.

F.J. (Frank) Smorenburg
Delft, November 2016

CONTENTS

Abstract iii

Preface v

List of Figures ix

List of Tables xv

Project map xvii

1 Introduction 1
- 1.1 Background information . . . 1
  - 1.1.1 Translation waves . . . 1
  - 1.1.2 Case study Juliana Canal . . . 1
- 1.2 Problem description . . . 2
- 1.3 Research questions . . . 2
- 1.4 Methodology . . . 2
- 1.5 Scope . . . 3
- 1.6 Thesis outline . . . 3

2 Literature study 5
- 2.1 Translation waves . . . 5
  - 2.1.1 What is a translation wave? . . . 5
  - 2.1.2 Propagation of a translation wave in a prismatic canal . . . 6
  - 2.1.3 Prismatic canal with changes in direction and cross section . . . 9
  - 2.1.4 Currents in the canal . . . 10
- 2.2 Method of characteristics . . . 13

3 Juliana Canal, case study 17
- 3.1 The Juliana Canal . . . 17
- 3.2 Functional conditions of the locks . . . 22
- 3.3 Defining limit state and downtime . . . 22

4 The translation wave model 25
- 4.1 Approach . . . 25
- 4.2 Determine the existence of translation waves in the Juliana Canal . . . 26
- 4.3 Propagation celerity of wave . . . 27
- 4.4 Discharge lock . . . 29
- 4.5 Reflections and beta's . . . 30
- 4.6 Propagation of the wave at location X . . . 32
  - 4.6.1 Calibration of the model . . . 32
- 4.7 Calculating from wave height to current . . . 35

5 Multiple scenarios 37
- 5.1 The scenarios . . . 37
- 5.2 Locations of interest . . . 39
  - 5.2.1 Parameters to obtain and compare . . . 40

6 Results 41
- 6.1 Different discharges . . . 42
  - 6.1.1 Discharge-time relations . . . 43
  - 6.1.2 Results with different discharges at 5 locations . . . 43

6.2 Different intervals . . . 49
6.2.1 Two culverts used at lock . . . 49
6.2.2 One culvert used at lock . . . 55

7 Conclusions and recommendations **61**
7.1 Conclusions . . . 61
7.2 Discussion . . . 65
7.3 Recommendations . . . 65

Bibliography **67**

A Analysis **69**
A.1 System description of the Juliana Canal . . . 69
A.2 Functional conditions of the locks . . . 73
A.3 Measurement devices . . . 74

B Spectrum analysis **77**
B.1 Data collection . . . 77
B.2 Analysis method to create a spectrum . . . 77
B.3 Interpretation of the results . . . 79
B.3.1 Observations and correlation with locks . . . 79

C Response of the pontoon **83**
C.1 Description on the pontoon . . . 83
C.2 Forces on pontoon . . . 83

D Literature study **87**
D.1 Translation waves according to Dietz . . . 87
D.2 Creating a wave spectrum using a Fourier analysis . . . 88
D.3 Ship induced waves . . . 90
D.3.1 Primary waves . . . 90
D.3.2 Secondary waves . . . 93

E Results in combined graphs **95**
E.1 Scenarios 1 up until 4 . . . 95
E.2 Scenarios 5 up until 7 . . . 100
E.3 Scenarios 8 up until 10 . . . 104

F Results of the model **109**
F.1 Group 1: Different Filling discharges . . . 109
F.2 Group 2: Different filling and emptying regimes . . . 137
F.2.1 Filling and emptying regimes with normal wave . . . 137
F.2.2 Filling and emptying regimes with low discharge waves . . . 157

List of Figures

1 Scheme of the bathymetry in modelled canal section. . . . iv
2 Results of 3 scenarios modelled at X1151 and X4000 . . . iv

3 Overview of the Juliana Canal system . . . xvii

2.1 Two examples of reasons for translation waves (lecture note CT3310 Open channel flow) . . . 6
2.2 Locations of the Juliana Canal and Twente Canal . . . 7
2.3 Translations waves at changes in cross section (lecture notes CT3310 Open channel flow) . . . 9
2.4 Current due to a positive translation wave . . . 11
2.5 Current due to a negative translation wave . . . 11
2.6 The resulting water level change and current when a negative and positive wave from opposite direction meet each other . . . 12
2.7 The resulting water level change and current when two positve waves from opposite directions meet each other . . . 12
2.8 (a) (x,t)-graph (b) (U,c)-graph (lecture notes CT3310 Open channel flow) . . . 14
2.9 (x,t)-diagram with multiple characteristics (lecture notes CT3310 Open channel flow [4]) . . . 15

3.1 Overview of the Juliana Canal system . . . 18
3.2 Overview of a canal cross section . . . 19
3.3 Heights of ground level near Born (ahn.maps.arcgis.com) . . . 19
3.4 Overview Maaswerken (www.grensmaas.nl) . . . 20
3.5 Cross section of the canal canal widened with a sheet pile construction (www.julianakanaal.nl) 20
3.6 Construction pontoon the Mattedoor . . . 21
3.7 The discharges measured at Eisden, from 2011 untill 2015 . . . 22
3.8 Base current in the Juliana Canal under the pontoon . . . 23

4.1 Steps to be taken to model the translation waves . . . 26
4.2 Translation wave propagating in the canal, at 4 locations . . . 27
4.3 Schematisation of the system as modelled . . . 28
4.4 Development of the celerity of the wave in the canal . . . 28
4.5 Discharges over time at Middle chamber with 1 or 2 culverts . . . 29
4.6 Discharges over time at East chamber with 1 or 2 culverts . . . 30
4.7 Primairy wave with 43 reflections in S-t diagram . . . 30
4.8 Amplificationfactors as percentage of the original wave . . . 31
4.9 Individual waves at X=1900 . . . 32
4.10 Model compared to measurement after calibration . . . 33
4.11 Differences between model compared to measurement after calibration . . . 34
4.12 Normal distribution over the difference between the model and measurements . . . 34
4.13 Two identical waves with 5 minutes in between, at X=1900 . . . 35

5.1 Overview of the schematized system, with calculation locations . . . 39

6.1 The resulting water level change and current when a negative and positive wave from opposite direction meet each other . . . 42
6.2 The resulting water level change and current when two positve waves from opposite directions meet each other . . . 42
6.3 The four modelled discharge-time relations . . . 43
6.4 Currents of scenarios 1, 2, 3 and 4 at location XBorn . . . 45
6.5 Water level changes due to scenarios 1, 2, 3 and 4 at location X1151 . . . 45
6.6 Currents of scenarios 1, 2, 3 and 4 at location X1151 . . . 46

6.7 Water level changes due to scenarios 1, 2, 3 and 4 at location X4000 . . . 46
6.8 Currents of scenarios 1, 2, 3 and 4 at location X4000 . . . 47
6.9 Currents of scenarios 1, 2, 3 and 4 at location X5900 . . . 47
6.10 Currents of scenarios 1, 2, 3 and 4 at location X6001 . . . 48
6.11 Discharge-time relations with 2 culverts used at Middle and East chamber . . . 49
6.12 Water level changes due to scenarios 5, 6 and 7 at location X1151 . . . 51
6.13 Currents of scenarios 5, 6 and 7 at location X1151 . . . 52
6.14 Water level changes due to scenarios 5, 6 and 7 at location X4000 . . . 52
6.15 Currents of scenarios 5, 6 and 7 at location X4000 . . . 53
6.16 Currents of scenarios 5, 6, 7 and 11 at location X1151 . . . 53
6.17 Currents of scenarios 5, 6, 7 and 11 at location X4000 . . . 54
6.18 Discharge-time relations with 1 culvert used at Middle and East chamber . . . 55
6.19 Water level changes due to scenarios 8, 9 and 10 at location X1151 . . . 56
6.20 Currents of scenarios 8, 9 and 10 at location X1151 . . . 57
6.21 Water level changes due to scenarios 8, 9 and 10 at location X4000 . . . 57
6.22 Currents of scenarios 8, 9 and 10 at location X4000 . . . 58

7.1 Schematisation of the system as modelled . . . 63

A.1 Overview of the Juliana Canal system . . . 70
A.2 Overview of a canal cross section . . . 71
A.3 Heights of ground level near Born (ahn.maps.arcgis.com) . . . 71
A.4 Overview Maaswerken (www.grensmaas.nl) . . . 72
A.5 Cross section of the canal canal widened with a sheet pile construction (www.julianakanaal.nl) 72
A.6 The discharges measured at Eisden, from 2011 untill 2015 . . . 74
A.7 Locations of the four pressure mats . . . 74
A.8 Example of ADCP data . . . 75

B.1 Locations pressure measure devices on April 25th . . . 78
B.2 Wave spectrum Obbicht March 2016 . . . 79
B.3 Wave periods of the whole spectrum . . . 80
B.4 Spectral analysis with a secondary model, including wave angles . . . 81

D.1 Example of observed surface elevation and its amplitude and phase spactrum ([16]) . . . 89
D.2 definitions of squat and sinkage . . . 91
D.3 Ship-fixed co-ordinate system . . . 92

E.1 Water level changes in scenarios 1, 2, 3 and 4 at location XBorn . . . 96
E.2 Currents in scenarios 1, 2, 3 and 4 at location XBorn . . . 96
E.3 Water level changes in scenarios 1, 2, 3 and 4 at location X1151 . . . 96
E.4 Currents in scenarios 1, 2, 3 and 4 at location X1151 . . . 97
E.5 Water level changes in scenarios 1, 2, 3 and 4 at location X4000 . . . 97
E.6 Currents in scenarios 1, 2, 3 and 4 at location X4000 . . . 97
E.7 Water level changes in scenarios 1, 2, 3 and 4 at location X5900 . . . 98
E.8 Currents in scenarios 1, 2, 3 and 4 at location X5900 . . . 98
E.9 Water level changes in scenarios 1, 2, 3 and 4 at location X6001 . . . 98
E.10 Currents in scenarios 1, 2, 3 and 4 at location X6001 . . . 99
E.11 Water level changes in scenarios 5, 6 and 7 at location XBorn . . . 100
E.12 Currents in scenarios 5, 6 and 7 at location XBorn . . . 101
E.13 Water level changes in scenarios 5, 6 and 7 at location X1151 . . . 101
E.14 Currents in scenarios 5, 6 and 7 at location X1151 . . . 101
E.15 Water level changes in scenarios 5, 6 and 7 at location X4000 . . . 102
E.16 Currents in scenarios 5, 6 and 7 at location X4000 . . . 102
E.17 Water level changes in scenarios 5, 6 and 7 at location X5900 . . . 102
E.18 Currents in scenarios 5, 6 and 7 at location X5900 . . . 103
E.19 Water level changes in scenarios 5, 6 and 7 at location X6001 . . . 103
E.20 Currents in scenarios 5, 6 and 7 at location X6001 . . . 103

E.21 Water level changes in scenarios 8, 9 and 10 at location XBorn . . . 104
E.22 Currents in scenarios 8, 9 and 10 at location XBorn . . . 105
E.23 Water level changes in scenarios 8, 9 and 10 at location X1151 . . . 105
E.24 Currents in scenarios 8, 9 and 10 at location X1151 . . . 105
E.25 Water level changes in scenarios 8, 9 and 10 at location X4000 . . . 106
E.26 Currents in scenarios 8, 9 and 10 at location X4000 . . . 106
E.27 Water level changes in scenarios 8, 9 and 10 at location X5900 . . . 107
E.28 Currents in scenarios 8, 9 and 10 at location X5900 . . . 107
E.29 Water level changes in scenarios 8, 9 and 10 at location X6001 . . . 108
E.30 Currents in scenarios 8, 9 and 10 at location X6001 . . . 108

F.1 The three modelled discharge-time relations . . . 110
F.2 Sc1: Water depth changes in original situation at location XBorn . . . 111
F.3 Sc1: Currents in original situation at location XBorn . . . 112
F.4 Sc2: Water depth changes in scenario with one culvert at location XBorn . . . 112
F.5 Sc2: Currents in scenario with one culvert at location XBorn . . . 113
F.6 Sc3: Water depth changes in scenario with four culverts at location XBorn . . . 113
F.7 Sc3: Currents in scenario with four culverts at location XBorn . . . 114
F.8 Sc1: Water level changes in scenario with the original situation at location X1151 . . . 115
F.9 Sc1: Currents in scenario with the original situation at location X1151 . . . 116
F.10 Sc2: Water level changes in scenario with one culvert at location X1151 . . . 116
F.11 Sc2: Currents in scenario with one culvert at location X1151 . . . 117
F.12 Sc3: Water level changes in scenario with four culverts at location X1151 . . . 117
F.13 Sc3: Four culverts at location X1151 . . . 118
F.14 Sc1: Water level changes in scenario with the original situation at location X4000 . . . 119
F.15 Sc1: Currents in scenario with the original situation at location X4000 . . . 120
F.16 Sc2: Water level changes in scenario with one culvert at location X4000 . . . 120
F.17 Sc2: Currents in scenario with one culvert at location X4000 . . . 121
F.18 Sc3: Water level changes in scenario with four culverts at location X4000 . . . 121
F.19 Sc3: Currents in scenario four culverts at location X4000 . . . 122
F.20 Sc1: Water level changes in scenario with the original situation at location X5900 . . . 123
F.21 Sc1: Currents in scenario with the original situation at location X5900 . . . 124
F.22 Sc2: Water level changes in scenario with one culvert at location X5900 . . . 124
F.23 Sc2: Currents in scenario with one culvert at location X5900 . . . 125
F.24 Sc3: Water level changes in scenario with four culverts at location X5900 . . . 125
F.25 Sc3: Currents in scenario with four culverts at location X5900 . . . 126
F.26 Sc1: Water level changes in scenario with original situation at location X6001 . . . 127
F.27 Sc1: Currents in scenario with original situation at location X6001 . . . 128
F.28 Sc2: Water level changes in scenario with one culvert at location X6001 . . . 128
F.29 Sc2: Currents in scenario with one culvert at location X6001 . . . 129
F.30 Sc3: Water level changes in scenario with four culverts at location X6001 . . . 129
F.31 Sc3: Currents in scenario with four culverts at location X6001 . . . 130
F.32 Sc4: Water level changes due to 2 x 2 culverts simultaneously at location XBorn . . . 131
F.33 Sc4: Currents due to 2 x 2 culverts simultaneously at location XBorn . . . 132
F.34 Sc4: Water level changes due to 2 x 2 culverts simultaneously at location X1151 . . . 132
F.35 Sc4: Currents due to 2 x 2 culverts simultaneously at location X1151 . . . 133
F.36 Sc4: Water level changes due to 2 x 2 culverts simultaneously at location X4000 . . . 133
F.37 Sc4: Currents due to 2 x 2 culverts simultaneously at location X4000 . . . 134
F.38 Sc4: Water level changes due to 2 x 2 culverts simultaneously at location X5900 . . . 134
F.39 Sc4: Currents due to 2 x 2 culverts simultaneously at location X5900 . . . 135
F.40 Sc4: Water level changes due to 2 x 2 culverts simultaneously at location X6001 . . . 135
F.41 Sc4: Currents due to 2 x 2 culverts simultaneously at location X6001 . . . 136
F.42 Discharge-time relations with 2 culverts used at Middle and East chamber . . . 137
F.43 Sc4: Water level changes in scenario with Middle and East chamber filled with 2 culverts, 5 minutes in between, at location XBorn . . . 138

F.44 Sc4: Currents in scenario with Middle and East chamber filled with 2 culverts, 5 minutes in between, at location XBorn . . . 138
F.45 Sc5: Water level changes in scenario with Middle and East chamber filled with 2 culverts, 10 minutes in between, at location XBorn . . . 139
F.46 Sc5: Currents in scenario with Middle and East chamber filled with 2 culverts, 10 minutes in between, at location XBorn . . . 139
F.47 Sc6: Water level changes in scenario with Middle and East chamber filled with 2 culverts, 15 minutes in between, at location XBorn . . . 140
F.48 Sc6: Currents in scenario with Middle and East chamber filled with 2 culverts, 15 minutes in between, at location XBorn . . . 140
F.49 Sc4: Water level changes in scenario with Middle and East chamber filled with 2 culverts, 5 minutes in between, at location X1151 . . . 141
F.50 Sc4: Currents in scenario with Middle and East chamber filled with 2 culverts, 5 minutes in between, at location X1151 . . . 142
F.51 Sc5: Water level changes in scenario with Middle and East chamber filled with 2 culverts, 10 minutes in between, at location X1151 . . . 142
F.52 Sc5: Currents in scenario with Middle and East chamber filled with 2 culverts, 10 minutes in between, at location X1151 . . . 143
F.53 Sc6: Water level changes in scenario with Middle and East chamber filled with 2 culverts, 15 minutes in between, at location X1151 . . . 143
F.54 Sc6: Currents in scenario with Middle and East chamber filled with 2 culverts, 15 minutes in between, at location X1151 . . . 144
F.55 Sc4: Water level changes in scenario with Middle and East chamber filled with 2 culverts, 5 minutes in between, at location X4000 . . . 145
F.56 Sc4: Currents in scenario with Middle and East chamber filled with 2 culverts, 5 minutes in between, at location X4000 . . . 146
F.57 Sc5: Water level changes in scenario with Middle and East chamber filled with 2 culverts, 10 minutes in between, at location X4000 . . . 146
F.58 Sc5: Currents in scenario with Middle and East chamber filled with 2 culverts, 10 minutes in between, at location X4000 . . . 147
F.59 Sc6: Water level changes in scenario with Middle and East chamber filled with 2 culverts, 15 minutes in between, at location X4000 . . . 147
F.60 Sc6: Currents in scenario with Middle and East chamber filled with 2 culverts, 15 minutes in between, at location X4000 . . . 148
F.61 Sc4: Water level changes in scenario with Middle and East chamber filled with 2 culverts, 5 minutes in between, at location X5900 . . . 149
F.62 Sc4: Currents in scenario with Middle and East chamber filled with 2 culverts, 5 minutes in between, at location X5900 . . . 150
F.63 Sc5: Water level changes in scenario with Middle and East chamber filled with 2 culverts, 10 minutes in between, at location X5900 . . . 150
F.64 Sc5: Currents in scenario with Middle and East chamber filled with 2 culverts, 10 minutes in between, at location X5900 . . . 151
F.65 Sc6: Water level changes in scenario with Middle and East chamber filled with 2 culverts, 15 minutes in between, at location X5900 . . . 151
F.66 Sc6: Currents in scenario with Middle and East chamber filled with 2 culverts, 15 minutes in between, at location X5900 . . . 152
F.67 Sc4: Water level changes in scenario with Middle and East chamber filled with 2 culverts, 5 minutes in between, at location X6001 . . . 153
F.68 Sc4: Currents in scenario with Middle and East chamber filled with 2 culverts, 5 minutes in between, at location X6001 . . . 154
F.69 Sc5: Water level changes in scenario with Middle and East chamber filled with 2 culverts, 10 minutes in between, at location X6001 . . . 154
F.70 Sc5: Currents in scenario with Middle and East chamber filled with 2 culverts, 10 minutes in between, at location X6001 . . . 155
F.71 Sc6: Water level changes in scenario with Middle and East chamber filled with 2 culverts, 15 minutes in between, at location X6001 . . . 155

F.72 Sc6: Currents in scenario with Middle and East chamber filled with 2 culverts, 15 minutes in between, at location X6001 . . . 156
F.73 Discharge-time relations with 1 culvert used at Middle and East chamber . . . 157
F.74 Sc7: Water level changes in scenario with Middle and East chamber filled with 1 culverts, 5 minutes in between, at location XBorn . . . 158
F.75 Sc7: Currents in scenario with Middle and East chamber filled with 1 culverts, 5 minutes in between, at location XBorn . . . 158
F.76 Sc8: Water level changes in scenario with Middle and East chamber filled with 1 culverts, 10 minutes in between, at location XBorn . . . 159
F.77 Sc8: Currents in scenario with Middle and East chamber filled with 1 culverts, 10 minutes in between, at location XBorn . . . 159
F.78 Sc9: Water level changes in scenario with Middle and East chamber filled with 1 culverts, 15 minutes in between, at location XBorn . . . 159
F.79 Sc9: Currents in scenario with Middle and East chamber filled with 1 culverts, 15 minutes in between, at location XBorn . . . 160
F.80 Sc7: Water level changes in scenario with Middle and East chamber filled with 1 culverts, 5 minutes in between, at location X1151 . . . 161
F.81 Sc7: Currents in scenario with Middle and East chamber filled with 1 culverts, 5 minutes in between, at location X1151 . . . 162
F.82 Sc8: Water level changes in scenario with Middle and East chamber filled with 1 culverts, 10 minutes in between, at location X1151 . . . 162
F.83 Sc8: Currents in scenario with Middle and East chamber filled with 1 culverts, 10 minutes in between, at location X1151 . . . 163
F.84 Sc9: Water level changes in scenario with Middle and East chamber filled with 1 culverts, 15 minutes in between, at location X1151 . . . 163
F.85 Sc9: Currents in scenario with Middle and East chamber filled with 1 culverts, 15 minutes in between, at location X1151 . . . 164
F.86 Sc7: Water level changes in scenario with Middle and East chamber filled with 1 culverts, 5 minutes in between, at location X4000 . . . 165
F.87 Sc7: Currents in scenario with Middle and East chamber filled with 1 culverts, 5 minutes in between, at location X4000 . . . 166
F.88 Sc8: Water level changes in scenario with Middle and East chamber filled with 1 culverts, 10 minutes in between, at location X4000 . . . 166
F.89 Sc8: Currents in scenario with Middle and East chamber filled with 1 culverts, 10 minutes in between, at location X4000 . . . 167
F.90 Sc9: Water level changes in scenario with Middle and East chamber filled with 1 culverts, 15 minutes in between, at location X4000 . . . 167
F.91 Sc9: Currents in scenario with Middle and East chamber filled with 1 culverts, 15 minutes in between, at location X4000 . . . 168
F.92 Sc7: Water level changes in scenario with Middle and East chamber filled with 1 culverts, 5 minutes in between, at location X5900 . . . 169
F.93 Sc7: Currents in scenario with Middle and East chamber filled with 1 culverts, 5 minutes in between, at location X5900 . . . 170
F.94 Sc8: Water level changes in scenario with Middle and East chamber filled with 1 culverts, 10 minutes in between, at location X5900 . . . 170
F.95 Sc8: Currents in scenario with Middle and East chamber filled with 1 culverts, 10 minutes in between, at location X5900 . . . 171
F.96 Sc9: Water level changes in scenario with Middle and East chamber filled with 1 culverts, 15 minutes in between, at location X5900 . . . 171
F.97 Sc9: Currents in scenario with Middle and East chamber filled with 1 culverts, 15 minutes in between, at location X5900 . . . 172
F.98 Sc7: Water level changes in scenario with Middle and East chamber filled with 1 culverts, 5 minutes in between, at location X6001 . . . 173
F.99 Sc7: Currents in scenario with Middle and East chamber filled with 1 culverts, 5 minutes in between, at location X6001 . . . 174

F.100Sc8: Water level changes in scenario with Middle and East chamber filled with 1 culverts, 10 minutes in between, at location X6001 174
F.101Sc8: Currents in scenario with Middle and East chamber filled with 1 culverts, 10 minutes in between, at location X6001 175
F.102Sc9: Water level changes in scenario with Middle and East chamber filled with 1 culverts, 15 minutes in between, at location X6001 175
F.103Sc9: Currents in scenario with Middle and East chamber filled with 1 culverts, 15 minutes in between, at location X6001 176

List of Tables

2.1 Parameters used in Thijsse's formulae . . . 7
2.2 Effects of changes in β . . . 10

3.1 Characteristics of CEMT-class Va and Vb (Rijkwaterstaat, 2016 [10]) . . . 20
3.2 Dimensions of lock chambers in the lock system . . . 21
3.3 Filling and emptying per lock, numbers of 2014 and 2015 (Rijkswaterstaat, 2016 [12]) . . . 22

4.1 Celerities of the waves per location . . . 36

5.1 Scenario's . . . 37
5.2 Currents due to shipping (Arcadis, 2015 [14]) . . . 38

6.1 Overview of extreme values and downtime at 5 locations . . . 44
6.2 Overview of extreme values and downtime of scenarios 5, 6 and 7, at 5 locations . . . 51
6.3 Overview of extreme values and downtime of scenarios 8, 9 and 10, at 5 locations . . . 56
6.4 Overview of the downtime per scenario and per location . . . 59

7.1 Best scenario for each location, scenarios with one wave . . . 64
7.2 Best scenario for each location, scenarios with two waves . . . 64

A.1 Characteristics of CEMT-class Va and Vb (Rijkwaterstaat, 2011 [10]) . . . 72
A.2 Dimensions of lock chambers in the lock system . . . 73
A.3 Filling and emptying per lock, numbers of 2014 and 2015 (Rijkswaterstaat, 2016 [12]) . . . 73

B.1 Information of the dataset . . . 77
B.2 Emptying and Filling times of the lock chambers . . . 79

C.1 Parameters in current calcuation . . . 84
C.2 Parameters for block section . . . 84
C.3 Currents due to shipping . . . 84
C.4 Results of combining different currents . . . 85

D.1 Symbols used in Dietz' derivation . . . 87
D.2 Dimensions of CEMT-class Va and Vb (Rijkswaterstaat 2011 [17]) . . . 90
D.3 Symbols and dimensions of parameters used in ship wave formulae . . . 92

E.1 Extreme values and downtime in scenarios 1, 2, 3 and 4 . . . 95
E.2 Extreme values and downtime in scenarios 5, 6 and 7 . . . 100
E.3 Extreme values and downtime of Scenarios 8, 9 and 10 . . . 104

F.1 Extreme values at X_Born in Scenario 1,2 and 3 . . . 111
F.2 Extreme values at X_1151 in Scenario 1,2 and 3 . . . 115
F.3 Extreme values at X_4000 in Scenario 1,2 and 3 . . . 119
F.4 Extreme values at X_5900 in Scenario 1,2 and 3 . . . 123
F.5 Extreme values at X_6001 in Scenario 1,2 and 3 . . . 127
F.6 Overview of extreme values and downtime of scenarios 1 and 4, at 5 locations . . . 131
F.7 Extreme values at X_Born in Scenario 5, 6 and 7 . . . 138
F.8 Extreme values at X_1151 in Scenario 5, 6 and 7 . . . 141
F.9 Extreme values at X_4000 in Scenario 5, 6 and 7 . . . 145
F.10 Extreme values at X_5900 in Scenario 5, 6 and 7 . . . 149

F.11 Extreme values at X_6001 in Scenario 5, 6 and 7 153
F.12 Extreme values at X_Born in Scenario 8,9 and 10 157
F.13 Extreme values at X_1151 in Scenario 8,9 and 10 161
F.14 Extreme values at X_4000 in Scenario 8,9 and 10 165
F.15 Extreme values at X_5900 in Scenario 8,9 and 10 169
F.16 Extreme values at X_6001 in Scenario 8,9 and 10 173

PROJECT MAP

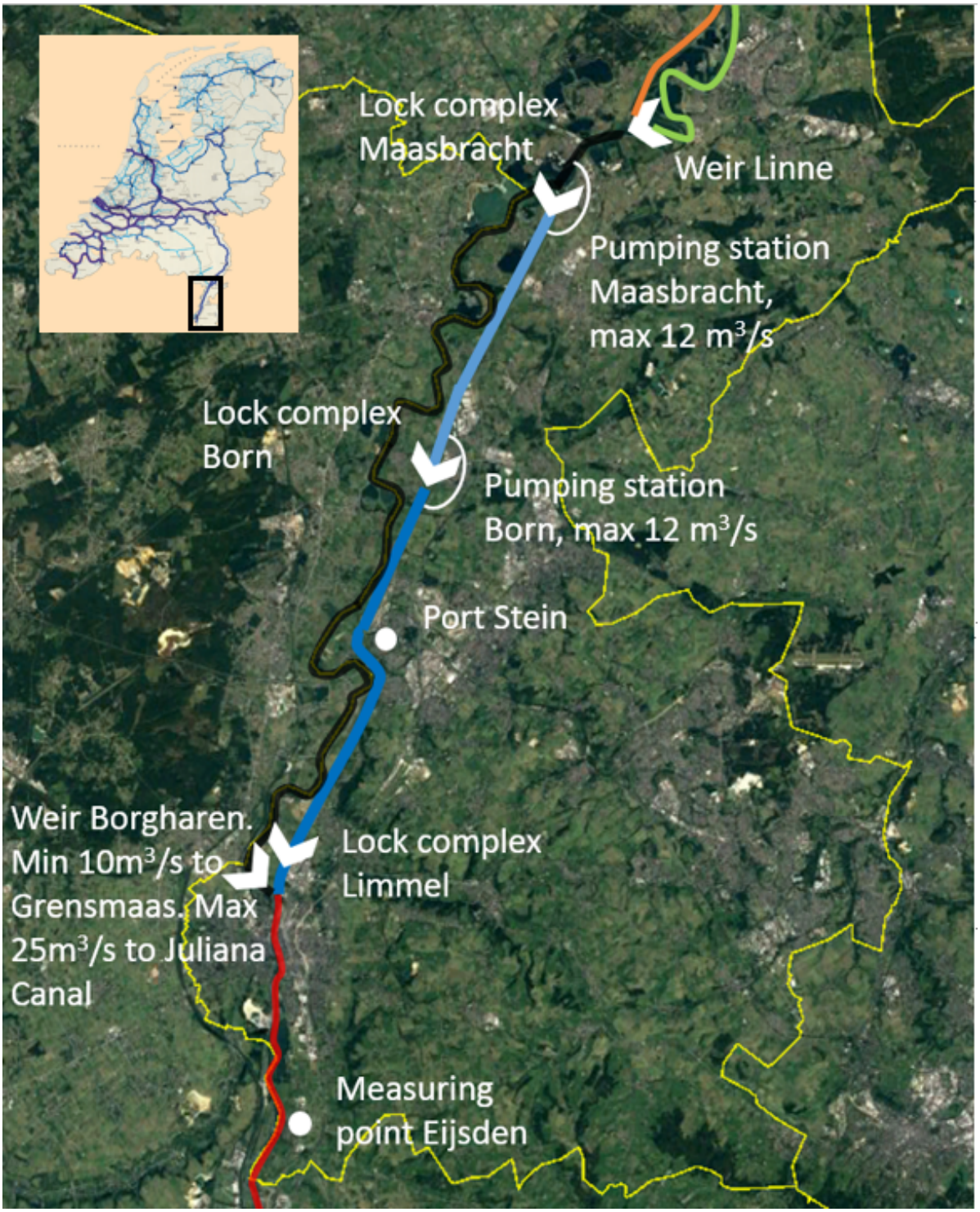

Figure 3: Overview of the Juliana Canal system

1

INTRODUCTION

1.1. BACKGROUND INFORMATION

The rate of transport to the hinterland over inland waterways is increasing in Europe. The vessels that transport the cargo continue to become larger. To provide the network that meets the markets demand, the dimensions of the waterways, canals and other hydraulic infrastructure, such as lock complexes, are being enlarged. To improve the European Waterways the European Commission has granted the TenT-subsidy (Balazs, 2015 [1]).

The hydraulic infrastructure increased over the last century. Lock complexes are an example of the hydraulic infrastructure which are enlarged. The lock complexes generate the translation waves in a canal but there has not been much research on what the effects of the larger complexes are on translation waves. The last large scientific researches on this topic were performed in the 30's and 40's of the past century by J. Th. Thijsse (Thijsse, 1935 [2]) and theoretical research added by D.N. Dietz (Dietz, 1941 [3]).

1.1.1. TRANSLATION WAVES

Translation waves are pulsatory travelling disruptions of the discharge and water depth which results in a more-or-less uniform change of velocity. A single translation wave creates the link between two different flow regimes. This is different than at for instance wind waves, these are oscillating waves which go up and down around the normal water depth. Translation waves are discussed in this research. Translation waves can be induced by multiple reasons, e.g. opening or closing of a weir, emptying and filling of lock systems or even a tsunami.
The focus of this research are translation waves induced by lock systems. To fill a lock chamber at a high head lock complex, a large volume of water is required. At the upstream side of the lock water flows to the lock chamber, resulting in a lower water level at the upstream side of the lock. Water from upstream in the canal flows towards the lower section close to the lock system, creating a new lower section because the water at that section is now in front of the gate. This process continuous, resulting in a translation wave propagation through the canal.

1.1.2. CASE STUDY JULIANA CANAL

The case study Juliana Canal is about the propagation and effects of translation waves in a canal situated in the south of the Netherlands, parallel to the Maas river. See the overview figure in the Project map. The Juliana Canal bifurcates at the Maas river near the village of Limmel and ends near the village of Maasbracht, where it confluences back with the Maas. An overview of the Juliana Canal is given in figure 3 in the project map. The construction of the canal was completed in 1935. The water level in the Juliana Canal is regulated with two lock complexes. The head difference between the two sides of both lock complexes is more than 11 meters, the highest head differences in the Netherlands. This is considered a high head lock system.
In current state the Juliana Canal meets the demands of a CEMT Va canal. The Juliana Canal is part of the North Sea - Mediterranean corridor. European legislation have determined that inland waterways should comply with the regulations of CEMT Vb vessels ([1]). The upgrade of the Juliana Canal is part of the larger construction works "Maaswerken". The canal has to be widened and deepened, to meet the demands of the

higher CEMT class. These activities started in 2013 and are expected to be completed in 2018. The project is awarded by "Rijkswaterstaat" and the "Ministerie van Infrastructuur en Milieu" to DEME-group and is executed by *de Vries & van de Wiel*. *Arcadis*' role is to deliver design support. The construction works are performed from the banks of the canal and with water-borne construction equipment.

1.2. PROBLEM DESCRIPTION

Currents induced by translation waves can have a negative effect on the workability of water-borne construction equipment. The Middle lock chamber of the lock complex near Born has already been enlarged. This results in larger translation waves and higher currents in the Juliana Canal since the dimensions of the cross sections of the canal itself, have not increased. High currents in the canal create highly undesirable working conditions which reduce the workability for the water-borne construction works.

1.3. RESEARCH QUESTIONS

To obtain more insight in the intensity and effects of the translation waves in a canal, research on the water level changes and currents induced by these waves has to be performed. The effects of the currents and water level changes on water-borne construction equipment is unknown. To gain the knowledge to answer these cases, the main research question is defined as:

How do translation waves, induced by high head lock systems, evolve in a canal and what are the possibilities by the lock system to create suitable working conditions for water-borne construction works?

To support the main question, a number of sub-questions are conceived.

- How does a translation wave propagate through a canal?
- What are the limit states of a water-borne construction equipment?
- What are the adaptation possibilities of a high head lock system?
- What is the best scenario to prevent downtime, caused by translation waves, for the construction works?

1.4. METHODOLOGY

The approach of this case study is divided in 6 steps:

1. System analysis
2. Develop a translation wave model
3. Determine the discharge-time relations of the lock chamber
4. Development different simulation scenario
5. Analysis of the model results
6. Determine best situation for water-borne construction works

First the system at its present state is analysed. In this analysis, the outline of the canal is observed, where the hydraulic structures, side canals and other points of interest are located.
Secondly, with the knowledge on translation waves, a model to simulate the propagation of translation waves in the canal is developed.
Third, the input parameter for translation waves, the discharge over time relation of filling the lock chambers is modelled.
Fourth, different scenarios that present insight in the reaction of the system, to different translation waves are used as input in the translation wave model.
Fifth, the results of the model under different scenarios are analysed and the consequences of the different waves on the water-borne construction equipment is presented.
Sixth, the outcomes of the different scenarios are compared and the most favourable result is determined.

1.5. SCOPE

In this research the area of interest will be limited to the upstream section of Born up to the bend upstream of the port of Stein in the Juliana Canal. During graduation this section of the canal was the part where construction works were executed by the contractor.
Currents induced by other external factors than translation waves induced by the lock complex are not investigated.
The measures which are analysed are adaptations related to the lock complex only. Adaptations to the waterborne construction equipment or to the bathymetry of the canal is excluded in this research.

1.6. THESIS OUTLINE

The build up of the report is presented according to the following division.

Chapter 1 Background information on translation wave and the case study of this research given in the first chapter. After the background information, an introduction to the subject and the problem definition which follows from subject and background information.

Chapter 2 To obtain a better understanding of the characteristics of a translation wave, a theoretical background is given. Largely according to the findings by Thijsse (Thijsse, 1935 [2]).

Chapter 3 This research covers the case study Juliana Canal. An introduction to, and an analysis on, the case study is given in chapter 3. The Juliana Canal system, construction equipment, limit states and downtime will elaborated upon in this chapter.

Chapter 4 A model to simulate the translation waves in the canal is made. In chapter 4 a description on how the model is set up and what the model can do is given.

Chapter 5 & 6 An elaboration on which scenarios are investigated, is given in chapter 5. The scenarios are implemented in the model as input for the translation waves. The results which follow from the different scenarios are given in chapter 6.

Chapter 7 The final chapter of the main report is chapter 7. The conclusions which follow from the results are presented here. Answers to the main- and sub-questions are given as well. After the conclusions, recommendations for future research is given.

2

LITERATURE STUDY

In this chapter will be elaborated on the theory on translation waves as far as it is currently known. Thereafter will the theory on the Method of Characteristic be explained. The theoretical approach on translation waves by Dietz and theory on spectrum analysis and ship induced waves can be found in Appendix D.

2.1. TRANSLATION WAVES

First the translation waves will be elaborated upon. The translation waves are the primary topic of this thesis. First a brief description will be given what the basics and origin of a translation wave is. Then the propagation of a translation wave through a canal will be discussed, according to the theories of Thijsse (Thijsse, 1935 [2]). This theory will be used to make a model to predict the water level changes and currents due to the translation waves. After the theory on translation waves, theory on the Method of Characteristics is discussed.

2.1.1. WHAT IS A TRANSLATION WAVE?

Unlike "normal" oscillating waves which go up and down around the normal water depth, translation waves are discussed in this chapter. Translation waves are pulsatory travelling disruptions of the discharge and water depth which results in a more-or-less uniform change of velocity. A single translation wave creates the link between two different flow regimes.

Translation waves causes multiple possible dangers in a canal:

- Change or increase of the water velocity may effect the bank protection
- Ships may be pressed against bridges or run aground due to the rising an falling of the water-level. This may also affect the bottom protection
- Steep gradients in the water surface may be dangerous for shipping

In this chapter, relatively low translation waves will be explained. In the situation of low translation waves the advection terms and local changes in cross sections can be neglected (lecture notes CT3310, Labeur, 2011 [4]). High translation waves will not be discussed because these kind of waves do not occur in the Juliana Canal.

LOW TRANSLATION WAVES

Low translation waves occur when a wave propagates fast but the discharge and water depth changes are relatively small. The discharge per travelling wave can be expressed as:

$$\delta Q = Bc\delta h \tag{2.1}$$

$$\text{with } c = \sqrt{\frac{gA_s}{B}} \tag{2.2}$$

With:
δh $[m]$ = Water level change due to translation wave

δQ $[m^3/s]$ = Discharge of the translation wave
B $[m]$ = Width of the canal
c $[m/s]$ = Wave celerity
A_s $[m^2]$ = Cross section of the canal
d $[m]$ = Depth
g $[m/s^2]$ = Gravitational acceleration

When there are no changes in the depth (δh) over the width B of the canal, this formula can be reduce to:

$$\delta U = \frac{\delta h}{d} c = \sqrt{\frac{g}{d}} \delta h = \frac{g}{c} \delta h \tag{2.3}$$

In the figure above, figure 2.1, two examples are given of a translation wave. In the first sketch an illustration is given of opening a lock or sluice, the discharge at $t = 0$ is zero but there is a height difference between both sides of the gate. In the second figure a discharge is partly closed. The discharge is no longer constant in time on both sides, a δQ arises. The abruptness of the response of the canal depends on the velocity in which the modifications to the systems are implemented. A very abrupt opening of a lock chamber will give a steep wave front. At the opening of a lock chamber, for instance, changes the discharge from second to second. After some minutes the discharge will have grown from zero to its maximum discharge and return back to zero. To determine the shape of the wave it can be described as elementary pulses travelling away from the lock chamber. Every pulse has its own height, depending on the discharge at that time. These pulses of different heights join creating a single wave. This principle is used in the translation wave model, discussed in Chapter 4.

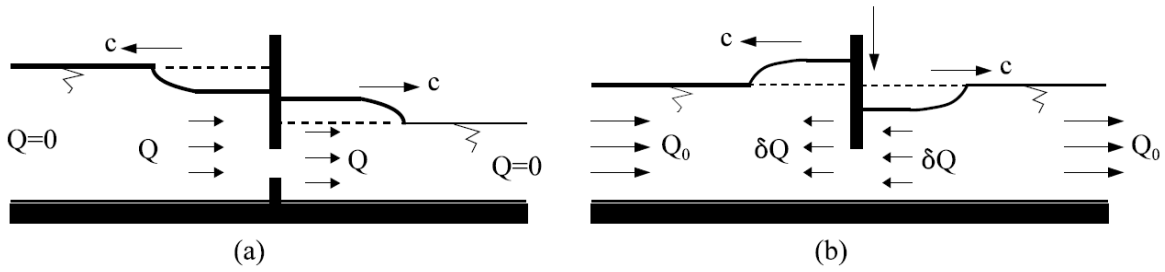

Figure 2.1: Two examples of reasons for translation waves (lecture note CT3310 Open channel flow)

2.1.2. PROPAGATION OF A TRANSLATION WAVE IN A PRISMATIC CANAL

In the 1930's Thijsse wrote a paper on translation waves (Thijsse, 1935 [2]). In the 30's large projects were constructed to counteract the unemployment in the Netherlands, the Juliana Canal was constructed in this period as well. The locations of these canals are presented in figure 2.2. The research of Thijsse was done in the Twente Canal, a similar canal as the Juliana Canal. In this canal large locks have been build with a large height difference of approximately seven meters (depending on the water level of the river IJssel and canal depth). At the lock systems at Born and Maasbracht the height difference is more than 11 meters, the effects of translation waves will be even more severe.

Figure 2.2: Locations of the Juliana Canal and Twente Canal

In this chapter the formula for the propagation of a translation wave will be explained, as derived by Thijsse. The symbols used in the derivation are given in table 2.1.

Table 2.1: Parameters used in Thijsse's formulae

Symbol	Meaning	Dimensions
z	Wave height	m
Q	Discharge through lock	m^3/s
b	Width	m
c	Wave propagation velocity, celerity	$^m/_s$
g	Gravitational acceleration	$^m/_{s^2}$
F	Area of wet cross section	m^2
h	Canal depth	m
v	Snelheid dempingsstroom	$^m/_s$
R	Hydraulic radius of the canal	m
k	Roughnessfactor	$m^{1/2}/s$
Z_0	Wave height at $x = 0$	m
z_0	Height of the top of the wave	m
x	Distance from origin wave	m
y	Passed distance till amplitude is half of original amplitude	m
n	Frequency of the composed wave	$^{rad}/_s$
c_w	Celerity, with friction	$^m/_s$
δ	Aid angle	rad

Assume the canal can be simplified to a prismatic canal. The following calculations can be made.

$$z = \frac{Q}{bc} \tag{2.4}$$

If the height of the wave can be neglected compared to the water depth:

$$c^2 = gh \tag{2.5}$$

The water depth:

$$h = \frac{F}{b} \tag{2.6}$$

If the wave height of the translation wave cannot be neglected compared to the water depth:

$$c^2 = gh * \left(1 + \frac{3}{2} * \frac{z}{h}\right) \tag{2.7}$$

Taking the curvature of the wave into account:

$$c^2 = gh * \left(1 + \frac{3}{2} * \frac{z}{h} + \frac{h^2}{3z} * \frac{d^2z}{dx^2}\right) \tag{2.8}$$

The value of z is negative for a negative wave. When this is inserted in formula 2.7 it results in a lower speed in the troughs than at undisturbed water level. The curvature at the front of the wave becomes flatter, at the back it becomes steeper until the curvature becomes in equilibrium with the waterline.

FRICTION ON TRANSLATION WAVES

The propagation velocity of the wave decreases over time in a prismatic canal due to friction. A current is created by the wave in a lower layer in the canal. This current encounters resistance due to friction along the sides of the canal. The velocity of the current underneath the translation wave can be calculated with:

$$u = \frac{cz}{h} \tag{2.9}$$

If the wave is a positive translation wave, the current is in the same direction as the propagation direction of the wave. In case the translation wave is a negative translation wave, the current is to the opposite direction. The resistance depends on three aspects:

- Current
- Roughness of the walls or banks
- Dimensions of the walls

The volume of the wave is reduced due to friction, the top or trough of the wave decreases. The sharp edge on the back of the wave dissipates and finally the diffuses over the canal.

A rough approximation can be expressed in the quadratic friction law:

$$v = k * \sqrt{R\frac{dh}{dx}} \tag{2.10}$$

After combining 2.9 and 2.10, the expression for the height of the wave can be written as:

$$z = \frac{Z_0}{1 + \frac{x}{y}} \tag{2.11}$$

$$\text{with } y = \frac{\varphi * k^2 * R}{g * Z_0} * h \tag{2.12}$$

The coefficient φ is a function of the shape of the wave. The coefficient does not vary much and can be taken at $\varphi = 3$. As can be seen in formula 2.12 a higher wave will decrease relatively faster than a smaller wave. The celerity of the wave decreases due to the friction. The influence is expressed with the parameter δ.

$$tg\delta = \frac{g}{k^2 Rn} v \tag{2.13}$$

In this expression, v is a velocity a little smaller than the maximum velocity underneath the wave, as calculated in equation 2.10. The largest uncertainty in this method is to choose the correct value for v. When this is done, the celerity with friction included is calculated:

$$c_w = c\frac{\sqrt{cos\,\delta}}{cos^{\,1}/_2\,\delta} \tag{2.14}$$

With c the original celerity, without friction.

2.1.3. PRISMATIC CANAL WITH CHANGES IN DIRECTION AND CROSS SECTION

In the previous section the celerity and friction of a translation wave in a prismatic canal (Thijsse, 1935 [2]) has been discussed. In the theory written in the previous paragraph the changes of the translation waves in a bend was elaborated upon nor investigated in Thijsses research. It is assumed that when the radius of the bend is large, the canal section can be calculated with the same method and assumptions as a straight section. Sections with an abrupt change of direction the wave can be reflected or partially reflected. The exact data on this topic is still not well known.
The changes of height and celerity of a translation wave caused by changes in the cross section can be explained theoretically. The waves are primarily determined by the canal width and celerity. Celerity depends largely on the water depth. The height of the wave changes if the product of b*c changes. When a wave travels from a cross section with a certain width to a section with another width the height of the wave changes according to the following formula.

$$z_1 = z\frac{2}{1+\beta} \tag{2.15}$$

With:
$\beta = \frac{b_1 c_1}{b_0 c_0}$
z = original wave height
z_1 = wave height in new cross section
z_2 = wave height of the reflected wave

A part of the wave travels to the new cross section, another part of the wave is reflected. The direction of the reflected wave is the opposite of the original wave, this is illustrated in figure 2.3. The height of the reflected wave is:

$$z_2 = z_1 - z = z\frac{1-\beta}{1+\beta} \tag{2.16}$$

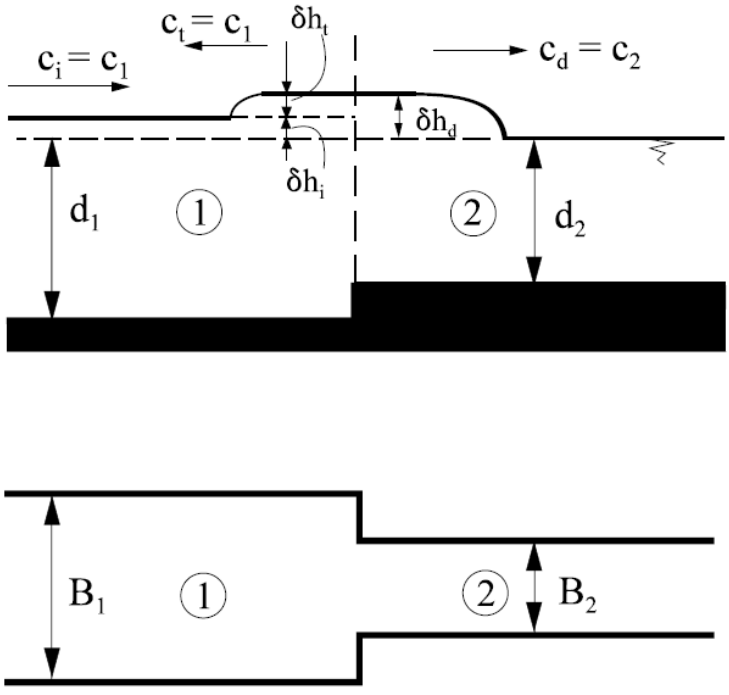

Figure 2.3: Translations waves at changes in cross section (lecture notes CT3310 Open channel flow)

If the secondary cross section is larger than the primary cross section then $\beta > 1, z_1 < z$ and $z_2 < 0$. When a positive translation wave propagates into a wider cross section, the reflective wave is a negative wave travelling in opposite direction.

If the opposite case, when the secondary section is narrower, then $\beta < 1, z_1 > z$ and $z_2 > 0$. The amplitude of propagating wave is larger than the original wave, the reflected wave has the same sign as the primary wave.

There are two extreme cases for $\beta, \beta = \infty$ and $\beta = 0$. In the extreme case $\beta = \infty$, this occurs for instance at the outflow of a canal in a lake or sea. In that case, the continuing wave is zero and the reflected wave has the same amplitude as the original wave but the opposite sign, $z_2 = -z$.

In the case $\beta = 0$ the canal stops due to e.g. a weir or lock. The amplitude of the continuing wave becomes $z_1 = 2z$ in theory, but at the end of a canal there is no continuing wave. This results in an elevation or depression of the water level of $z_1 = 2z$ at the closure only. The reflected wave has the same sign and amplitude as the original wave, $z_2 = z$.

In summary:

Table 2.2: Effects of changes in β

$\beta = bc$	Continuing wave	Reflected wave
$\beta > 1$	$z_1 < z$	$z_2 < 0$
$\beta < 1$	$z_1 > z$	$z_2 > 0$
$\beta = \infty$	$z_1 = 0$	$z_2 = -z$
$\beta = 0$	$z_1 = 2z$	$z_2 = z$

The translation wave can encounter a temporary change of the cross section. The water level change of the wave will always be smaller than before the change of cross section. The water level change of the wave after the wider or narrower section, so when the canal is back to the original shape is expressed as follow:

$$z_3 = z\frac{4\beta}{(1+\beta)^2} \tag{2.17}$$

The change of the cross section has to be of significant length to have an effect on the translation wave. A narrowing at for instance a bridge will not have an effect on the water level change.
A harbour or the mouth of a branch have more impact on the decreasing the amplitude of the wave. The bc of the side branch is included in the bc for z_1, the bc is the combination of the canal before the side canal and the side canal. The water level change of the wave is the same in the canal and the side branch, decreasing the water level change significantly compared to a situation without side branch. The wave in the branch can reflect back to the canal, depending on the length of the branch. If the length of the side canal is small or a change of profile occurs close to the main canal in the side canal, a reflected wave will arise. When the reflected wave from the branch reaches the canal, it splits again in both directions of the canal, decreasing the water level change even further. To detect the reflected wave, the side canal has to be long enough. If the side canal is not too small, the reflected wave will merge back with the original wave and will not be detectable nor result in a lowering of the water level change. The length of the canal has to be a least as long as it takes the head of the translation wave in the side canal to arrive back at the canal when the back of the primary wave in the canal has passed by.

2.1.4. CURRENTS IN THE CANAL

The direction of the currents depend on the sign of the translation wave, whether it is a positive or negative wave. In a positive translation wave the current is pushed in the same direction as the propagation direction of the wave. This is visualized in figure 2.4.

The currents resulting from negative translation waves are in the opposite direction of the propagation direction of the wave. A lowering of the water level occurs during the passing of a negative translation wave. The volume at the back end of the wave has to be restored to the original water level, a volume of water is transported to the opposite side than the propagation direction of the negative wave. This is illustrated in figure 2.5.

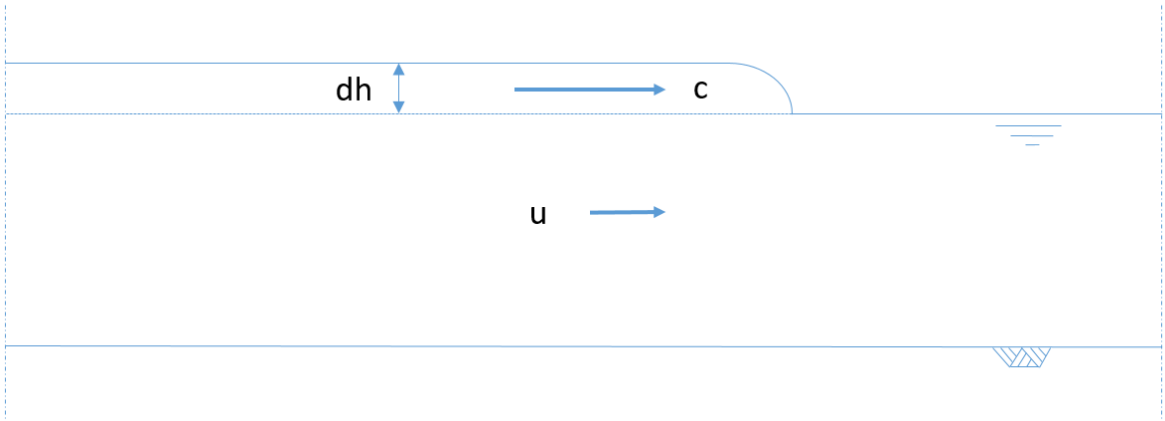

Figure 2.4: Current due to a positive translation wave

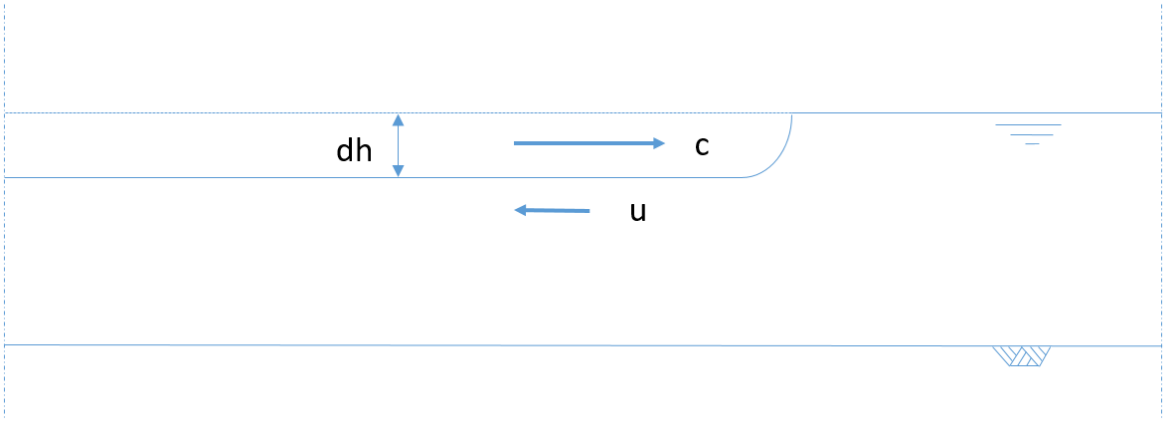

Figure 2.5: Current due to a negative translation wave

When there is interference between two waves from opposite directions, the waves can enlarge or reduce each other. If a positive wave from one side interacts with a negative wave from the opposing side of a canal, the water level changes will reduce. If in this situation the positive and negative translation wave are exactly of the same magnitude, the water level changes will be neutralized. The current however will double in magnitude because the current of the negative wave is in the opposite direction of the propagation direction of the wave and the current of the positive wave is in the propagation direction of the positive wave. This is visualized in figure 2.6.
The opposite situation happens when two positive or two negative waves interact. If the magnitudes of the waves are equal again, the water level change will double but the currents will cancel each other out. This can be seen for the situation with two positive waves in figure 2.7. The effect of interacting waves can be opposite for currents as to water level changes.

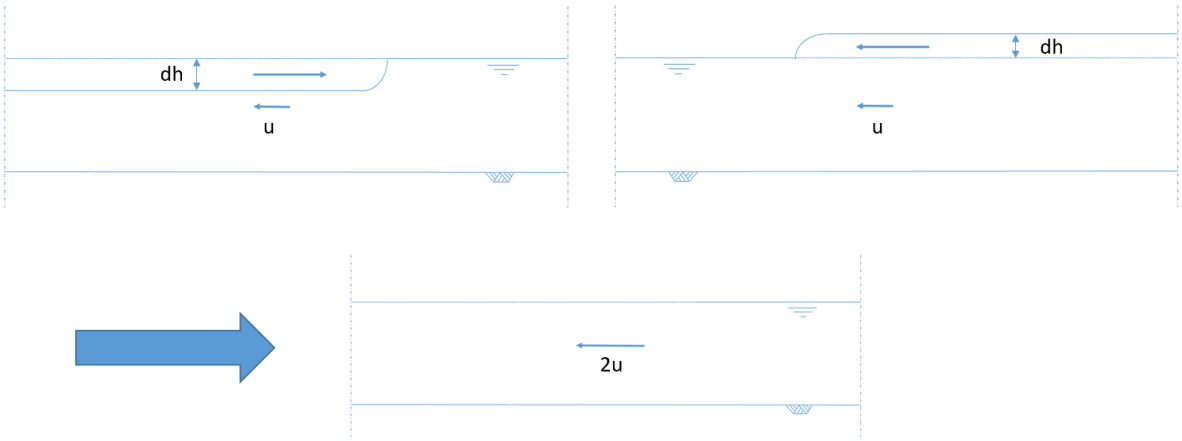

Figure 2.6: The resulting water level change and current when a negative and positive wave from opposite direction meet each other

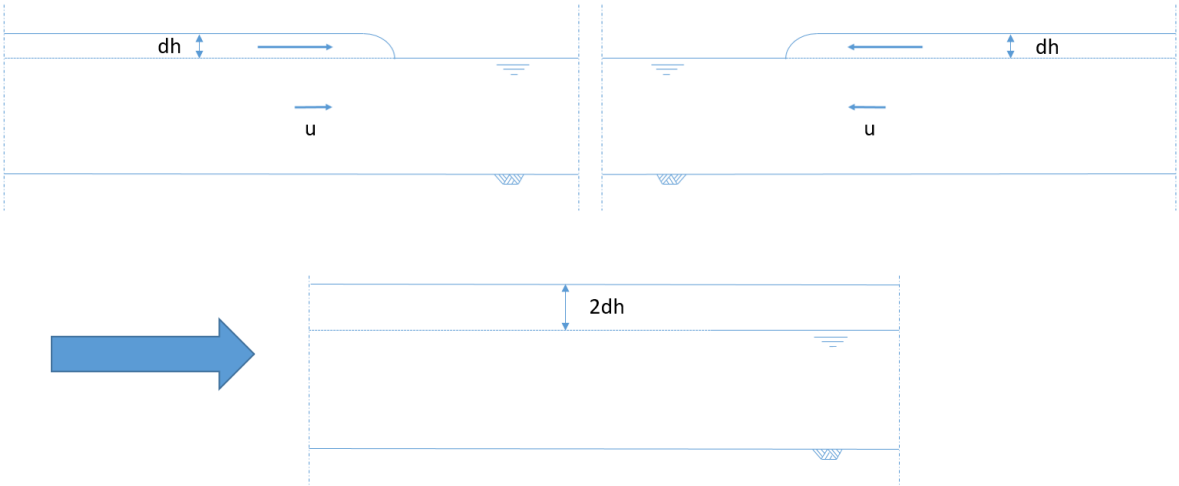

Figure 2.7: The resulting water level change and current when two positve waves from opposite directions meet each other

The formula used for the calculation from water level change to current is:

$$u = \frac{1}{f_p}\frac{cz}{h} \tag{2.18}$$

In which:
u $[m/s]$ = Current
c $[m/s]$ = Wave celerity
z $[m]$ = Water level change
h $[m]$ = Water depth
f_p [-] = Reduction factor of net water surface of the canal due to the water-borne equipment

The currents have to be calculated from each individual wave and can than be added together to calculate the net current on that location, on that time. The net current on a location cannot be calculated by the implementing the net water level change z in formula 2.18.

2.2. METHOD OF CHARACTERISTICS

The explanations and derivations of the Method of Characteristics will be done according to the lecture notes of CT3310 Open Channel Flow ([4]) course at TU Delft.

The waves considered in this chapter and in this system travel through the system with a finite velocity. The influence of local interventions, such as filling or emptying of a lock chamber, arise on other locations in the canal after time. The magnitude and when the intervention arrive at another location in the channel has to be calculated. The method used is the method of characteristics.
Simplify the canal as a 1D-system over the x-axis which changes over time. The changes can be represented in a (x,t)-diagram. The changes over time can be expressed as $\frac{dx}{dt}$, the celerity. The $\frac{dx}{dt}$ form in this situation linear lines (when resistance is neglected), the lines are called characteristics. The characteristics represent the information travelling through the canal.

The derivation of the method of characteristics start with the transport-equation (bottom friction is neglected) and the continuity-equation, assuming a horizontal bottom and no changes in side directions.

$$\frac{\partial U}{\partial t} + U\frac{\partial U}{\partial x} + g\frac{\partial d}{\partial x} = 0 \tag{2.19}$$

$$\frac{\partial d}{\partial t} + \frac{\partial Ud}{\partial x} = 0 \tag{2.20}$$

With:
U $[m/s]$ = velocity
d $[m]$ = depth
x $[m]$ = distance
t $[s]$ = time

The variable d is replace by $c = \sqrt{gd}$ and substituted in equations 2.19 and 2.20, resulting in:

$$\frac{\partial U}{\partial t} + U\frac{\partial U}{\partial x} + 2c\frac{\partial c}{\partial x} = 0 \tag{2.21}$$

$$2\frac{\partial c}{\partial t} + c\frac{\partial U}{\partial x} + 2U\frac{\partial c}{\partial x} = 0 \tag{2.22}$$

Defining $R^+ = U + 2c$, adding equations 2.21 and 2.22 and substitute R^+ into the new equation result in:

$$\frac{\partial R^+}{\partial t} + (U + c)\frac{\partial R^+}{\partial x} = 0 \tag{2.23}$$

The left side of equation 2.23 is the derivative of R^+ to t, which is 0 if the observer travels at $dx/dt = U + c$. So equation 2.23 can be represented by:

$$\frac{\partial R^+}{\partial t} = 0 \tag{2.24}$$

If

$$\frac{\partial x}{\partial t} = U + c \tag{2.25}$$

If equations 2.21 and 2.22 are subtracted, R^+ defined as $R^- = U - 2c$ and substituted in the new equation result in:

$$\frac{\partial R^-}{\partial t} + (U - c)\frac{\partial R^-}{\partial x} = 0 \tag{2.26}$$

And

$$\frac{\partial R^+}{\partial t} = 0 \tag{2.27}$$

If

$$\frac{\partial x}{\partial t} = U - c \tag{2.28}$$

The velocities U ± c are called the characteristic velocities, the lines in the (x,t)-graph in which $dx/dt = U \pm c$ are called the positive c.q. negative characteristics. $dx/dt = U \pm c$ are defined as $K^{\pm}$, these are called the characteristic relations. The characteristics U ± c, defined as $R^{\pm}$. $R^{\pm}$, are constant along the lines of $K^{\pm}$.

If two point in the (x,t)-graph are located close to each other and the values of the variables U and c at these two points are also known, the values and location of a third location can be calculated as well. The locations of the known point are drawn in figure 2.8a as 1 and 2, in figure 2.8b as T_1 and T_2. The derivatives of locations 1 and 2 are known as well according to equation 2.25 and 2.28. These are the velocities along the x-axis, corresponding with the directions in the (x,t)-plane. Extrapolating a line from the points 1 and 2 with an angle according to dx/dt, the lines will cross in the new point 3. The accompanying variables U and c are determined with the Riemann invariants R^+ and R^-. Where the lines cross represent the values for U and c in point 3. This is graphically represented in figure 2.8.

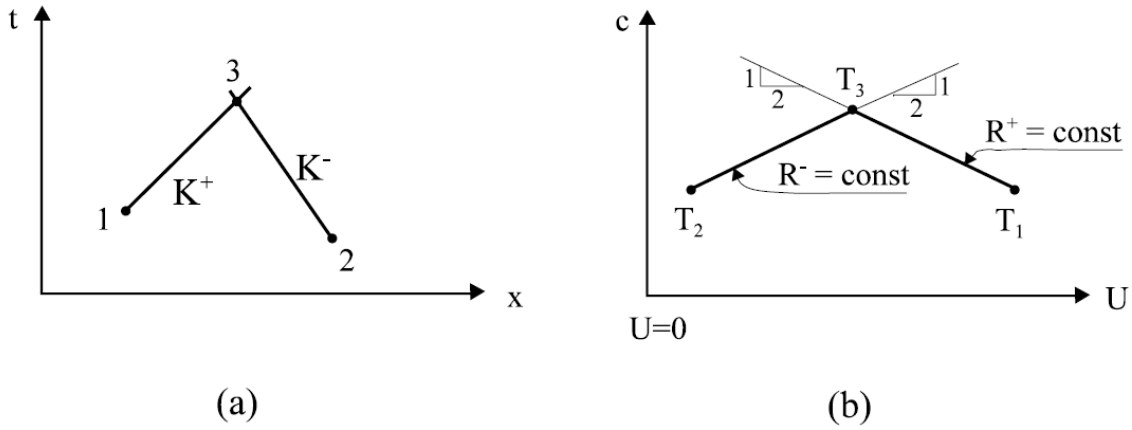

Figure 2.8: (a) (x,t)-graph (b) (U,c)-graph (lecture notes CT3310 Open channel flow)

The values for U and c at point 3 can be calculated as well. Along the characteristic relations K^+ and K^- are the characteristic velocities R^+ and R^- constant. At point 3 the variables correspond to:

$$R_3^+ = R_1^+ \tag{2.29}$$

$$R_3^- = R_2^- \tag{2.30}$$

Or:

$$U_3 + 2c_3 = U_1 + 2c_1 \tag{2.31}$$

$$U_3 - 2c_3 = U_2 - 2c_2 \tag{2.32}$$

Solving equations 2.31 and 2.32 for U_3 and c_3 result in:

$$U_3 = \frac{1}{2}(U_1 + U_2) + (c_1 - c_2) \tag{2.33}$$

$$c_3 = \frac{1}{4}(U_1 - U_2) + \frac{1}{2}(c_1 + c_2) \tag{2.34}$$

The method described above can be applied throughout the canal if the base points are known. From the new points can further points be calculated, as can be seen in figure 2.9.

Further explanations and derivations on the theory of the method of characteristic can be found in the lecture notes of CT3310 Open Channel Flow ([4]), at TU Delft.

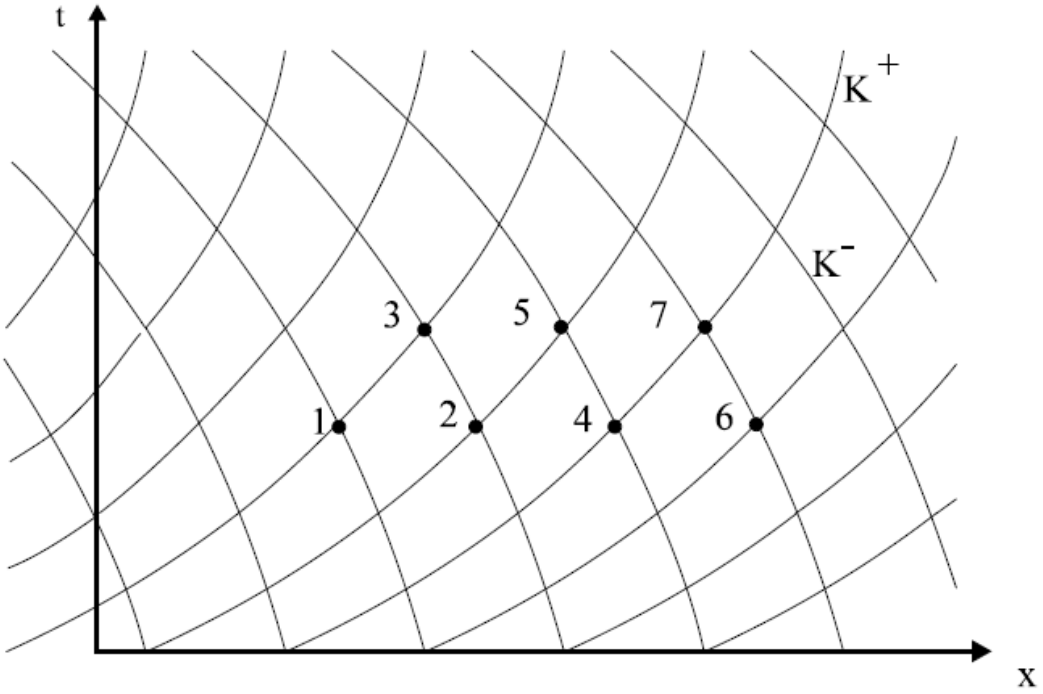

Figure 2.9: (x,t)-diagram with multiple characteristics (lecture notes CT3310 Open channel flow [4])

3

JULIANA CANAL, CASE STUDY

The theoretical principles of translation waves have been explained in chapter 2. To investigate the consequences of translation waves induced by high head lock systems, research is done applying the theory on a case study. In this research, the case study in done in the Juliana Canal. In this chapter an introduction on the area and boundary conditions are given.

3.1. THE JULIANA CANAL

The Juliana Canal is a canal in the south of the Netherlands. The canal was constructed to overcome the steep part of the Maas, the Grensmaas. The translation of Grensmaas is "border Maas", the border between the Netherlands and Belgium. The location of the Juliana Canal is determined by political motivations (Rouvroye/Schreurs, 1996), more detailed information about this topic can be found in *Aanleg Julianakanaal 1935* by *H. Rouvroye / L. Schreurs*, commissioned by *Heemkundevereniging Maasstreek*.

The canal is 35 km long, start at the Maas at Limmel near Maastricht and ends in Maas in Maasbracht, as can be seen in figure 3.1. The difference in altitude over the canal is 23 meter and is regulated with 3 locks, at Limmel, Born and Maasbracht. At each lock complex a pump station is installed to compensate in the upstream canal section for the water losses due to emptying and filling of the lock. The lock at Limmel is a guard lock, this lock is only closed when high water levels in the Maas occur.

The weir at Borgharen, regulates the distribution of the discharge between Maas and Juliana Canal. The weir maintains the water level at a design level at which vessels of class CEMT Va can sail the canal.

The water discharge which flows to the Juliana canal depends on the Maas discharge. The maximum inflow at Limmel is $25 m^3/s$ (Rijkswaterstaat, 2012 [5]), the excessive discharge flows to the Grensmaas. The locks at Limmel act as a narrowing in the canal, the flow velocity increases as it flows through the locks resulting in a lower water level. If the discharge would exceed the maximum discharge, ships would be unable to sail through the locks. The minimum discharge to the Grensmaas is set at $10 m^3/s$ for environmental reasons (Imtech, 2015 [6]).

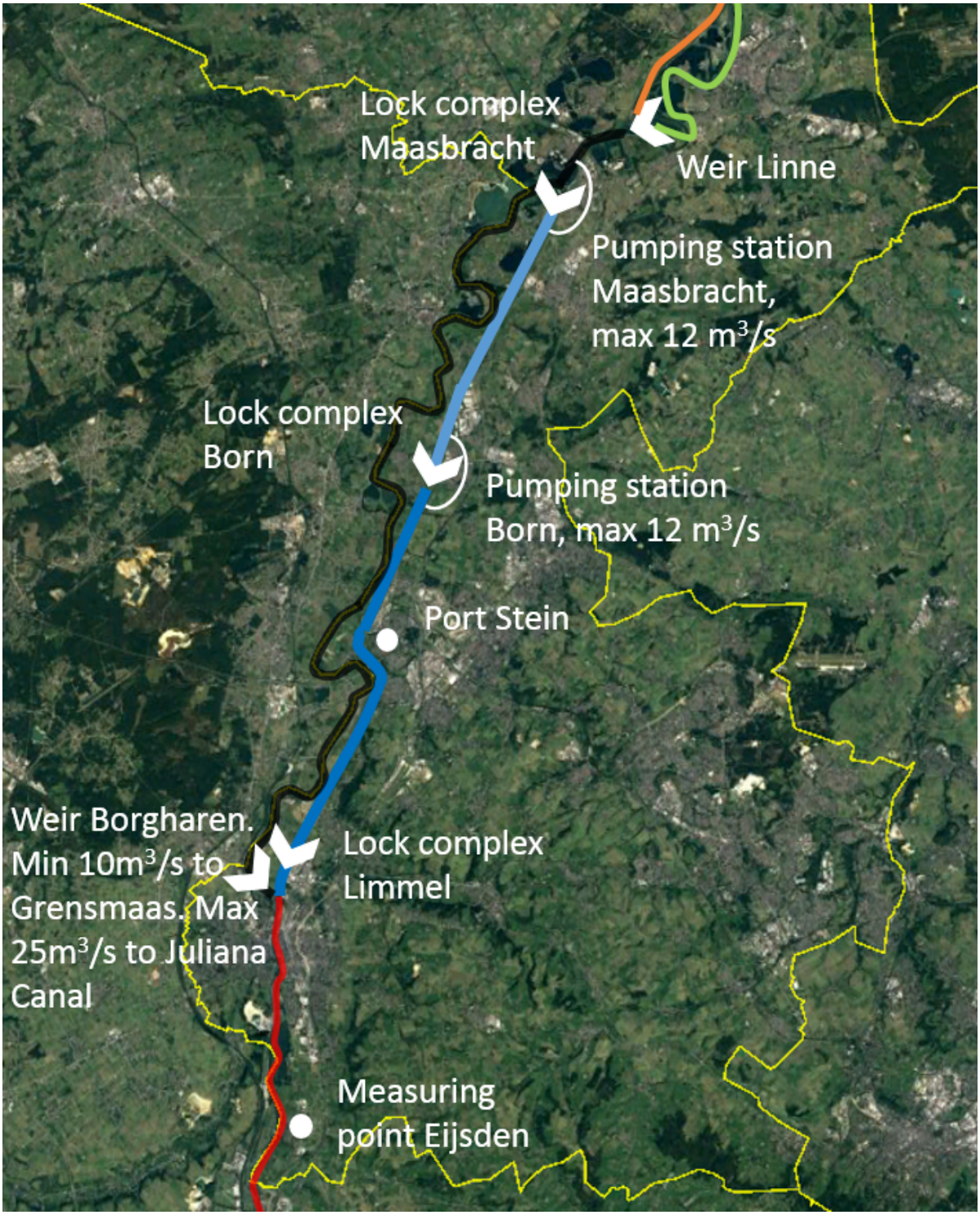

Figure 3.1: Overview of the Juliana Canal system

The water level in the Juliana Canal is higher than the surface level next to the canal. The canal has been built on top of the surface area. The surrounding soils are mostly sand and gravel layers, to make the canal watertight the bottom of the canal has been coated with a clay layer of 70cm.

In the figure below, figure 3.3, a visualisation is given of the heights of the ground level near Born. Higher grounds are presented in orange, lower areas in green and blue. The bottom level of the Juliana Canal is higher than the surrounding areas as well, not only the water level.

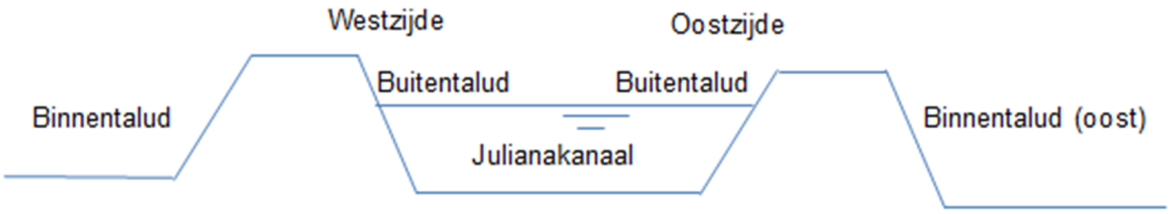

Figure 3.2: Overview of a canal cross section

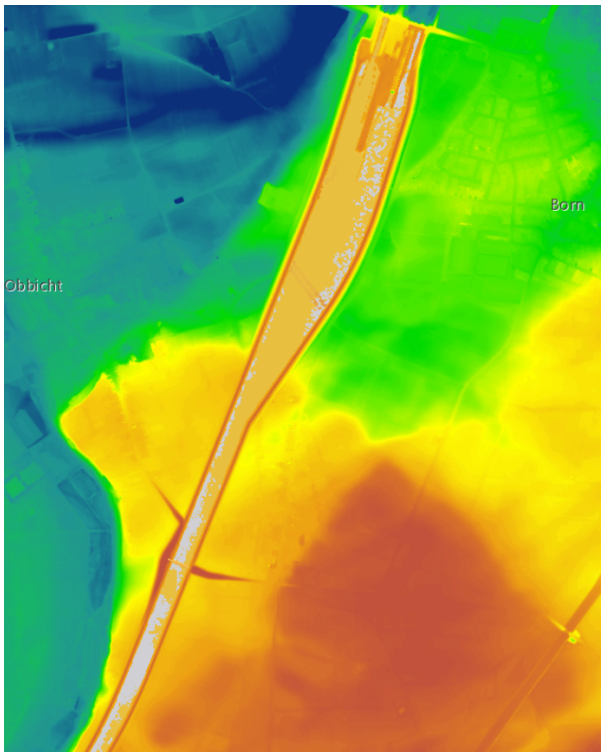

Figure 3.3: Heights of ground level near Born (ahn.maps.arcgis.com)

The projects at the Juliana Canal are part of a larger project, the Maaswerken. In these works the whole Maas system is maintained and upgraded, it includes the projects Grensmaas, Zandmaas and Julianakanaal. An overview of the projects is given in figure 3.4 below. To comply with the European ambition to improve the North Sea – Mediterranean connection (Balazs, 2015 [1]), the Juliana Canal is upgraded from CEMT Va to CEMT Vb. These activities started in 2013 and are expected to be completed in 2018, the project is awarded by Rijkswaterstaat Ministerie van Infrastructuur en Milieu to DEME-group and is executed by “de Vries & van de Wiel”. Arcadis’ roll is to deliver design support.

Several measures are implemented at the Juliana Canal. A large part of the canal, 26 km, has to be dredged back to the original bottom height of 39m +NAP, these are maintenance works. One and a half km of the canal has to be deepened by 1 meter, the canal will be made watertight again with bentonite mats. The dredging works will be done by dredging with a backhoe on a pontoon.

Ten percent of the canal has to be widened, two techniques are applied. First, where possible, the dike is moved back to create a wider canal. The second option is applied if there is not enough space to displace the dike. Sheet piles are placed in the old dike, the soil on the waterside of the old dike is excavated, resulting in a wider waterline and due to the vertical sheet piles, in a much wider sailing cross section. The clay layer on the dike section is removed as well. To make it watertight again bentonite mats are placed on the bottom. A new technique has been developed to implement the bentonite mats, with the construction vessel *Mattedoor*. A more detailed description of the *Mattedoor* is given further in this chapter. An illustration of a cross section where this method is applied, is given in figure 3.5.

In 2012 there were about 23.000 ship passages on the Juliana Canal (Bureau Voorlichting Binnenvaart,

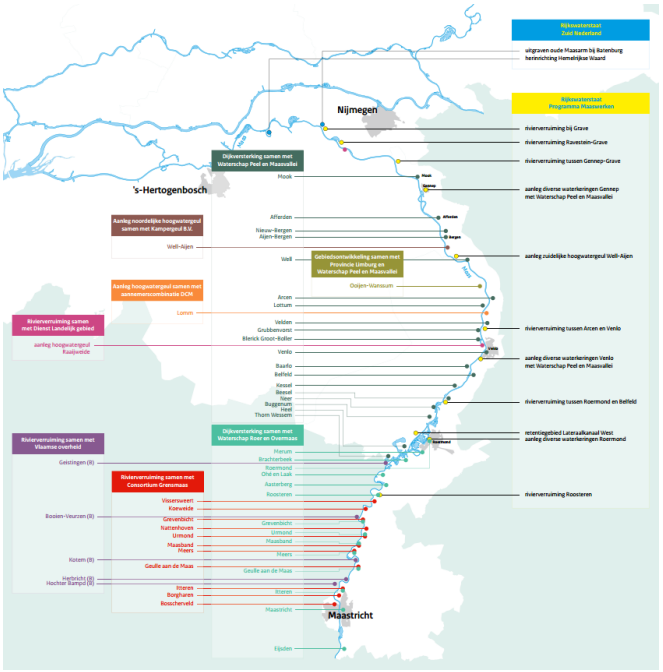

Figure 3.4: Overview Maaswerken (www.grensmaas.nl)

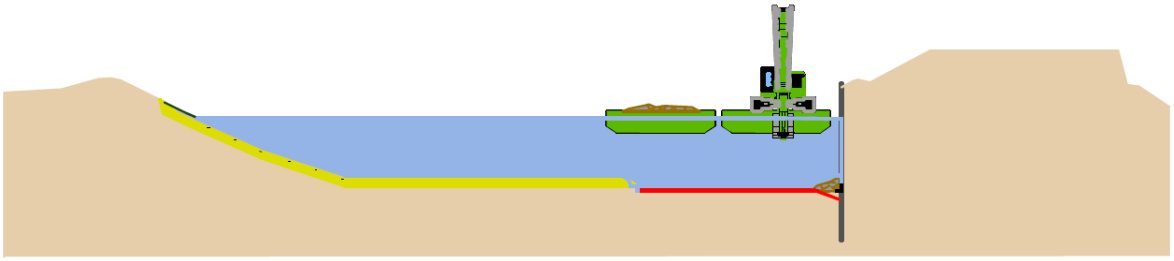

Figure 3.5: Cross section of the canal canal widened with a sheet pile construction (www.julianakanaal.nl)

2016 [7]). There is an expected shipping intensity of 1500 vessels of CEMT-class Va per year (Deltares, 2015 [8]). Current CEMT class is Va Groot Rijnschip and Duwvaart with 1 barge (Binnenvaart in beeld, 2016 [9]).

Table 3.1: Characteristics of CEMT-class Va and Vb (Rijkwaterstaat, 2016 [10])

Class	Va	Vb
Length [m]	110	170-190
Width [m]	11.4	11.4
Draught (laden) [m]	3.5	3.5
Load [tons]	2051-3300	3951-7050

As mentioned before, there are 3 lock complexes in the lock system of the Juliana Canal. These are located at the beginning of the canal at Limmel, about halfway at Born and near the confluence at Maasbracht. There used to be a fourth lock system at Roosteren but this lock complex was closed and removed in 1965 to improve navigability in the canal. To accomplish this, the canal had to be widened and the dikes made higher between Born and Maasbracht. The lock systems at Born and Maasbracht were upgraded as well. The height difference at the locks at Maasbracht increased to 11.85m, making it the locks with the highest water level difference in the Netherlands (KanaleninNederland.nl, 2010 [11]).
The lock complex at Born originates from the opening of the canal in 1935. In 1965 the lock was upgraded to meet the new specifications after the removal of the Roosteren locks. The lock complex consists of three

locks, the East, Middle and Old lock. The middle lock chamber has been lengthened in 2009 to 225m to meet the requirements for CEMT Vb vessels. Further characteristics of the Born lock complex can be found in table 3.2.
The lock complex at Maasbracht originates from 1935 and has been upgraded in 1965 as well. One of the three lock chambers has been lengthened to 225m, the other two locks are 142m in length (Rijkswaterstaat, 2016 [10]). The lock complex at Limmel contains of two locks, these locks are only used when there is a high water discharge at the Maas. The lock complex is under construction at the moment and will be replaced with a flood gate. The construction works are expected to be completed in 2018. An overview of the current locks in given in table 3.2.

Table 3.2: Dimensions of lock chambers in the lock system

Complex	Lock chamber	Length [m]	Width [m]	Depth [m]	Height difference [m]
Limmel	Lock chamber 1	136	16	5	min: 0, max: 2
	Lock chamber 2	136	16	5	min: 0, max: 2
Born	East	136	16	5	11.35
	Middle	225	16	5	11.35
	Old	136	16	5	11.35
Maasbracht	East	225	16	4.1	11.85
	Middle	142	16	4.1	11.85
	West	142	16	4.1	11.85

The Juliana Canal is currently being upgraded from a CEMT class Va to a CEMT class Vb. These works are performed from the banks of the canal and from pontoons. One of the pontoons is the Mattedoor, see figure 3.6. The Mattedoor is a pontoon with a crane mounted on top, which can move over the width of the pontoon. A bentonite mat is picked up by the crane and put tightly at the junction of sheet pile and bottom and then rolled over the bottom of the canal. This is a delicate job, where external flow fluctuations can cause major problems for the construction process. If the mat is not placed on the right spot, or correctly attachment to the sheet pile and the previous mat is not watertight, a leak can occur in the canal. It is a sensible job as well, if currents under the pontoon are too high, the mat can flip over, making it useless. After the mat is placed on the bottom, a first protection layer is deposited on top of the mat to secure the stability during construction.

Figure 3.6: Construction pontoon the Mattedoor

The translation waves in a canal can be induced by emptying and filling of the lock chamber. A large volume of water is extracted from the upstream side of the canal in a relatively short time period when the lock is filling. This causes a negative translation wave. When the lock emptying, a large volume of water is deposited in the downstream side of the lock resulting in a positive translation wave. This process is known, but the

magnitude of the water level change due to translation waves is under debate. The amplitude of translation waves of 15cm are to be expected in the Juliana Canal according to Rijkswaterstaat (Rijkswaterstaat, 2012 [5]).

3.2. FUNCTIONAL CONDITIONS OF THE LOCKS

There are 3 lock complexes situated in the Juliana Canal lock system. The lock complexes near the villages of Limmel and Born are located within the geographical boundary conditions and will be elaborated upon.

Lock complex at Born: The lock complex near the village of Born consists of 3 locks. The dimensions of the lock chambers are given in table 3.2. The frequency of filling and emptying each chamber is given in table 3.3.

Table 3.3: Filling and emptying per lock, numbers of 2014 and 2015 (Rijkswaterstaat, 2016 [12])

Name lock	2014		2015	
	With ships	Without ships	With ships	Without ships
East	8742	2326	7328	2035
Middle	3795	909	6452	1653
Old	4966	1301	3322	915

The volume of water which flows through the lock gates depends on the ships in the lock. The flow velocities depend on the volume, the difference in water level and the outflow area. These data has to be collected.

Lock complex near the village of Limmel:
The lock complex near the village of Limmel is only in use at high Maas discharges, if the discharge is higher than 1280 m^3/s, measured at Borgharen. In other situations, the locks are open. The lock complex near Limmel consists of two lock chambers, each with a width of 16 meters and a length of 136 meters.
In figure 3.7 an overview is given of the discharges of the Maas of the past 5 years. In orange is the limit discharge of $Q = 1280 m^3/s$ drawn. The lock system is used a few times in the past 5 years, about once every year but sometimes a year not at all. When the discharge is high it occasionally lasts for about a week.

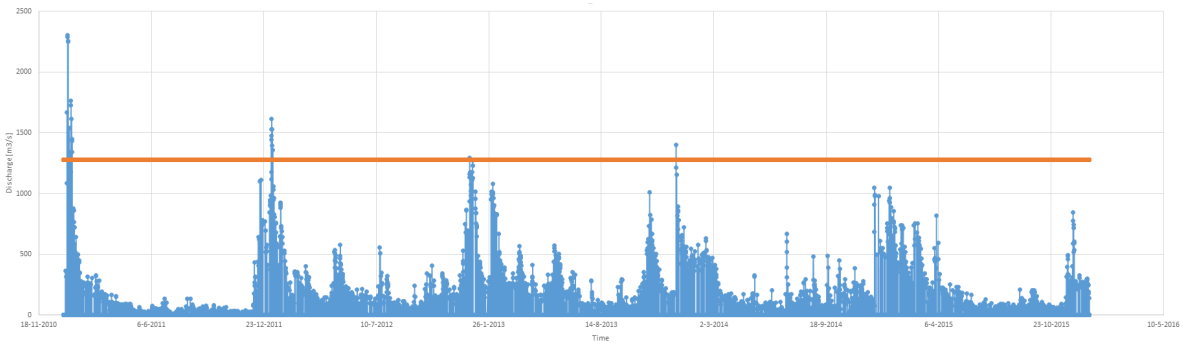

Figure 3.7: The discharges measured at Eisden, from 2011 untill 2015

The lock complex near the village of Limmel is going to be replaced by a flood gate. The construction works start in 2015 and will be finished in 2018. The sluice will be 50 meters wide, which is wider than in the current situation, making it easier to pass for vessels of the higher CEMT class Vb. Another positive effect could be that the increase of flow velocities creating a decrease of the water level due to the narrowing of the canal by the construction will decrease.

3.3. DEFINING LIMIT STATE AND DOWNTIME

In the model the water level changes are calculated first. The currents are calculated with the water level changes, wave celerity, water depth and the correction factor for the construction equipment. To establish the relation between the current and downtime, the benchmark up till which current the construction equipment is still capable to continue construction works is determined. Several processes have been evaluated to see

which process results in the decisive limit states. First calculations had been made to see whether the water-borne equipment will start to move. This is not the case in the range of magnitude of the currents that occur due to translation waves. This is further explained in Appendix C.
The construction works, such as the placed bentonite mats and first protection layer, have to be inspected by divers. This is the second process calculated. A benchmark for this criterion has been set according to the "Regulations on working conditions in hydraulic engineering" ([13]). In the regulations is defined that inspection divers can work without a diver on stand-by up to a current of 0.5 knots, about $0.3 m/s$. This has been set a limit state for the maximum allowable current for the construction pontoon to continue working. The base current in the canal to compensate for extracted water volumes is measured with an ADCP (Acoustic Doppler Current Profiler) and determined at $u_{base} = 0.17 m/s$. This can be seen in figure 3.8.

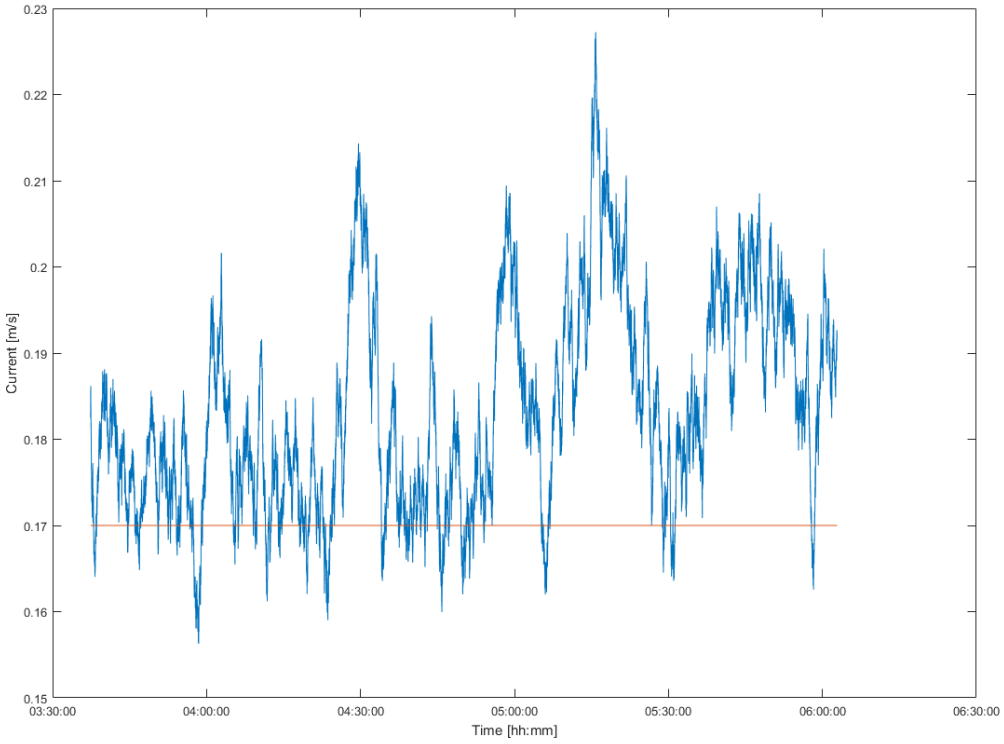

Figure 3.8: Base current in the Juliana Canal under the pontoon

The maximum allowable current in the situation in the Juliana Canal is in both directions $u_{max} = \pm 0.30$ m/s. The base current flows from south to north and is determined at $u_{base} = 0.17$ m/s. The maximum allowable current due to translation waves in the direction of lock Born, can be calculated as $u_{trans} = u_{total} - u_{base} = 0.13 m/s$.
The maximum allowable current due to translation waves with base current included is $u_{trans} = u_{total} - u_{base} = +0.30 - (-0.17) = +0.47 m/s$. In the situation that the Maas encounters discharges larger than $Q_{Maas} = 1280 m^3/s$ the lock complex at Limmel will close. There will no longer be a base current. The upper limit for translation waves in a situation without base current is $u_{trans} = 0.3 m/s$. This is a conservative value and will be implemented in the model.

4

THE TRANSLATION WAVE MODEL

The translation waves are calculated and modelled to determine the water level changes and currents which impact on the construction equipment. In this chapter the translation wave model is explained. The input parameters, methods and build up of the model are elaborated upon.
There was an alternative method available, a Delft3D model created by Deltares and calibrated by DEME group. Still the choice had been made to make a 1D model for several reasons:

- Apply the theory and understand the simplifications that are made and the impact of these simplifications
- To acquire more insight how the system works and its sensitivity to adaptations
- Acquire the knowledge how and which components and parameters can be adapted to modify the system to create a workable situation for the construction works

4.1. APPROACH

Generally the frequencies and amplitudes related to waves impacting structures are calculated with a spectral analysis and expressed in a wave spectrum. The theory of spectral analysis is explained in appendix D. This method was applied on the available data but had to be concluded that this is not applicable in this canal, with these waves. The waves from one translation wave keep travelling back and forth, with different water level changes and currents due to reflections. The locks fill and empty often due to the intensity on the canal, resulting in multiple translations waves with a lot reflections, on random intervals as a result of the human decision when to empty and fill the lock. On top of this are the waves caused by shipping. The result is a canal full of random waves where a spectral analysis cannot give any reliable results. The research to apply this method and the results are presented in Appendix B.
Another method can be used to determine the water level changes and currents in the canal, the method of characteristics. How this method is used and applied in the model is explained in this chapter, theoretical background is elaborated on in chapter 2. The approach can roughly be divided in 7 step:

1 Determine the characteristic terms and reflection location
2 Simplify wave as a pulse to determine the water level changes over the canal of 1 wave
3 Calculate the real shape of a translation wave, divide this wave in pulses of 1 second
4 Calculate for each pulse the water level change and time on pre-set locations
5 Add pulses on a location to result in a graph of amplitudes over time
6 Calibration of the model
7 Calculating waves to currents

These steps are visualized in the figure below, figure 4.1. The figures are discussed later in this chapter.

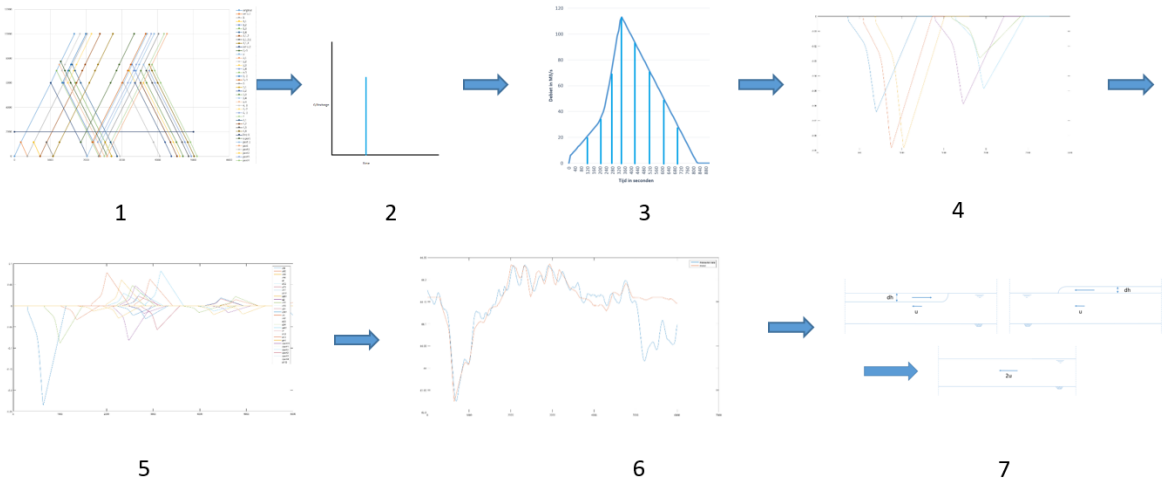

Figure 4.1: Steps to be taken to model the translation waves

To get results for the steps, several side steps have to be taken to get the model running. This is done according to the following steps: First the existence of translation waves in the Juliana Canal is demonstrated. Then an elaboration on how the celerity of the wave in the canal is calculated is given. The next input for the eventual model is the primary translation wave. This wave is derived from the discharge to empty and fill the lock. The beta's and amplification factors are calculated. Finally, these parameters are imported in a Matlab model which is based on the theory of the method of characteristics. An extension on the basic method of characteristics is that the shape of the wave is now implemented into the model as well. Since the wave has a long period, between 10 and 15 minutes, the total shape of the wave has a large impact when reflections are included.

4.2. DETERMINE THE EXISTENCE OF TRANSLATION WAVES IN THE JULIANA CANAL

Observations by the contractor have been made of translation waves with a water level change of 30cm in the Juliana Canal. For research purposes it needs to be established by measurements. High frequency pressure mats are placed in the Juliana Canal. These mats measure the water depths in the canal. The locations of the pressure mats are given in figure A.7 in appendix A. From these measurements, a first indication of the propagation of the translation waves can be abstracted, this is graphically visualized in figure 4.2. At Born, the lock system extracts a large volume of water, resulting in a lowering of the water level. At Obbicht the same shape is observed in the measurements about 1.5 minutes later. Berg aan de Maas is located 4km upstream of Born, the translation wave arrives about 4 minutes later than it started at Born. Finally, the wave arrives at Stein as well. The lines in figure 4.2 indicate the lowering of the water level due to the translation wave. The dotted lines indicate the propagation of the translation wave.

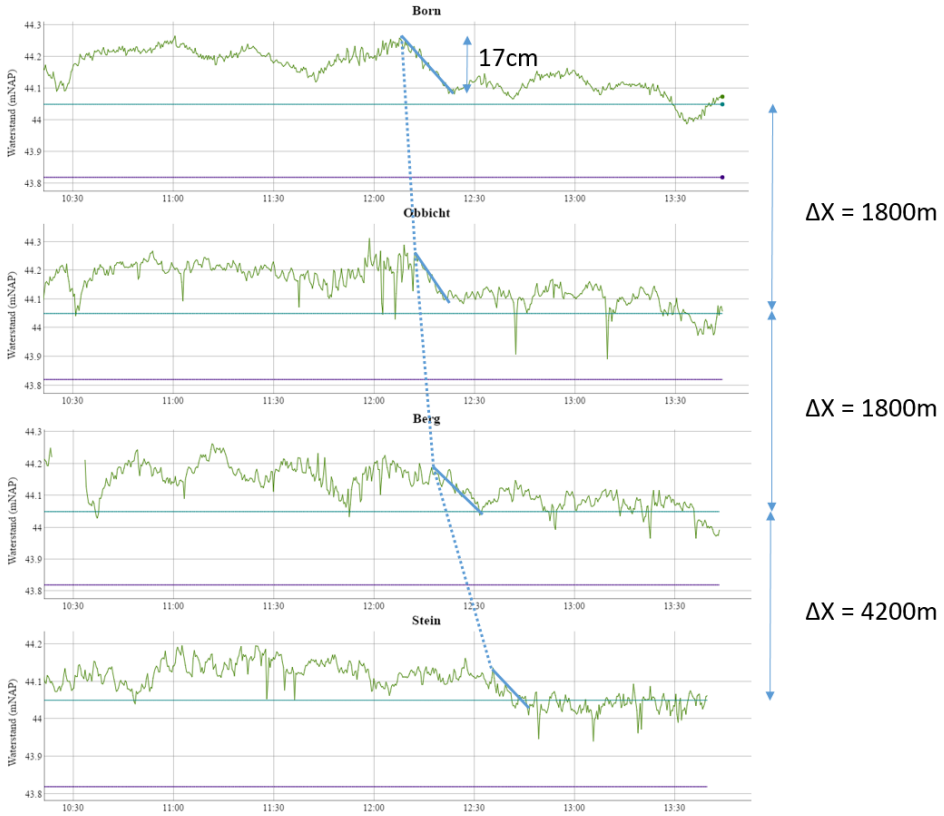

Figure 4.2: Translation wave propagating in the canal, at 4 locations

4.3. PROPAGATION CELERITY OF WAVE

The celerity of the waves propagation through the canal is calculated according to the theory of Thijsse [2] and the expansion on this theory by Dietz [3]. The formula which is used is:

$$c = \sqrt{gh}\left\{1 + \left(1 - \frac{2\tau h}{3b}\right)\frac{3}{2}\eta - \frac{g\sqrt{gh}}{2C^2 h}\left(\int A\,dt + B\frac{dt}{d\eta}\right)\right\} \tag{4.1}$$

An elaboration on the derivation and further understanding of the formula has already been given in Chapter 2 and in the research report of Thijsse (Thijsse,1935).

Three main components can be distinguished in formula 4.1. First, the driving celerity, known from the shallow water equations. Second, an added or negative celerity for the higher or lower depth due to a passing wave, corrected for a trapezium cross-section. The correction for the shape of the cross section is given in the symbol τ and defined as the tangent between the berm and the bottom. The value for τ is estimated to be $\tau = tan(30)$ Final term is a resistance term for bottom friction. All these terms depend either on the depth or on the width of the canal. The change of the water level is highly influenced by the width as well.
A schematisation is made to decrease calculation time and to keep the overview of the situation. More detail in the schematization gives a more accurate model, with a higher resolution. Smaller reflections can then be included. This will give more transition points and more reflections which will increase the calculation time. It is a trade-off between resolution and calculation time. The schematisation used in this model is given in figure 4.3. In the calibration has been proven that the resolution of the schematization for this system is high enough.

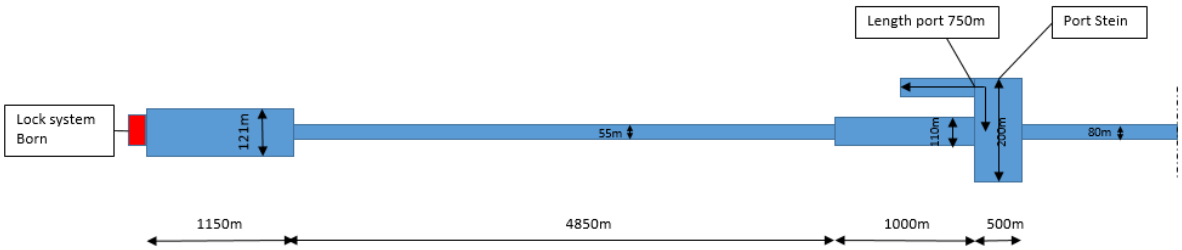

Figure 4.3: Schematisation of the system as modelled

Due to the changes in depth, the value for the Chezy coefficient should change as well. The equation of Manning is used to comprehend with these changes, the formula is given in 4.2

$$C = \frac{1}{n} R^{\frac{1}{6}} \tag{4.2}$$

In which n in the Manning roughness coefficient, estimated at $n = 0.03$(www.engineeringtoolbox.com, www.fsl.orst.edu). R is the hydraulic radius, dependent on the width and depth in the canal. This results in Chezy coefficients between 41 and 43,5 $m^{\frac{1}{2}}/s$. These formulae are programmed, the results can be seen in the figure below, figure 4.4

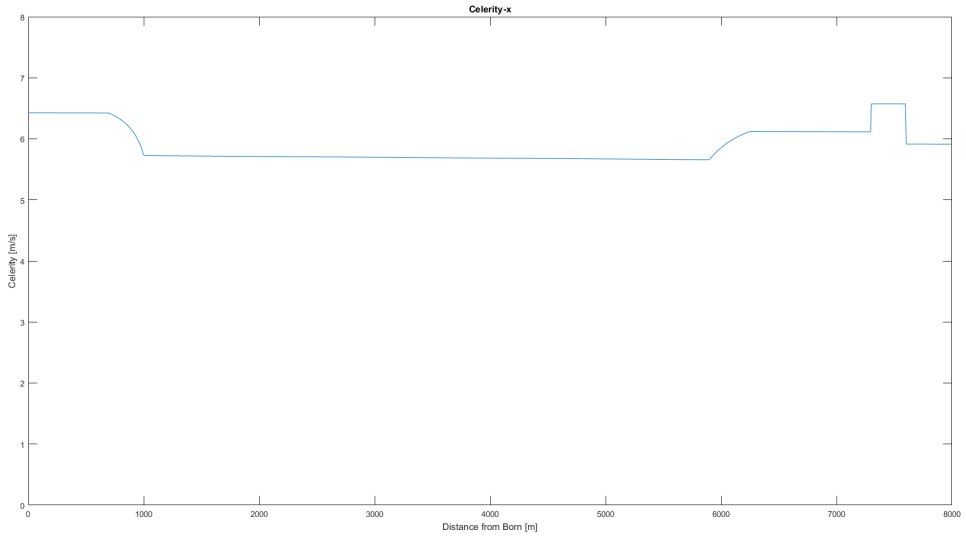

Figure 4.4: Development of the celerity of the wave in the canal

In this figure, an initial wave height of $h = -0,15m$ is assumed. The wave height increases at $x = 1000$ meaning in this situation, with a negative wave, that the water depth decreases further than at the start of the wave. As a result, the celerity of the wave decreases as well. When the canal widens again, near the port of Stein, the height of the wave decreases, resulting in a higher water level and a higher celerity. The celerity of the wave near the lock is $6.4m/s$. After the narrowing, the celerity drops to $5.8m/s$ and due to resistance decreases to about $5.7m/s$ at the end of the narrowing. At the beginning of the port, the celerity increases again to $6m/s$, increases even further at the port entrance and reduces again after the next narrowing to $5.9m/s$. These calculations are done according to Thijsse and Dietz. Reflections are not included in this calculation.

4.4. DISCHARGE LOCK

The discharge into the lock creates the translation wave in the canal. Water flows through the valves to the culverts and into the lock chamber. There are two culverts per chamber available. The discharge to the lock chamber depends on how much the valves are opened and how many valves/culverts are used. Measurements at the lock-operator are done to determine the percentage of opening of the valve. This is done calibrate the discharge into the chamber and create a model in which the discharge through the valves is calculated. If the discharge through the valves is high, the emptying and filling of the lock will create a steeper and larger wave in the canal.
The discharge to the lock chamber and thereby the discharge from the canal has been modelled in Mathcad, taking into account the number of locks, number of culverts, height difference and velocity at which the valve is opened. The results of the discharge at the Middle lock chamber at full capacity and and half capacity are shown in 4.5. The discharges at the East lock chamber are given in 4.6.

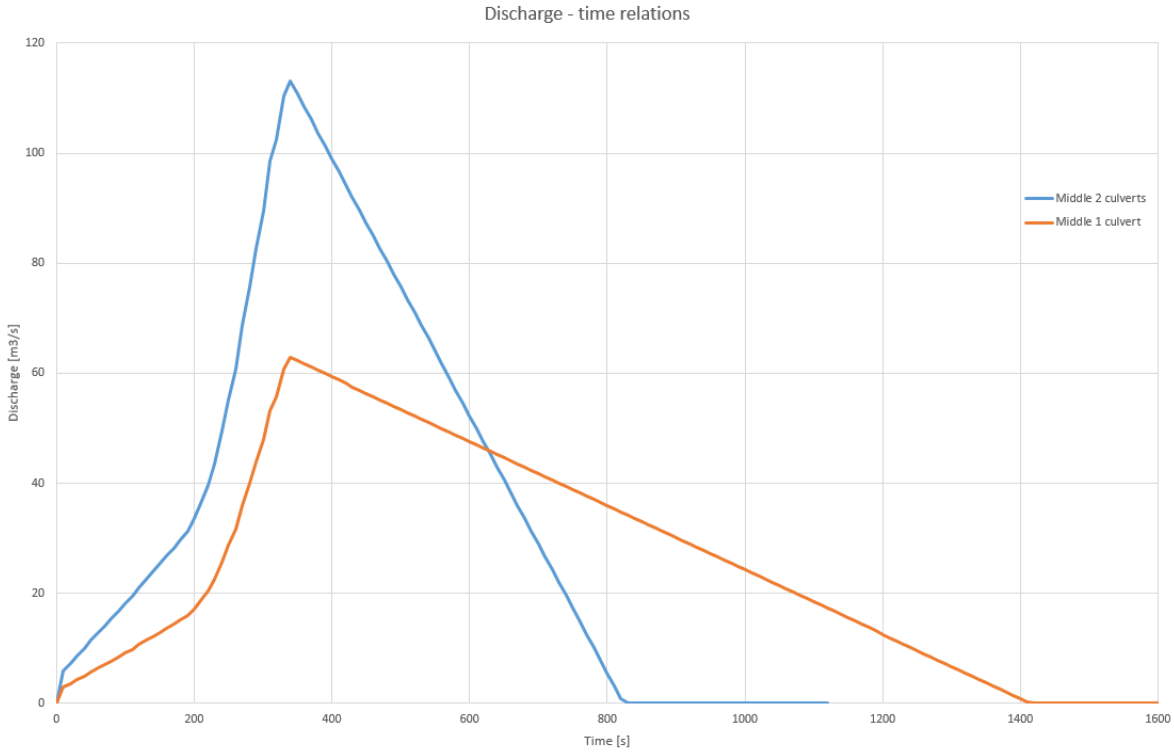

Figure 4.5: Discharges over time at Middle chamber with 1 or 2 culverts

The total volume is in both cases $40,860 m^3$. The maximum discharge is $113 m^3/s$ with 2 culverts open. This is the combined discharge of the culverts. The maximum discharge with only one culvert open is $63 m^3/s$. The maxima occur both at $t = 340 s$, this originates from the input parameters obtained from the lock-operator. Total duration to fill the chamber is 830s with both culverts in use and 1420s with only one culvert.

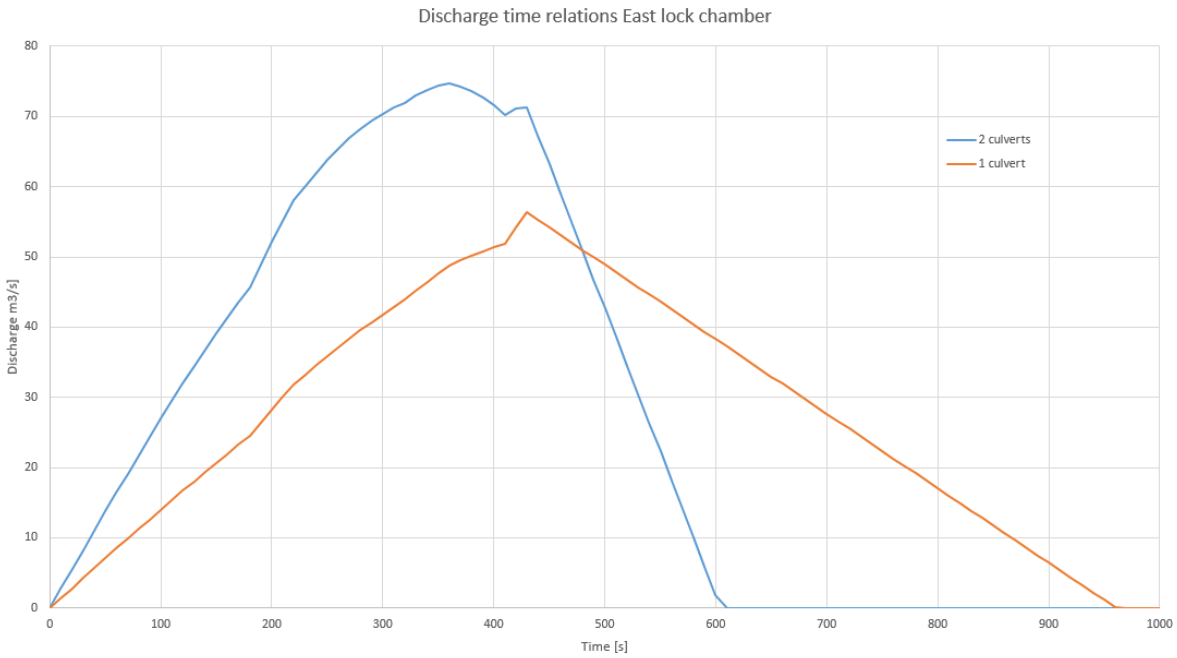

Figure 4.6: Discharges over time at East chamber with 1 or 2 culverts

4.5. REFLECTIONS AND BETA'S

In the model reflections are taken into account. The height of the reflected wave is determined and calculated using beta's from the theory of Thijsse. Reflections of which the first reflections are 20% of the original wave or more are implemented in the model, 42 reflections are implemented, so 43 waves in total. An overview of the waves implemented in the model is given in figure 4.7.

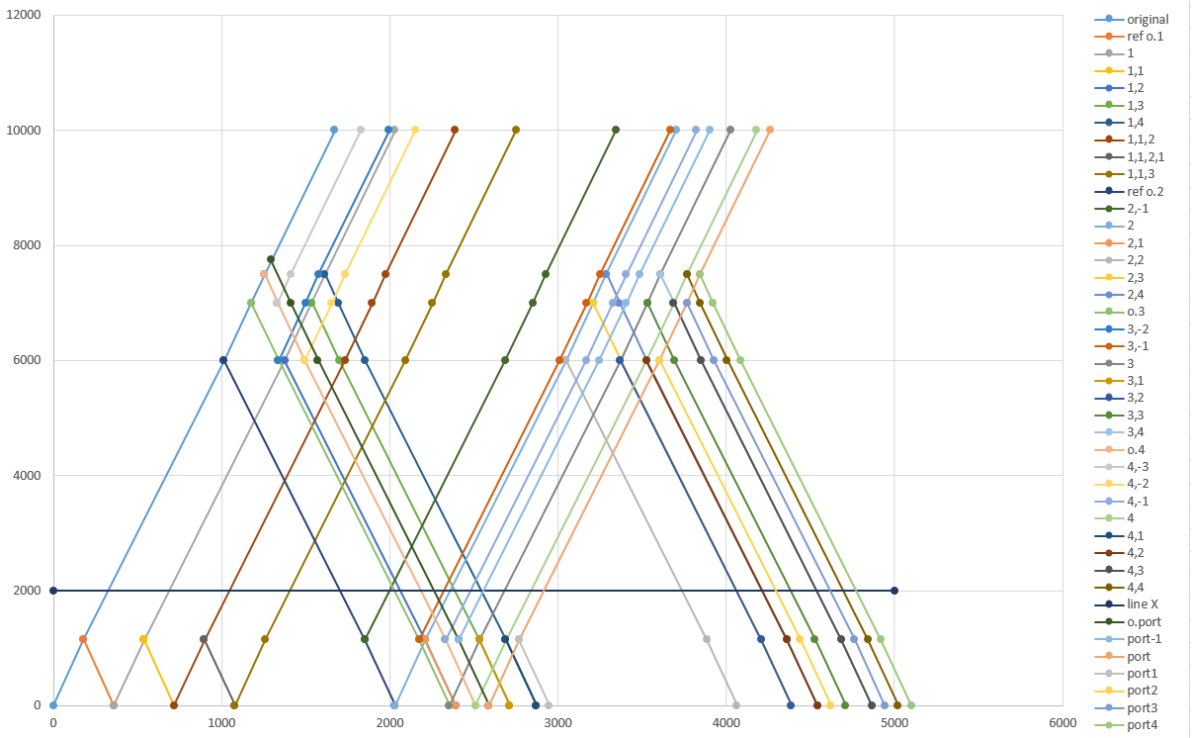

Figure 4.7: Primairy wave with 43 reflections in S-t diagram

Figure 4.7 is a S-t diagram, distance from the lock over time. It should be noted that this is a schematisation, the locations over time describe the arrival of the wave at that location. This is the pulse, as described in step 2 of the approach. In figure 4.7 the primary wave starts at $t = 0$ and $S = 0$, the wave is generated by the lock and should start at $S = 0$. The dots represent the changes in bathymetry, these are also the locations where reflections arise. The waves are numbered according to the reflection location and the reflection at the lock. So the "0.1" wave in the figure is the wave from the first reflection point of the "original" wave. Wave "1.1" is the first reflection of the first wave that has reflected already and so on. At every transition point a beta was calculated. A part of the wave before a transition point continues in the same direction, a part reflects. The amount that continues or reflects can be expressed as an percentage of the original wave. An overview of these percentages of the original wave is given in figure 4.8.

	wave number	beta 0		beta 1		beta 2		beta 3		beta 4		
location		A	>	B	<	C	<	D	>	E		F
original wave	0	1	1,000	→	1,375	→	0,917	→	0,651	→	0,929	→
First reflection B	o.1		0,375	←								
	1		0,375	→	0,516	→	0,344	→	0,244	→	0,349	→
	1,1		0,141	←		↓		↓		↓		
	1,2		-0,107	←	-0,172	←		↓		↓		
	1,3		-0,083	←	-0,133	←	-0,100	←		↓		
	1,4		0,112	←	0,180	←	0,135	←	0,105	←		
	1,1,2		0,141	→	0,193	→	0,129	→	0,091	→	0,131	→
	1,1,2,1		0,053	←								
	1,1,3		0,053	→	0,073	→	0,048	→	0,034	→	0,049	→
	1,1,3,1		0,020	←								
	1,1,4		0,020	→	0,027	→	0,018	→	0,013	→	0,018	→
First reflection C	0.2		-0,286	←	-0,458							
	2,-1		↓		0,172	→	0,115	→	0,081	→	0,116	→
	2		-0,201	→	-0,276	→	-0,184	→	-0,130	→	-0,186	→
	2,1		-0,075	←		↓		↓		↓		
	2,2		0,057	←	0,092	←		↓		↓		
	2,3		0,044	←	0,071	←	0,053	←		↓		
	2,4		-0,060	←	-0,096	←	-0,072	←	-0,056	←		
First reflection D	0.3		-0,222	←	-0,355	←	-0,266					
	3.-2		↓		↓		-0,089		-0,063	→	-0,090	→
	3.-1		↓		0,133	→	0,089	→	0,063	→	0,090	→
	3.0		-0,266	→	-0,366	→	-0,244	→	-0,173	→	-0,247	→
	3,1		-0,100	←		↓		↓		↓		
	3,2		0,076	←	0,122	←		↓		↓		
	3,3		0,059	←	0,094	←	0,071	←		↓		
	3,4		-0,080	←	-0,128	←	-0,096	←	-0,074	←		
First reflection E	0.4		0,300	←	0,480	←	0,360	←	0,279			
	4,-3		↓		↓		↓		0,081	→	0,116	→
	4,-2		↓		↓		0,120	→	0,085	→	0,122	→
	4,-1		↓		-0,180	→	-0,120	→	-0,085	→	-0,122	→
	4		0,240	→	0,330	→	0,220	→	0,156	→	0,223	→
	4,1		0,090	←		↓		↓		↓		
	4,2		-0,069	←	-0,110	←		↓		↓		
	4,3		-0,053	←	-0,085	←	-0,064	←		↓		
	4,4		0,072	←	0,115	←	0,086	←	0,067	←		
First reflection P	o.port		-0,175	←	-0,280	←	-0,210		-0,163			
	port,-1				0,105	→	0,070	→	0,050	→	0,071	→
	port		-0,350	→	-0,481	→	-0,321	→	-0,228	→	-0,325	→
	port1		-0,131	←		↓		↓		↓		
	port2		0,100	←	0,160	←		↓		↓		
	port3		0,078	←	0,124	←	0,093	←		↓		
	port4		-0,105	←	-0,168	←	-0,126	←	-0,098	←		

Figure 4.8: Amplificationfactors as percentage of the original wave

In figure 4.8 the green sections are waves travelling from north to south, so away from the lock system. The blue sections travel towards the lock. Positive numbers are waves with the amplitude in the same direction as the original wave. In the Juliana Canal case water is extracted from the canal, lowering the water level which result in a negative wave. So the original wave is negative, a positive number in the table represents a lowering of the water level.

4.6. PROPAGATION OF THE WAVE AT LOCATION X

In the Matlab model all previous described sections come together. In the model, the water level change at each point, extracted from the lock-discharge model, is calculated at which time it arrives at the transition points. When the amplitudes and time of each point of the wave is known, it can be calculated by interpolation at which time each point of the wave arrives at a defined point X, assuming a constant celerity at that section. In this model the section between the first narrowing and widening afterwards has been chosen, this is section $X = 1150$ till $X = 6000$ measured from the lock system at Born. This is the section where the difficulties with the translation waves occurred, according to the contractor. When the water level change of each wave are calculated, the waves are summed at a location. This results in a pattern of the water level changes of the wave at that location over time. The lowest water level is, as expected, a result of the emptying and filling of the lock, the primary wave. The origin of the other fluctuations in water level are visualised in figure 4.9.

N.B. the water level changes and currents induced by translation waves are location dependent. It is determined by the interaction between primary waves and reflection waves. Where the waves meet depends on the propagation direction and distance to transition points and is unique per location. Interpolation of the level of water level changes and magnitude of currents between locations is not possible. Interpolation of downtime periods between locations neither.

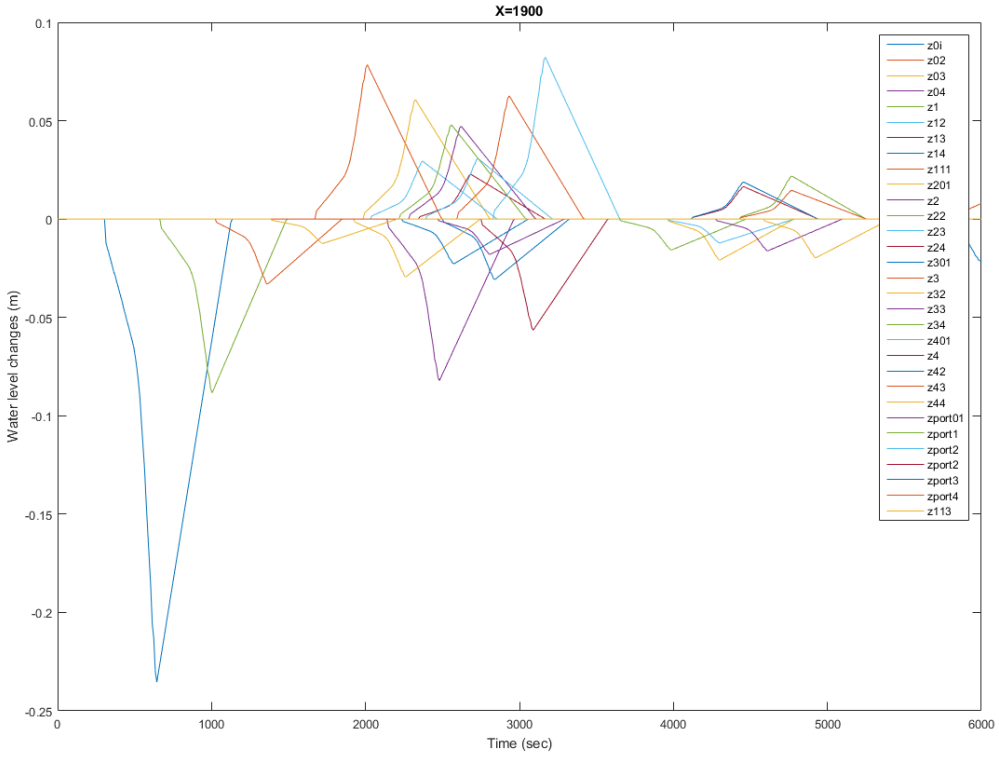

Figure 4.9: Individual waves at X=1900

4.6.1. CALIBRATION OF THE MODEL

The framework of the model has been set, next step is to calibrate the model to measurements. The calibration has to be done by comparing the model result with measurement where only translation waves disrupt the water levels. Measurement where done at night when there is no shipping. Normally the locks are not operational at night because there is no shipping but for these measurements the lock chambers where filled purely for the measurement. This results in fairly clean measurement to which the model is calibrated. The model is calibrated to a wave measured on the 21 of May with the high frequency pressure mat near Obbicht. The time interval of the calibration section is from 9:36 till 11:16, from visual analysis of the data this timeslot

represents a relatively unaffected translation wave. The location of Obbicht has been measured in Google Earth and is determined to be at $X = 1900m$.
The beginning, till about 2000s, of the modelled translation wave follows the measured line well. After $t = 2000$ the model deviates more from the measurement. The locations of the peaks are in most situations at the right time but there are minor differences in water level change. There is still a discrepancy between $t = 3400$ and $t = 4300$. This is most likely to be due to a small narrowing after the bend at Stein, where the highway crosses the canal. The difference between the measurement and model is at maximum 2cm and is not further investigated nor implemented in the model. After $t = 5000$ the water level drops significantly. This is assumed to be another wave and is not taken into account in this model. The maximum and minimum values match well and are accurate enough for first predictions.

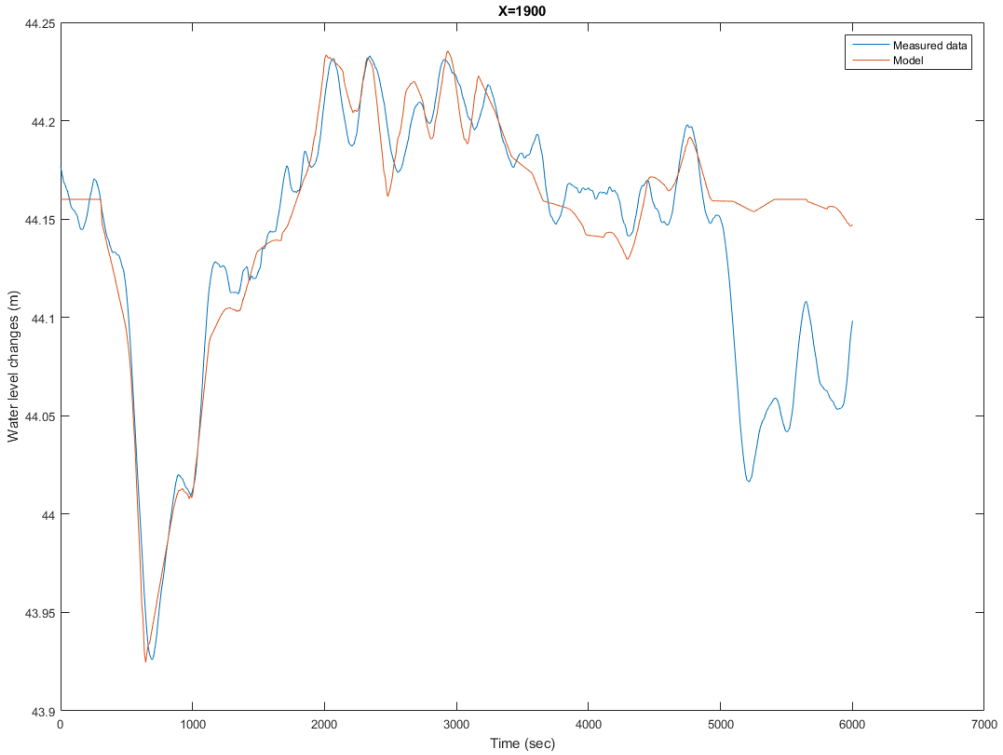

Figure 4.10: Model compared to measurement after calibration

The normal, unaffected, water level has been set at 44.16m +NAP. The translation wave created at the lock has a maximum water level change of 17cm near the lock. At X = 1900, the primary wave has a decrease of the water level of 23cm, resulting in a lowest water level of 43.93m +NAP. Due to reflections the water level rises above the normal water level, with a maximum water level of 44.24m +NAP. This is an increase of the water level of 8cm above normal water level.

The changes between the model and measurement are calculated and are presented in figure 4.11. The occurrences of the differences are plotted against the differences. A normal distribution can be made of the graph, this is presented in figure 4.12. The mean value μ and standard deviation σ are calculated, $\mu = 0.0050$ and $\sigma = 0.0136$. This means the average deviation of the model is only 5mm. A 95% confidence interval of the deviation of the model is calculated and determined to be between -0.0217m and 0.0317m.

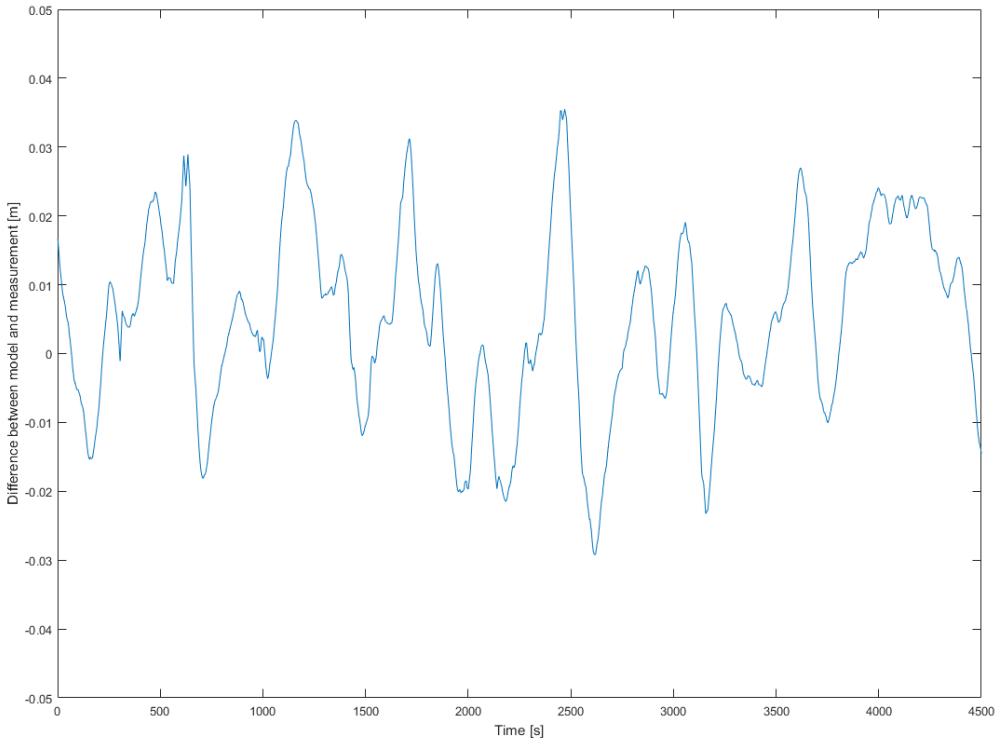

Figure 4.11: Differences between model compared to measurement after calibration

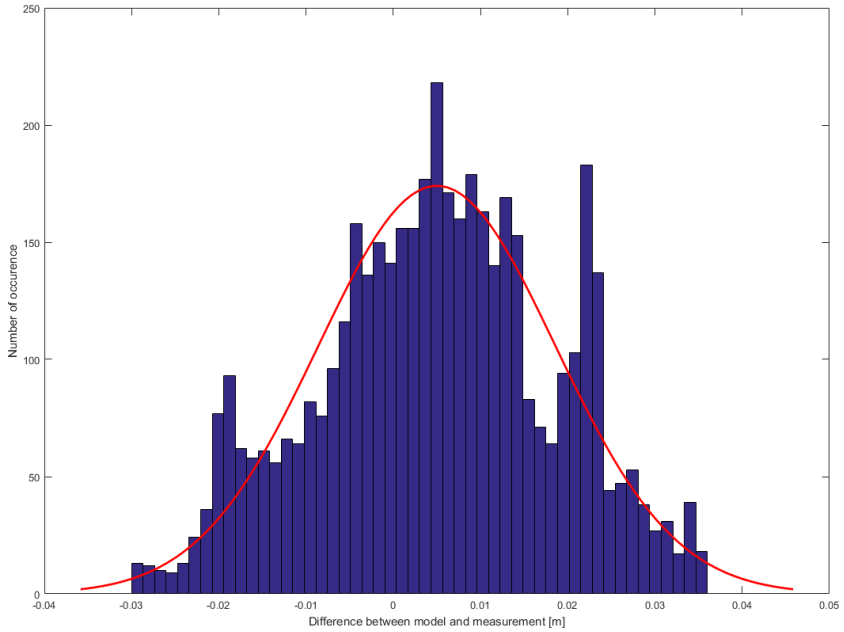

Figure 4.12: Normal distribution over the difference between the model and measurements

TWO WAVES

The extreme values resulting from one wave are -23cm and +8cm relative to the normal water level. When two waves behind each other arise due to the regime of the lock-operator the two waves and its reflections can interfere. The results of a situation with the same wave as in the section above but with a second identical wave five minutes behind the first wave are given in figure 4.13. The wave created near the lock has still a water level change of 17cm. At X=2000 the minimum water level is the same as with one wave but the difference is the maximum water level. Where the maximum value with one wave was +8cm, the maximum is more than +10cm with two waves. In figure 4.13 the time in between the two translation waves is 5 minutes. In the scenarios in the next chapter, multiple time intervals between sequel waves will be investigated.

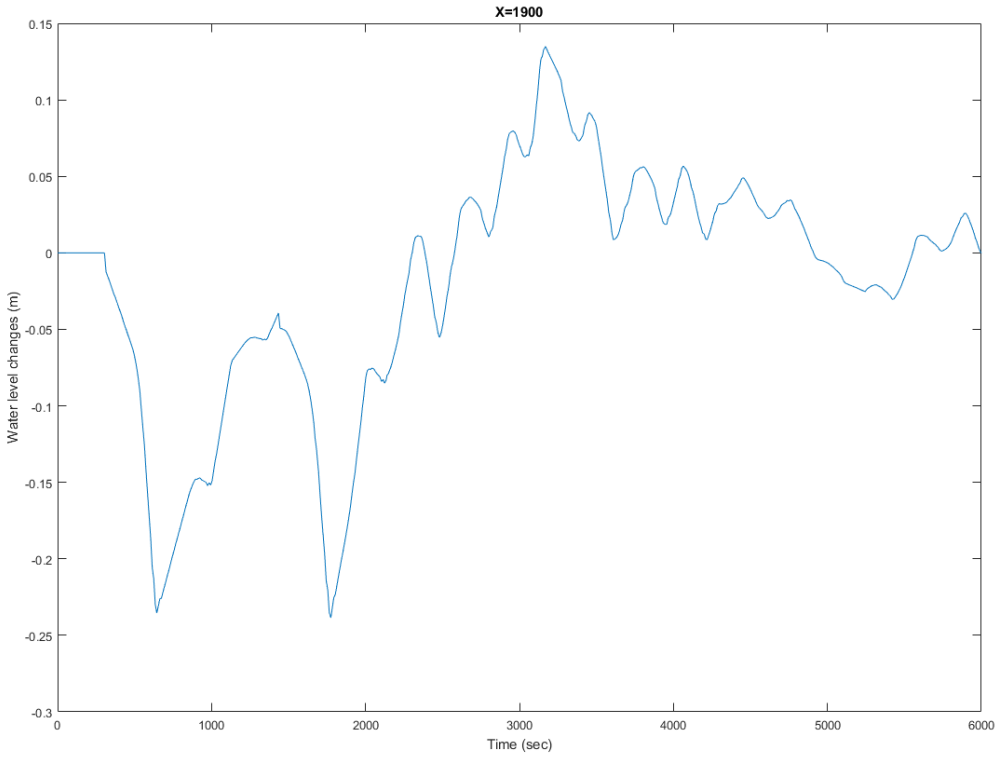

Figure 4.13: Two identical waves with 5 minutes in between, at X=1900

4.7. CALCULATING FROM WAVE HEIGHT TO CURRENT

In the model the water level changes are calculated first. The currents are calculated using the water level changes, the wave celerity and the water depth. The water depth is taken constant at $h = 5m$. The wave celerities are calculated as is described in the literature in chapter 2 and adapted during the calibration. The current as a result of the translation wave is calculated with equation 4.3.

$$u = \frac{cz}{h} \tag{4.3}$$

This is the situation without the water-borne construction equipment. At the cross section where the construction equipment is located is assumed that the current will increase because less water surface area is available. The construction equipment is a blunt surface in the canal which will created turbulent flow. The turbulent flow is implemented in the model as an increase of the surface of the construction equipment. The increase of the surface area is assumed to be 10% of the pontoon surface. The wet surface of construction pontoon the "Mattedoor" is $28,24m^2$. In the model the local narrowing resulting from the pontoon is expressed as an increase factor relative to the canal cross section, given in equation 4.4. The canal cross section is simplified as a prismatic canal with depth h and width B.

$$f_p = \frac{A_{canal} - A_{pontoon} * 1.1}{A_{canal}} \tag{4.4}$$

With: f_p = correction factor for obstruction in canal
$A_{canal}[m^2]$ = surface area of canal section
$A_{pontoon}[m^2]$ = surface area of the construction equipment

To calculate the currents at the locations, including the local narrowing by the construction equipment, equations 4.3 and 4.4 are combined to equation 4.5:

$$u = \frac{1}{f_p}\frac{cz}{h} \tag{4.5}$$

The parameters used in equation 4.5 are given in table 4.1. The locations X = 1151, X = 4000 and X = 5900 are on the narrow canal section and have the same dimensions.

Table 4.1: Celerities of the waves per location

Location	celerity [m/s]	B [m]	f_p [-]
X = 0	6.4	121	0,949
X = 1151	6.0	55	0,887
X = 4000	6.0	55	0,887
X = 5900	6.0	55	0,887
X = 6001	6.4	110	0,944

5

MULTIPLE SCENARIOS

In this chapter different alternatives will be presented. To evaluate under which circumstances which currents arise under the pontoon, different scenarios are drafted. In the scenarios different currents result from different sources.

5.1. THE SCENARIOS

The scenarios can be divided in two main categories, according to the origin of the current:

1. Only due to the Middle chamber of the lock system Born
2. Due to the Middle chamber followed by filling of the East chamber

The Middle chamber is represented in every scenario. This chamber is the largest chamber of the lock complex near Born, creating the largest translation waves under normal conditions. The lock chamber is filling through culverts. There are two culverts at each chamber at the Born lock complex. To reduce the discharge extracted from the canal, only one culvert can be used as well. A theoretical example with 4 culverts has been modelled to find out what the consequences on the canal would be. The consequences on the currents when two lock chambers are filled simultaneously is investigated as well.
When the next emptying and filling cycle is commenced depends on the lock-keeper. Scenarios at different intervals are modelled, after 5 minutes, 10 minutes and 15 minutes. Reflections of waves can result in interference between the first and second wave. Different scenarios which result in different currents affecting the pontoon are presented in table 5.1. Further explanation on the different scenarios will be given below.

Table 5.1: Scenario's

Chamber	Middle			East						
Delay time				0 min	5 min		10 min		15 min	
Scenarios / # Culverts	1	2	4	2	1	2	1	2	1	2
Scenario 1: 1 wave, original situation		✓								
Scenario 2: 1 wave, slow filling	✓									
Scenario 3: 1 wave, fast filling			✓							
Scenario 4: 1 wave, simultaneous filling		✓		✓						
Scenario 5: Normal filling, second wave after 5 min		✓				✓				
Scenario 6: Normal filling, second wave after 10 min		✓						✓		
Scenario 7: Normal filling, second wave after 15 min		✓								✓
Scenario 8: Slow filling, second wave after 5 min	✓				✓					
Scenario 9: Slow filling, second wave after 10 min	✓						✓			
Scenario 10: Slow filling, second wave after 15 min	✓								✓	

Scenarios with combinations with return currents from passing vessels are excluded. Return currents of shipping creates too large currents on its own, investigating what the effects in combination with currents due to translation waves would be otiose. This can be seen in table 5.2, the currents are about three times as high as is assumed to be workable for the Mattedoor.

Table 5.2: Currents due to shipping (Arcadis, 2015 [14])

Class	Length [m]	Width [m]	Depth [m]	Return Current [m/s]	Propeller wash [m/s]
M8 loaded	185	11.45	3.5	1.18	0.65
M8 unloaded	185	11.45	0.9	0.92	0.00
M9 loaded	135	11.45	3.5	1.18	0.83
M9 unloaded	135	11.45	0.8	0.92	0.00

SCENARIO 1: CURRENT SITUATION

In this scenario the standard situation is analysed. Only the currents created by translation waves are taken into account. The translation waves are assumed to be created by the middle lock chamber as it is used without adaptations to the filling and emptying regime. In the standard situation the chamber is filled by two culverts. This scenario is the reference situation.

SCENARIO 2: ONE CULVERT

The middle lock chamber is filled only by one culvert, resulting in about double the time to fill the chamber. The expectation is that a lower translation wave will arise. If this is true, the currents will be lower as well. This scenario will determine the difference in currents between normal filling and slower filling which can be useful for future measures.

SCENARIO 3: FOUR CULVERTS

The lock chamber is filled by four culvert, resulting in about half the time to fill the chamber. The expectation is that higher translation wave will arise. This scenario is purely a theoretical scenario, there are not 4 culverts implemented in the construction of the lock chamber. In this scenario is examined how the system reacts under circumstances with higher waves to see what the effects is on the currents in the system.

SCENARIO 4: FILLING MIDDLE AND EAST LOCK SIMULTANEOUS

In this scenario the Middle lock chamber and East lock chamber are filled at the same time. This is a situation which under normal circumstances should never occur. During extreme shipping intensity someone might make the decision to speed up the process and use two lock simultaneously. The effects of extracting two discharges from the canal is investigated in this scenario.

SCENARIO 5: 2 CULVERTS, 5 MINUTES IN BETWEEN

In situations with high shipping intensity the different lock chambers can be used with minor time between filling the first and second lock chamber. In this scenario the middle chamber will be filled first, 5 minutes later the east chamber is filled. Both locks will use 2 culverts to fill, as is common. When multiple waves are raised interference can occur between the secondary wave and the reflections of the primary wave. In this scenario the results with 5 minutes between the primary and secondary wave are analysed.

SCENARIO 6: 2 CULVERTS, 10 MINUTES

In this scenario the same conditions are applied as in scenario 4, except the time between the primary and secondary wave is now 10 minutes. In this scenario the findings with a longer period in between are analysed.

SCENARIO 7: 2 CULVERTS, 15 MINUTES

In this scenario the same conditions are applied as in scenario 4, except the time between the primary and secondary wave is now 15 minutes. In this scenario the findings with an even longer period in between than in scenario 5 are analysed to see what the differences of longer time periods in between is on the interference.

SCENARIO 8: 1 CULVERTS, 5 MINUTES

In this scenario the middle chamber will be filled first, 5 minutes later the east chamber will begin to fill. Difference with scenario 4 is that in this scenario only 1 culvert is used per chamber to fill. The waves will be longer and lower, the reflection points are at the same locations. The interference between the primary and secondary waves will be different than in the previous three scenarios. This scenario is performed to obtain insight in the behaviour of the system when longer waves are imposed.

SCENARIO 9: 1 CULVERTS, 10 MINUTES

In this scenario the same conditions are applied as in scenario 7, except the time between the primary and secondary wave is now 10 minutes. In this scenario the findings with a longer period in between are analysed.

SCENARIO 10: 1 CULVERTS, 15 MINUTES

In this scenario the same conditions are applied as in scenario 7, except the time between the primary and secondary wave is now 15 minutes. In this scenario the findings with an even longer period in between than in scenario 5 are analysed to see what the differences of longer time periods in between is on the interference.

5.2. LOCATIONS OF INTEREST

Calculating and investigating all sections of the canal would be too time-consuming and would not enlarge insight on the behaviour of the system. Five locations have been chosen to functions as representative locations for the canal. These five locations give an overview of the development of the wave through the canal section from Born to Stein. The locations are given in the summation below as well in figure 5.1. The locations are expressed as distance relative to the lock system near Born.

1. X = 0m, close to lock system Born
2. X = 1150m, section on narrow canal just after narrowing
3. X = 4000m, straight section in canal
4. X = 5900m, section on narrow canal before widening to port Stein
5. X = 6001m, after widening from narrow canal to wide port section.

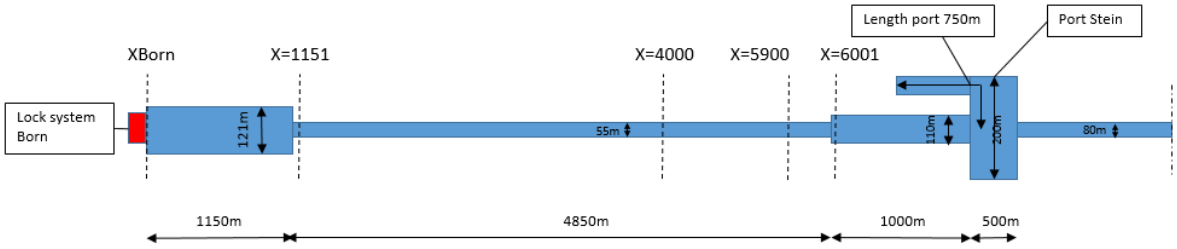

Figure 5.1: Overview of the schematized system, with calculation locations

The first section is close to the lock system near Born. This location is chosen to obtain more insight how the wave behaves at a closed boundary. Returning waves from other locations reflect at the boundary, resulting in large increases of the deviation of the water level. It is possible that reflected waves impact simultaneously with filling of the lock. This would lead to different wave heights.
The second location is at $X = 1150m$ from the lock complex near Born. The cross section changed from the wide section near the lock to the long, normal, canal cross section. Adaptations of the cross section result in reflection waves and changes in wave heights.
The third section is chosen at $X = 4000m$ from the lock complex. The largest reflection waves are expected to arise due to the port near Stein. At the location $X = 4000m$ the reflections of the port are expected to interact with a wave originating from a second filling of the lock, 10 minutes after the first filling. This, under the assumptions of both waves travelling at a wave celerity of $6m/s$.
The fourth section is at $X = 5900m$, the location on the narrow canal just before the widening to the wide port section of Stein. At the cross section adaptation new reflection waves arise. At this location the effects of these reflection waves on secondary waves can be observed.

The last location is situated at $X = 6001m$, just after the widening. The influence of changes in cross section between the narrow canal section and the wider section can be observed.

5.2.1. PARAMETERS TO OBTAIN AND COMPARE

To compare the results and to endorse the differences between a scenarios on different locations and differences on a locations between different scenarios the leading parameters have to be determined. These parameters have to be observed and compared. The to be compared parameters are:

1. z [m] = water level changes
2. z_{min}[m], minimum water level relative to h
3. z_{max}[m], maximum water level relative to d_0
4. u [m/s], current
5. u_{min} [m/s], minimum current
6. u_{max} [m/s], maximum current

To be able to compare differences in the water level, solely due to the translation waves, external factors are neglected and other parameters are kept constant. The constant parameters are:

1. h [m] = Water depth
2. A_{pon} [m^2] = Wet cross section pontoon
3. B [m] = Width at canal section
4. c [m/s] = Wave celerity
5. f_p [-] = Reduction factor of net water surface of the canal due to pontoon

6

RESULTS

In the previous chapter are the different scenarios specified. The locations at which the scenarios are calculated are determined as well. The results of the scenarios at different locations will be discussed in this chapter. The results can be divided in two sections:

- Scenarios with different discharges to fill a lock chamber. Scenarios 1 up till 4.
- Scenarios with different intervals between filling of the first and second lock chamber. Scenarios 5 up till 10.

The discharge relations of each scenario will be given since these are the driving factor of the translation waves. Of the scenarios with two waves, one scenario of each discharge is analysed. The results of the scenarios which are not addressed in this chapter are given in Appendix D. In each section results of the water level changes are given to obtain understanding of the magnitudes and reactions of the system to the induced waves. Then, the currents resulting from the waves are presented. The currents will be elaborated upon in extend since these are the critical parameter for downtime in water-borne construction equipment.
A small recap of the theory, how the currents are calculated from the water level changes is given below. Elaboration on the theory of translation waves is given in chapter 2 and appendix E.

The primary formula used for the calculation from water level change to current is:

$$u = \frac{1}{f_p}\frac{cz}{h} \tag{6.1}$$

In which:
u $[m/s]$ = Current
c $[m/s]$ = Wave celerity
z $[m/s]$ = Water level change
h $[m]$ = Water depth
f_p [-] = Reduction factor of net water surface of the canal due to the water-borne equipment

In formula 6.1 the direction of the current is taken equal to the positive or negative sign of the water level change. The propagation direction of the wave is not included. In the model the summation of the individual waves are taken to calculate the total water level and current. For the summation of the currents the propagation direction of the wave is highly important, this is visualized in figures 6.1 and 6.2. The adaptations of the water level changes can oppose the changes in current during interference between waves. This will stand out in the figures in this chapter.

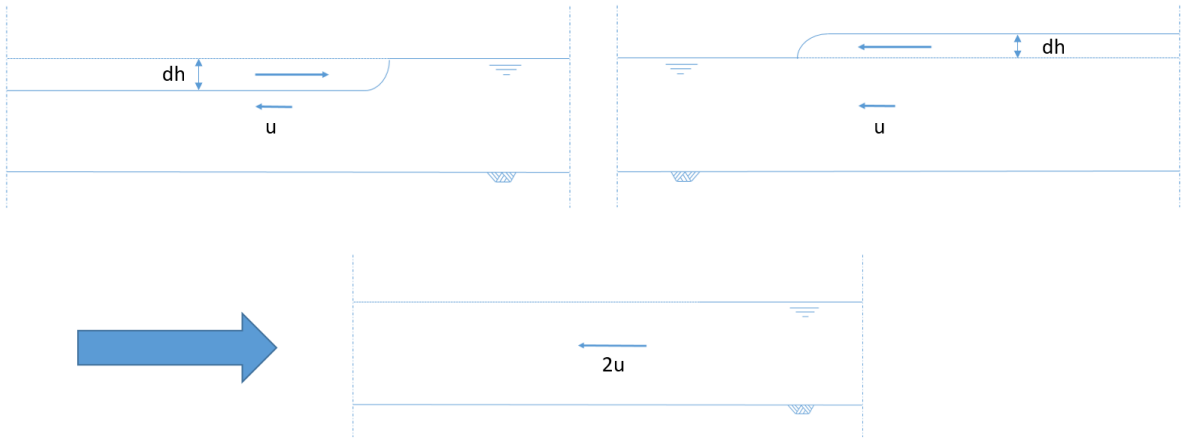

Figure 6.1: The resulting water level change and current when a negative and positive wave from opposite direction meet each other

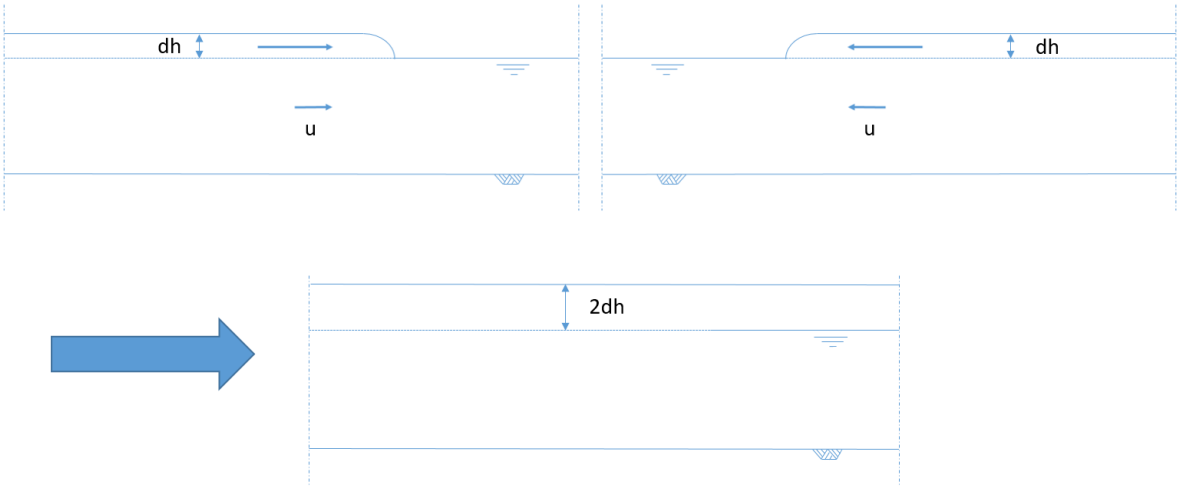

Figure 6.2: The resulting water level change and current when two positve waves from opposite directions meet each other

In the figures in this chapter are the currents away from lock system Born are taken positive. So negative currents are towards lock system Born. The locations are defined as distance from the lock system, towards the south is taken positive as well. The limit currents are defined as $u_{min} = -0.13\ m/s$ and $u_{max} = 0.3\ m/s$, as explained in chapter 2.

6.1. DIFFERENT DISCHARGES

The Middle lock chamber at lock complex Born is used to model different discharges. The translation waves are created using three different discharge-time relations. The discharge into the lock chamber can be varied in several ways, e.g. the valves to the culverts can be regulated, opening slower or faster or opening the valves not fully. Another way to adapt the discharge to the chamber is by regulating the number of culverts used. In present situation there are two culvert implemented in the system.

6.1.1. DISCHARGE-TIME RELATIONS

In this section scenarios 1, 2, 3 and 4 are handled. In these scenarios the discharge-time relations are varied by changing the number of culverts used to fill the lock chamber or the number of lock chambers filled. This is a realistic situation, implemented at the lock complex sometimes already. The first discharge-time relation, scenario 1, is the present situation. In this situation 2 culverts are used to fill the chamber. This is the scenario to which regulation measures can be compared to. Scenario 2 is the situation utilizing only one culvert. This will probably reduce the wave height and current in the canal. The third discharge-time relation, scenario 3, is based on a theoretical situation in which four culverts are applied. The final discharge-time relation is scenario 4. The Middle lock chamber and East lock chamber are filled simultaneous. The four discharge-time relations are visualized in figure 6.3.

1. Present discharge
2. Lower discharge
3. Higher discharge
4. Simultaneous discharges

Figure 6.3: The four modelled discharge-time relations

6.1.2. RESULTS WITH DIFFERENT DISCHARGES AT 5 LOCATIONS

The discharges as presented in figure 6.3 are implemented in the model as input. The results of the water level changes of two locations are given in figures 6.5 and 6.7. The differences between water level changes and currents due to interference with reflections can be seen between these figures and the figures of the currents. The currents resulting from the translation waves are presented in figures 6.4, 6.6, 6.8, 6.9 and 6.10. These figures show how the discharges evolve over time, at different locations in the Juliana Canal. The extreme values of the currents due to negative as well as positive translation waves are given in table 6.1, the downtime ($Dtime$ in the table) resulting from high currents are given in table 6.1 as well.
Scenarios 1 up till 3 will be analysed first, in these scenarios is one lock chamber filled. Hereafter is scenario 4 discussed and compared to scenario 1.
The difference in discharge between one culvert and two culverts is very large compared to the discharge difference between two culverts and four culverts. The difference between the maximum discharge with two culverts and one culvert is about $50 m^3/s$, between four culverts and two culverts the difference between the maximum discharges is only $14 m^3/s$. This is visible in the difference in maximum currents due to the translation waves created by the discharge to the lock chambers. The difference in currents between scenarios 1 and scenario 2 is $0.052 m/s$, while the difference between scenario 1 and scenario 3 is $0.027 m/s$. Even though the

discharge capacity doubles in scenario 3 compared to scenario 1, the maximum current does not increase that much. The head difference between the filling chamber and the water level of the canal becomes too small before the discharge in scenario 3 can reach its maximum discharge capacity.
The maximum discharge results in a peak for the currents. The other effect is the length or period of the translation wave. In all situations the same volume of water has to be transported into the lock chamber to fill it. For low discharges, the period and length of the translation wave will increase. This is visible in figure 6.3. The wave in scenario 2 is 1.7 times as long as scenario 1 and 2.8 times as long as scenario 3.
The moderate current difference between scenario 1 and 3 and the large difference between scenario 1 and 2 are also visible in the graphs of the currents at the five locations, figures 6.4 till 6.10, as well as the long and short lengths of the primary translation waves.
The long period of scenario 2 makes the water level changes and corresponding currents look smoother and more gentle. The relatively short period of scenario 3 result in sharper current changes. The different waves and reflections are more clearly visible in the graphs. The fluctuations around zero current are frequent and extremer as well, this is for instance noticeable in figure 6.9. The present situation, situation is in between the extremes of scenarios 2 and 3.
The wave length of the translation wave in scenario 4 is the same as the wave length of scenario 1. The interference with reflections will occur on the same moment. Difference between the first and fourth scenario is the magnitude of the discharge and with that the resulting water level change. The maximum discharge of scenario 4 is $185 m^3/s$ compared to $113 m^3/s$ in scenario 1. The maximum discharge results in a current of more than 0.5 m/s at location X1151 and X4000 and even currents of almost 0.7 m/s at location X5900.
About the first 1000 seconds, after arrival of the translation wave, is the influence of the discharge-time relation clearly visible. After that time, the influence of reflection waves become more influential. The magnitude of the reflection waves are a result of the discharge but the interval when reflections occur are determined by the bathymetry of the system. The sections where the discharge-time relations are clearly visible is also where the currents are highest and the most downtime occurs.

Table 6.1: Overview of extreme values and downtime at 5 locations

Scenario	Parameter	X_Born	X_1151	X_4000	X_5900	X_6001
Sc1	z_{min} [m]	-0,173	-0,235	-0,235	-0,170	-0,154
	z_{max} [m]	0,117	0,106	0,076	0,074	0,069
	u_{min} [m/s]	-0,231	-0,318	-0,318	-0,416	-0,217
	u_{max} [m/s]	0,065	0,082	0,132	0,168	0,156
	$Dtime$ [min:sec]	04:48	08:59	16:26	10:13	07:48
Sc2	z_{min} [m]	-0,135	-0,136	-0,133	-0,095	-0,086
	z_{max} [m]	0,082	0,079	0,039	0,042	0,034
	u_{min} [m/s]	-0,128	-0,184	-0,194	-0,278	-0,147
	u_{max} [m/s]	0,017	0,056	0,101	0,092	0,127
	$Dtime$ [min:sec]	00:00	10:15	18:24	02:08	16:07
Sc3	z_{min} [m]	-0,193	-0,266	-0,266	-0,180	-0,177
	z_{max} [m]	0,118	0,109	0,070	0,086	0,084
	u_{min} [m/s]	-0,261	-0,359	-0,359	-0,477	-0,246
	u_{max} [m/s]	0,073	0,124	0,138	0,171	0,175
	$Dtime$ [min:sec]	05:33	08:24	15:34	12:27	05:58
Sc4	z_{min} [m]	-0,285	-0,389	-0,389	-0,274	-0,253
	z_{max} [m]	0,167	0,152	0,104	0,112	0,117
	u_{min} [m/s]	-0,382	-0,527	-0,527	-0,703	-0,362
	u_{max} [m/s]	0,107	0,141	0,196	0,243	0,258
	$Dtime$ [min:sec]	07:18	12:03	22:10	17:48	10:36

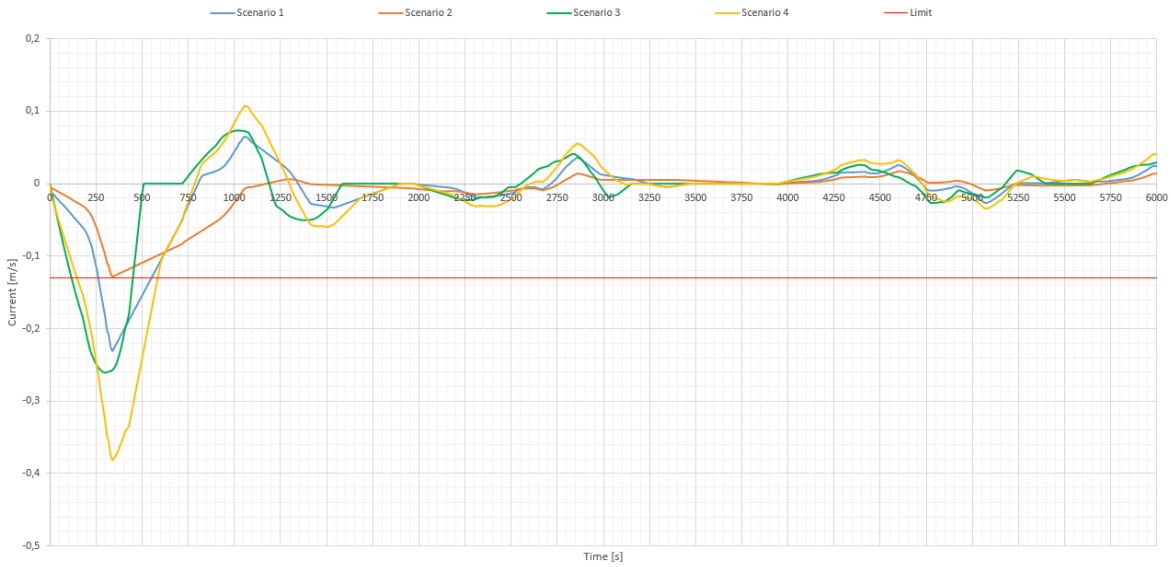

Figure 6.4: Currents of scenarios 1, 2, 3 and 4 at location XBorn

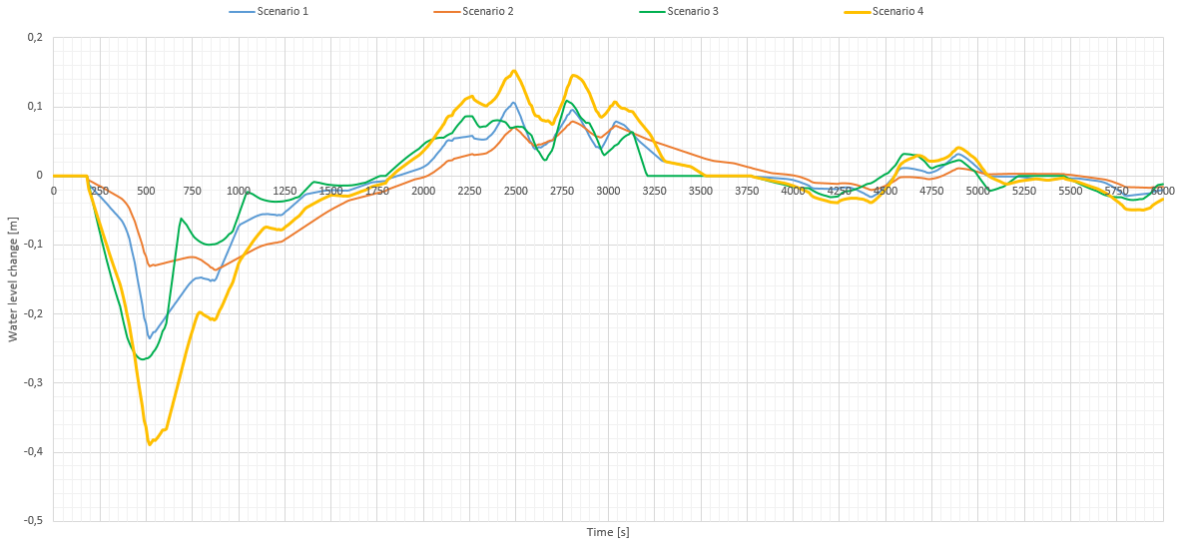

Figure 6.5: Water level changes due to scenarios 1, 2, 3 and 4 at location X1151

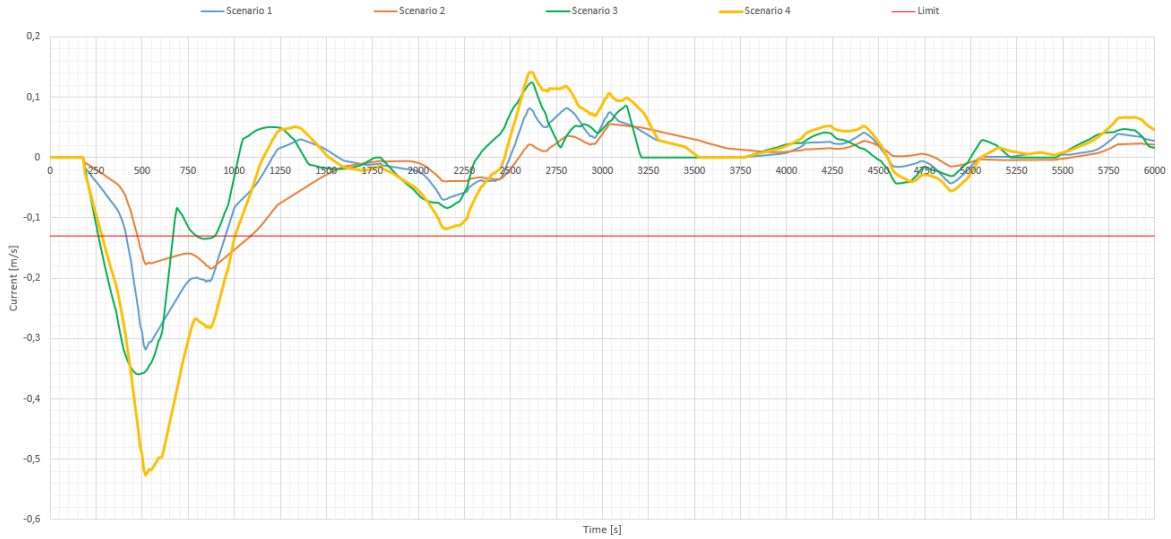

Figure 6.6: Currents of scenarios 1, 2, 3 and 4 at location X1151

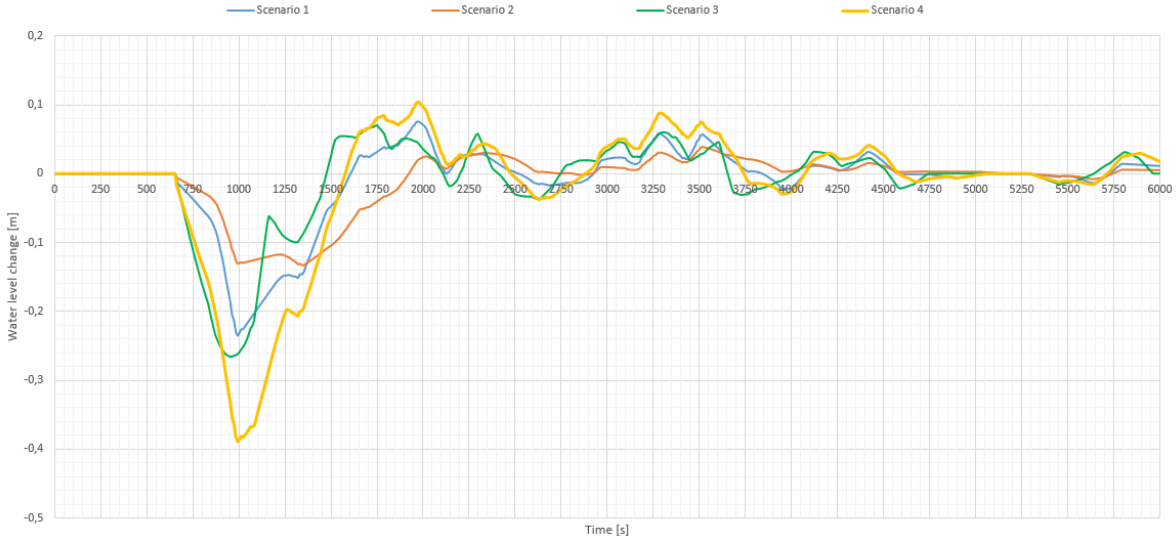

Figure 6.7: Water level changes due to scenarios 1, 2, 3 and 4 at location X4000

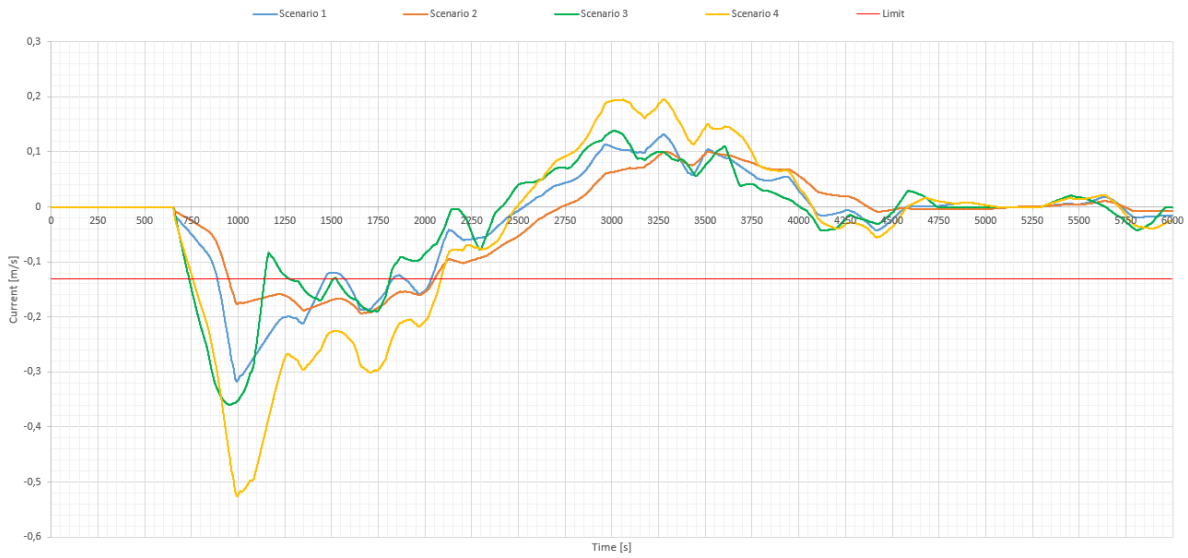

Figure 6.8: Currents of scenarios 1, 2, 3 and 4 at location X4000

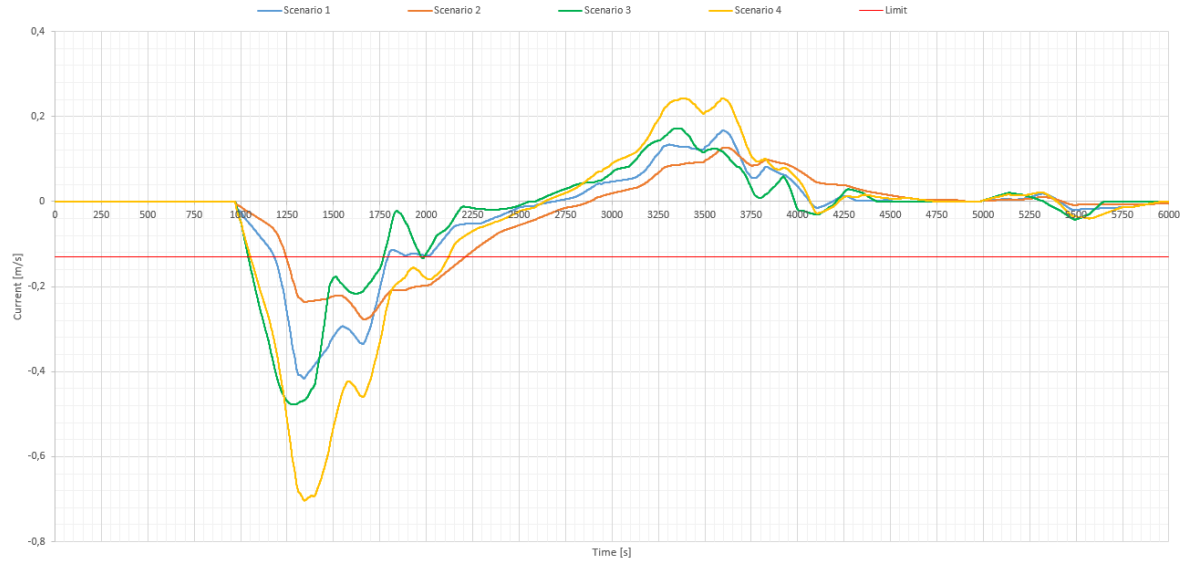

Figure 6.9: Currents of scenarios 1, 2, 3 and 4 at location X5900

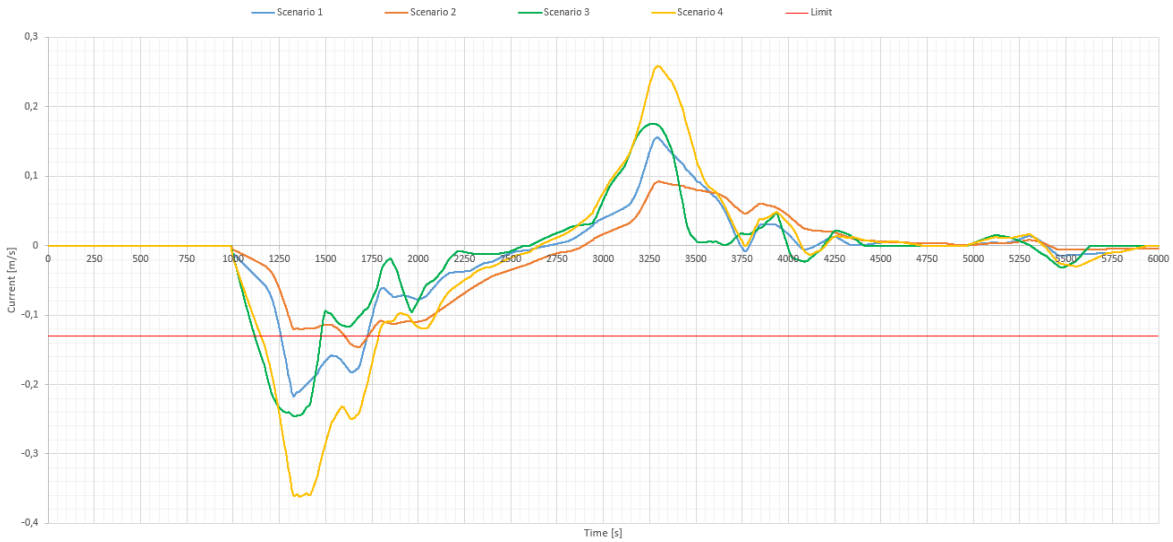

Figure 6.10: Currents of scenarios 1, 2, 3 and 4 at location X6001

6.2. DIFFERENT INTERVALS

In this section 6 scenarios are addressed, scenarios 5 up until 10. These scenarios involve differences in the filling regime, two waves are modelled in sequence. The 6 scenarios are divided in two subsection, with the main difference being the number of culverts used to fill the lock chamber. The first subsection is modelled with a wave created by the Middle lock chamber using two culverts, after which a second wave is created by the East lock chamber, again using two culverts. In the second subsection is again first a wave created by the Middle lock chamber, then a wave created by the East lock chamber. In the second subsection the filling of the lock chambers is done using one culvert for each chamber.
Six scenarios are addressed in this chapter, in each subsection 3 scenarios. The first subsection addresses scenarios 5, 6 and 7. The second subsection scenarios 8, 9 and 10. In scenarios 5 and 8, the time interval between the first and second wave is 5 minutes. In scenario 6 and 9 an interval of 10 minutes and in scenarios 7 and 10, 15 minutes in between the waves.

6.2.1. TWO CULVERTS USED AT LOCK

Scenarios 5, 6 and 7 are handled in this subsection. The discharge-time relations of these scenarios are given in figure 6.11. For each scenario, the first wave starts at t = 0 s. The difference between the scenarios is the interval in between the waves, visualized in figure 6.11 with the blue, red and green lines, corresponding to 5, 10 and 15 minutes in between the waves.

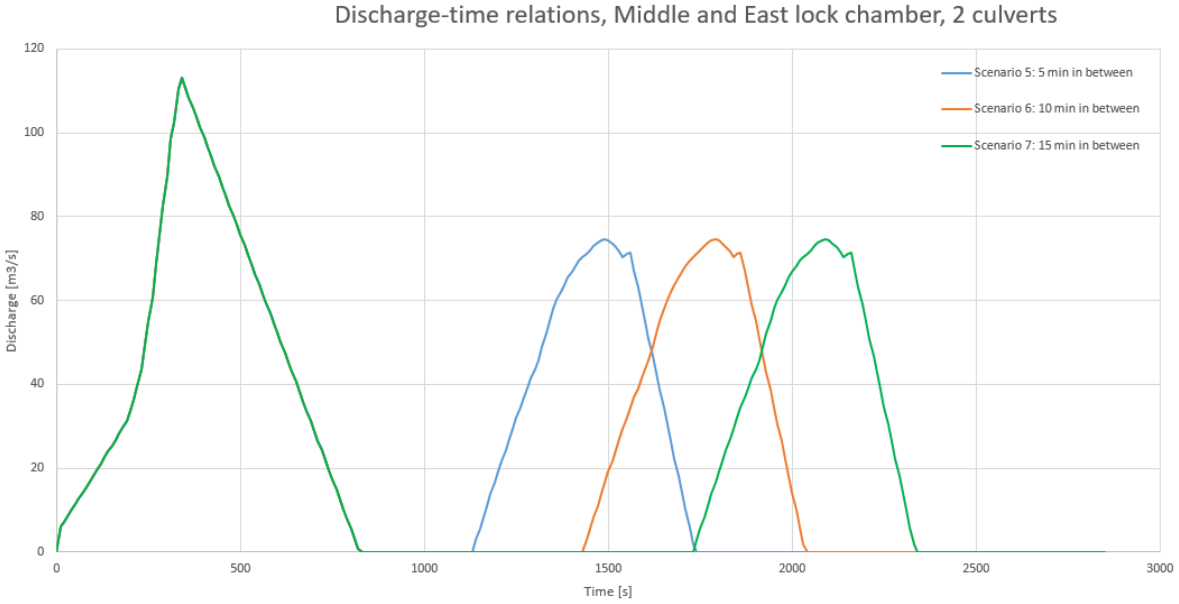

Figure 6.11: Discharge-time relations with 2 culverts used at Middle and East chamber

The results of the modelling of scenarios 5, 6 and 7 are presented in figures 6.12 up until 6.15. These two locations have been chosen to represent the results of this section. Both locations are situated on the narrow section of the canal, there are no transition points in between. The only factors by which the figures differ is by the interaction of the waves created by filling the lock chamber and the reflections. This way the differences due to the filling regime can be observed. At each location the water level changes and currents are given.
The maximum current due to negative translation waves is at both locations $u_{max} = 0.318 m/s$, as can be seen in table 6.2. This is a result of the primary wave of the first wave, originating from a water level change of $z_{min} = -0.235$. This is in all three situations the same. The time period between the arrival of the first and second wave is in figure 6.13 and figure 6.15 the same, as it is defined in the input data. The magnitude of the currents are different. The magnitude of the currents at figure 6.13 decrease, while the magnitude in figure 6.15 increase. On the contrary at the water level change figures 6.12 and 6.14.
These figures indicate that at location X1151, first (around $t = 1250s$) a negative wave travels towards Born. This gives a positive current and a negative water level change. Then around $t = 2200s$, a positive reflection wave propagating towards Born. The water level change decreases, the current towards Born (negative) in-

creases. These phenomena can be observed in figures 6.5 and 6.6. First a negative water level change in the blue line around t = 1250 and a positive current. Then a negative current around t = 2200 and a positive water level change.
The same phenomena can be observed at location X4000 but at other time intervals. A decrease of the water level change around t = 2100 and an increase of the negative current (towards Born). This indicates a positive translation wave towards Born. At t = 2750 the current is significantly decreased but the magnitude of the negative current increases in scenario 7 compared to scenario 5. This indicates a negative reflection wave towards Born.
The differences when reflection waves coincide is the result of the distance to the next transition points, where waves are reflected. The time interval between the first and second wave can also result in interaction of the second wave with the reflection of the first transition point, located at X = 1150. The combination of all these reflections result in different shapes and magnitudes of the waves at every location of the canal. To take the currents created by the translation waves into account in the planning of the construction works, the model has to be run for that location with different filling regimes. It is a location specific property of the system, with large influences on the downtime. Understanding the reactions of system to amplifications and reflections, the system can be used to reduce downtime as well. If the lock-keeper starts to fill the second lock chamber at the right time, the positive currents can decrease the negative currents. This can even result in fully removing the downtime created by the second wave at some locations. At location X1151 there would still be a time interval where downtime caused by the second wave has to be expected. At location X4000 the downtime resulting from the second wave can be taken away when the interval between the first and second wave is between 19 minutes and 25 minutes. This hypotheses has been modelled for a time interval between first and second wave of 20 minutes. The figures 6.16 and 6.17 confirmed that with 20 minutes between the subsequent waves, the downtime due to the second wave is zero at location X4000. As expected, the downtime at location X1151 could not be reduce to a current less than the limit current but the current decreased as well. These are modelled time intervals, if it is applicable in reality should be evaluated.
In scenario 5 the downtime at location X = 1151 is almost 15 minutes, at location X = 4000 about 23 minutes. The downtime at X = 4000 is 54% more than at location X = 1151, in that scenario. Where as the downtime in scenarios 7, with 15 minutes in between the waves, is 16 minutes at location X = 1151 and 21 minutes at location X = 4000. This is 30% more downtime at location X = 4000 than at location X = 1151. An overview of the extreme values of the currents and the downtime is given in table 6.2. There is not a clear line to see between the three scenarios. Every location is affected by a unique combination of individual waves and currents. These combinations result in different downtimes and for each location should another regime of subsequent waves be determined. The difference in downtime at a location between the scenarios does not vary that much. Comparing these scenarios with the original wave, with one filling cycle, the additional downtime due to the second wave is about 7 minutes at location X = 1151 and about 6 minutes at location X = 4000. The downtime with 20 minutes has increased nothing compared to the scenario with one wave, this means there is no second exceedance of the limit current.
This is highly beneficial for the construction works because the contractor knows the water-borne construction equipment can proceed working. Controlling the filling regime in a clever way can definitely pay off.

Table 6.2: Overview of extreme values and downtime of scenarios 5, 6 and 7, at 5 locations

Scenario	Parameter	X_Born	X_1151	X_4000	X_5900	X_6001
Sc5	z_{min} [m]	-0,173	-0,235	-0,235	-0,170	-0,154
	z_{max} [m]	0,096	0,092	0,076	0,066	0,062
	u_{min} [m/s]	-0,231	-0,318	-0,318	-0,416	-0,217
	u_{max} [m/s]	0,065	0,078	0,106	0,157	0,129
	$Dtime$ [min:sec]	08:58	14:54	22:55	18:49	12:47
Sc6	z_{min} [m]	-0,173	-0,235	-0,235	-0,170	-0,154
	z_{max} [m]	0,086	0,077	0,091	0,066	0,054
	u_{min} [m/s]	-0,231	-0,318	-0,318	-0,416	-0,217
	u_{max} [m/s]	0,065	0,109	0,073	0,131	0,123
	$Dtime$ [min:sec]	09:03	16:44	23:21	17:29	10:49
Sc7	z_{min} [m]	-0,173	-0,235	-0,235	-0,170	-0,154
	z_{max} [m]	0,076	0,074	0,103	0,075	0,046
	u_{min} [m/s]	-0,231	-0,318	-0,318	-0,416	-0,217
	u_{max} [m/s]	0,071	0,102	0,095	0,120	0,107
	$Dtime$ [min:sec]	08:16	16:06	20:56	16:01	07:48

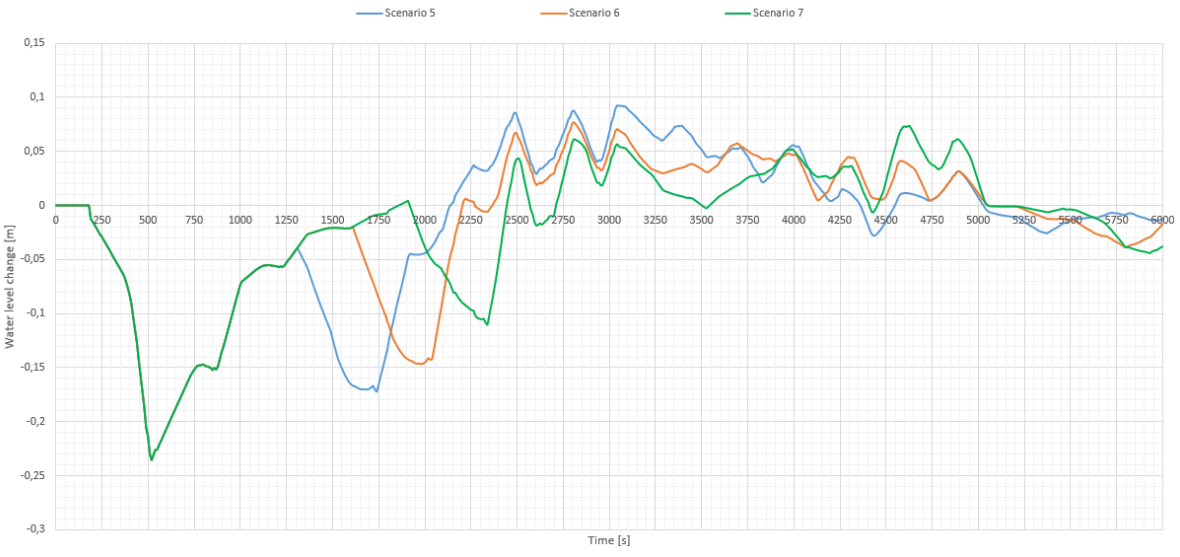

Figure 6.12: Water level changes due to scenarios 5, 6 and 7 at location X1151

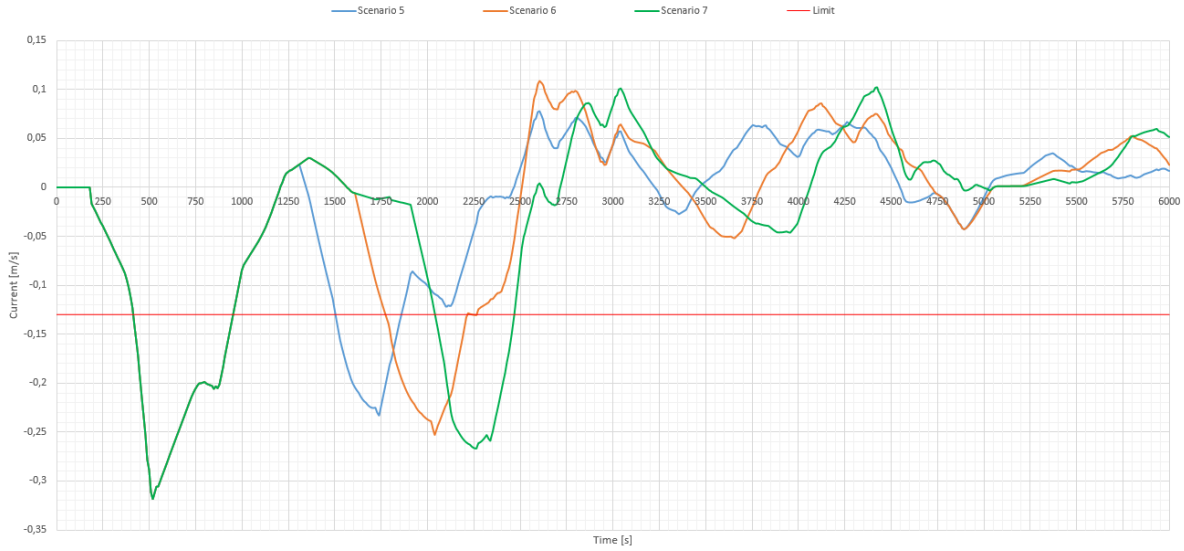

Figure 6.13: Currents of scenarios 5, 6 and 7 at location X1151

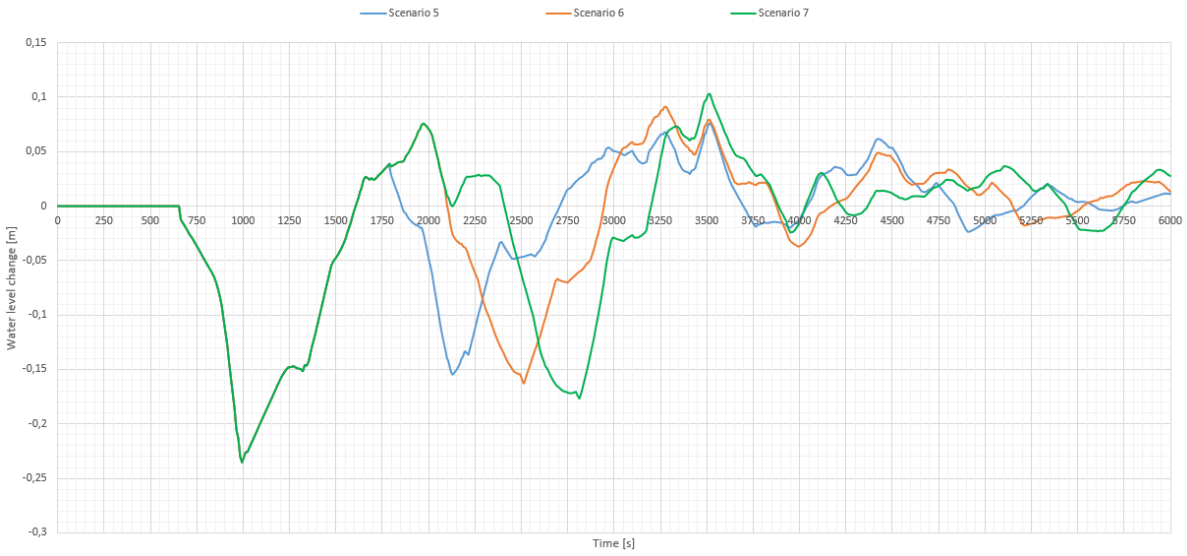

Figure 6.14: Water level changes due to scenarios 5, 6 and 7 at location X4000

Figure 6.15: Currents of scenarios 5, 6 and 7 at location X4000

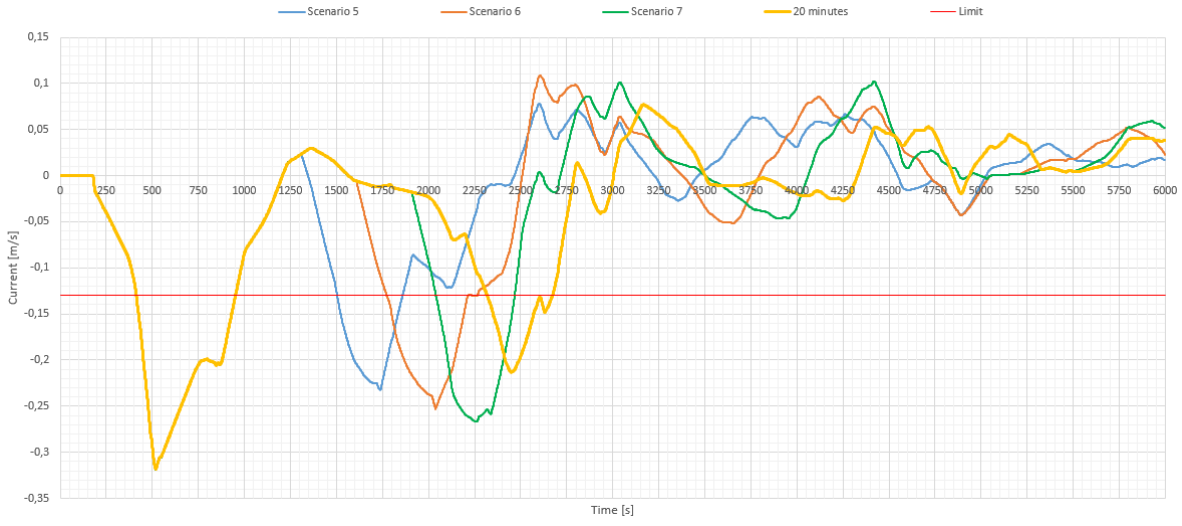

Figure 6.16: Currents of scenarios 5, 6, 7 and 11 at location X1151

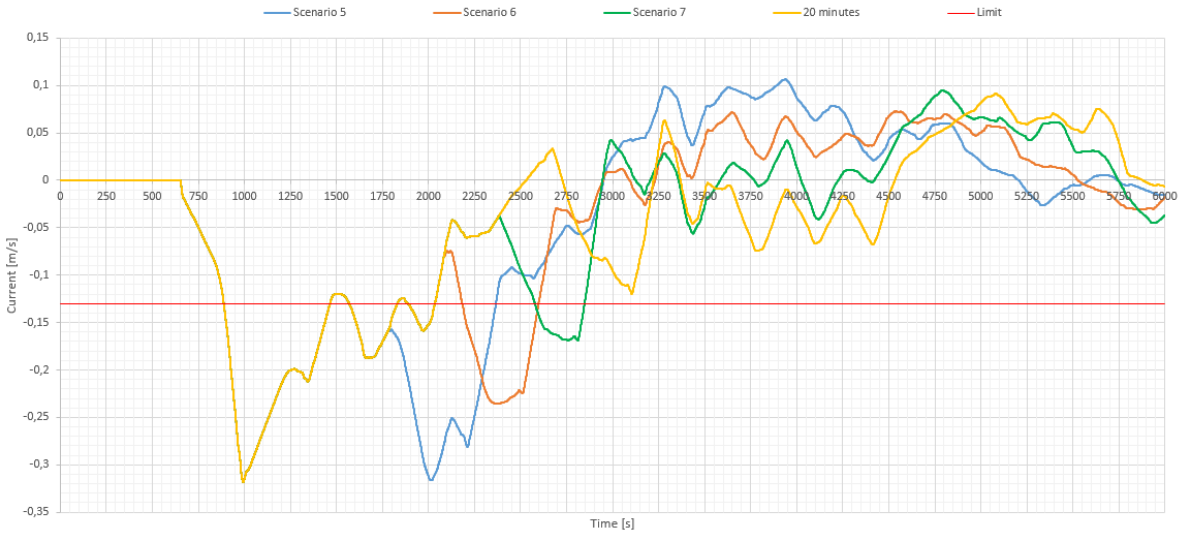

Figure 6.17: Currents of scenarios 5, 6, 7 and 11 at location X4000

6.2.2. ONE CULVERT USED AT LOCK

The results of scenarios 8, 9 and 10 are explained in this subsection. The discharge-time relations of these scenarios are given in figure 6.18. The difference between the scenarios is the interval between the first and second wave, this is visualized in figure 6.18. In this figure the 5, 10 and 15 minutes in between the waves are presented with respectively the blue, red and green lines.
The first wave draws a maximum discharge of 62 m^3/s, the second waves have a maximum discharge of 56 m^3/s. The wave period is much longer than in the situation with 2 culverts, 1420 seconds compared to 830 seconds.

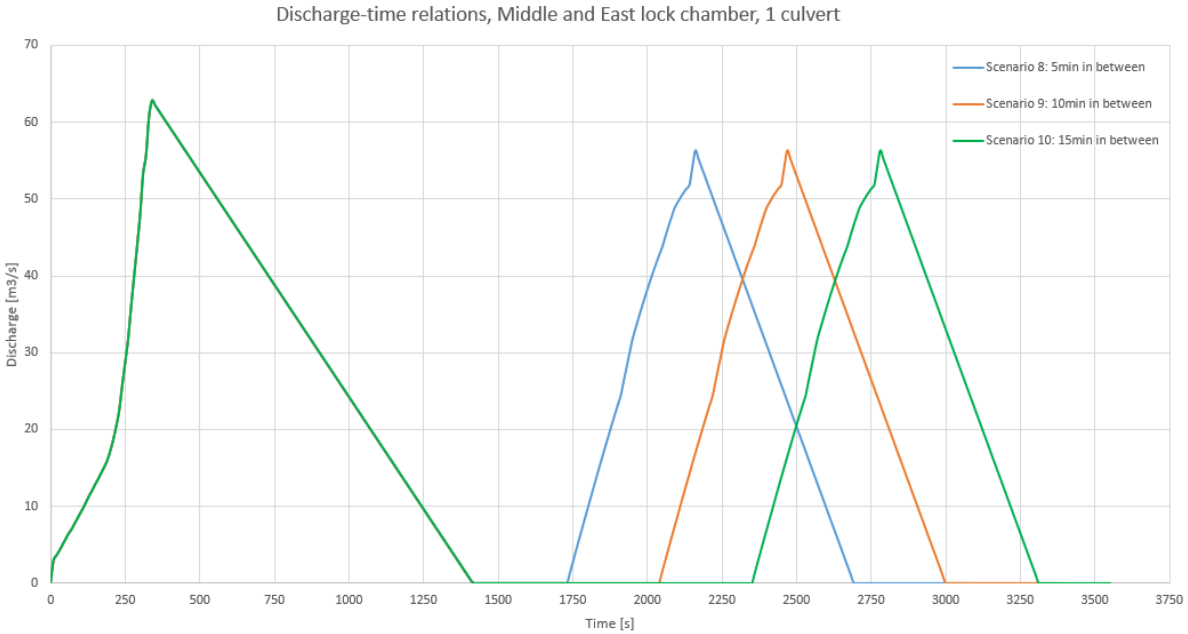

Figure 6.18: Discharge-time relations with 1 culvert used at Middle and East chamber

To compare the situation with one culvert with the situation with two culverts, the same locations have been chosen. The results of the model at locations X = 1151 and X = 4000 are presented in figures 6.19 up till 6.22.
The maximum currents occur at location X = 1151 in scenarios 6 and 7 and at location X = 4000 in all three scenarios due to the primary wave and first reflection of the first wave. The primary wave is the first trough, the first reflection is the second trough about 400 seconds later. Filling the lock chamber with one culvert creates a longer wave. Location X = 4000 is located closer to the transition point at X = 6000, the reflection from that point is visible as the third trough around $t = 1650$.
Remarkable to see is that the second wave in scenario 8 at location X = 1151 results in a larger current than the primary wave of the first wave. This is due to the negative current which is visible in figure 6.6 as well. Scenarios 9 and 10 arrive later at the location and create a smaller current, almost less than the critical current of $u_{max} = -0.13 m/s$.
The currents arising from the second wave at location X = 1151, could be corrected to currents above the critical current by extending the period between sequel to 17 minutes. This way the maximum negative current of the second wave would coincide with the maximum positive current resulting from the first wave, around $t = 3100$ in figure 6.6. This by using the same method as in the previous section where scenarios 5, 6 and 7 where discussed. To compensate the currents from the second wave at location X = 4000, an interval between the two waves of 8 minutes would suffice. This is, again, concluded by comparing the troughs of figure 6.22 with the peaks in figure 6.8.
The wide trough at location X = 4000 in scenarios 8, 9 and 10 can not be compensated for by the filling regime, these are a result of the systems bathymetry and reflections by the first wave. A downtime of 18:24 minutes will not be avoidable if the lock chamber is filled with one culvert. An overview of the currents and downtime is given in table 6.3.

Table 6.3: Overview of extreme values and downtime of scenarios 8, 9 and 10, at 5 locations

Scenario	Parameter	X_Born	X_1151	X_4000	X_5900	X_6001
Sc8	z_{min} [m]	-0,135	-0,136	-0,133	-0,097	-0,086
	z_{max} [m]	0,055	0,049	0,059	0,043	0,028
	u_{min} [m/s]	-0,128	-0,202	-0,194	-0,278	-0,147
	u_{max} [m/s]	0,042	0,062	0,071	0,096	0,086
	$Dtime$ [min:sec]	00:00	17:22	21:11	21:07	02:08
Sc9	z_{min} [m]	-0,135	-0,136	-0,133	-0,095	-0,086
	z_{max} [m]	0,057	0,061	0,045	0,042	0,033
	u_{min} [m/s]	-0,128	-0,184	-0,194	-0,278	-0,147
	u_{max} [m/s]	0,034	0,041	0,076	0,088	0,082
	$Dtime$ [min:sec]	00:00	13:16	18:24	17:25	02:08
Sc10	z_{min} [m]	-0,135	-0,136	-0,133	-0,095	-0,086
	z_{max} [m]	0,065	0,070	0,047	0,020	0,034
	u_{min} [m/s]	-0,128	-0,184	-0,194	-0,278	-0,147
	u_{max} [m/s]	0,033	0,039	0,080	0,085	0,092
	$Dtime$ [min:sec]	00:00	11:12	18:24	17:31	02:08

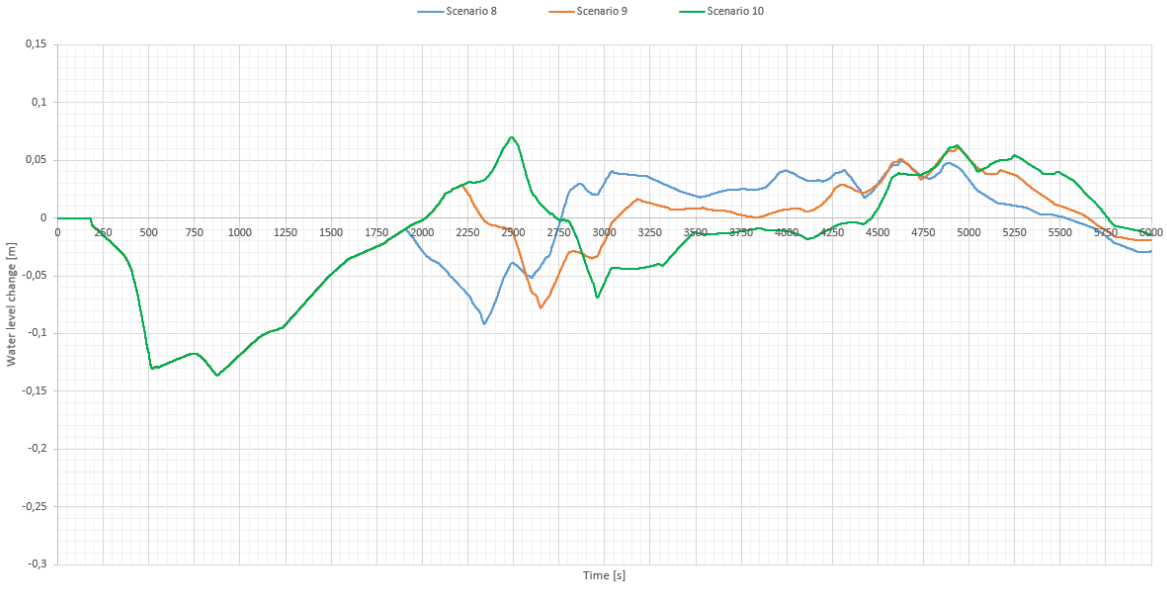

Figure 6.19: Water level changes due to scenarios 8, 9 and 10 at location X1151

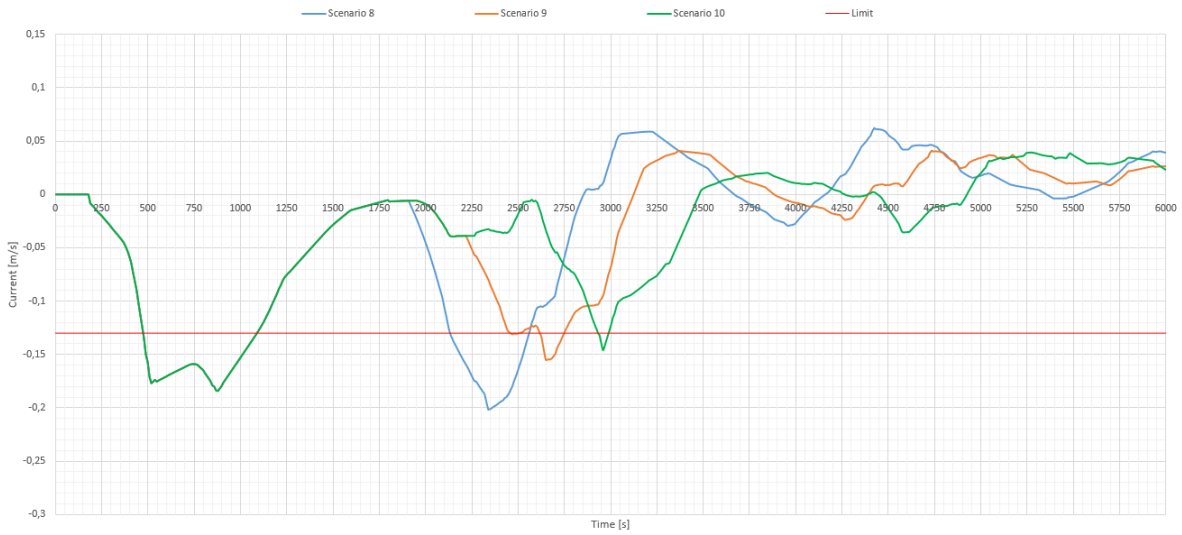

Figure 6.20: Currents of scenarios 8, 9 and 10 at location X1151

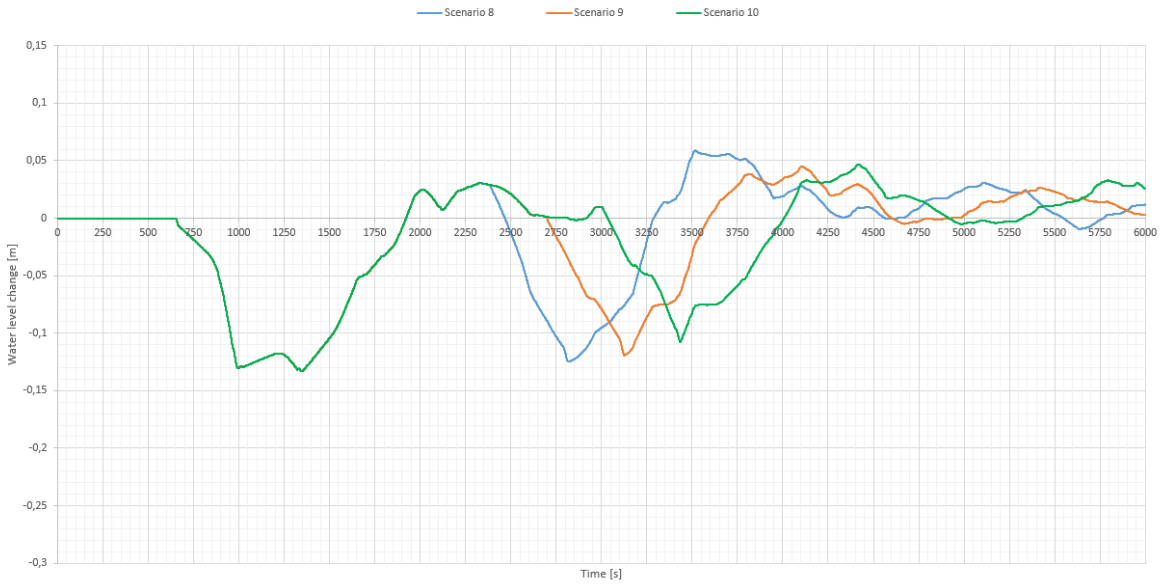

Figure 6.21: Water level changes due to scenarios 8, 9 and 10 at location X4000

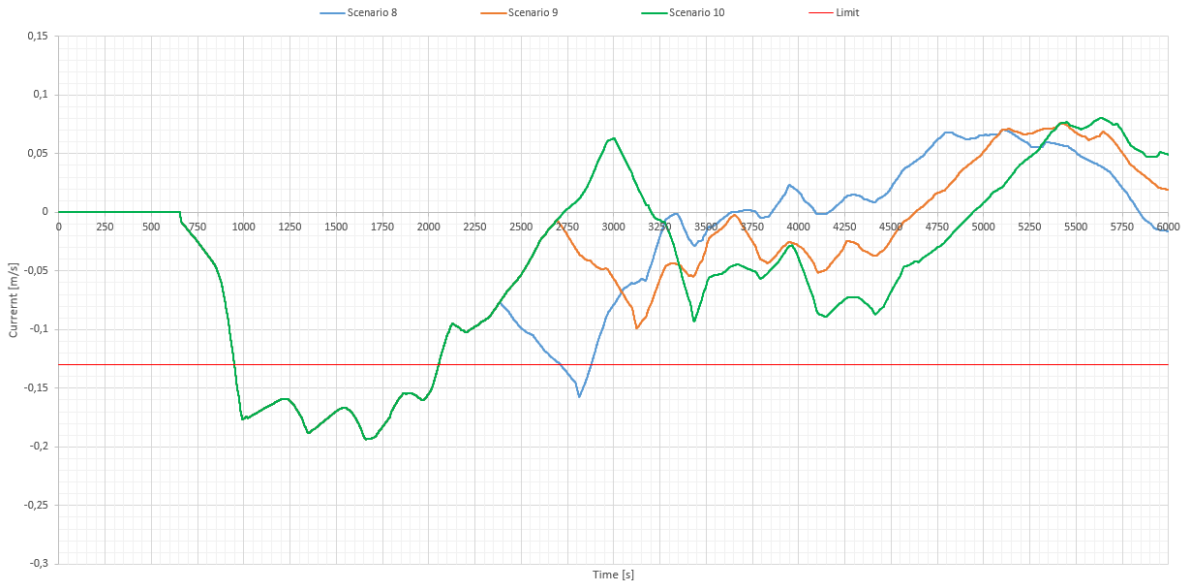

Figure 6.22: Currents of scenarios 8, 9 and 10 at location X4000

An overview of the downtime in all different scenarios is given in table 6.4. Here can be seen that the downtime is per location different, depending on the filling regime and discharge-time relation.

Table 6.4: Overview of the downtime per scenario and per location

Downtime overview		Downtime per location [min:sec]				
Scenario number	Name	0	1150	4000	5900	6001
Sc1	Original (2 culverts)	04:48	08:59	16:26	10:13	07:48
Sc2	1 culvert	00:00	10:15	18:24	16:07	02:08
Sc3	4 culverts	05:33	08:24	15:34	12:27	05:58
Sc4	2 x 2 culverts	07:18	12:03	22:10	17:48	10:36
Sc5	2 waves, 2 culverts, 5 minutes	08:58	14:54	22:55	18:49	12:47
Sc6	2 waves, 2 culverts, 10 minutes	09:03	16:44	23:21	17:29	10:49
Sc7	2 waves, 2 culverts, 15 minutes	08:16	16:06	20:56	16:01	07:48
Sc8	2 waves, 1 culverts, 5 minutes	00:00	17:22	21:11	21:07	02:08
Sc9	2 waves, 1 culverts, 10 minutes	00:00	13:16	18:24	17:25	02:08
Sc10	2 waves, 1 culverts, 15 minutes	00:00	11:12	18:24	17:31	02:08

7

CONCLUSIONS AND RECOMMENDATIONS

Different scenarios are explored and were modelled. The results from the model are analysed in chapter 6. In this chapter conclusions are drawn in section 7.1, in the discussion, section 7.2, is reflected on the conclusions. Recommendations for future researches and possibilities to explore are given section 7.3.
The conclusions will be considered according to the research question and sub-questions. In the introduction the research question for this case study was defined as:

How do translation waves, induced by high head lock systems, evolve in a canal and what are the possibilities by the lock system to create suitable working conditions for water-borne construction works?

7.1. CONCLUSIONS

The conclusions are presented according to the numeration of the sub-questions, given in chapter 1. The conclusion will shortly be introduced first and be elaborated on after.

Conclusion 1 *Propagation of a translation wave?*

The water level changes, due to translation waves, react to changes in width of the canal and celerity of the wave. At transition points in the canal-profile the wave is partly reflected, the other part of the translation wave continues. The water level changes and current increases or decreases or even change sign at these points. These variations on the translation waves were described in theory (Thijsse, 1935 [2]) and were validated in the model. First for the changes of a single pulse, as was described in theorem. Thereafter validated for the complex situation, where the discharge to the lock chamber was modelled as a combination of subsequent pulses. **The implemented discharge-over-time relations as subsequent pulses in the model, proved to be a good representation for the propagation of a translation wave, compared to the measurements.**

Conclusion 2 *Limit states?*

The limit states have been calculated for two situations. First the situation that inspections of the construction works by divers would no longer be possible due to high currents. Second, the water-borne equipment would no longer be stable and would float away by the currents. Calculations determined that the decisive limiting situation is the situation with the inspection divers. **The limit states for currents due to translation waves are defined at $u_{low} = -0.13 m/s$ to the north and $u_{high} = +0.30 m/s$ to the south.** The difference between the limit state to the north and to the south is caused by the base current in the canal.

Conclusion 3 *Adaptation options of a lock complex?*

Two options show to be dominant in the behaviour of the canal. These are: 1) the number of culverts used, and 2) the filling regime. The number of culverts used determines the discharge-time relations. These relations determine the length of the wave and the magnitude of the water level change. The filling regime controls how much time is kept between subsequent waves. This determines the interaction between reflections and the second wave. Multiple scenarios, by varying the first group, second group and combinations of both groups, were investigated and modelled. **Both options influence the behaviour and show to be well modelled and tuned.**

Conclusion 4 *Best scenario to increase workability?*

In the present situation a number of currents exceed the defined limit state due to translation waves. Alternatives, as described in conclusion 3, have been investigated. There cannot be concluded that one scenario is the best scenario at all locations. At every location the combinations of primary waves and reflection waves result in a best scenarios for that location. In the scenarios implementing the first control option, the best scenario at the locations vary between scenarios 1, 2 and 3, in these scenarios are respectively 1,2 or 4 culverts used. The scenario with simultaneous filling of two chambers is never the best scenario. In the scenarios implementing the second control option, the scenarios with 2 subsequent waves, scenario 10 is at 4 of the 5 locations the best option. At the other location scenario 7. In situations with subsequent waves, the scenarios with longer time between waves are preferred. **Since there is no prevailing scenario for all locations, the model has to be run with different scenarios for each new location.**

Elaboration on the enumerated conclusions.

Conclusion 1:
The water level change due to translation waves are dependent on the celerity of the waves and the width of the canal. The differences in celerity between the canal-sections is mostly influenced by the added or lowered depth as a result of the wave height. The wave celerities vary between $c = 5.7 m/s$ and $c = 6.4 m/s$, assuming a wave of 15cm.
At transition points a part of the wave is reflected, the other part of the wave continues through the canal. In the model, first the propagation of a single pulse through the canal is calculated. The water level changes and current adaptations of this pulse is used to define the response of the system. In the complex situation of filling the lock chamber there is not a single wave height, the discharge-time relation is divided in small intervals, like one or two seconds. For each pulse adaptations to the transition points are calculated. These pulses are put behind each other in the model resulting in the translation wave according to the discharge-time relation. The transition points modelled in this part of the Juliana Canal system are located at X = 0 (Born), X = 1151, X = 6000, X = 7000, X = 7500 and the port. An overview of the transition points is given in figure 7.1. When a reflection wave encounters previous transition points, the reflection wave reflects another part while the reflection wave continues, this way it creates more and more reflections. In the model the canal-section between Born and the bend south of Stein is schematized with 5 transition points and the lock complex. In total the original wave and 42 reflections are included in the model.
This 1D-model results in a light and accurate prediction tool for the propagation of translation waves and could be a good alternative for modelling tools, like Delft 3D, for exploratory researches of water-movements in a canal. The model calculates scenarios in less than 5 minutes on a standard laptop. The mean error of the model is $\mu = 0.005 m$, the standard deviation is $\sigma = 0.0136 m$ and the 95% confidence interval of the deviation of the model is determined to be between -0.0217m and 0.0317m.

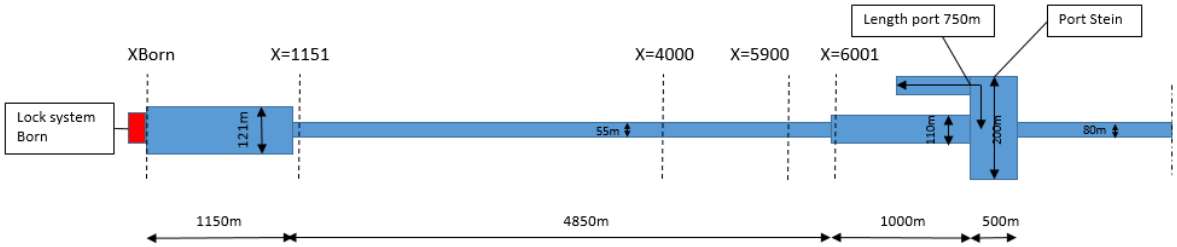

Figure 7.1: Schematisation of the system as modelled

The response of ships to waves is usually calculated using spectral calculations. The propagation of a translation wave and its accompanied currents cannot be represented in a spectrum, as is proven in appendix A. The model developed during this research, gives a good representation of the water level changes and currents that construction equipment will have to endure during the passage of translation waves.

Conclusion 2:
The limit states for two situations were calculated. The first situation is to determine the maximum currents for inspections of the construction works to be performed. The inspections are done by divers. The maximum current to which divers are allowed to work is set at 0.5 knots (www.waterbouw.nl, 2015 [13]), that is about $u_{max} = 0.3 m/s$.
The second situation for which the limit states are calculated, is to whether the water-borne construction equipment would move as a whole. In this calculation the horizontal driving forces were the pressure gradients to the vertical wet surface of the pontoon. For the construction equipment used in the Juliana Canal, the current would be $u = 3.23 m/s$. The wave height to create this current, by a single translation wave, would be $z = 1.68 m$. This is not a realistic wave height for translation waves due to this lock complex.
The decisive situation for the limit states is the inspection of the construction works by divers. The critical current at which divers are allowed to work during inspection is determined at $u_{max} = 0.3 m/s$ [13]. In the canal is a base current measured (see figure 3.8, stated at $u_{base} = -0.17\ m/s$. The base current is in the direction towards Born. At the construction equipment an absolute value of the current is $u_{max} = 0.3 m/s$, so for a current towards the lock complex near Born, a maximum current of $u_{trans} = u_{total} - u_{base} = 0.13 m/s$. The maximum allowable current due to translation waves with base current included is $u_{trans} = u_{total} - u_{base} = +0.30 - (-0.17) = +0.47 m/s$. In the situation that the Maas encounters discharges larger than $Q_{Maas} = 1280 m^3/s$ the lock complex near the village of Limmel will close. There will no longer be a base current. The upper limit for translation waves in a situation without base current is $u_{trans} = 0.30 m/s$. This is a conservative value. So, for currents towards the lock complex at Born, north, the maximum current is 0.13 m/s. For currents induced by translation waves away from the lock complex, south, the maximum current is 0.30m/s.

Conclusion 3:
The first option on changing the controlling mechanism by the lock complex is to vary with the number of culverts used to fill the lock chamber or chambers. Adaptations in the number of culverts create different discharge-time relations. The different situations explored in this research are: the original situation with 2 culverts, 1 culvert, 4 culverts and filling the Middle and East chamber simultaneous, but the same volume has to be transported from the canal to the lock chamber. The time it takes to fill the lock chamber and thereby the resulting wave length, will increase if the discharge is lower. The maximum discharges are respectively 110 m^3/s, 63 m^3/s, 127 m^3/s and 185 m^3/s. The time to fill the lock chamber is respectively 830s, 1420s, 520s and 830s. The time to fill the Middle chamber only, or the Middle and East chamber simultaneous, are equal. The Middle and East chamber start to fill at the same time during simultaneous filling, but the East chamber is smaller and will be filled before the Middle chamber. So, the Middle chamber is decisive for the wave-period. The wave lengths resulting from the time to fill the lock chambers are roughly 5km, 8.5km and 3km.
The second option on changing the control mechanism is the time given between two subsequent fillings of the lock chambers, so the time between two translation waves. If the time between the first filling and the second filling of a chamber is at the right time, the reflection waves of the first wave can be used to compensate for currents induced by the second filling. If done incorrectly, the interaction of the reflection waves

and second waves can result in amplifications of the currents. Long waves have longer interaction periods with reflection waves but are less severe. The duration of interference of waves with a higher discharge with reflections is less but the effects are more fierce.
In this research, the situations at relatively fast filling after each other have been investigated. This was with 5, 10 and 15 minutes between the first and second wave. These scenarios have been investigated for filling with one culvert and with two culverts.

Conclusion 4:
Distinction is made between the first and second control option, as is described in conclusion 3. The control options are treated separately.

Control option 1: vary with the number of culverts
The scenarios 1 up until 3 refer to the scenarios with respectively 2, 1 or 4 culverts used to fill the lock chamber. In these three scenarios is the Middle lock chamber filled only. In scenarios 4 are the East and Middle lock chamber filled simultaneous.
In the scenarios of the first control option there is not a trend visible for a particular scenario. The scenarios with 1, 2 or 4 culverts all appear in table 7.1, the overview of the best scenarios per location. Scenario 4 is in non of the scenarios the scenario with least downtime and should not be implemented in the filling regime of the lock-operator!

Table 7.1: Best scenario for each location, scenarios with one wave

Location	Scenario one wave	Downtime $[min:sec]$	u_{min} $[m/s]$	u_{max} $[m/s]$
X = 0	Sc 2, 1 culvert	00:00	-0,128	0,017
X = 1151	Sc 3, 4 culverts	08:24	-0,359	0,124
X = 4000	Sc 3, 4 culverts	15:34	-0,359	0,138
X = 5900	Sc 1, 2 culverts	10:13	-0,416	0,168
X = 6001	Sc 2, 1 culvert	02:08	-0,147	0,092

Control option 2: varying the time between two subsequent fillings
In the second group of control options first the Middle chamber is filled, subsequently the East chamber. Distinction is made between scenarios 5 up until 7, where the lock chambers are filled with 2 culverts, and scenarios 8 up until 10, where the lock chambers are filled with 1 culvert. In scenarios 5 and 8 there is 5 minutes between filing of the Middle and East chamber. In scenarios 6 and 9 there is 10 minutes between filling of the two chambers. In scenario 7 and 10 there is 15 minutes between subsequent fillings.
The best scenarios of the second control option are presented per location in table 7.2. At three locations are multiple scenarios the scenario with least downtime. In these situation the downtime is the result of the primary wave of the Middle lock chamber only and is the downtime between those scenarios the same. Scenario 10 is in 4 of the 5 locations the best scenario. In 2 of the 5 locations filling with one culvert is sufficient to result in the best scenario unrelated to the time between the fillings. At location X = 5900 the lowest downtime period is when scenario 7 is applied on the system. The time between subsequent waves is 15 minutes in both scenarios 7 as in scenario 10. A longer period between sequent waves reduces the downtime period significantly.

Table 7.2: Best scenario for each location, scenarios with two waves

Location	Scenario two waves	Downtime $[min:sec]$	u_{min} $[m/s]$	u_{max} $[m/s]$
X = 0	Sc 8, 9 or 10, 1 culvert, 5, 10 or 15 minutes	00:00	-0,128	0,042
X = 1151	Sc 10, 1 culvert, 15 min	11:12	-0,184	0,039
X = 4000	Sc 9 or 10, 1 culvert, 10 or 15 minutes	18:24	-0,194	0,080
X = 5900	Sc 7, 2 culverts, 15 minutes	16:01	-0,416	0,120
X = 6001	Sc 8, 9 or 10, 1 culvert, 5, 10 or 15 minutes	02:08	-0,147	0,092

In summary, the theorem on the propagation of translation wave from Thijsse in 1935 (Thijsse, 1935 [2]) still holds according to calculations. The propagation of a complex wave, such as the filling of a lock chamber, can practically not be performed with calculations as done by Thijsse. The 1D-model developed during this case study, can accurately calculate and describe how the translation wave evolve over the canal.
The options on changing the controlling mechanism of the lock complex are: the number of culverts used during filling of the lock chamber, or the time between subsequent waves. From the model calculations it cannot be concluded that one control option is de best scenario for the whole canal-system. The interaction between primary waves and reflections develop for each location under each discharge-time relation, other water level changes and currents. In order to determine the best option for the construction works and to reduce the downtime for water-borne construction equipment, the model has to be run with different scenarios for that work location.

7.2. DISCUSSION

A reflection on the research is given in this paragraph. This includes critical notes on the research and elaboration on the applicability to other situations.

The model
The model gives a good representation of the situation in reality. There are still deviations between the water level changes in the model and measurements. Further calibrations could improve the model but is very time consuming and would probably not increase the accuracy that much.
The model could relatively easy be adapted to another canal-system by changing the bathymetry, lock discharges and transition points.
If the complexity, e.g. changes in width, ports or other transition points, of a canal system becomes larger, the size of the model will increase more-than-linear. If another transition point is added to the model, not only new reflections have to be added to the model but also the reflections of the previous reflections that were already in the model.
The waves and reflection waves are put in the model manually. For large scale canal-systems, this would be very time consuming. An interface where reflections at transition points are automatically included could be a useful addition to the model to make it more user-friendly and less prone to programming errors.

The results
In the results, the total downtime is given based on the inspection by divers. Recording the number of limit state crossings and the time between downtime periods could give another insight for the construction works.
The results are presented in the form of downtime for water-borne construction equipment, this is a specific parameter for the equipment. Standardized guidelines could give more universal interpretations of the results.
The results are location specific and cannot be used in other canal-systems directly. The model can be used in other canal-systems after adaptations and calibration to the system.

7.3. RECOMMENDATIONS

Based on findings during the research, the following subjects are recommended to investigate further.

- *Investigate the limit state for horizontal movement of the construction equipment*
  After the calculations on the stability of the water-borne construction equipment, it was concluded that the equipment used in the Juliana Canal would not move. This calculation was done according to the horizontal balance. In that situation it will not move. In the situation that the water level is lowered due to a negative wave passing by, the water-borne construction is assumed to move even less. There is less buoyancy because the equipment stand higher above the water, resulting in more vertical pressure, resulting in more horizontal bottom friction. If a positive translation wave passes by, the water level rises, buoyancy increases, pressure on the spud-poles is assumed to decrease if they cannot adjust quickly, this can result in a decrease of the vertical forces. If the vertical forces decrease, the horizontal bottom friction will decrease. In the most extreme situation the spud-poles will come of the ground, then the construction equipment will move. The changes to the vertical forces due to positive or negative translation waves and the resulting effects on the bottom friction should be investigated. In canal sections with dominantly positive translation waves it is recommended to monitor this already.

- *Research on the behaviour of bentonite mats under currents*
  A subject that was excluded from this research was the vulnerability of bentonite mats. The effects of currents on the behaviour of bentonite mats under water is a topic that should be investigated for future construction works. The placement of bentonite mats could possibly be a second of even the decisive limit state for the construction works.
- *Further research in the behaviour of translation waves around a blockage in the canal on a local level.*
  In the model the assumption has been made that local changes on the velocity of the current is linear dependent on the relative narrowing of the canal due to the construction equipment. This was done according to the ratio between the old wet surface and new wet surface $f_p = (A_w - A_{pon})/A_w$. The construction equipment is a blunt object with sharp edges, water will not flow smoothly around the construction equipment. To compensate for turbulent flow around the area, the wet area of the construction equipment was enlarged with 10%. The assumption that the net wet surface decrease more due to turbulent flow should be checked and which percentage would be reasonable for this construction equipment should be investigated further.
- *Validation in other canal systems*
  The model has only been calibrated and validated to the Juliana Canal. The theory is applicable to all other translation waves in canal systems but more testing of the model to check whether it is universally applicable would be desirable.
- *Integration of the model in other applications*
  Development of an expansion of the model where the bathymetry automatically can be loaded in the system, scenarios can be defined and optimizations to reduce downtime can be calculated. So a program where all aspects are integrated.
- *Effects of translation waves on shipping*
  The effects of translation waves on water-borne construction equipment is investigated in this research. The effects of currents and water level changes as a result of translation waves on the navigability of vessels in a canal is not. This is out of the scope of this case study but can be investigated in future research.
- *Predicting an economical optimization between downtime for the construction works and waiting time for shipping*
  Numerous control options at the lock complex involve either longer time between sequent fillings or filling the lock chamber with less culverts. Both options result longer periods to pass the lock complex and a delay in shipping time. Downtime at the construction works increases the construction time of the project and increases the costs. A research for the economical optimization can be performed.

BIBLIOGRAPHY

[1] P. Balazs, *North Sea Mediterranean*, Tech. Rep. (European Commission, 2015).

[2] J. T. Thijsse, *Golfbewegingen en langsstroomingen in kanaalpanden,* (1935).

[3] D. N. Dietz, *A new method for calculating the conduct of translation waves,* (1941).

[4] R. J. Labeur and J. A. Battjes, *CT3310 Open Channel Flow, Lecture notes,* (2011).

[5] Rijkswaterstaat, *Nota randvoorwaarden bij VS1 Julianakanaal 09-10-2012*, Tech. Rep. (Rijkswaterstaat, 2012).

[6] Imtech and Rijkswaterstaat, *Technische handleiding Regelalgoritme Stuw/vispassage Borgharen* (2015) p. 36.

[7] Bureau Voorlichting Binnenvaart, *Waardevol Transport*, Tech. Rep. (Bureau voorlichting binnenvaart, 2016).

[8] R. Schroevers, H. Verheij, K. Berends, and T. Vermaas, *Stabiliteitsproeven Julianakanaal 2014*, Tech. Rep. (Deltares, Delft, 2015).

[9] Www.binnenvaartinbeeld.nl, *Binnenvaart in Beeld, Julianakanaal,* (2016).

[10] Rijkswaterstaat, *Vaarwegen in Nederland,* , 194 (2016).

[11] R. Raat, *Kanalen in Nederland, Julianakanaal,* (2010).

[12] E. van de Lockant, *Schuttingen Born,* (2016).

[13] Waterbouw.nl, *Arbo catalogus waterbouw,* (2015).

[14] H. G. Tuin, *Bepaling maatgevende belastingen retourstroom,* (2015).

[15] H. Rouvroye and L. Schreurs, *Aanleg Julianakanaal 1935*, Tech. Rep. (Stein, 1996).

[16] L. H. Holthuijsen, *Waves in Oceanic and Coastal Waters (Emergency Notes)* (Cambridge University Press, 2010).

[17] Rijkswaterstaat, *Waterway Guidelines 2011*, Tech. Rep. (Rijkswaterstaat, Delft, 2011).

A

ANALYSIS

A.1. SYSTEM DESCRIPTION OF THE JULIANA CANAL

The demand for transport capacity to the hinterland is still increasing. With a share of 37% in 2014 (Bureau Voorlichting Binnenvaart, 2016 [7]) of the total transported weight in the Netherlands, inland waterways are a major contributor. Transport on inland waterways is still increasing and is assumed to continue growing the coming years. The discharge of the Maas is heavily influenced by rainfall in the catchment area, resulting in high fluctuations in water depth. High water depth in the winter, low water depth during summer. This is not preferable for navigation purposes. To improve navigability to the cities along the Maas upstream, e.g. Maastricht, Liege, a system of 7 weirs and two canals was constructed, namely the Juliana Canal and the Lateral Canal.

The Juliana Canal was constructed to overcome the steep part of the Maas, the Grensmaas. The translation of Grensmaas is border Maas, the border between the Netherlands and Belgium. The location of the Juliana Canal is determined by political motivations (Rouvroye/Schreurs, 1996), more detailed information about this topic can be found in *Aanleg Julianakanaal 1935* by *H. Rouvroye / L. Schreurs* [15], commissioned by *Heemkundevereniging Maasstreek*.

The canal is 35 km long, start at the Maas at Limmel near Maastricht and ends in Maas in Maasbracht, as can be seen in figure A.1. The difference in altitude over the canal is 23 meter and is regulated with 3 locks, at Limmel, Born and Maasbracht. At each lock complex a pump station is installed to compensate in the upstream canal section for the water losses due to emptying and filling of the lock. The lock at Limmel is a guard lock, this lock is only closed when high water levels in the Maas occur.

The weir at Borgharen, regulates the distribution of the discharge between Maas and Juliana Canal. The weir maintains the water level at a design level at which vessels of class CEMT Va can sail the canal.

The water discharge which flows to the Juliana canal depends on the Maas discharge. The maximum inflow at Limmel is $25 m^3/s$ (Rijkswaterstaat, 2012 [5]), the excessive discharge flows to the Grensmaas. The locks at Limmel act as a narrowing in the canal, the flow velocity increases as it flows through the locks resulting in a lower water level. If the discharge would exceed the maximum discharge, ships would be unable to sail through the locks. The minimum discharge to the Grensmaas is set at $10 m^3/s$ for environmental reasons (Imtech, 2015 [6]).

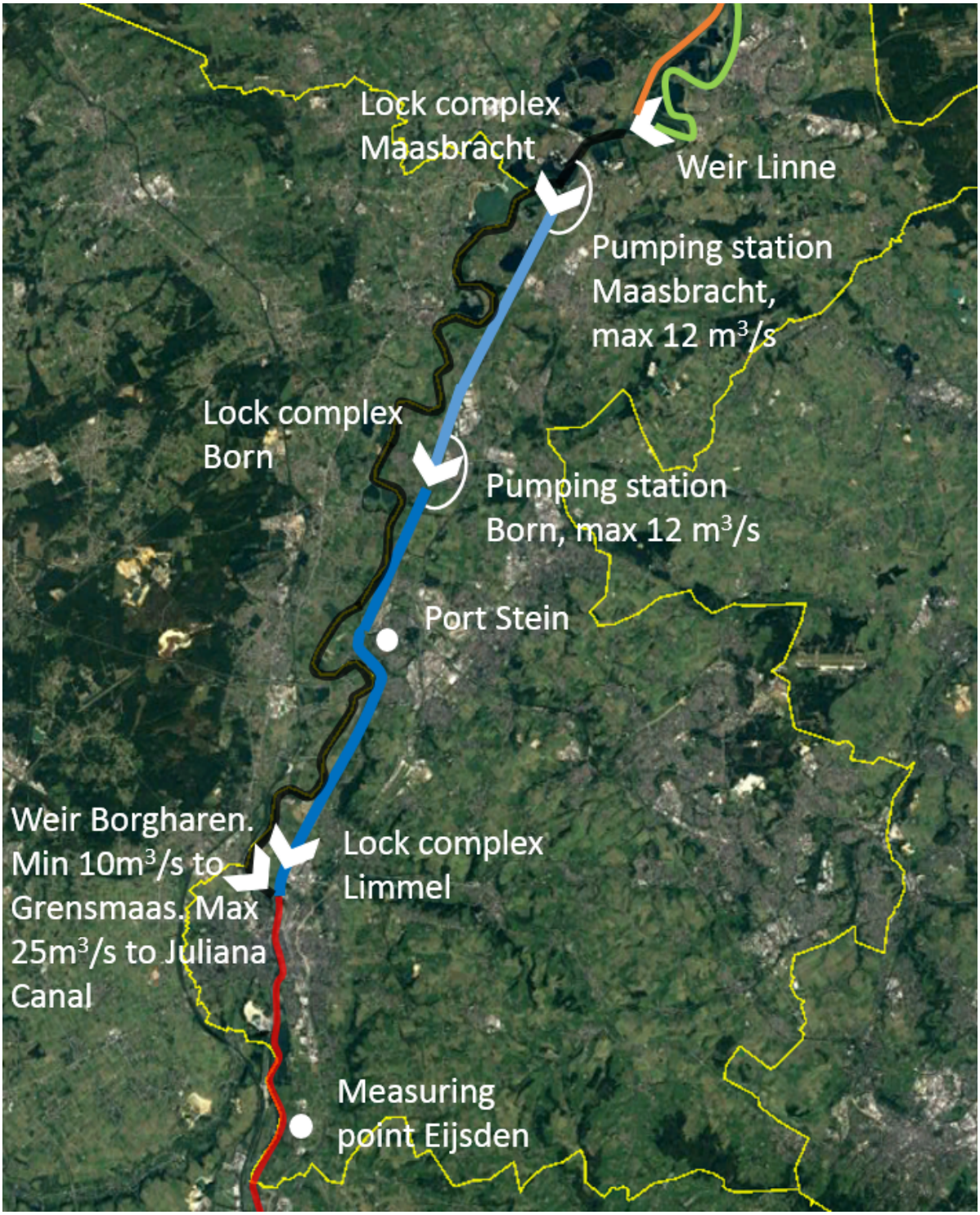

Figure A.1: Overview of the Juliana Canal system

Unlike in most canals, the water level in the Juliana Canal is higher than the surface level next to the canal. The canal has been built on top of the surface area. The surrounding soils are mostly sand and gravel layers, to make the canal watertight the bottom of the canal has been coated with a clay layer of 70cm.

In the figure below, figure A.3, a visualisation is given of the heights of the ground level near Born. Higher grounds are presented in orange, lower areas in green and blue. The bottom level of the Juliana Canal is higher than the surrounding areas as well, not only the water level.

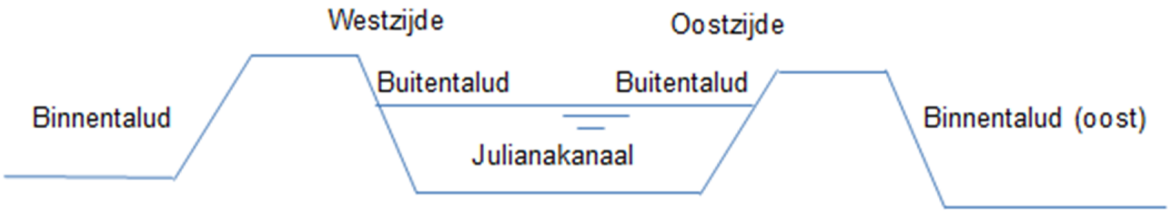

Figure A.2: Overview of a canal cross section

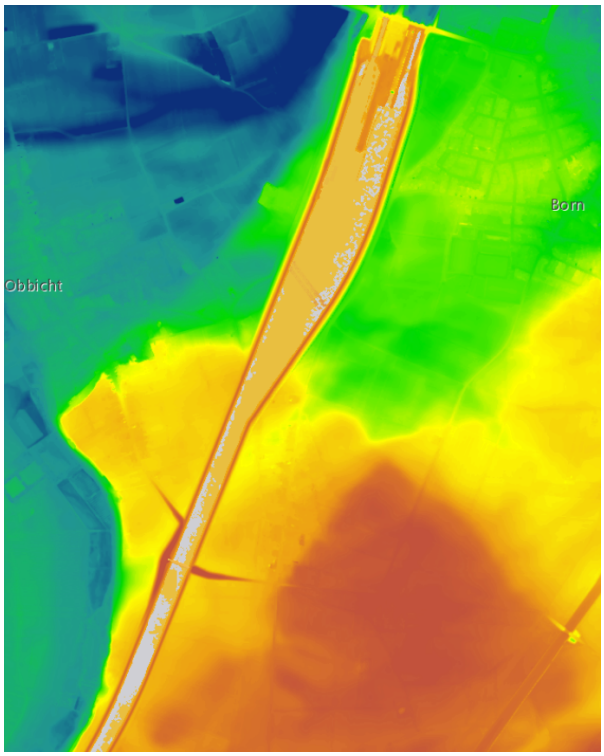

Figure A.3: Heights of ground level near Born (ahn.maps.arcgis.com)

The projects at the Juliana Canal are part of a larger project, the Maaswerken. In these works the whole Maas system is maintained and upgraded, it includes the projects Grensmaas, Zandmaas and Julianakanaal. An overview of the projects is given in figure A.4 below. To comply with the European ambition to improve the North Sea – Mediterranean connection (Balazs, 2015 [1]), the Juliana Canal is upgraded from CEMT Va to CEMT Vb. These activities started in 2013 and are expected to be completed in 2018, the project is awarded by Rijkswaterstaat Ministerie van Infrastructuur en Milieu to DEME-group and is executed by “de Vries & van de Wiel”. Arcadis’ roll is to deliver design support.

Several measures are implemented at the Juliana Canal. A large part of the canal, 26 km, has to be dredged back to the original bottom height of 39m +NAP, these are maintenance works. One and a half km of the canal has to be deepened by 1 meter, the canal will be made watertight again with bentonite mats. The dredging works will be done by dredging with a backhoe on a pontoon.

Ten percent of the canal has to be widened, two techniques are applied. First, where possible, the dike is moved back to create a wider canal. The second option is applied if there is not enough space to displace the dike. Sheet piles are placed in the old dike, the soil on the waterside of the old dike is excavated, resulting in a wider waterline and due to the vertical sheet piles, in a much wider sailing cross section. The clay layer on the dike section is removed as well. To make it watertight again bentonite mats are placed on the bottom. A new technique has been developed to implement the bentonite mats, with the construction vessel Mattedoor. In chapter 2 a more detailed description of the Mattedoor is given. An illustration of a cross section where this method is applied, is given in figure A.5.

In 2012 there were about 23.000 ship passages on the Juliana Canal (Bureau Voorlichting Binnenvaart,

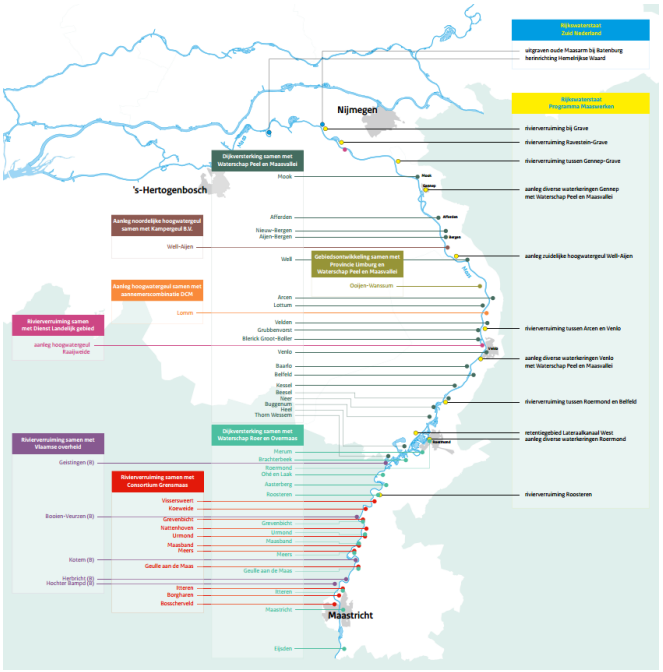

Figure A.4: Overview Maaswerken (www.grensmaas.nl)

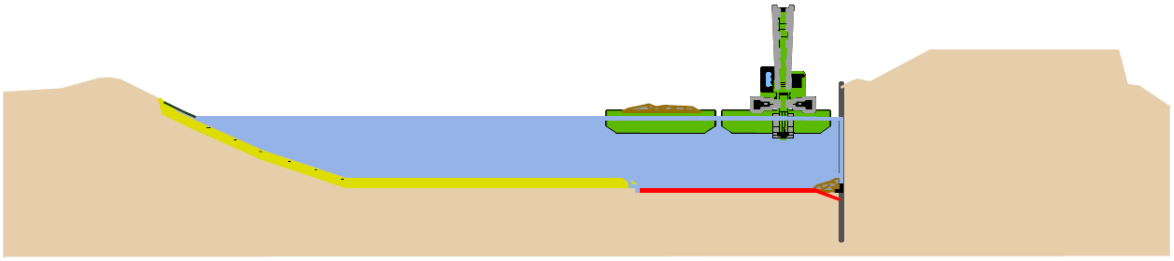

Figure A.5: Cross section of the canal canal widened with a sheet pile construction (www.julianakanaal.nl)

2016 [7]). There is an expected shipping intensity of 1500 vessels of CEMT-class Va per year (Deltares, 2015 [8]). Current CEMT class is Va Groot Rijnschip and Duwvaart with 1 barge (Binnenvaart in beeld, 2016 [9]).

Table A.1: Characteristics of CEMT-class Va and Vb (Rijkwaterstaat, 2011 [10])

Class	Va	Vb
Length [m]	110	170-190
Width [m]	11.4	11.4
Draught (laden) [m]	3.5	3.5
Load [tons]	2051-3300	3951-7050

As mentioned before, there are 3 lock complexes in the lock system of the Juliana Canal. These are located at the beginning of the canal at Limmel, about halfway at Born and near the confluence at Maasbracht. There used to be a fourth lock system at Roosteren but this lock complex was closed and removed in 1965 to improve navigability in the canal. To accomplish this, the canal had to be widened and the dikes made higher between Born and Maasbracht. The lock systems at Born and Maasbracht were upgraded as well. The height difference at the locks at Maasbracht increased to 11.85m, making it the locks with the highest water level difference in the Netherlands (KanaleninNederland.nl, 2010 [11]).
The lock complex at Born originates from the opening of the canal in 1935. In 1965 the lock was upgraded to meet the new specifications after the removal of the Roosteren locks. The lock complex consists of three

locks, the Eastern, Middle and Old lock. The middle lock chamber has been lengthened in 2009 to 225m to meet the requirements for CEMT Vb vessels. Further characteristics of the Born lock complex can be found in table A.2.
The lock complex at Maasbracht originates from 1935 and has been upgraded in 1965 as well. One of the three lock chambers has been lengthened to 225m, the other two locks are 142m in length (Rijkswaterstaat, 2016 [10]). The lock complex at Limmel contains of two locks, these locks are only used when there is a high water discharge at the Maas. The lock complex is under construction at the moment and will be replaced with a sluice. An overview of the current locks in given in table A.2.

Table A.2: Dimensions of lock chambers in the lock system

Complex	Lock chamber	Length [m]	Width [m]	Depth [m]	Height difference [m]
Limmel	Chamber 1	136	16	5	min: 0, max: 2
	Chamber 2	136	16	5	min: 0, max: 2
Born	East	136	16	5	11.35
	Middle	225	16	5	11.35
	West	136	16	5	11.35
Maasbracht	East	225	16	4.1	11.85
	Middle	142	16	4.1	11.85
	West	142	16	4.1	11.85

A.2. FUNCTIONAL CONDITIONS OF THE LOCKS

There are 3 lock complexes situated in the Juliana Canal lock system. The lock complexes of Limmel and Born are located within the geographical boundary conditions and will be elaborated upon.

Lock complex at Born: The lock complex at Born consists of 3 locks. The dimensions of the lock chambers are given in table A.2. The frequency of filling and emptying each chamber is given in table A.3.

Table A.3: Filling and emptying per lock, numbers of 2014 and 2015 (Rijkswaterstaat, 2016 [12])

Name lock	2014		2015	
	With ships	Without ships	With ships	Without ships
Oost	8742	2326	7328	2035
Midden	3795	909	6452	1653
West	4966	1301	3322	915

The volume of water which flows through the lock gates depends on the ships in the lock. The flow velocities depend on the volume, the difference in water level and the outflow area. These data has to be collected.

Lock complex at Limmel:
The lock complex at Limmel is only in use at high Maas discharges, if the discharge is higher than 1280 m3/s, measured at Borgharen. In other situations, the locks are open. The lock complex at Limmel consists of two lock chambers, each with a width of 16 meters and a length of 136 meters.
In figure A.6 an overview is given of the discharges of the Maas of the past 5 years. In orange is the limit discharge of $Q = 1280 m^3/s$ drawn. The lock system is used a few times in the past 5 years, about once every year but sometimes a year not at all. When the discharge is high it occasionally lasts for about a week.

The lock complex at Limmel is going to be replaced by a sluice. The construction works start in 2015 and will be finished in 2018. The sluice will be 50 meters wide, which is wider than in the current situation, making it easier to pass for vessels of the higher CEMT class Vb. Another positive effect could be that the increase of flow velocities creating a decrease of the water level due to the narrowing of the canal by the construction will decrease.

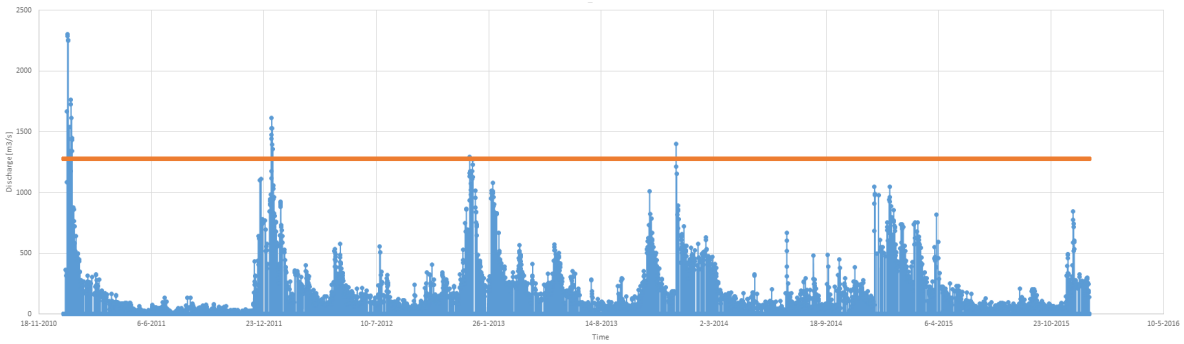

Figure A.6: The discharges measured at Eisden, from 2011 untill 2015

A.3. MEASUREMENT DEVICES

Two types of measuring devices are used to collect data: high frequency pressure mats and an ADCP. The pressure mats measure the water depth, the ADCP the currents.

THE HIGH FREQUENCY PRESSURE MATS

The high frequency pressure mats measure the pressure above the mat. From the pressure, the water depths are determined. The water level changes can be calculated from this data. There are 4 pressure mats used in the canal section between Born and Stein. The locations of the pressure mats are given in figure A.7.

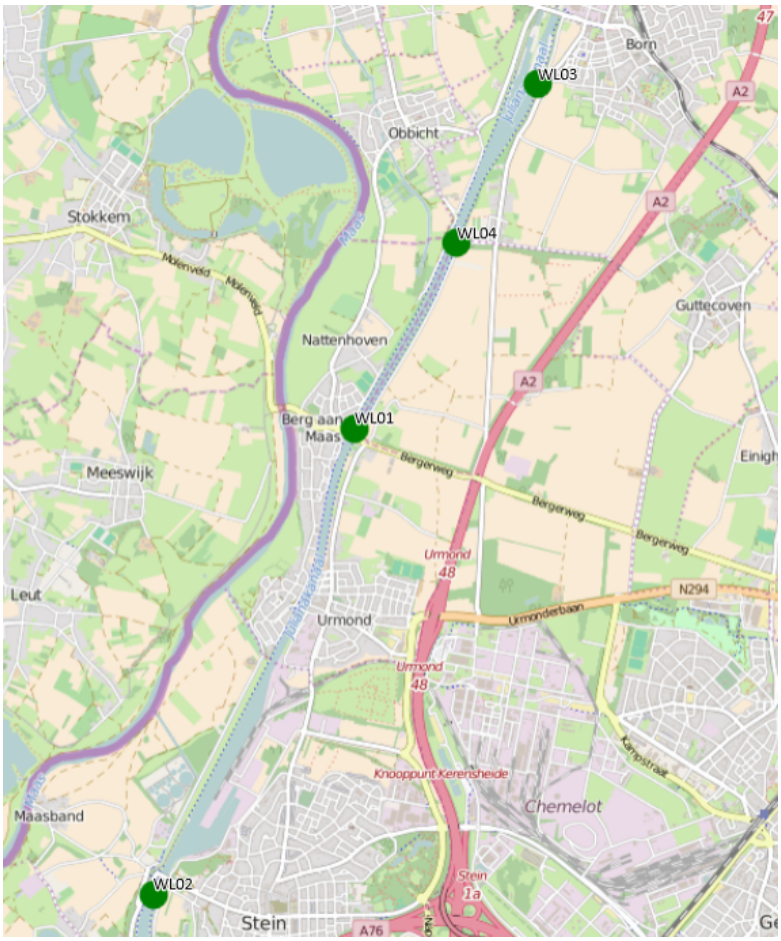

Figure A.7: Locations of the four pressure mats

THE ADCP

The ADCP is a device that measures the currents in the canal. ADCP is an abbreviation for Acoustic Doppler Current Profiler. An example of the data from the ADCP is given in figure A.8. The ADCP is used to determine the base current in the canal. The base current is determined at $u_{base} = 0.17 m/s$, as can be seen in figure A.8. The ADCP is placed at the construction pontoon *Mattedoor*.

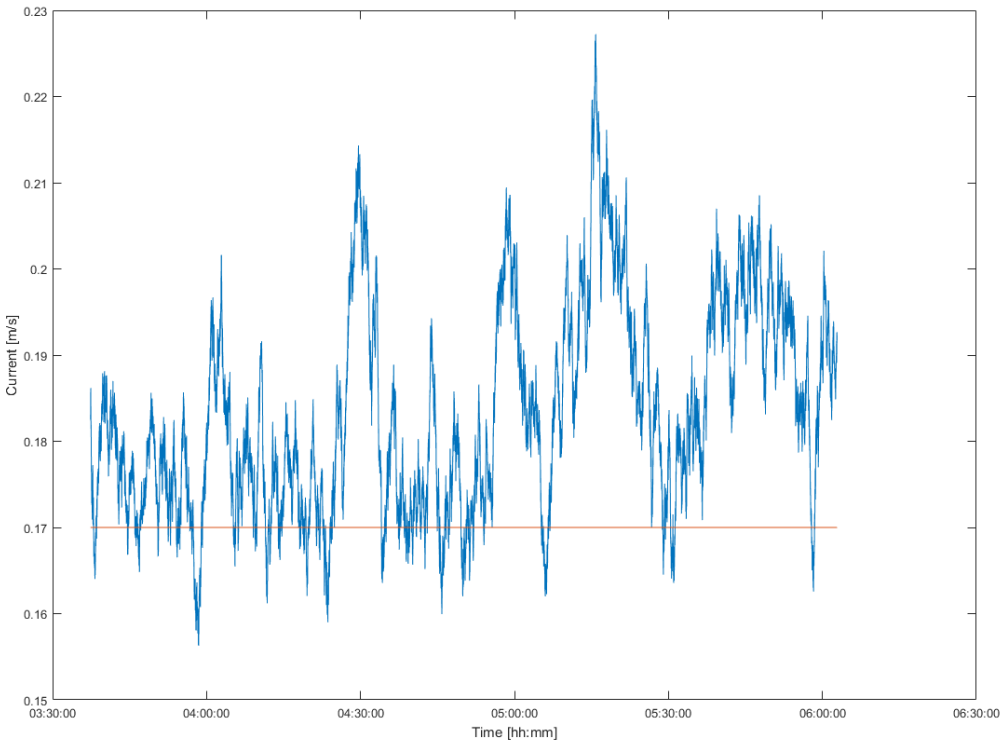

Figure A.8: Example of ADCP data

B

SPECTRUM ANALYSIS

This appendix is about the spectrum analysis of the depth measurements. Spectral analyses is the generally the first step to determine the significant wave heights in a system. This method has been applied to the Juliana Canal as well. Unfortunately the conclusion had to be made that a spectral analysis is not applicable on this system. The number of reflections in the canal result is such a randomness that a Fourier transformation did not give any accurate results that could be worked with. For integrity, the methodology of the analysis is described in this Appendix.

B.1. DATA COLLECTION

The analysis to make the spectrum has been executed with depth measurements. The depth measurements are done with high frequency pressure measure devices. These are placed on the bottom of the canal on locations of interest. Figure B.1 gives an overview where the devices lay on April 25th. Location W03 is close to the lock complex of Born, the place where the translation waves are generated. Location W02 is "upstream" of the port of Stein. Due to the port, reflection waves can occur making this an interesting location to explore the effects of changes in the profile. Locations W01 and W04 are on the canal section in between. The interaction between reflected waves can be observed on two different locations but on the same section. This is interesting data for calibration of the translation waves model.

As can be seen in table B.1 , the devices on location W02 and W04 were placed in begin March. The other two were added in begin April.

Info on the pressure devices:

The measurements are performed at a rate of 1Hz, 1 measurement per second.

Table B.1: Information of the dataset

Number	Location	Longitude	Latitude	Period
W01	Berg aan de Maas	5.7748167	51.0047167	10-04-2016 t/m 24-04-2016
W02	Stein	5.7508000	50.9698500	08-03-2016 t/m 21-03-2016
W02	Stein	5.7508000	50.9698500	10-04-2016 t/m 24-04-2016
W03	Born	5.7972800	51.0307300	10-04-2016 t/m 24-04-2016
W04	Obbicht	5.7873667	51.0184333	02-03-2016 t/m 21-03-2016
W04	Obbicht	5.7873667	51.0184333	10-04-2016 t/m 24-04-2016

B.2. ANALYSIS METHOD TO CREATE A SPECTRUM

The data is analyse in Matlab using a Fourier Transformation. The output after the transformation is a set of sinusoidal equations with an amplitude and a frequency. The high frequencies are filtered out, these frequencies correspond with shipping movements and aerial induced waves. At this time the translation waves are of interest, these have a lower frequency. The frequencies which are filtered out are lower than 0.01Hz, or

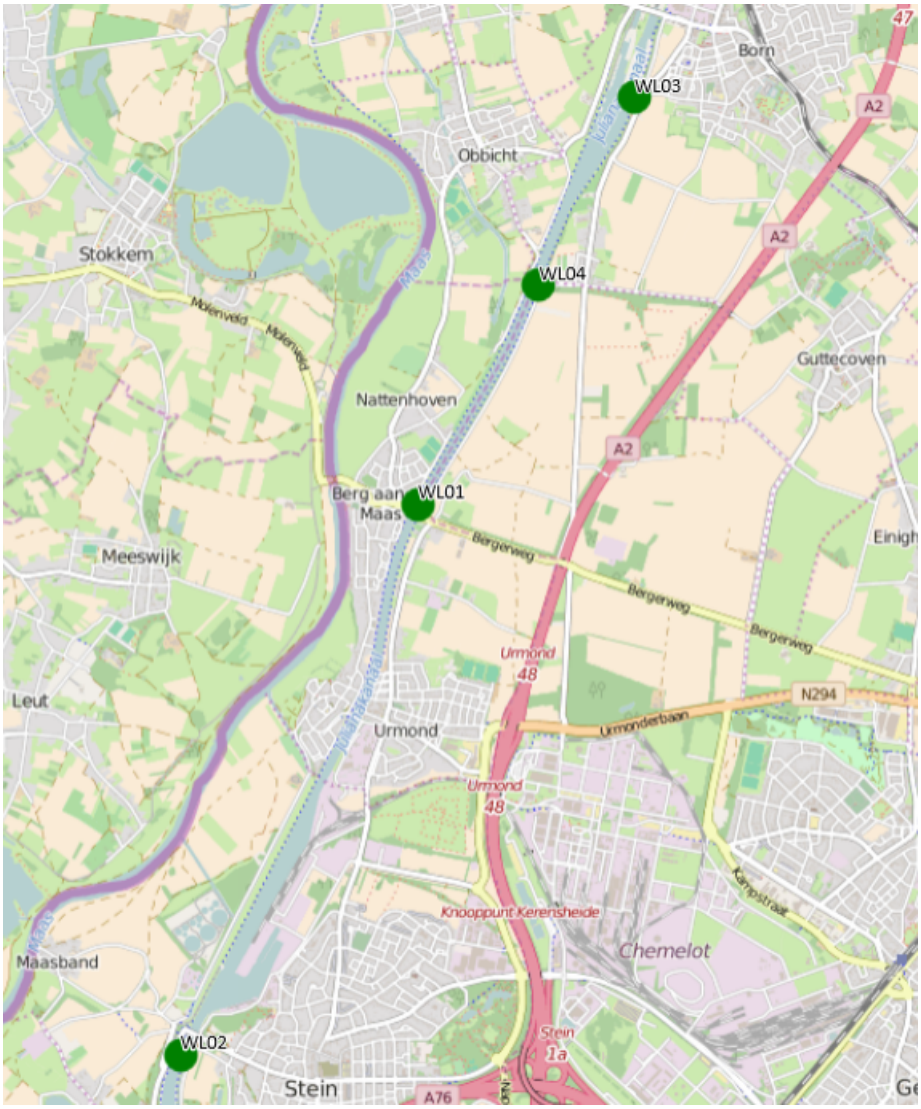

Figure B.1: Locations pressure measure devices on April 25th

100 seconds. The filtration is done with a Butterworth filter technique. Frequencies with a period higher than an hour are also assumed not to be in the region where the translation waves are positioned and are ignored. Frequencies are converted to periods to make the interpretation easier. The periods which are analysed have a period between 100 seconds and one hour. The amplitudes and periods are plotted in graphs per dataset. Peaks occur in the graph when that period occurs with a high amplitude.

B.3. INTERPRETATION OF THE RESULTS

The results still have a lot of fluctuation in the graphs. To obtain a more clear view, the floating average of the datapoints has been taken every 50 and 100 steps.

B.3.1. OBSERVATIONS AND CORRELATION WITH LOCKS

From theory it is known that there is a direct correlation between a translation wave and the filling and emptying of a lock chamber. So to make comments on the results and whether it makes any sense with respect to translation waves, the time it takes to fill and empty a lock chambers has to be known. The periods of the lock chambers are as follows:

Table B.2: Emptying and Filling times of the lock chambers

Lock chamber	Filling and Emptying	
	Minutes	Seconds
Oost	10:46	646
Midden	12:54	774
West (or old)	14:20	860

The lock times given above are based on a single measurement with a stopwatch. The time periods should be dealt with, with caution.

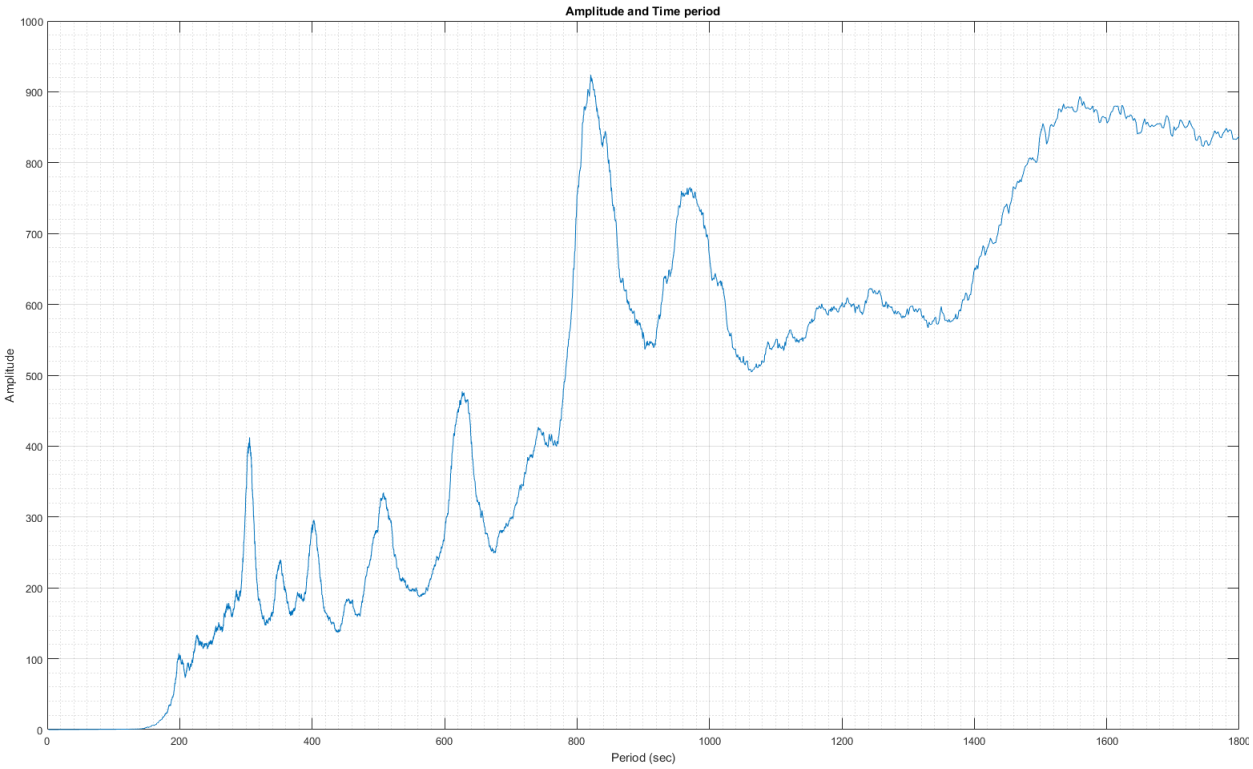

Figure B.2: Wave spectrum Obbicht March 2016

Looking at the spectrum in figure B.2 and taking the lock times in account, the results can roughly be

divided in three categories:

1. period < 600 s
2. 600s ≤ period ≤ 1000s
3. period > 1000s

This classification can be seen in the other spectra as well. The periods between 600s and 1000s are the area where the translation waves are expected, on the basis of the filling and emptying times of the locks. In figureB.2 three clear peaks can be distinguished in the period between 600s and 1000s: around 630s, 820s and 970s. These are believed to be the result of the lock chambers respectively Oost, Midden and West.
In the regime below 600s, 5 different peaks are observed. The current theory is that translation waves in the canal generate higher order harmonic waves. A higher order harmonic wave is a positive integer multiple of the frequency of the fundamental wave, of the original wave. So the second order wave, also known as the first higher order wave, is double the frequency of the fundamental wave. In the spectrum above, the period is plotted on the x-axis, the period is $1/frequency$, so the first higher order harmonic is half the period. This results in the measurement for Obbicht during March 2016 in a first order harmonic wave for the Oost chamber at about 300s and for the Midden chamber at about 400s.
Around 1500 seconds there is in all spectra a peak, in some instances a very high clear peak.
These results all look very promising but the results are only plotted at the time periods where the translation waves are most likely situated, not taking account for the whole spectrum. The whole spectrum is presented in figure B.3. The interval discussed is just a tiny section of the spectrum. The energy levels at longer periods are much higher making the section with periods up to 1400 seconds negligible.

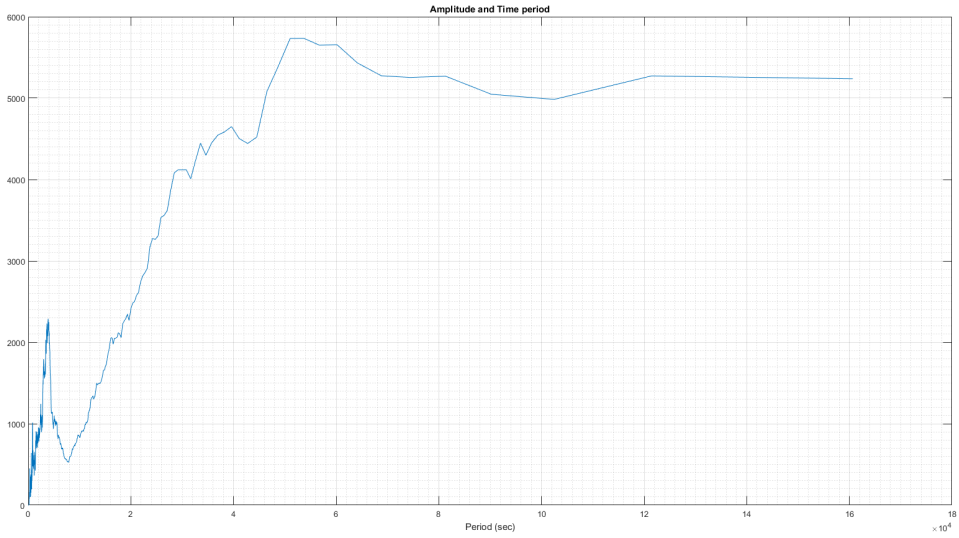

Figure B.3: Wave periods of the whole spectrum

To rule out modelling mistakes, the spectrum has been analysed with another model as well. In this model is the wave angle included as well. In figure B.4 are the results of this analysis presented. The phases cover the whole graph, it is completely random where the waves come from. The amplitudes are spread out over the width of the graph as well and are extremely small. Only one conclusion can be taken, this method is not suitable for this case.

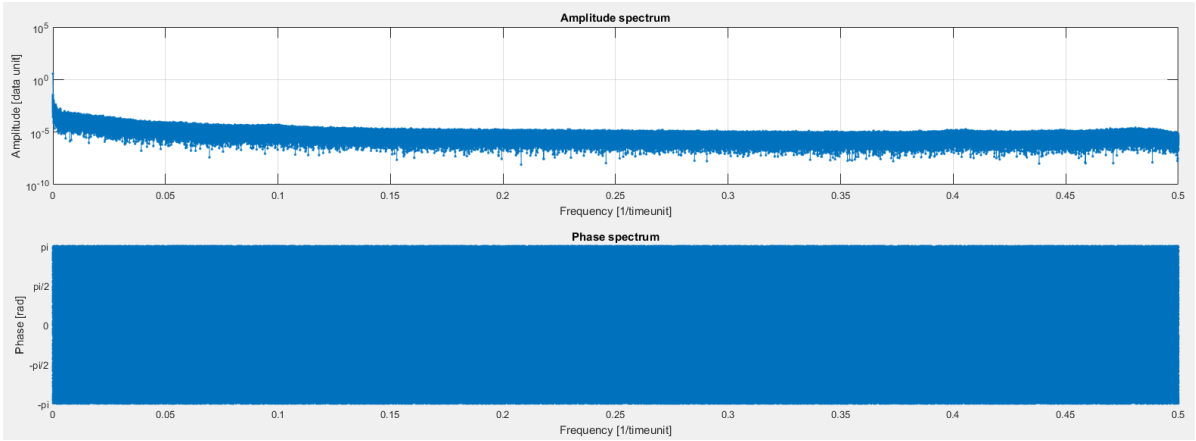

Figure B.4: Spectral analysis with a secondary model, including wave angles

C

RESPONSE OF THE PONTOON

In this chapter the response of the pontoon to translation waves and at which currents the pontoon will start to move, will be discussed. The calculation is a simplified calculation to quickly acquire insight in the magnitude of forces.

C.1. DESCRIPTION ON THE PONTOON

In this section a description of pontoon the "Mattedoor" will be given. This is the pontoon carrying out the construction works at the Juliana Canal. A top view with dimensions is given in figure ??. The depth of the Mattedoor is 1 meter. The pontoon is kept at its place by four spud-poles. Each spud-pole has a diameter of 60cm. On the bottom of a spud-pole is a 2x2 meter steel plate attached to distribute the vertical forced over the canal bottom and prevent it to subside in the mud.

C.2. FORCES ON PONTOON

The calculation is a 1D simplification of the situation, only forces in the lateral direction of the canal are included. The forces to keep the pontoon at its location are the resistance forces of the spud-poles which are pulled downward with 20 tonnes per pole. The friction between the bottom and the pole result in a resistance force. Described in formula form:

$$F_{fric} = n * \mu * N \tag{C.1}$$

In which:
n [-] = number of poles
μ [-] = friction coefficient between pole and bottom
N [N] = vertical force on bottom

There are 3 type of driving forces included: the translation waves, return currents by shipping and wind waves. Each will be explained below.

First, the currents due to translation waves. Before the forces can be calculated the magnitude of the current has to be known. A large volume of water is extracted at the lock when the lock is filling. This "gap" has to be filled up, water flows from the adjacent section to the section with lower water level. This continues on and on, creating a negative wave travelling away from the lock. The wave moves away from the lock but the current to fill the "gap" move toward the lock, in the opposite direction of the propagation direction. The magnitude of the current depends on the wave height:

$$u = \frac{c \cdot h}{d} \tag{C.2}$$

In which:
u [m/s] = current of the water
c [m/s] = celerity of the wave

h [m] = wave height
d [m] = water depth

In this calculation assumptions are made for the parameters, conservative values are taken. The values of the parameters are presented in table C.1.

Table C.1: Parameters in current calcuation

Parameter	Symbol	Value	Unit
Celerity of the wave	c	6	m/s
Wave height	h	0.5	m
Water depth	d	5	m
Current of the water	u	0.71	m/s

The maximum current is determined at $u = 0.71 m/s$, the force resulting from the current can now be calculated. This is done according to the following formula:

$$F = 1/2 * \rho_{water} * u^2 * Cd_{block} * A_{blocked} \tag{C.3}$$

Formula C.3 is used to calculate the drag forces of the water over the pontoon and for the force resulting from wind on the top side of the pontoon. The forces of the current on the pontoon is divided in a square part and the cylindrical parts of the spud poles. The parameters used in the formula C.3 for the three forces are listed in table C.2.

Table C.2: Parameters for block section

Parameter	Symbol	Value	Unit
Density water	ρ_{water}	1000	kg/m^3
Density air	ρ_{air}	1	kg/m^3
Current	u	0.71	m/s
Wind velocity	u_{wind}	30	m/s
Drag coefficient block	Cd_{block}	1.05	-
Drag coefficient cylinder	$Cd_{cylinder}$	0.48	-
Drag coefficient top side	$Cd_{topside}$	1.05	-
Area block	A_{block}	24.24	m^2
Area cylinder	$A_{cylinder}$	2.4	m^2
Area top side	$A_{topside}$	35	m^2

The wind speed is estimated at a storm with wind speeds of $30 m/s$, a conservative value. The top side of the pontoon consists of two containers on top of each other, with stairs on the side. A 20 feet container is about 6 meters wide, add the stair, a total width of 7 meters is assumed with a total hight of 5 meters. Resulting in a total top side area of 35 m^2.

Finally, the return currents due to shipping. The return currents are taken from the design values used by the contractor. The return current is determined per ship class, difference is made between laden and unladen vessels as well. The maximum return currents in the canal at 90% of the limit velocity are given in table C.3.

Table C.3: Currents due to shipping

Class	Length [m]	Width [m]	Depth [m]	Return Current [m/s]	Propeller wash [m/s]
M8 laden	185	11.45	3.5	1.18	0.65
M8 unladen	185	11.45	0.9	0.92	0.00
M9 laden	135	11.45	3.5	1.18	0.83
M9 unladen	135	11.45	0.8	0.92	0.00

The driving force can occur simultaneously, the results after combining different formats of the forces are presented in table C.4. The currents as a result of passing vessels simultaneous with the translation wave are combined in the calculations for the cylinder force and block force.
The unity check is the resistance terms divided by the driving terms. In this situation the bottom friction forces divided by the drag forces. Looking at the situation with only translation waves the UC is more than 20, this means that the resistance terms are 20 times larger than the driving terms. It is safe to say that the pontoon will not move. In the situation that a ship passes the pontoon while a translation wave is travelling through the canal, the UC is still almost 3. Even in the situation with the translation wave, shipping and a heavy storm all at the same time under conservative condition, the unity check is more than 2. Horizontal movement in lateral direction will not occur.

Table C.4: Results of combining different currents

Force	Symbol	Unit	Only wave	Wave + wind	Wave + ship	Wave + ship + wind
Cylinder force	$F_{cylinder}$	kN	1.2	1.2	8.2	8.2
Block force	F_{block}	kN	6.4	6.4	45.4	45.4
Wind force	F_{wind}	kN	-	16.5	-	16.5
Total drag force	F_{driv_tot}	kN	7.6	24.1	53.6	70.2
Downward pressure	m_{pole}	kg	20000	20000	20000	20000
Friction coeff steel-mud	μ	-	0,2	0,2	0,2	0,2
#piles	n		4	4	4	4
Downward force	F_{down}	kN	196	196	196	196
Horizontal friction force	F_{fric_tot}	kN	157	157	157	157
Unity check	UC	-	20.77	6.51	2.93	2.24

‘

D

LITERATURE STUDY

D.1. TRANSLATION WAVES ACCORDING TO DIETZ

Dietz' research follows from the project carried out by Thijsse. The theory is expanded, with the primary focus on the resistance terms. Where Thijsse's theory was mostly based on pragmatic obtained results, is Dietz's research mostly based on mathematical and abstract points. The theory is verified in a flume in the laboratory, not in a case study.

In table D.1 an overview is given of the symbols used in the derivation of Dietz.

Table D.1: Symbols used in Dietz' derivation

Symbol	Parameter	Dimension
t	Time	s
x	Distance along the canal	m
z	Momentary average depth	m
h	Original average water depth	m
v	Water velocity, averaged over cross section	m/s
c	Wave velocity at a certain height	m/s
g	Gravitational acceleration	m/s^2
C	Resistance coefficient of Eytelwein (Chezy)	$m^{1/2}/s^2$
A	Area of cross section	m^2
u	Wet perimeter	m
b	Original width of the water surface	m
η	Wave height ratio with depth	[-]
τ	Average of the tangents of the angles the berms make with the perpendicular	rad

Dietz starts the derivation with the hydrodynamic equations:

$$\frac{\partial z}{\partial t} + \frac{\partial (vz)}{\partial x} = 0 \tag{D.1}$$

$$g\frac{\partial z}{\partial x} + \frac{\partial v}{\partial t} + v\frac{\partial v}{\partial x} + \frac{g}{C^2}\frac{u}{A}v^2 = 0 \tag{D.2}$$

After the hydrodynamic equations the Saint Venant equations are applied and assumptions are made. For the full derivation is referred to Dietz' paper "Conduct of translation waves in canals" (Dietz, 1941 [3]).

Assumptions:

- Vertical accelerations are neglected
- Advection terms are neglected
- Local changes in cross sections can be neglected

The parameter η is introduced, this is defined as the dimensionless ratio between the wave height and the original water-level.

$$\eta = \frac{z-h}{h} \tag{D.3}$$

After the derivations, Dietz concluded that the celerity of a translation wave in a prismatic canal can be described as:

$$c = \sqrt{gh}\left\{1+\frac{3}{2}\eta - \frac{g\sqrt{gh}}{2C^2h}\left(\int A\,dt + B\frac{dt}{d\eta}\right)\right\} \tag{D.4}$$

In which:

$$A = \frac{\eta^2}{\sqrt{1+\eta}} \quad \text{and} \quad B = \eta^2\sqrt{1+\eta} \tag{D.5}$$

The equations above are derived for a prismatic canal. In reality the canal will not have vertical walls. A correction has to be made for the slope of the berms. The parameter τ is introduced to take the slopes in account. τ is the average of the tangents of the angles the berms make with the perpendicular. The derivation is again in the paper "Conduct of translation waves in canals" by D.N. Dietz [3]. This results in following formula:

$$c = \sqrt{gh}\left\{1+\left(1-\frac{2\tau h}{3b}\right)\frac{3}{2}\eta - \frac{g\sqrt{gh}}{2C^2h}\left(\int A\,dt + B\frac{dt}{d\eta}\right)\right\} \tag{D.6}$$

D.2. CREATING A WAVE SPECTRUM USING A FOURIER ANALYSIS

Spectral analyses is the generally the first step to determine the significant wave height on a location. Calculations of the significant wave height is not of interest for this case study, the wave height will be determined by the lock-chamber-model. In this section only the frequency spectrum determination will be addressed.

The observations of the wave heights are treated as one realisation of a stochastic process. The the surface elevation of the measurements can be reproduced can be reproduced as the sum of a large number of harmonic wave components. The reproduction of the signal as the sum of harmonic waves is called a Fourier series. The Fourier series can be described as a formula as:

$$\eta(t) = \sum_{i=1}^{N} a_i \cos(2\pi f_i t + \alpha_i) \tag{D.7}$$

With:
η [m] = surface elevation
a_i [m] = amplitude
α [rad] = phase
f [s^{-1}] = frequency
t [s] = time

a_i and α_i are the amplitude and phase of each frequency, $f_i = i/D$. D is the duration of the measurement. The values of the amplitude and phase for each frequency can be determined by Fourier analysis of the wave record. The results of the amplitudes and phases can be plotted in a amplitude and phase spectrum. As can be seen in the left figure of figure D.1.

As can be seen in the right figure in figure D.1 the phases α_i do not have a dominant direction. For most records the the phase does not have any preference, the phase spectrum will be ignored. Only the amplitude spectrum is left to analyse. As said before, the measurements are one observation of a stochastic process. If the measurements would be performed again, under the same conditions, the amplitude spectrum would still be different. To reduce the error between the samples, the average of a large quantity of measurements can be taken:

$$\overline{a}_i = \frac{1}{M}\sum_{i=1}^{M} a_i \tag{D.8}$$

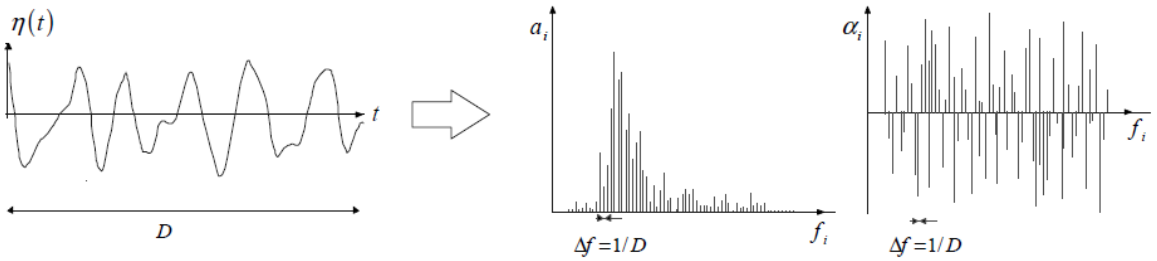

Figure D.1: Example of observed surface elevation and its amplitude and phase spactrum ([16])

The larger the amount of measurement M, the smaller the error, the value of $\overline{a}_i$ converges towards a constant value. But, there is still a dissimilarity. In nature, all frequencies are present. In the amplitude spectrum in figure D.1 only the frequencies $f_i = i/D$ are taken in account. To minimize the dissimilarity, the average amplitude $\overline{a}_i$ over the frequency interval Δf can be taken. This gives the amplitude density $\overline{a}_i/\Delta f$ at each frequency.
An better alternative is to take the variance. The variance is statistically a more relevant quantity than the amplitude. Furthermore, the energy of the waves is proportional to the variance, according to the linear theory for surface gravity waves. From above two reasons can be concluded that a connection might be made between variance and wave energy, as well as to particle velocity and pressure variations. The variance of each wave component is given by $^1/_2\overline{a_i^2}$. Dividing the variance per wave component by the frequency interval gives the variance density, $^1/_2\overline{a_i^2} \rightarrow ^1/_2\overline{a_i^2}/\Delta f$. The variance jumps from one frequency band to another, to solve this the frequency interval has to be decreased, approaching zero, $\Delta f \rightarrow 0$. The variance density spectrum is now defined as:

$$E(f) = \lim_{\Delta f \rightarrow 0} \frac{1}{\Delta f} \frac{1}{2} \rho g \overline{a}^2 \tag{D.9}$$

For more thorough information and further applications of the spectrum is referred to "Waves in Oceanic and Coastal Waters" by L.H. Holthuijsen ([16]).

D.3. SHIP INDUCED WAVES

There are three main categories for ship induced currents:

- Primary waves
- Secondary waves
- Propeller wash

The waves induced by vessels depend on the dimensions and velocity of the vessels. The velocity differs between vessel. The dimensions of the vessels are restricted because of the dimensions and bathymetry of the canal. In the Juliana Canal ships of the CEMT Va are allowed, after constructions CEMT Vb class is permitted. A distinction is made between Motor vessels and barges and Pushed convoys. In the table below the dimensions according to the CEMT classes are given.

Table D.2: Dimensions of CEMT-class Va and Vb (Rijkswaterstaat 2011 [17])

Class	Length (m)	Beam (m)	Draught (m)	Tonnage (T)	Minimum height under bridges (m)
Motor vessels and barges					
Va	95-110	11.40	2.50-2.80	2500-3000	5.25
Vb	95-110	11.40	2.50-2.80	2500-3000	7.00 or 9.10
Pushed convoys					
Va	95-110	11.40	2.50-4.50	2500-3000	5.25
Vb	172-185	11.40	2.50-4.50	2500-3000	7.00 or 9.10

D.3.1. PRIMARY WAVES

The primary waves are directly linked to the water displacement by the ship. The primary waves are formed by the combination of the water level depression and the return current. The theoretical background will be discussed according to the approach of Schijf. This approach is based on the theorem of Bernoulli and the equation of continuity. This method will be discussed later.

Due to the primary waves squat will occur. Squad is the combination of sinkage and trim. The water displacement by the ship causes a lowering in water level next to the ship. This effect creates a decrease in nautical depth, making the ship to sail at a lower level relative to the bottom, this phenomenon is called sinkage. Sinkage is more present at the aft part of the ship than at the bow resulting the vessel to sail under an slight angle.

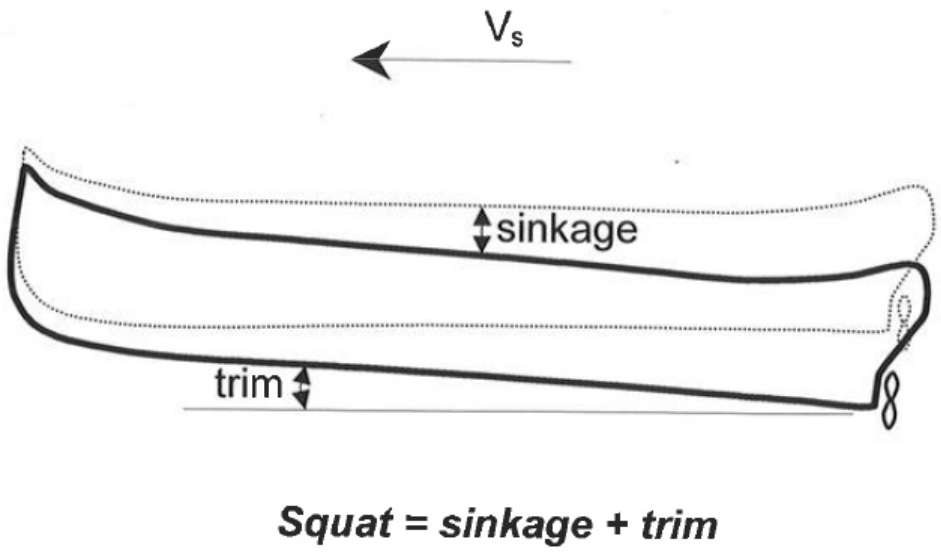

Figure D.2: definitions of squat and sinkage

The water motion around a sailing vessel is complicated and hard to describe. To give an expression for the effects of a sailing vessel, simplifications and assumptions have been made. The following assumptions are made in this theorem, according to Verheij, 2008.

- A straight, infinitely-long prismatic canal section
- A prismatic amidships cross-section over the total length of the ship
- A constant speed of the ship
- A uniform return current over the total wet-waterway profile, next to and below the ship
- A uniform water-level depression over the total width of the canal
- Sinkage of the ship equal to the water-level depression
- No trim of the ship
- No energy losses, omitting of shear stress and inertia losses
- No influence of ship-initiated waves or phenomena caused by helical motion

In the theory below a ship-fixed co-ordinate system is assumed, the axes are considered to move together with the ship. In this co-ordinate system the ships appears to be still in the water, the water appears to flow underneath the vessel with velocity V_s. The velocity alongside and under the ship will become equal to $(V_s + U_r)$. Applying Bernoulli's theorem between cross section 1 and 2 (see figureD.2, below) gives:

$$z = \frac{(V_s + U_r)^2}{2g} - \frac{V_s^2}{2g} = \frac{V_s + U_r}{2g} + \frac{U_r^2}{2g} \tag{D.10}$$

When the continuity conditions are applied for cross-section 1 and 2 the formula or the discharge is:

$$Q = V_s * A_c = (V_s + U_r) * (A_c - A_s - W_s * z) \tag{D.11}$$

After differentiating the discharge, dQ/dz, calculation the maximum water level depression z_{max}, applying $A_c = W_s * h$ and rearranging the formula, the maximum discharge Q_max is calculated:

$$\frac{Q_{max}}{W_s * g^{1/2} * h^{-3/2}} = \left\{ \frac{2}{3} \left(1 - \frac{A_s}{A_c} + \frac{1}{2} * \frac{V_l^2 im}{gh} \right) \right\} \tag{D.12}$$

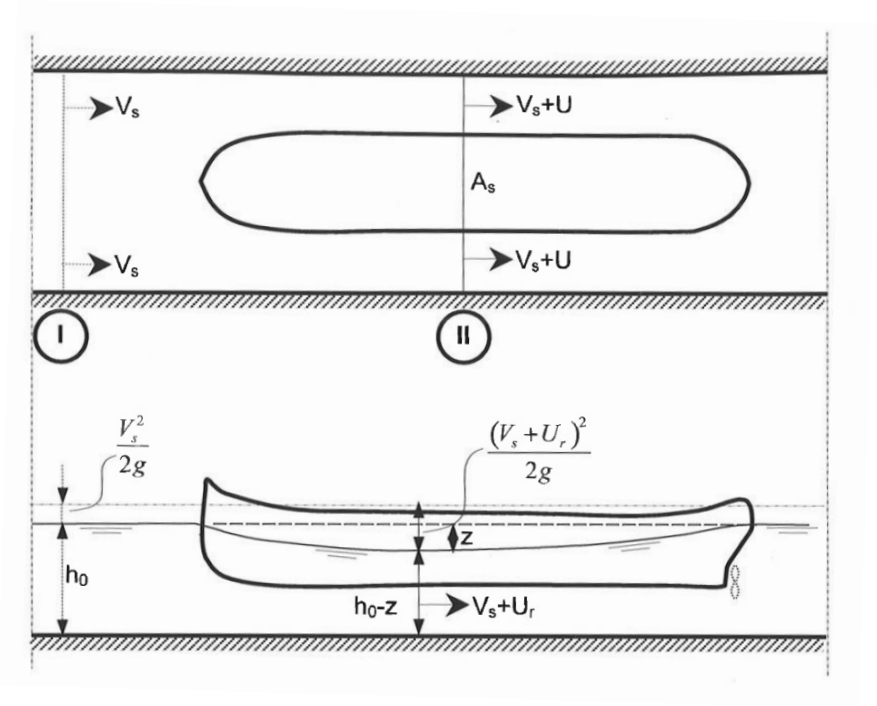

Figure D.3: Ship-fixed co-ordinate system

Table D.3: Symbols and dimensions of parameters used in ship wave formulae

Symbol	Parameter	Dimension
A_c	$W_s * h_0$ = wet cross section area of undisturbed canal	m^2
A_s	$B_s * D$ = ship's underwater amidships cross section	m^2
h_0	Water depth of undisturbed canal	m
W_s	Width at water-level of undisturbed canal	m
B_s	Ship's beam at midships section	m
D	Draught of ship at midships section	m
V_s	Ship's service speed	m/s
z	Maximum water-level depression at midships section	m
U_r	Maximum return current velocity along ship at midships section	m/s
Q	Discharge which passes along the vessel	m^3/s

The formulae written above are the core of the method of preserving equations.

The maximum speed of a ship is restricted to the waterways depth and width. The limiting speed of the vessel is reached when the return current has reached its maximum as a function of the water-level depression. The restriction takes into account the Froude number. At Fr=1, the flowing water reaches its critical depth. When the water depth alongside the ship is equal to the critical depth, the ships speed will not be able to increase its speed, the limiting speed has been reached according to Schijf.

After combining the formulae written above and rearranging the parameters the equations can be written as :

$$1 - \frac{A_s}{A_c} + \frac{1}{2}\left(\frac{V_{lim}}{\sqrt{gh}}\right)^2 - \frac{3}{2}\left(\frac{V_{lim}}{\sqrt{gh}}\right)^{2/3} = 0 \tag{D.13}$$

In the two extreme cases where:

1. $As/Ac = 0 \rightarrow V_{lim} = \sqrt{gh} = 1 \rightarrow V_{lim} = \sqrt{gh}$
2. $As/Ac = 1 \rightarrow V_{lim} = \sqrt{gh} = 0 \rightarrow V_{lim} = 0$

In the first situation the cross section of the ship is very small/negligible to the area of the canal.The maximum speed is equal to the velocity of a wave in shallow water. In the second situation the area of the canal is about the same size as the cross section of the ship. The ship is squeezed in the canal and will not be able to sail through the canal. Normally, the value for A_s/A_c is between 0.1 and 0.3.

After defining the maximum service speed V_s, the maximum return current can be determined:

$$\frac{U_{lim}}{\sqrt{gh}} = \sqrt{\frac{2}{3}\cdot\left(1-\frac{A_s}{A_c}+\frac{1}{2}\left(\frac{V_{lim}}{\sqrt{gh}}\right)^2\right)} - \frac{V_{lim}}{\sqrt{gh}} \tag{D.14}$$

The result after tests (executed by Delft Hydraulics, 1953) did not fully comply with the theory, the correction factor α was added. The correction factor compensates for the non-uniform distribution of the return current. In the theoretical approach a regular velocity distribution was assumed alongside and under the ship. The factor α can be calculated as:

$$\alpha = 1.4 - 0.4\cdot\frac{V_s}{V_{lim}} \tag{D.15}$$

The value of factor α normally varies between 1.05 and 1.2. The correction factor is implemented in the water depth, as:

$$z = \alpha\cdot\frac{(V_s+U_r)^2}{2\cdot g} - \frac{V_s^2}{2\cdot g} \tag{D.16}$$

D.3.2. SECONDARY WAVES

Secondary waves occur at two locations on the ship, a group of waves at the bow and at the stern region. the groups consists of two systems of waves, the divergent waves and transversal waves. Divergent waves become wider at both sides of the sailing line. The transversal waves are generated behind the pressure point. When divergent and transverse waves meet, inference cusps are formed. Where two or more waves meet at the same time, cusps arise. The summation of the single waves determine the height of the cusps. Each group of waves, bow and stern, create a system of interference cusps. The angle between the sailing line is in theory $\theta = 19°28'$, in practise the angle depends in reality between $10° < \theta < 19°28'$.

A distinction is made between deep water and shallow water. The linear wave theory is applied to determine the relation between the length of the ship-induced waves and the navigation speed. In deep water, there is no influence by the water depth. The gravity waves are described in the following relation:

$$c = \sqrt{\frac{g\cdot\lambda}{2\cdot\pi}} \rightarrow \lambda = c^2\cdot\frac{2\cdot\pi}{g} \tag{D.17}$$

With the wave number $k = \sqrt{\frac{2\cdot\pi}{\lambda}}$ the wave celerity becomes:

$$c = \sqrt{\frac{g}{k}} \tag{D.18}$$

The sailing speed can be thought of as the celerity of a certain point that induces waves. so V_s can be represented by:

$$V_s = \sqrt{\frac{g\cdot L_t}{2\cdot\pi}} \tag{D.19}$$

Shallow water is defined as the situation where the water depth becomes smaller than half the wave length $\left(\frac{h}{\lambda} < {}^1/_2\right)$, at which depth the waves start to get influenced by the bed. The celerity of the individual waves in described with:

$$c' = \sqrt{\frac{g}{k}\cdot\tanh kh} \tag{D.20}$$

When this is taken relative to the deep water celerity:

$$\frac{c'}{c} = \sqrt{\tanh \frac{g \cdot h}{c^2}} \tag{D.21}$$

Take the celerity at ship's speed. The deduction of the speed due to the bottom effects on the wave vary little in situations up to:

$$\tanh\left(\frac{g \cdot h}{V_s^2}\right) < 0.95 \text{ (Johnson, 1958, Sorensen, 1967, 1969)} \tag{D.22}$$

The Froude number can be used as well as an indication whether it is shallow or deep water. If $\frac{V_s}{\sqrt{g \cdot h_0}} <$ 0.74 deep water conditions are coming up.

With the Froude number the angle θ can be determined. Values of Froude number up to 0.74 result in $\theta = 19°28'$, which is the same as in deep water. If the velocity increases further to the limit speed angle θ increases rapidly, up to $\theta = 90°$. This occurs when $Fr = 1$. In that situation the transversal and divergent waves coincide.

E

RESULTS IN COMBINED GRAPHS

The results obtained from the Matlab model are presented in this appendix. The results which are already presented in the main report are included as well to give a full overview of the results from the scenarios. Of each subgroup are the extreme values and tables given in the tables.

E.1. SCENARIOS 1 UP UNTIL 4

In this section are the results presented from scenarios 1 up until 4. The extreme values are given in table E.1. The results are presented in figures E.1 up until E.10. At each location is first the water level change and then the currents given.

Table E.1: Extreme values and downtime in scenarios 1, 2, 3 and 4

Scenario	Parameter	XBorn	X1000	X4000	X5900	X6001
Sc1	z_{min} [m]	-0,173	-0,235	-0,235	-0,170	-0,154
	z_{max} [m]	0,117	0,106	0,076	0,074	0,069
	u_{min} [m/s]	-0,231	-0,318	-0,318	-0,416	-0,217
	u_{max} [m/s]	0,065	0,082	0,132	0,168	0,156
	$Downtime$ [min:sec]	04:48	08:59	16:26	10:13	07:48
Sc2	z_{min} [m]	-0,135	-0,136	-0,133	-0,095	-0,086
	z_{max} [m]	0,082	0,079	0,039	0,042	0,034
	u_{min} [m/s]	-0,128	-0,184	-0,194	-0,278	-0,147
	u_{max} [m/s]	0,017	0,056	0,101	0,127	0,092
	$Downtime$ [min:sec]	00:00	10:15	18:24	16:07	02:08
Sc3	z_{min} [m]	-0,193	-0,266	-0,266	-0,180	-0,177
	z_{max} [m]	0,118	0,109	0,070	0,086	0,084
	u_{min} [m/s]	-0,261	-0,359	-0,359	-0,477	-0,246
	u_{max} [m/s]	0,073	0,124	0,138	0,171	0,175
	$Downtime$ [min:sec]	05:33	08:24	15:34	12:27	05:58
Sc4	z_{min} [m]	-0,285	-0,389	-0,389	-0,274	-0,253
	z_{max} [m]	0,167	0,152	0,104	0,112	0,117
	u_{min} [m/s]	-0,382	-0,527	-0,527	-0,703	-0,362
	u_{max} [m/s]	0,107	0,141	0,196	0,243	0,258
	$Downtime$ [min:sec]	07:18	12:03	22:10	17:48	10:36

Figure E.3: Water level changes in scenarios 1, 2, 3 and 4 at location X1151

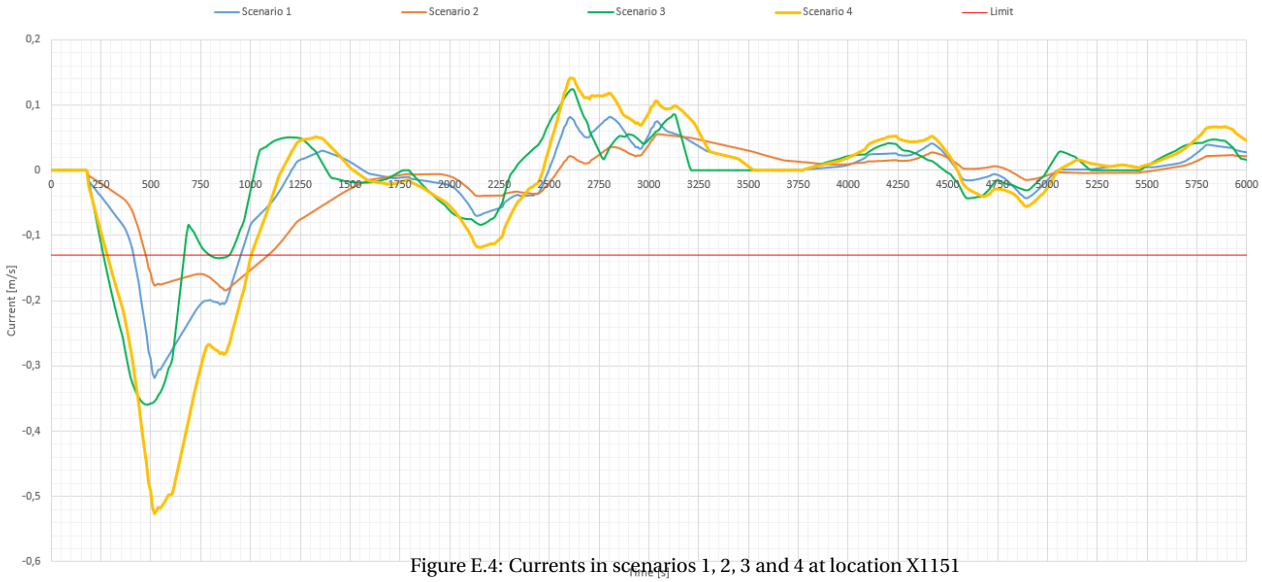

Figure E.4: Currents in scenarios 1, 2, 3 and 4 at location X1151

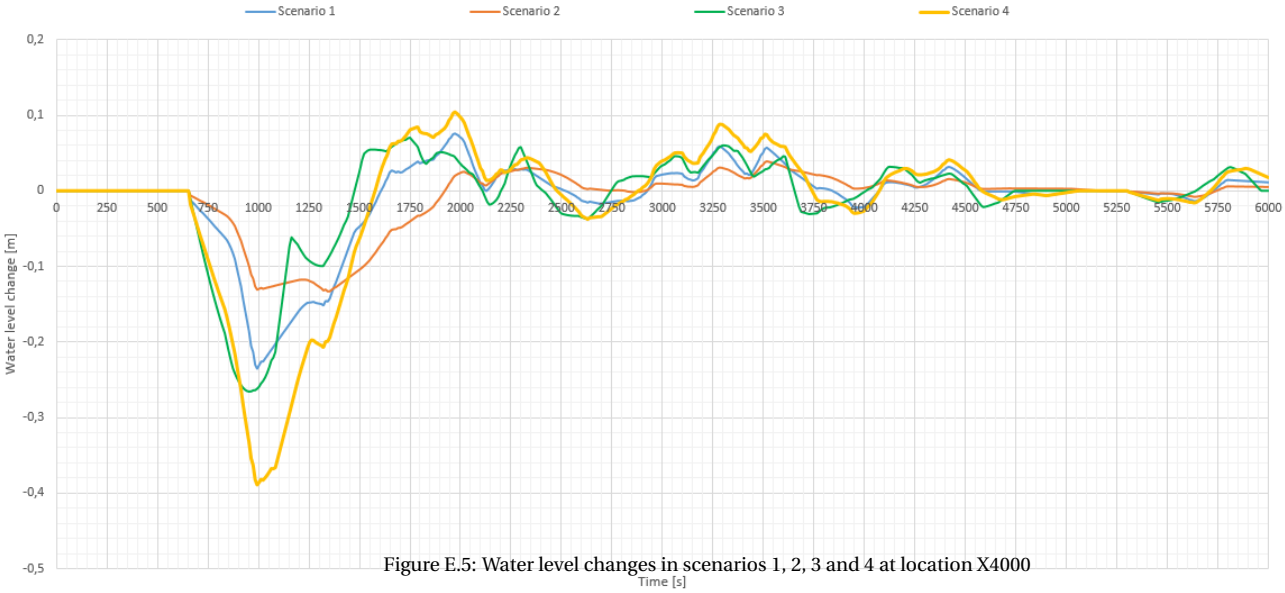

Figure E.5: Water level changes in scenarios 1, 2, 3 and 4 at location X4000

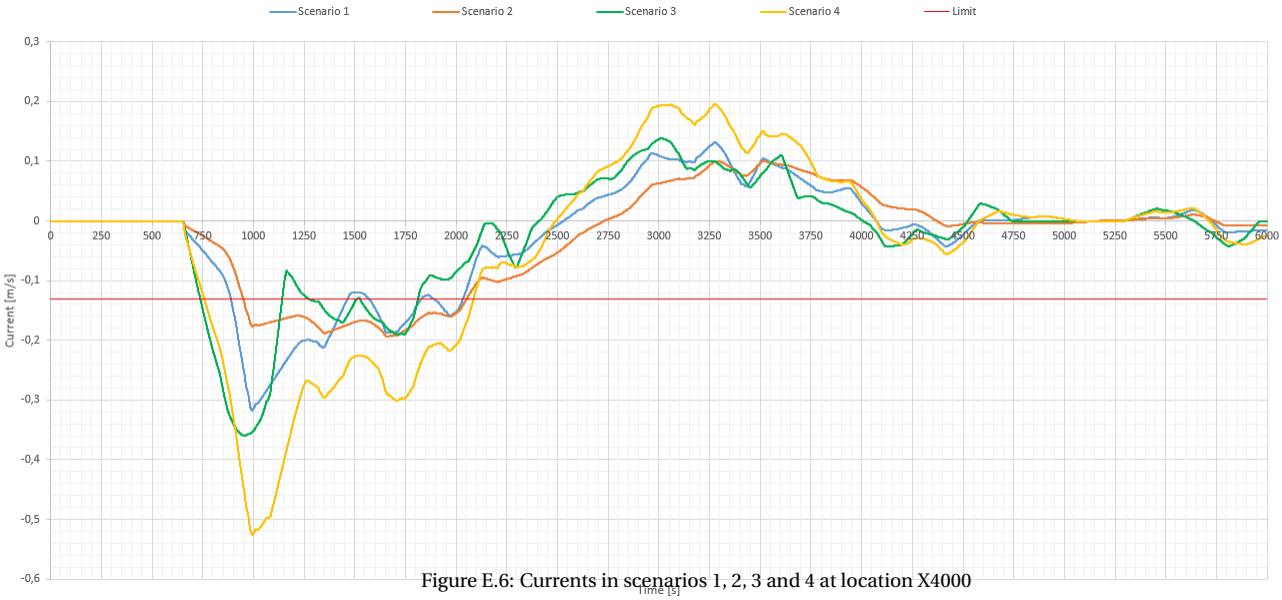

Figure E.6: Currents in scenarios 1, 2, 3 and 4 at location X4000

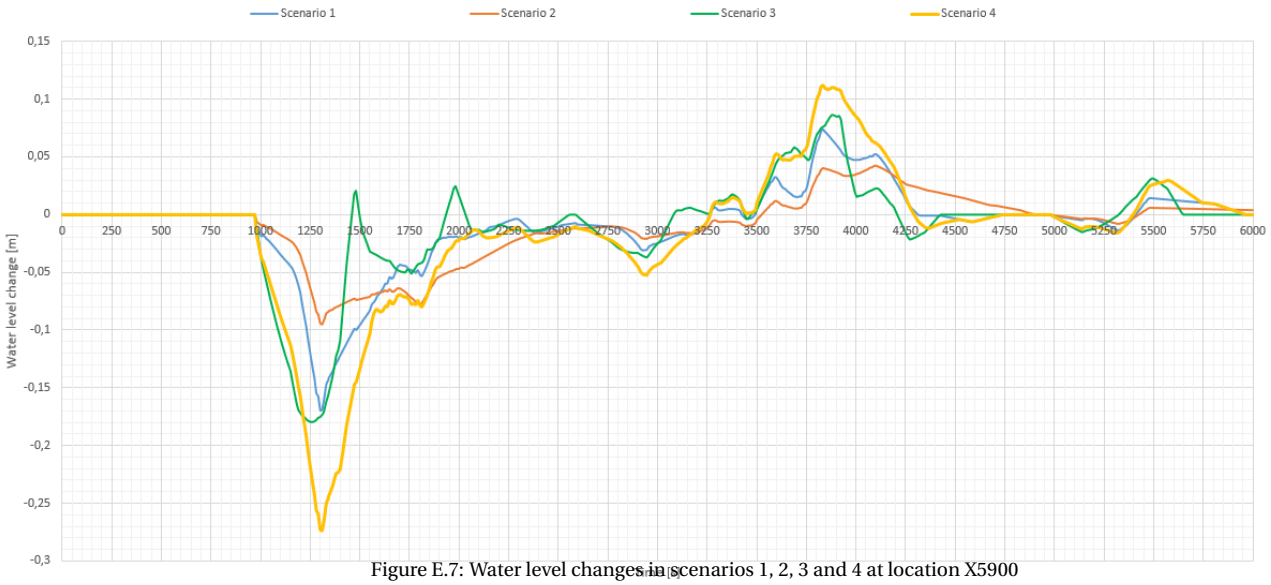

Figure E.7: Water level changes in scenarios 1, 2, 3 and 4 at location X5900

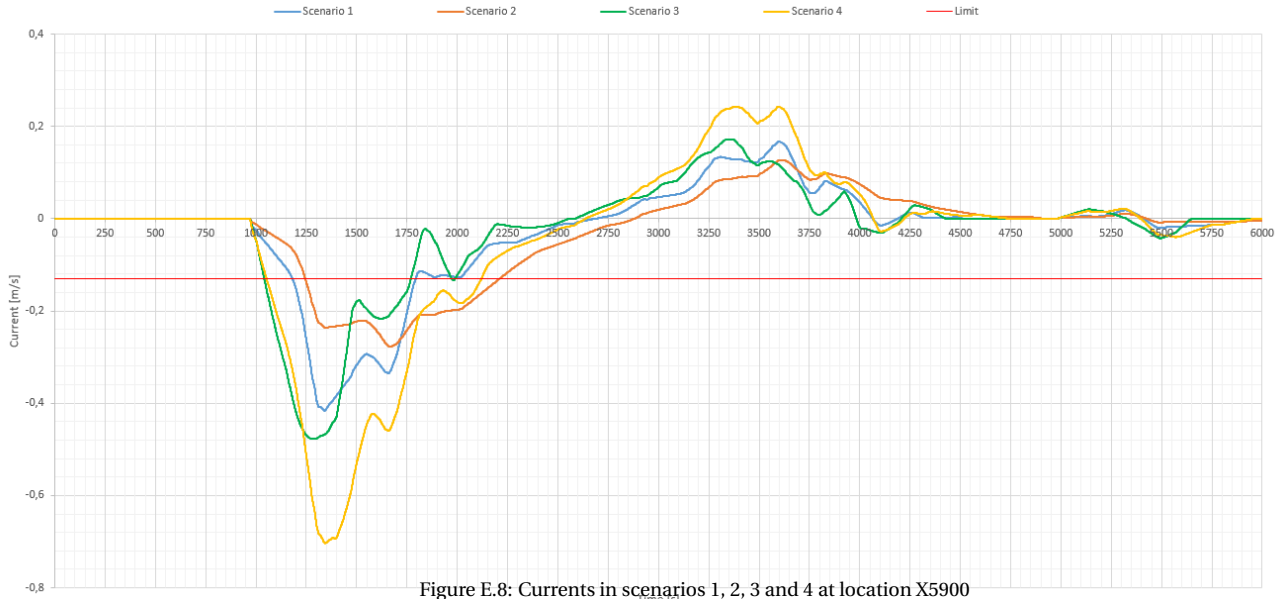

Figure E.8: Currents in scenarios 1, 2, 3 and 4 at location X5900

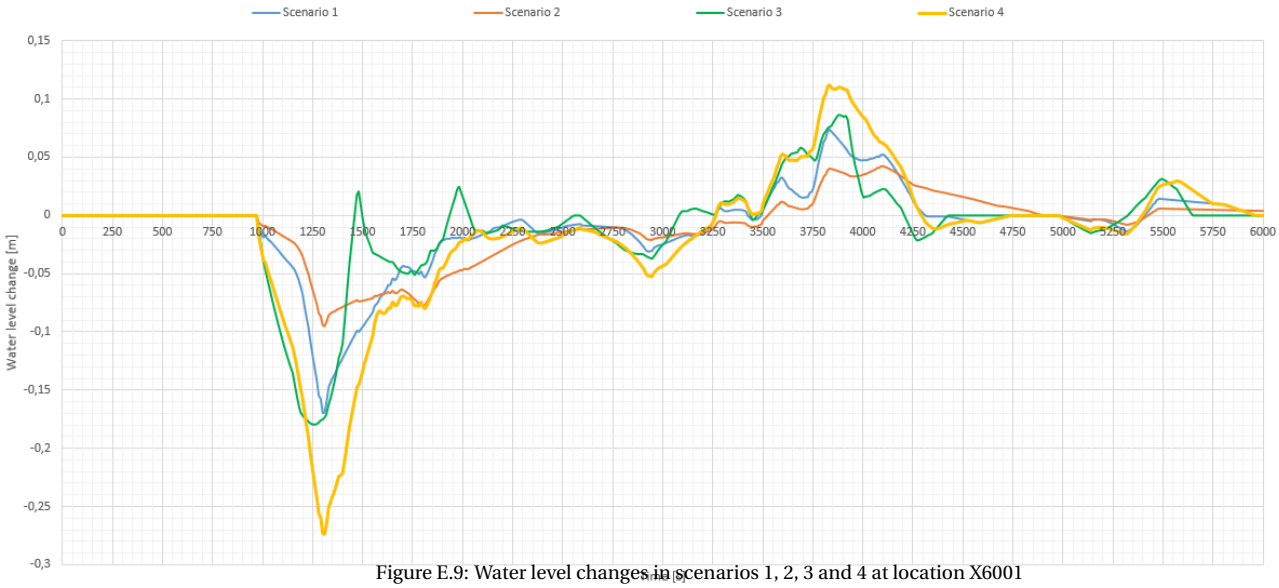

Figure E.9: Water level changes in scenarios 1, 2, 3 and 4 at location X6001

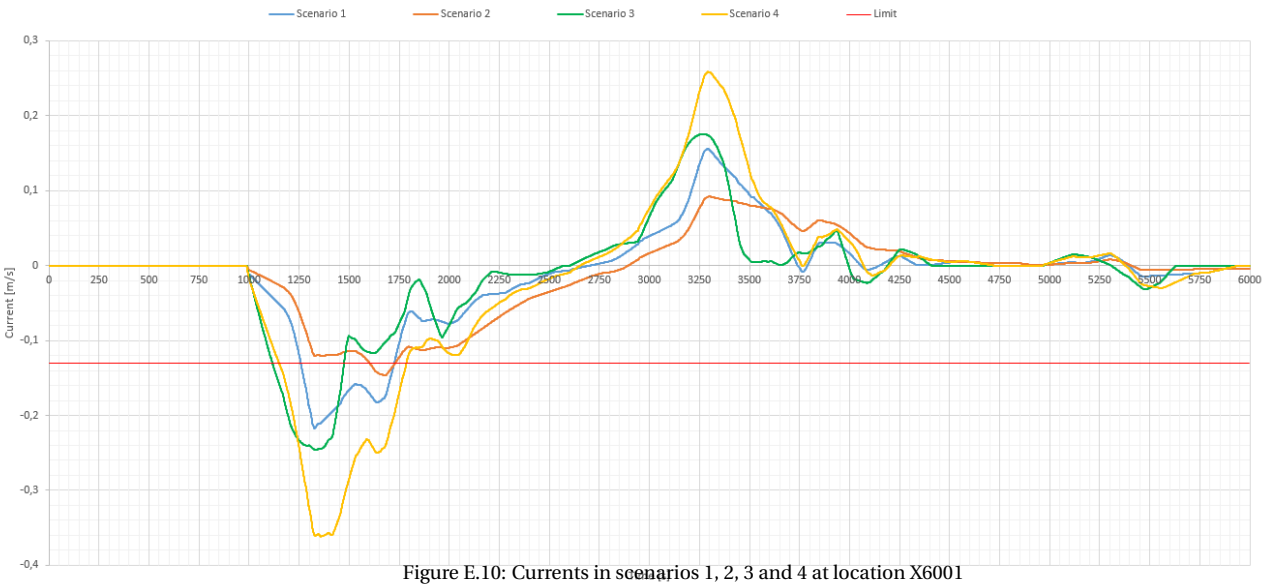

Figure E.10: Currents in scenarios 1, 2, 3 and 4 at location X6001

E.2. SCENARIOS 5 UP UNTIL 7

In this section are the results presented from scenarios 5, 6 and 7. The extreme values are given in table E.2. The results are presented in figures E.11 up until E.20. At each location is first the water level change and then the currents given.

Table E.2: Extreme values and downtime in scenarios 5, 6 and 7

Scenario	Parameter	XBorn	X1000	X4000	X5900	X6001
Sc5	z_{min} [m]	-0,173	-0,235	-0,235	-0,170	-0,154
	z_{max} [m]	0,096	0,092	0,076	0,066	0,062
	u_{min} [m/s]	-0,231	-0,318	-0,318	-0,416	-0,217
	u_{max} [m/s]	0,065	0,078	0,106	0,157	0,129
	$Downtime$ [min:sec]	08:58	14:54	22:55	18:49	12:47
Sc6	z_{min} [m]	-0,173	-0,235	-0,235	-0,170	-0,154
	z_{max} [m]	0,086	0,077	0,091	0,066	0,054
	u_{min} [m/s]	-0,231	-0,318	-0,318	-0,416	-0,217
	u_{max} [m/s]	0,065	0,109	0,073	0,131	0,123
	$Downtime$ [min:sec]	09:03	16:44	23:21	17:29	10:49
Sc7	z_{min} [m]	-0,173	-0,235	-0,235	-0,170	-0,154
	z_{max} [m]	0,076	0,074	0,103	0,075	0,046
	u_{min} [m/s]	-0,231	-0,318	-0,318	-0,416	-0,217
	u_{max} [m/s]	0,071	0,102	0,095	0,120	0,107
	$Downtime$ [min:sec]	08:16	16:06	20:56	16:01	07:48

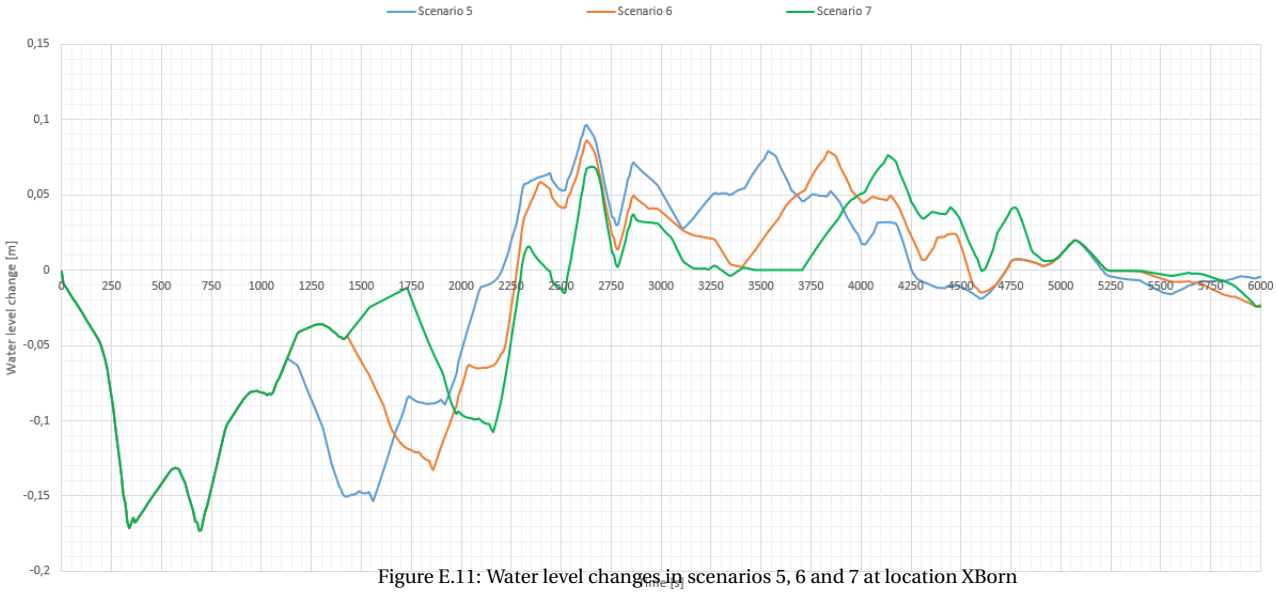

Figure E.11: Water level changes in scenarios 5, 6 and 7 at location XBorn

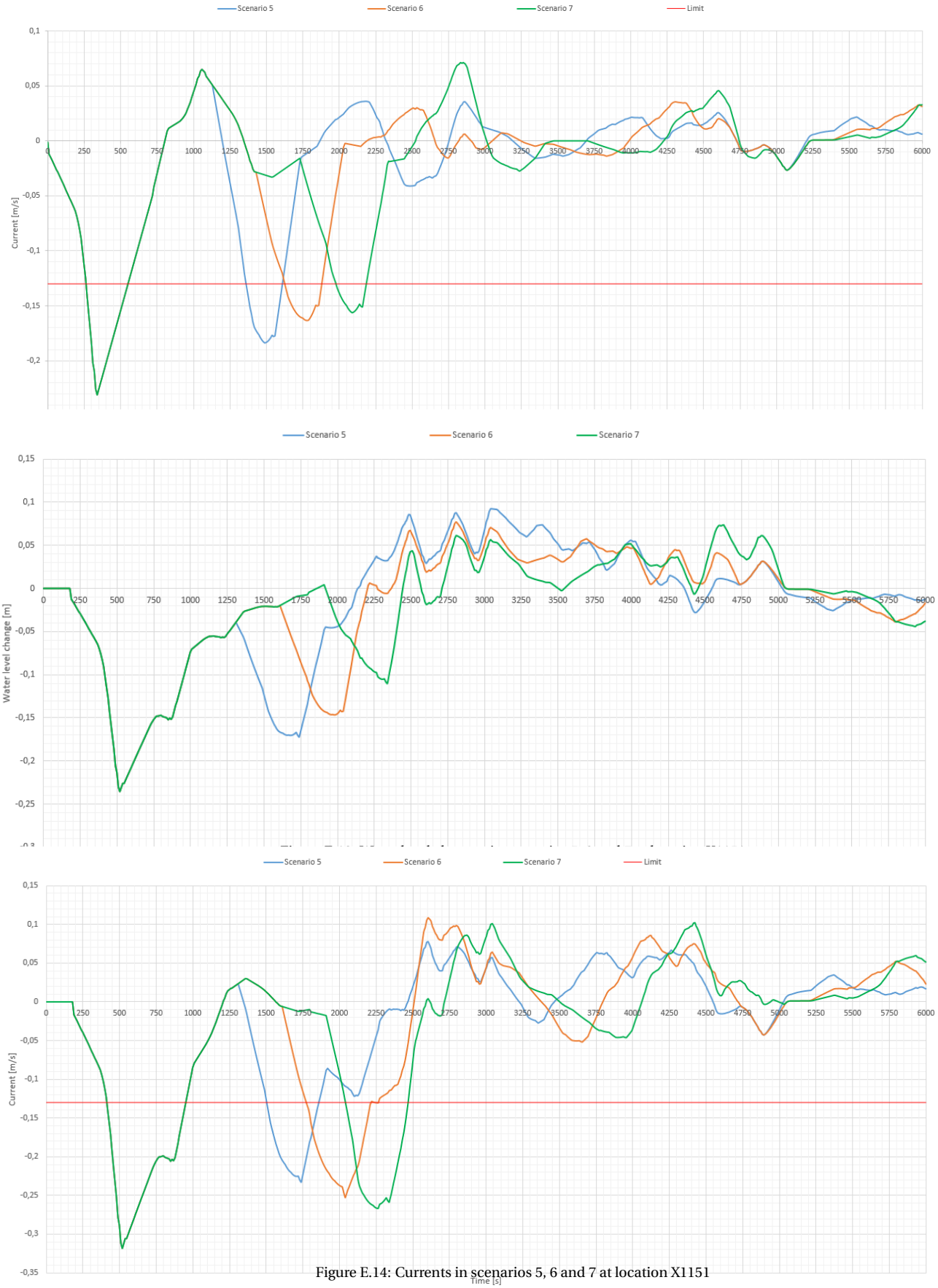

Figure E.14: Currents in scenarios 5, 6 and 7 at location X1151

Figure E.17: Water level changes in scenarios 5, 6 and 7 at location X5900

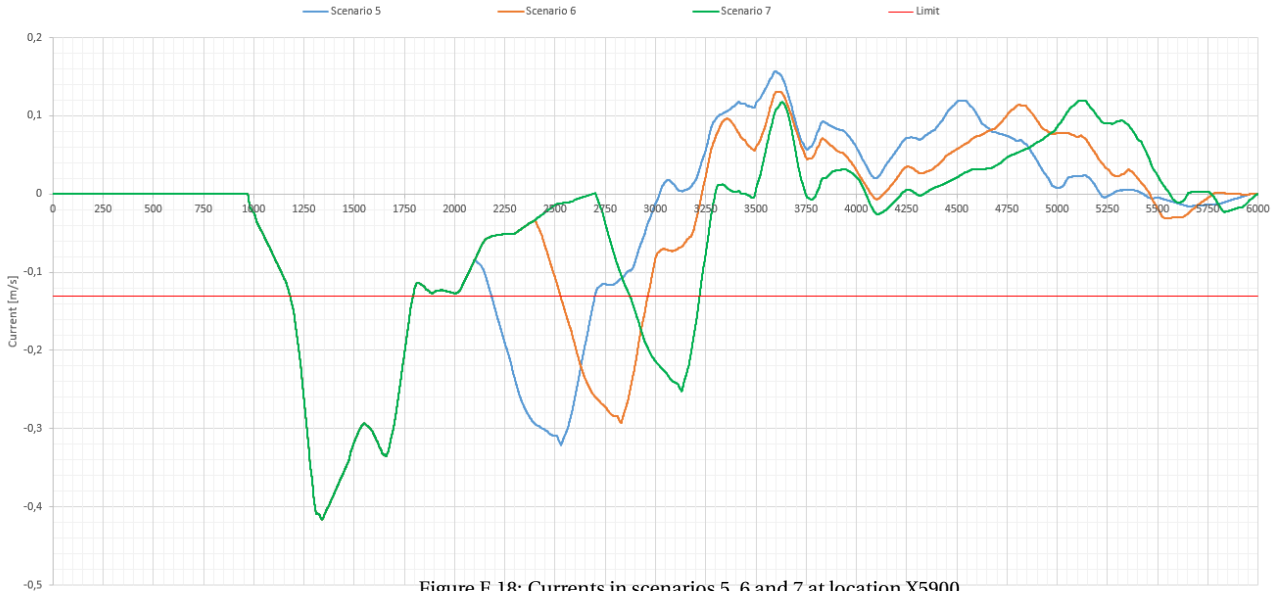

Figure E.18: Currents in scenarios 5, 6 and 7 at location X5900

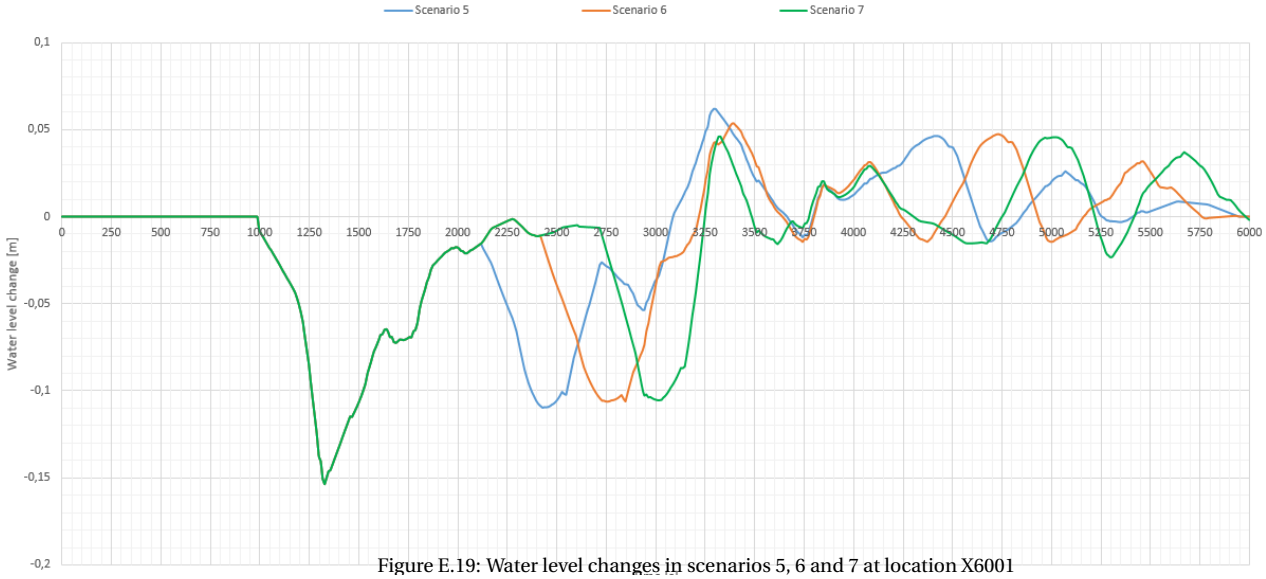

Figure E.19: Water level changes in scenarios 5, 6 and 7 at location X6001

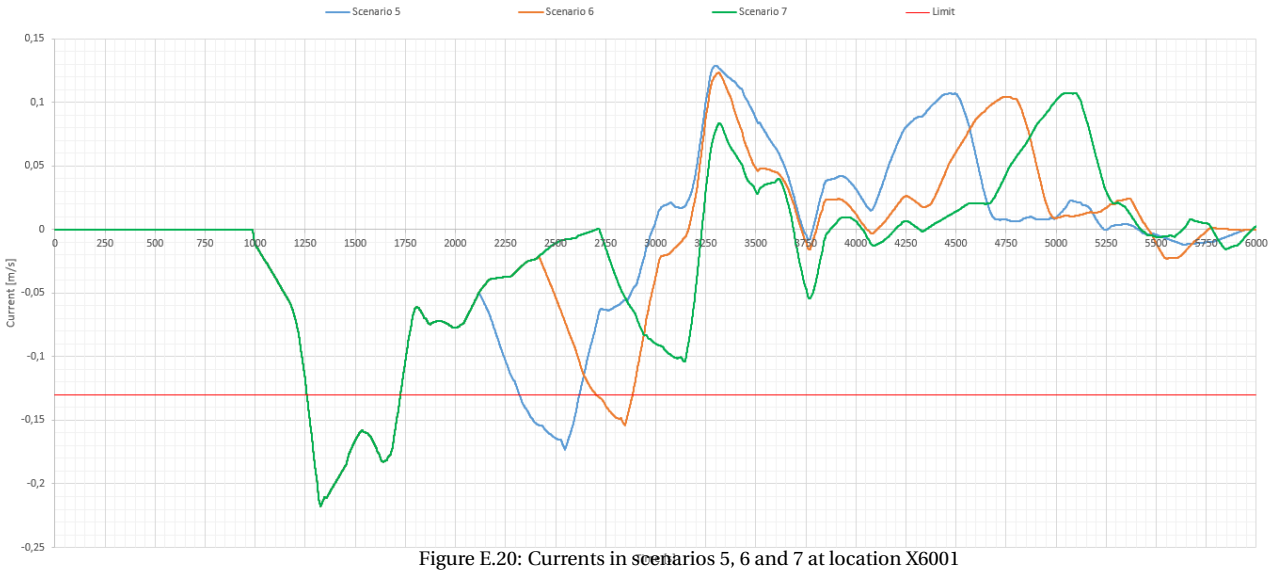

Figure E.20: Currents in scenarios 5, 6 and 7 at location X6001

E.3. SCENARIOS 8 UP UNTIL 10

In this section are the results presented from scenarios 8, 9 and 10. The extreme values are given in table E.3. The results are presented in figures E.21 up until E.30. At each location is first the water level change and then the currents given.

Table E.3: Extreme values and downtime of Scenarios 8, 9 and 10

Scenario	Parameter	XBorn	X1151	X4000	X5900	X6001
Sc8	z_{min} [m]	-0,135	-0,136	-0,133	-0,097	-0,086
	z_{max} [m]	0,055	0,049	0,059	0,043	0,028
	u_{min} [m/s]	-0,128	-0,202	-0,194	-0,278	-0,147
	u_{max} [m/s]	0,042	0,062	0,071	0,096	0,086
	$Downtime$ [min:sec]	00:00	17:22	21:11	21:07	02:08
Sc9	z_{min} [m]	-0,135	-0,136	-0,133	-0,095	-0,086
	z_{max} [m]	0,065	0,070	0,047	0,020	0,034
	u_{min} [m/s]	-0,128	-0,184	-0,194	-0,278	-0,147
	u_{max} [m/s]	0,033	0,039	0,080	0,085	0,092
	$Downtime$ [min:sec]	00:00	13:16	18:24	17:25	02:08
Sc10	z_{min} [m]	-0,135	-0,136	-0,133	-0,095	-0,086
	z_{max} [m]	0,065	0,070	0,047	0,020	0,034
	u_{min} [m/s]	-0,128	-0,184	-0,194	-0,278	-0,147
	u_{max} [m/s]	0,033	0,039	0,080	0,085	0,092
	$Downtime$ [min:sec]	00:00	11:12	18:24	17:31	02:08

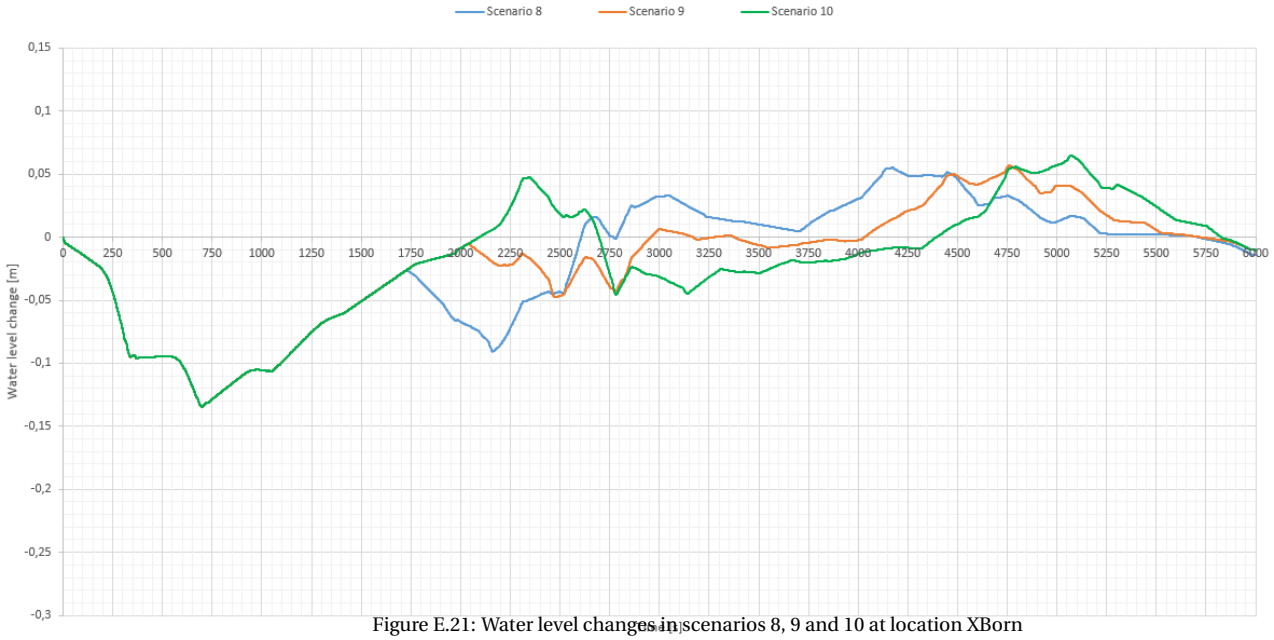

Figure E.21: Water level changes in scenarios 8, 9 and 10 at location XBorn

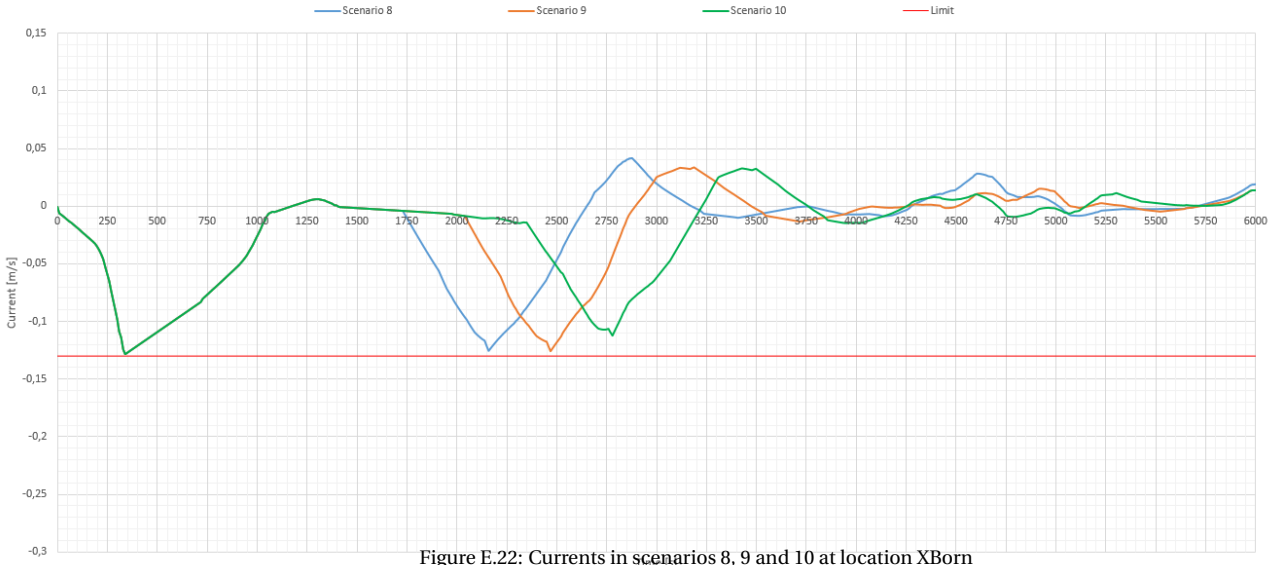

Figure E.22: Currents in scenarios 8, 9 and 10 at location XBorn

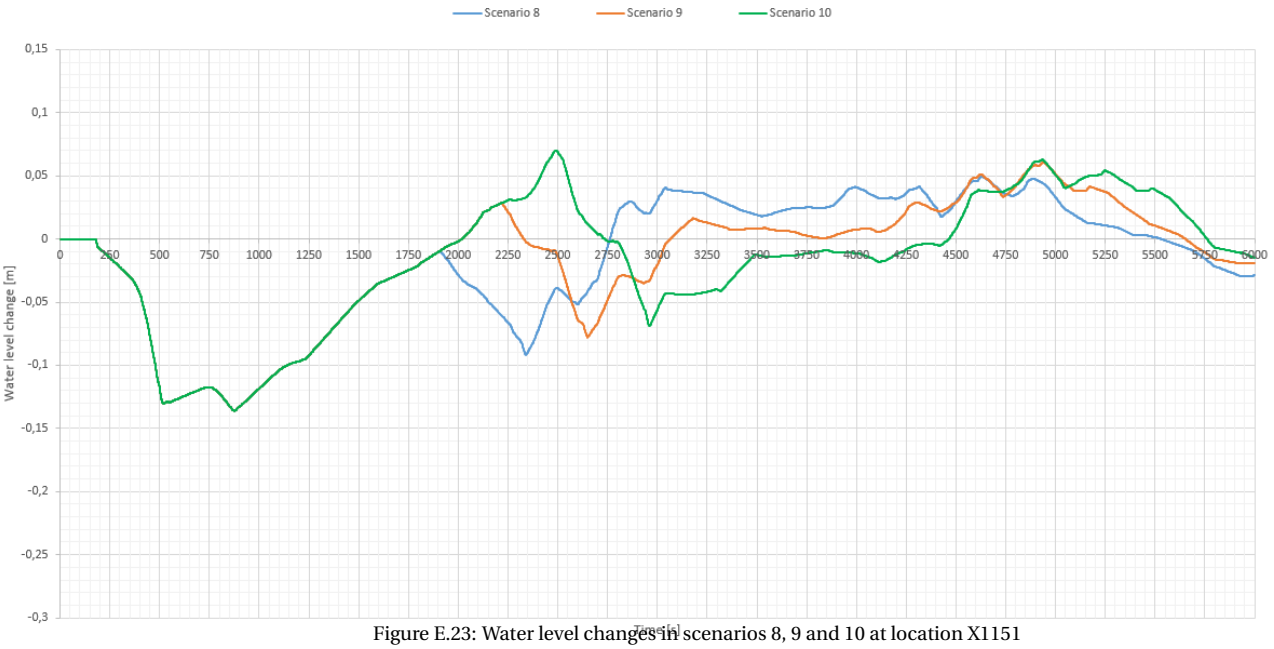

Figure E.23: Water level changes in scenarios 8, 9 and 10 at location X1151

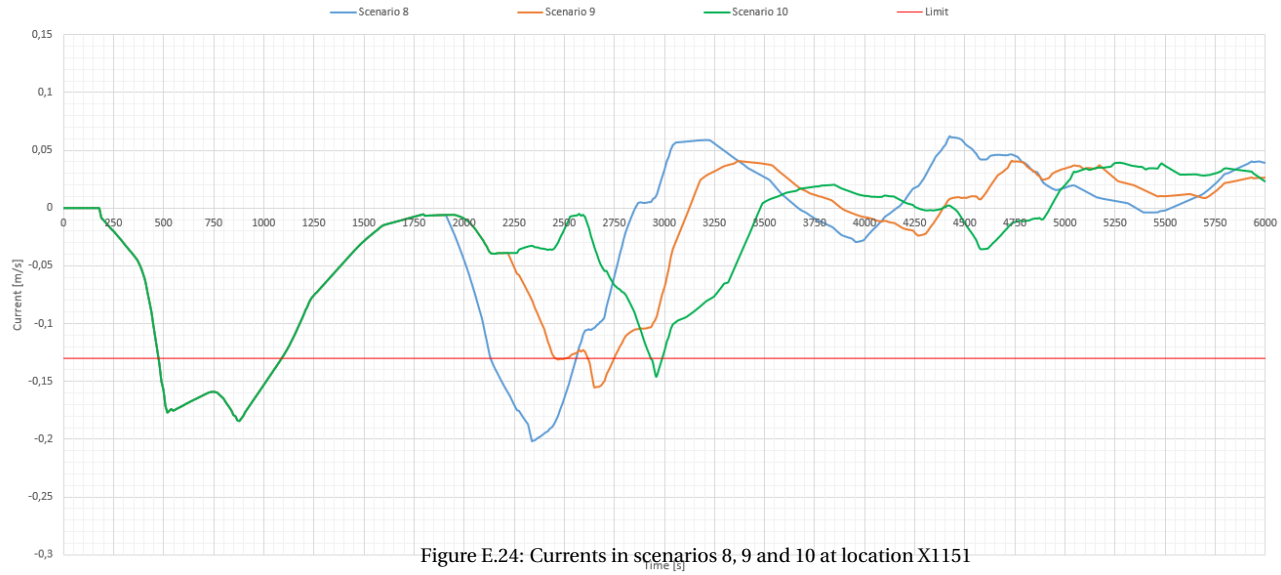

Figure E.24: Currents in scenarios 8, 9 and 10 at location X1151

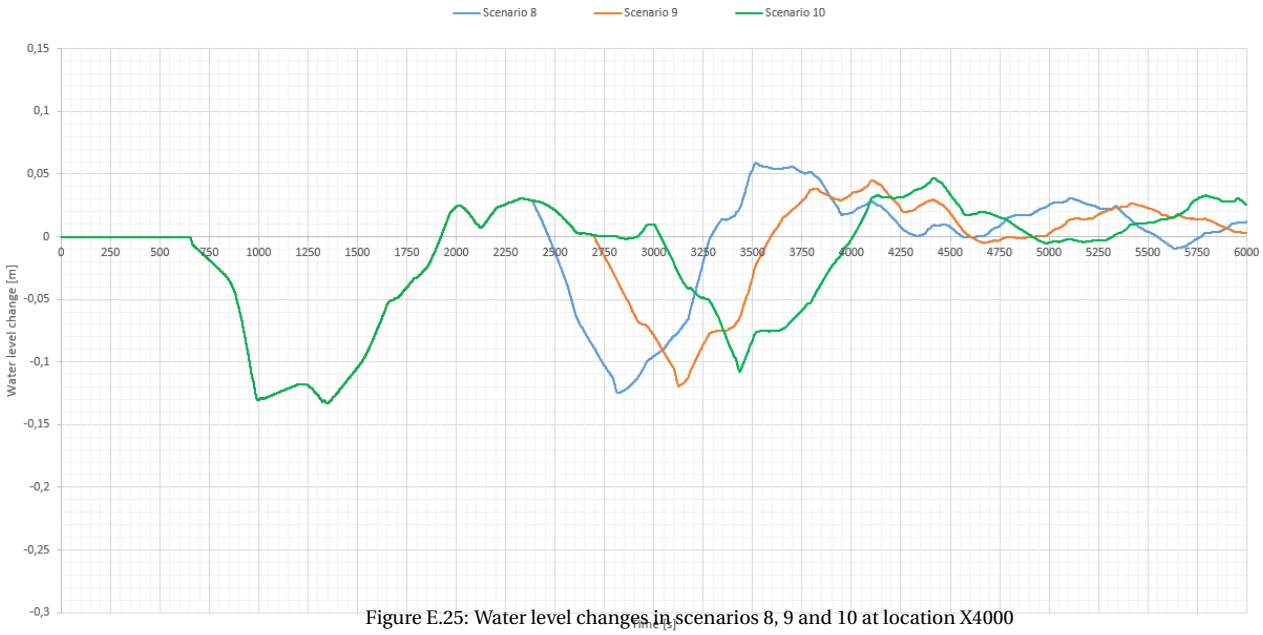

Figure E.25: Water level changes in scenarios 8, 9 and 10 at location X4000

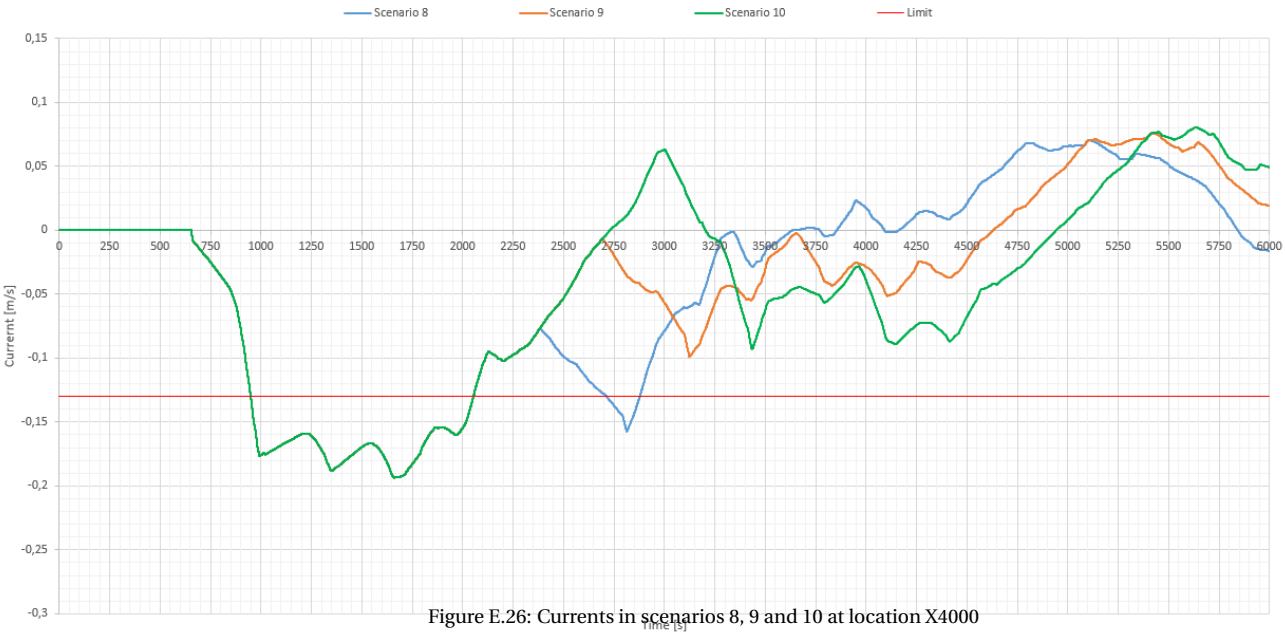

Figure E.26: Currents in scenarios 8, 9 and 10 at location X4000

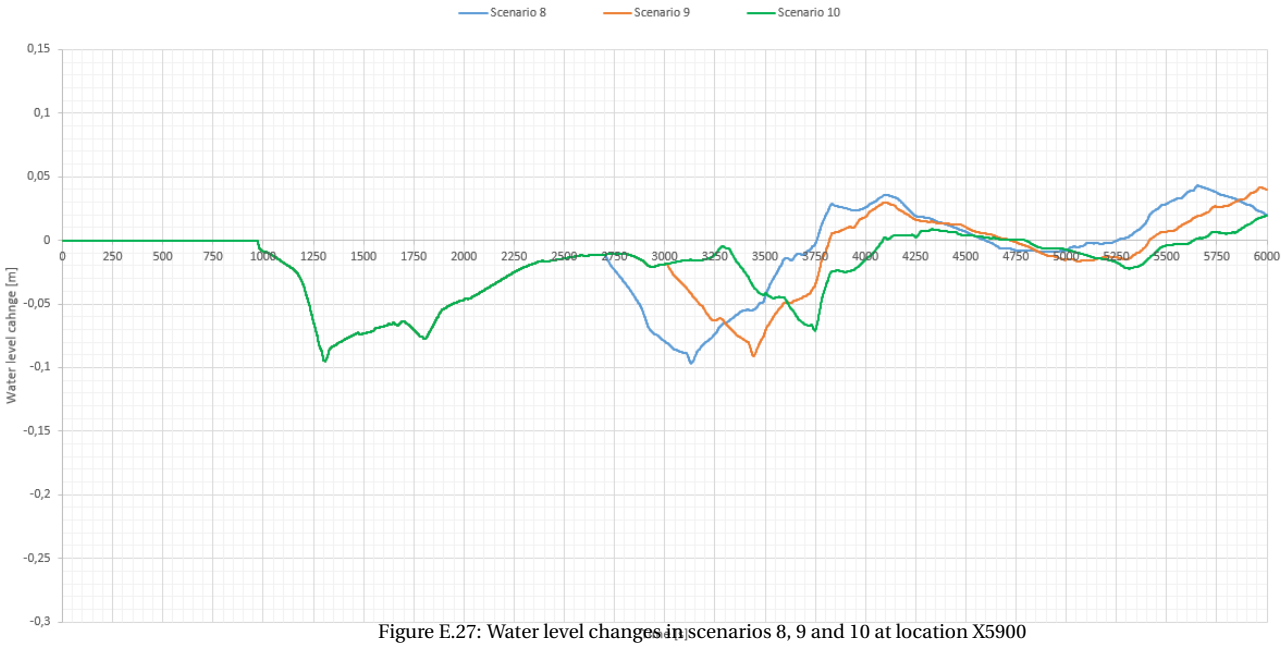

Figure E.27: Water level changes in scenarios 8, 9 and 10 at location X5900

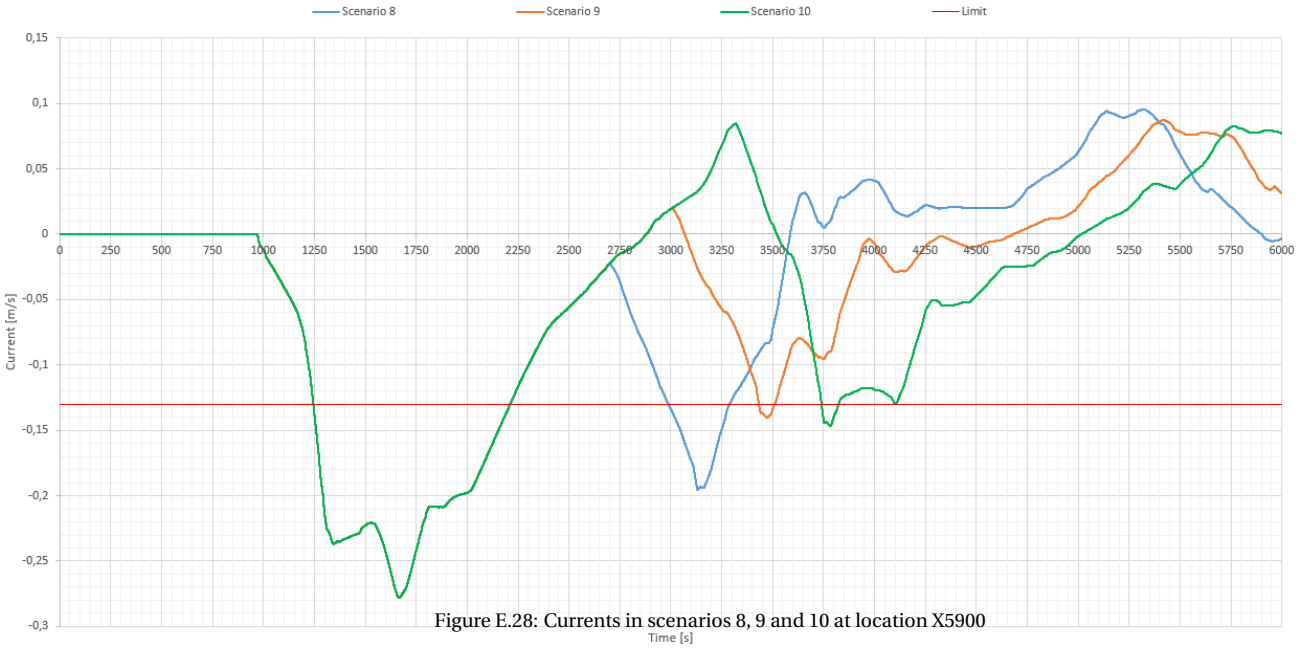

Figure E.28: Currents in scenarios 8, 9 and 10 at location X5900

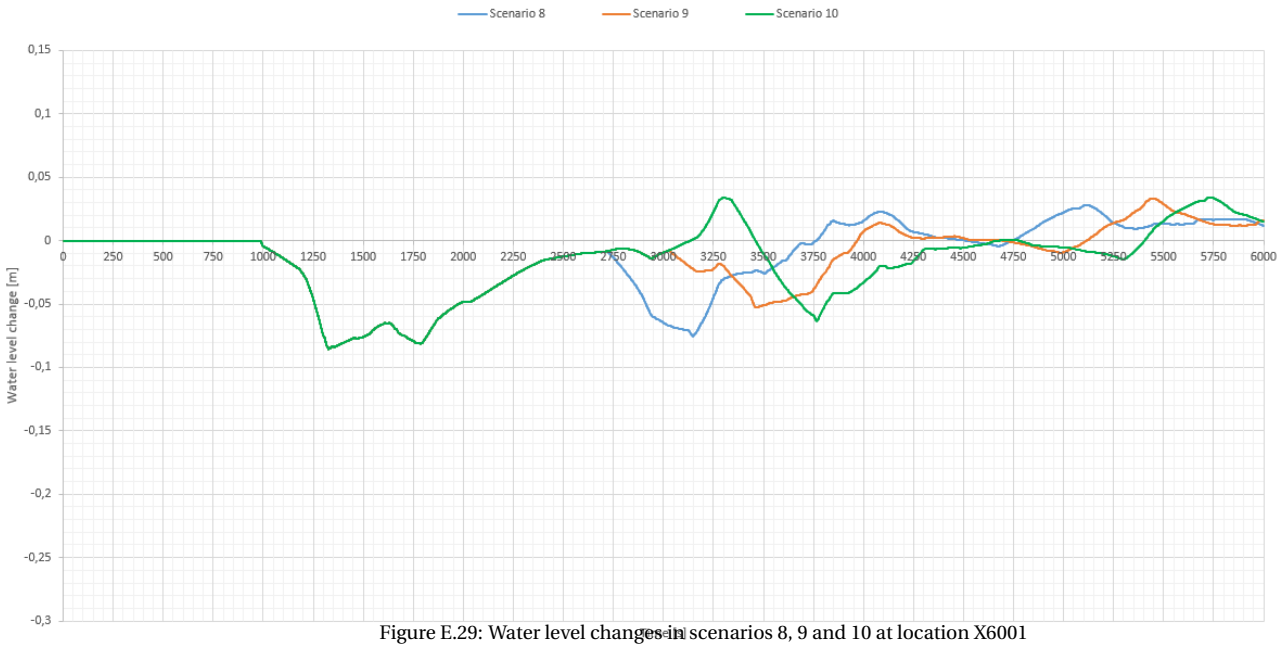

Figure E.29: Water level changes in scenarios 8, 9 and 10 at location X6001

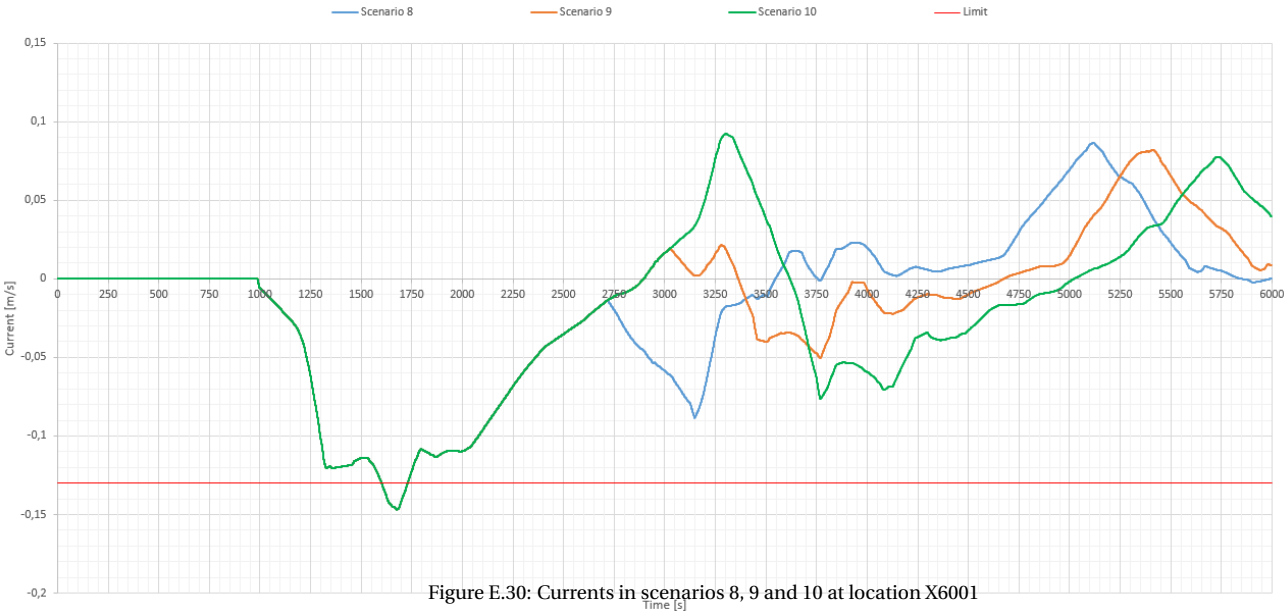

Figure E.30: Currents in scenarios 8, 9 and 10 at location X6001

F

RESULTS OF THE MODEL

In total 9 different scenarios have been developed to understand the system better and to come up with alternatives for more workable situations. To obtain more insight of the whole system, the scenarios have been calculated at 5 locations. Special attention has been made for the section between the first narrowing near Born and the section towards the port near Stein. 1 location near lock system Born (XBorn), 3 locations are on the narrow section (X1001, X4000 and X5900) and 1 at the wide port section of port Stein (X6001). The numbers between the brackets represent the distance from the location to lock system Born
Inspection divers can work without a diver on stand-by up to a current of 0.5 knots, about $0.26 m/s$, according to the Regulations on working conditions in hydraulic engineering ([13]. This has been taken as an indication for the maximum allowable current for the construction pontoon, determined at $0.3 m/s$. The base current in the canal to compensate for extracted water volumes is determined as $u_{base} = 0.17 m/s$. The current due to negative translation wave is in the opposite direction of the propagation direction of the wave. The current is towards the lock. The current due to positive translation waves is in the same direction as the propagation direction of the wave. Positive waves are assumed to be reflected waves, so moving towards the lock complex, thus the current as well. This is a conservative assumption which has to be investigated in further research. With the current of the positive, as well as the negative translation wave taken towards the lock complex near Born, the maximum allowed current for the translation waves can be calculated as $u_{trans} = u_{total} - u_{base} = 0.13 m/s$.

F.1. GROUP 1: DIFFERENT FILLING DISCHARGES

The situation in which the waves are created at the Middle lock chamber at Born is modelled using three different discharge-time relations. The discharge into the lock chamber can be varied in several ways, e.g. the valves to the culverts can be regulated, opening slower or faster or not fully. Another way to adapt the discharge to the chamber is by regulating the number of culverts used. In present situation there are two culvert implemented in the system.
In these runs the choice has been made to vary with the number of culverts. This is a realistic situation, implemented at the lock complex sometimes already. The first discharge-time relation, is the present situation. In this situation 2 culverts are used to fill the chamber. This is the 0-scenario to which regulation measures can be compared to. Second is the situation utilizing only one culvert. This will probably reduce the wave height and current in the canal. The final discharge-time relation is based on a theoretical situation in which four culverts are applied. The three discharge-time relations are visualized in figure F.1.

1. Present discharge
2. Lower discharge
3. Higher discharge

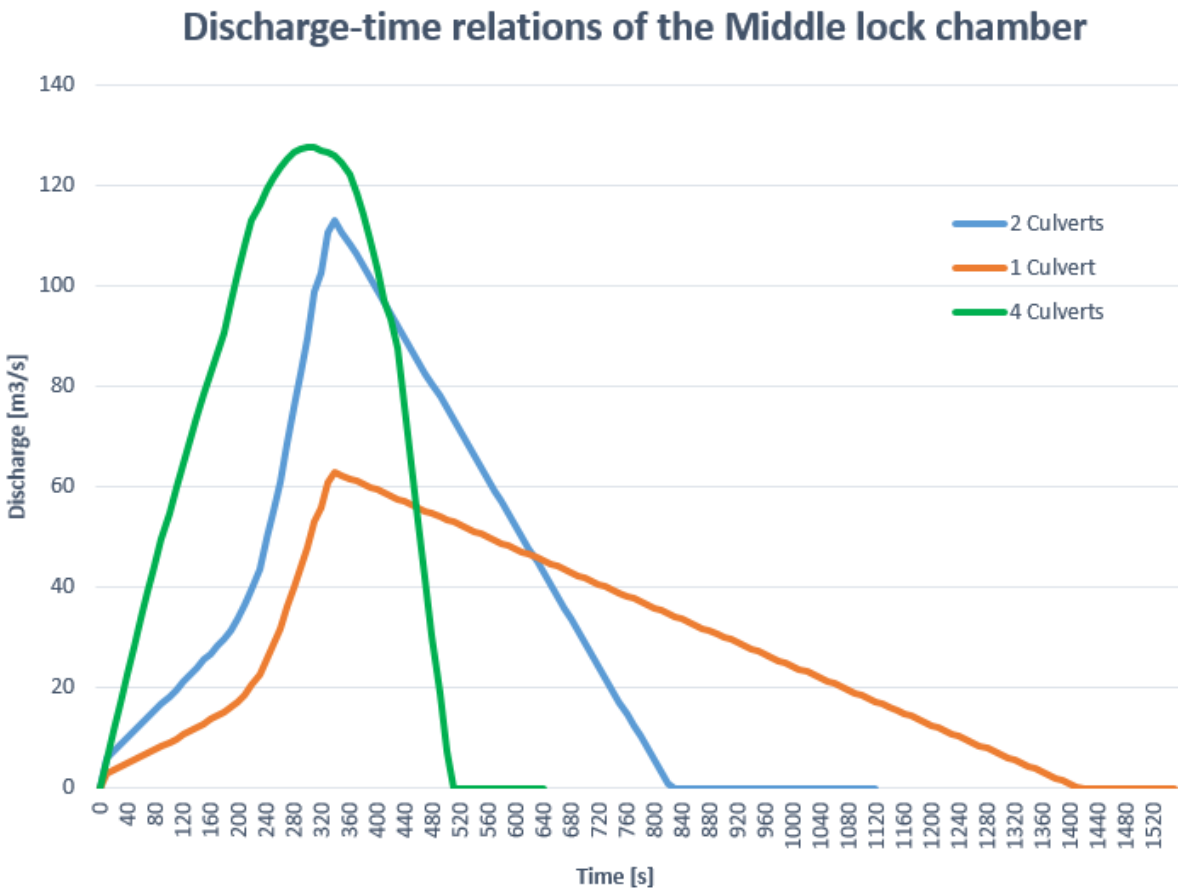

Figure F.1: The three modelled discharge-time relations

The adaptations of the water level in the canal, to the discharge of filling the lock chamber are modelled at five locations and presented over time. To interpret the differences how the waves develop between the three scenarios, the results are presented per location. The locations where the development of the waves over time are modelled are:

1. X = 0m, close to lock system Born
2. X = 1150m, section on narrow canal just after narrowing
3. X = 4000m, straight section in canal
4. X = 5900m, section on narrow canal before widening to port Stein
5. X = 6000m, after widening from narrow canal to wide port section.

LOCATION X=0 BORN

The waves are created due to filling the lock chamber at lock complex Born. The first location is right in front of the lock complex. The currents resulting from the translation waves at different Q-t relations are presented in figures F.3, F.5 and F.7. The shape of the waves in the section between the start and about $t = 1000$ stands out between the three figures. Where figure F.3 and F.7 have two clear troughs before $t = 1000$, the first due to the primary wave, the second as a result of the reflection a $X = 1150$, appears figure F.5 to have only one trough. This is a result of the long wave period. The peak, seen around $t = 800s$, is actually the result of the first reflection wave. The reflection wave amplifies the primary wave. The section roughly between $t = 2000$ and $t = 3000$ is another section where reflections interfere. Due to differences in wave length, the reflections amplify and damp each other at different time intervals resulting in different shapes of the water level changes.
The maximum and minimum values of the water level change and currents are given in table F.1. The u_{max} represents the maximum current as a result of the positive water level change, represented by h_{max}. The

current with a positive value is in the same direction as currents with a negative value, both are towards the lock complex. The values of the currents are still positive and negative to indicate the origin of the current (positive or negative water level change). The largest current occurs in all three scenarios due to the negative translations wave and are respectively 0.234, 0.182 and 0.261 m/s. A decrease of 22% between the second and first scenario and an increase of the current between the third and first scenario of 12%.

Table F.1: Extreme values at X_Born in Scenario 1,2 and 3

	Sc1	Sc2	Sc3
z_{min} [m]	-0,173	-0,135	-0,193
z_{max} [m]	0,117	0,082	0,118
u_{min} [m/s]	-0,234	-0,182	-0,261
u_{max} [m/s]	0,158	0,110	0,159
$Downtime$ [min:sec]	11:43	09:07	13:40

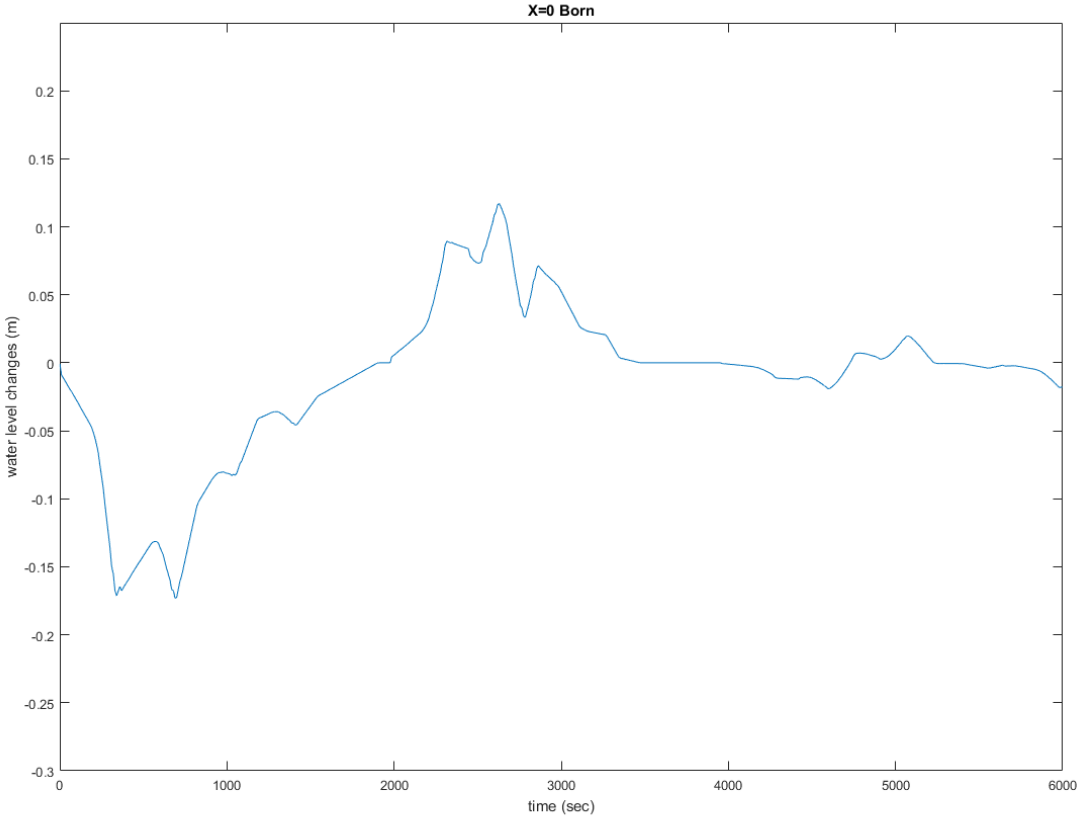

Figure F.2: Sc1: Water depth changes in original situation at location XBorn

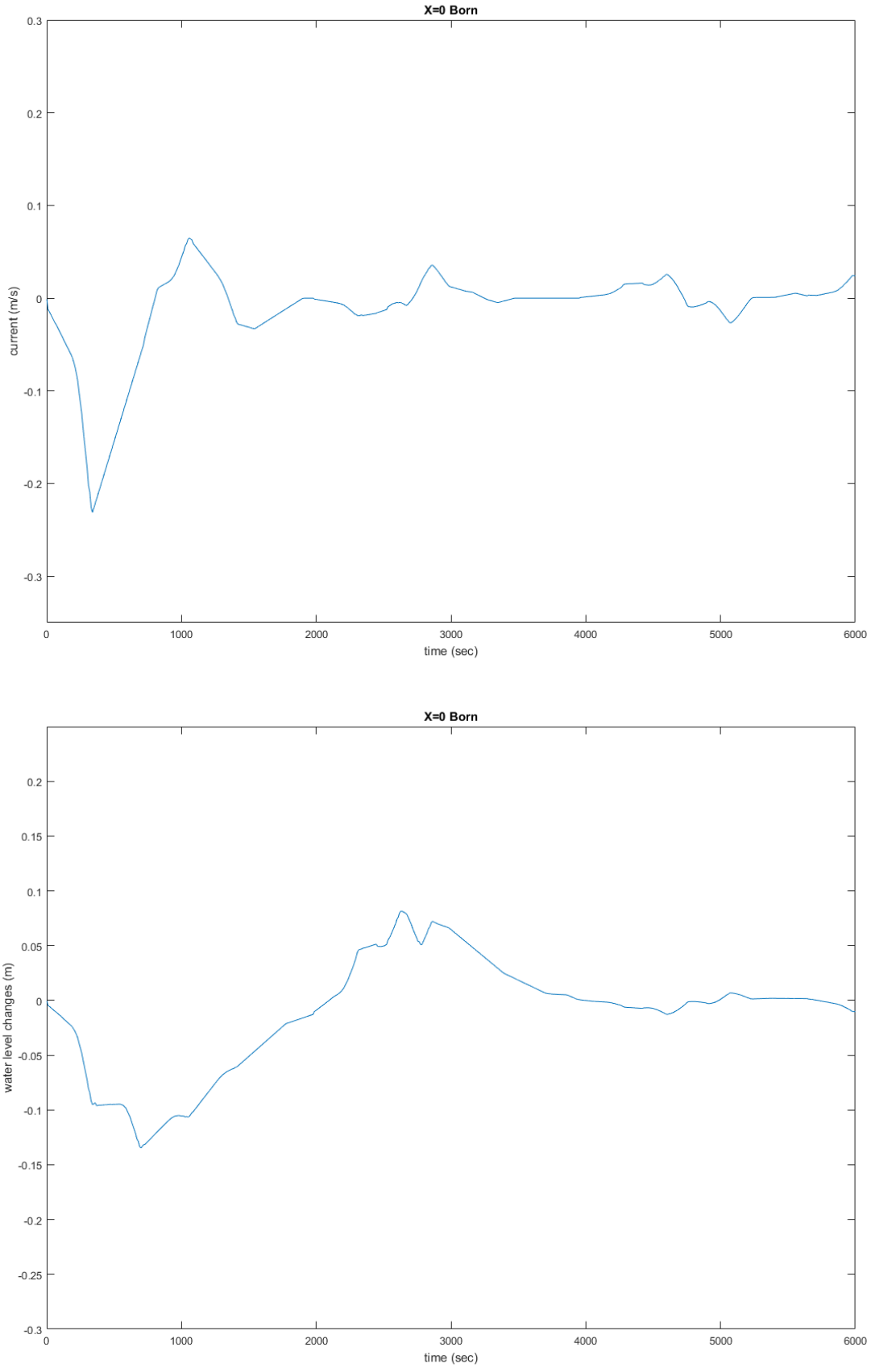

Figure F.4: Sc2: Water depth changes in scenario with one culvert at location XBorn

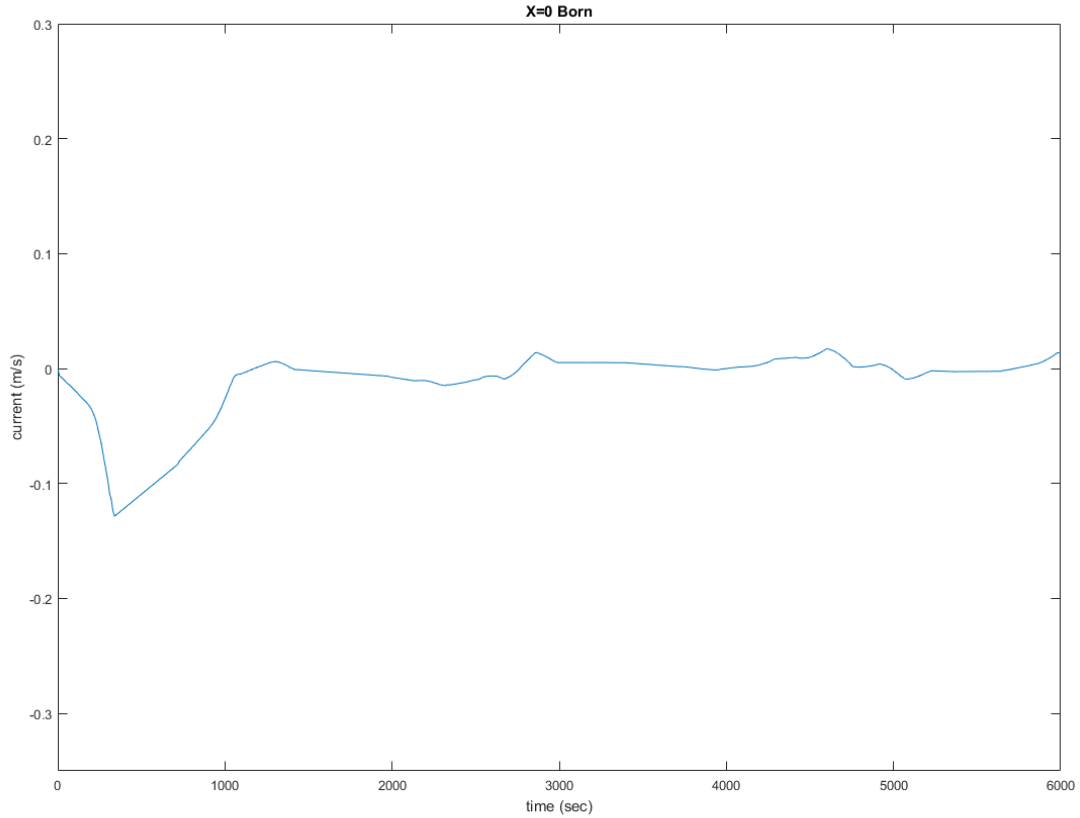

Figure F.5: Sc2: Currents in scenario with one culvert at location XBorn

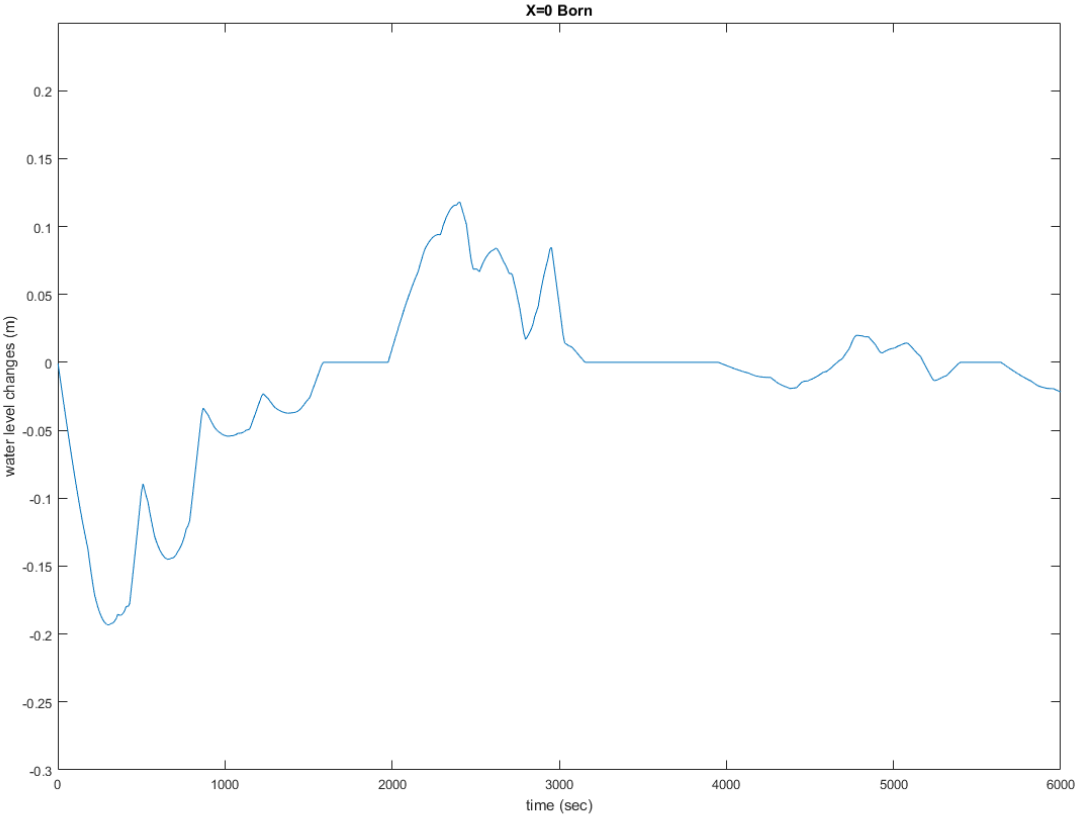

Figure F.6: Sc3: Water depth changes in scenario with four culverts at location XBorn

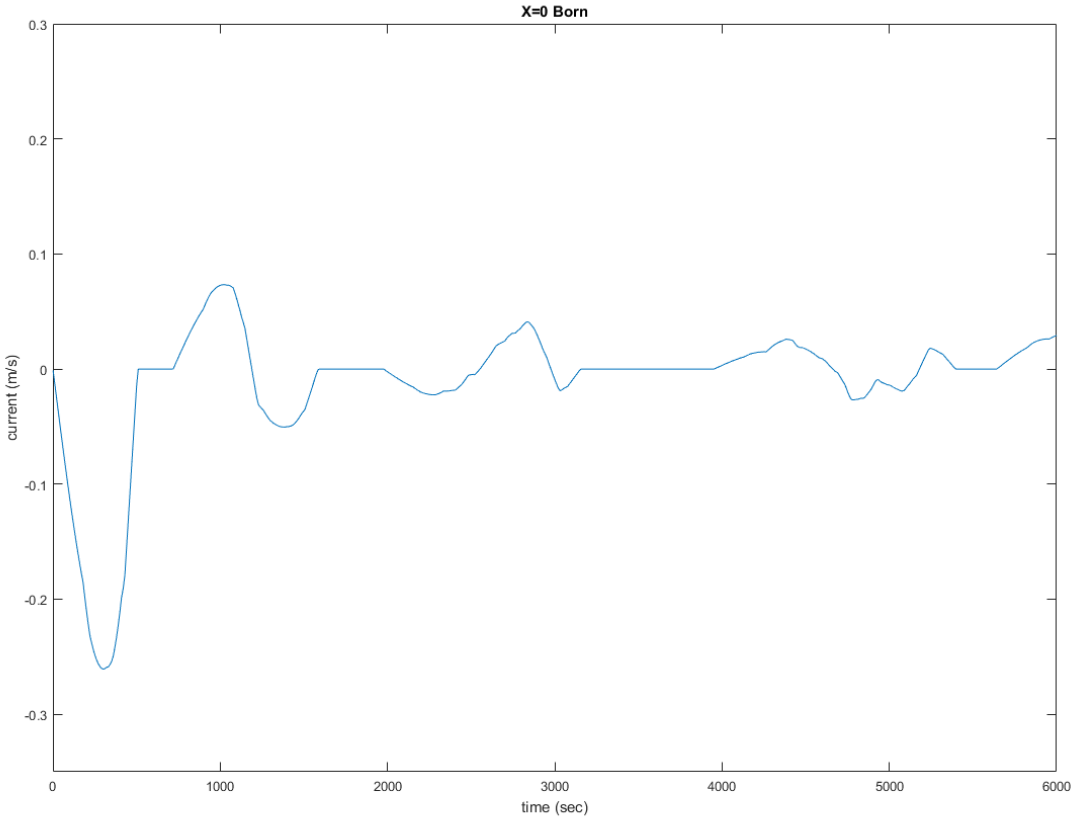

Figure F.7: Sc3: Currents in scenario with four culverts at location XBorn

LOCATION X1151

Location X1151 is located just south of the narrowing from lock basin to canal section. The primary waves have changed in shape, as can be seen in figures F.9, F.11 and F.13. The reflection of the first transition point is no longer coinciding as obvious with the primary wave as it was at location Born. It is still clearly visible but now as a second wave behind the primary wave. The second block of interference between waves shifted from t = 2000 till t = 3000 to t = 2200 till t = 3200. The waves of scenario 3 stops earlier than the waves of scenario 1 and 2 due to the shorter time period of the wave.
The extreme values of all the scenarios increase, mainly due to the first transition point. The largest in the three scenarios are 0.318, 0.184 and 0.359 m/s. The decrease in velocity of the current between the first and second scenario is 42%, between the first and third scenario an increase of 13%. Comparing location Born and X1151 the currents increases respectively 36%, 1% and 38%. The lack of increase in the second scenario is probably because the primary wave and first reflection amplified each other at location Born, which was no longer the case at location X1151.

Table F.2: Extreme values at X_1151 in Scenario 1,2 and 3

	Sc1	Sc2	Sc3
z_{min} [m]	-0,235	-0,136	-0,266
z_{max} [m]	0,106	0,079	0,109
u_{min} [m/s]	-0,318	-0,184	-0,359
u_{max} [m/s]	0,144	0,107	0,148
$Downtime$ [min:sec]	10:09	12:19	09:35

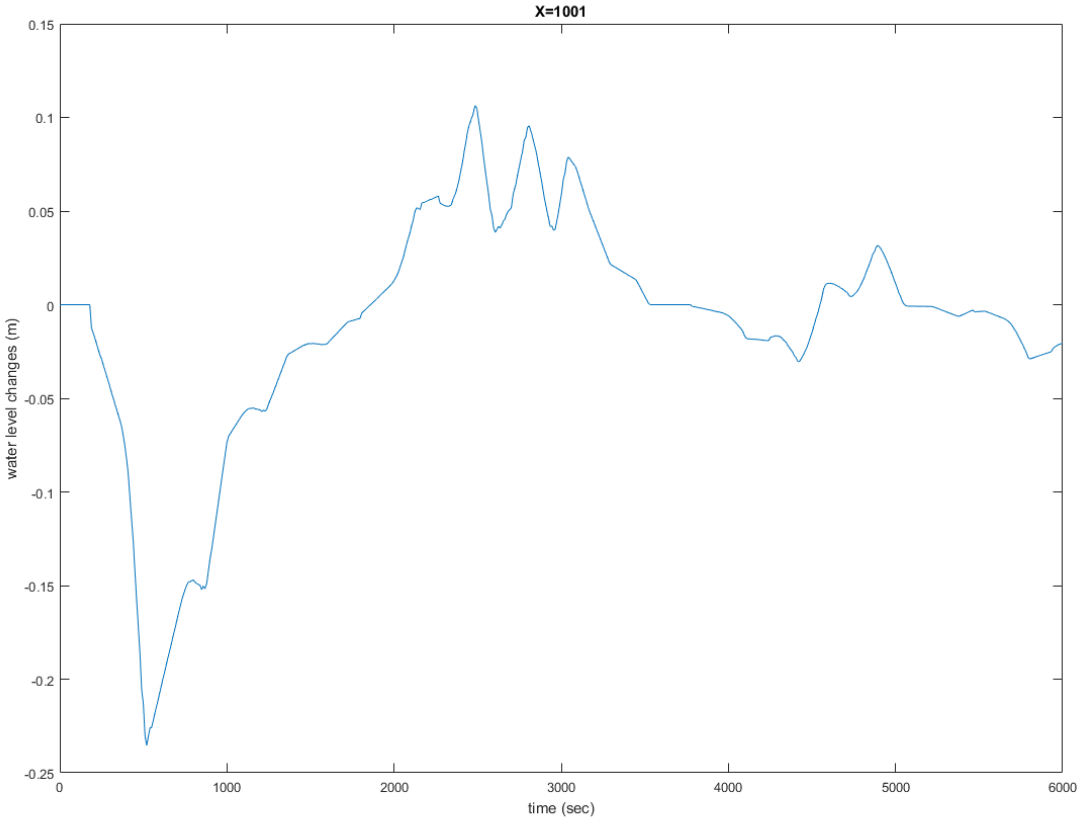

Figure F.8: Sc1: Water level changes in scenario with the original situation at location X1151

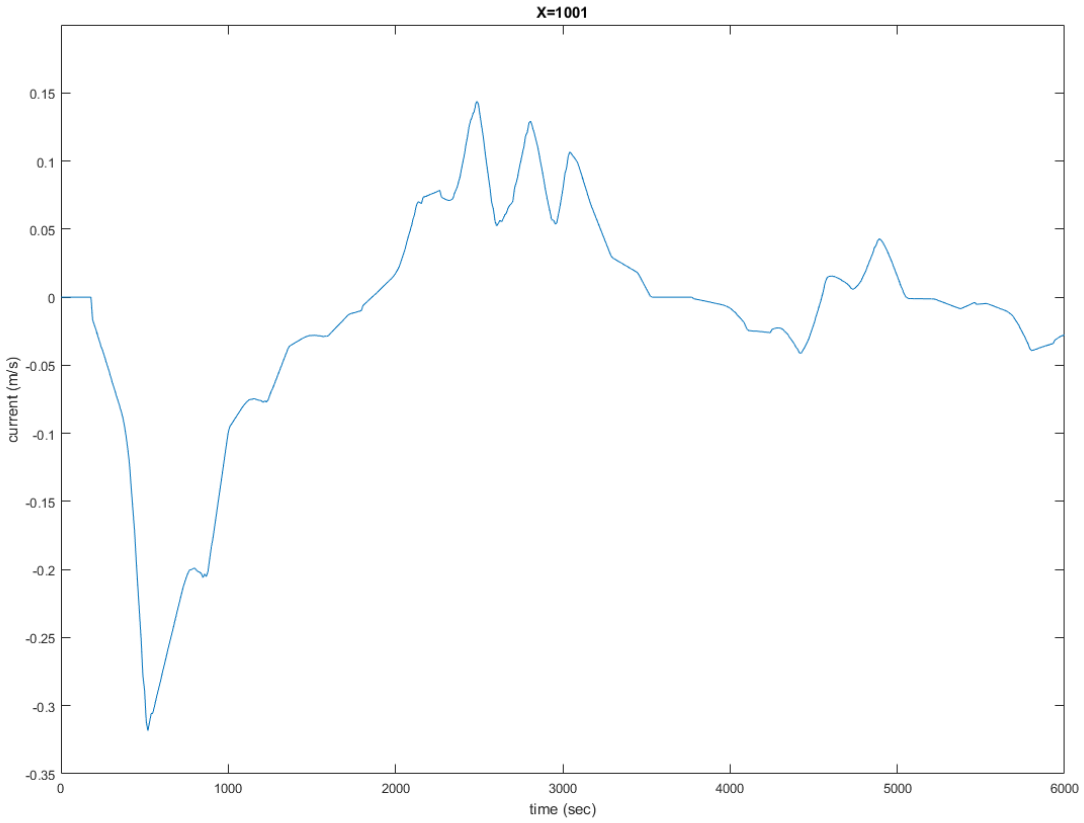

Figure F.9: Sc1: Currents in scenario with the original situation at location X1151

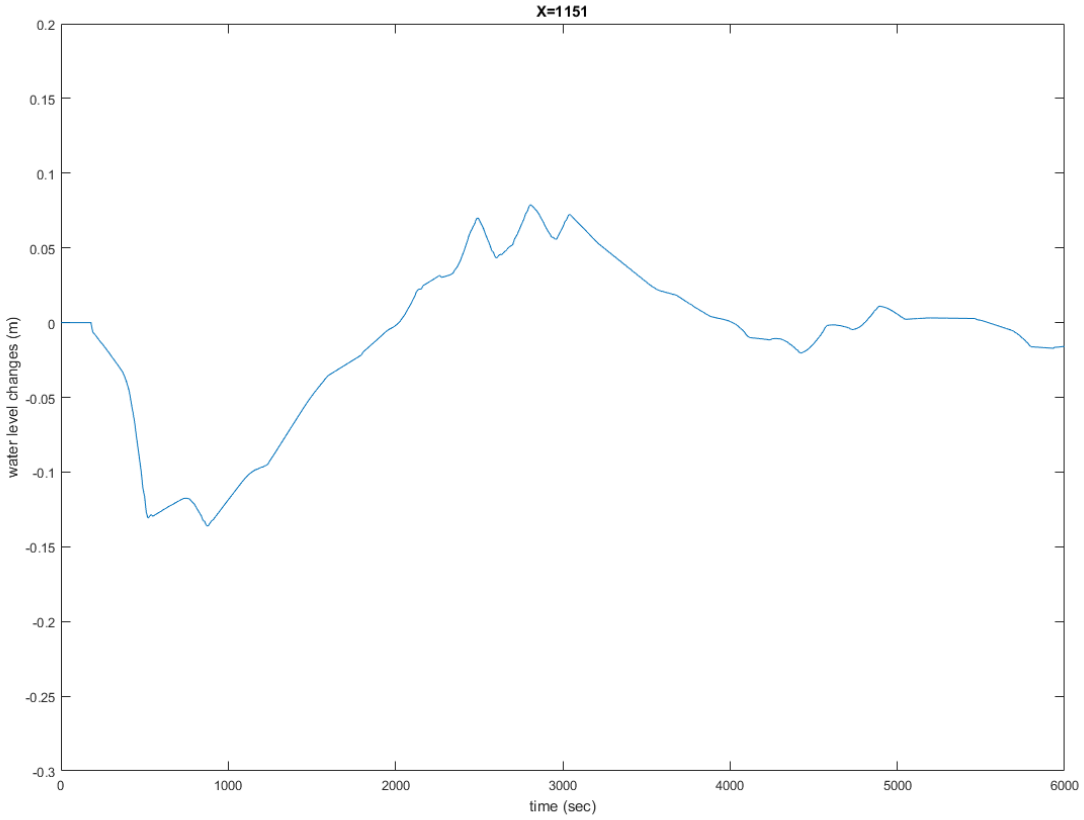

Figure F.10: Sc2: Water level changes in scenario with one culvert at location X1151

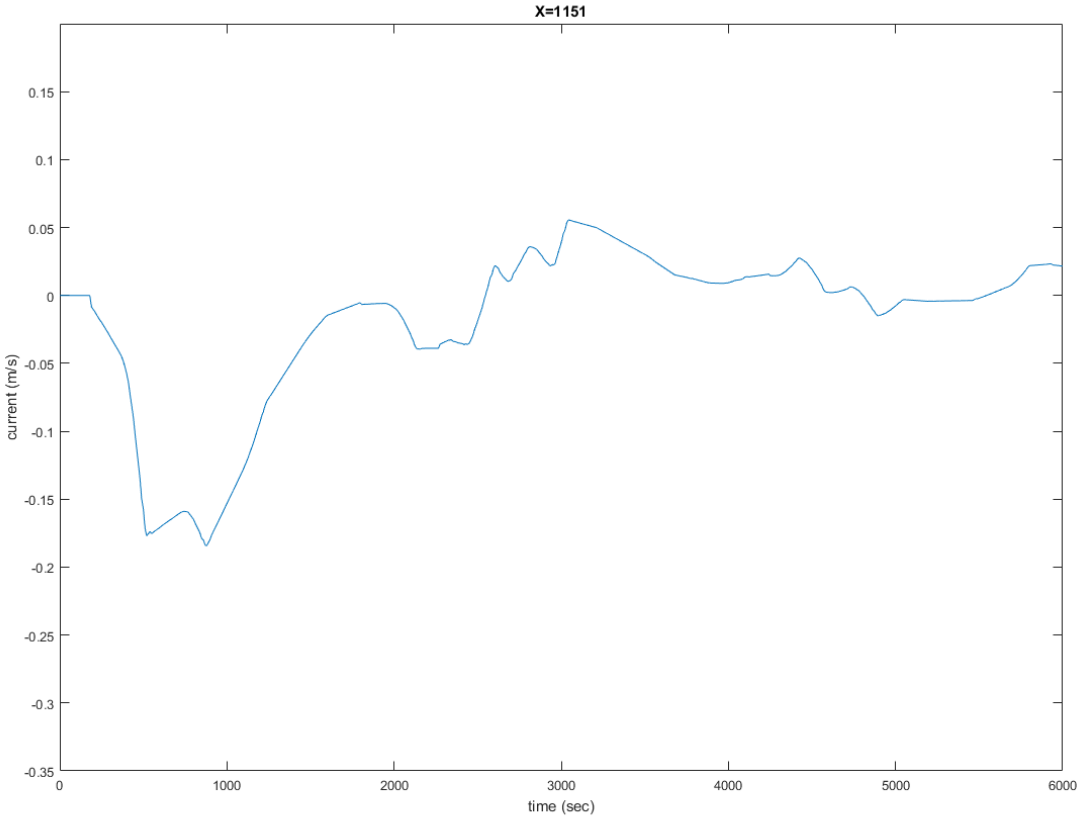

Figure F.11: Sc2: Currents in scenario with one culvert at location X1151

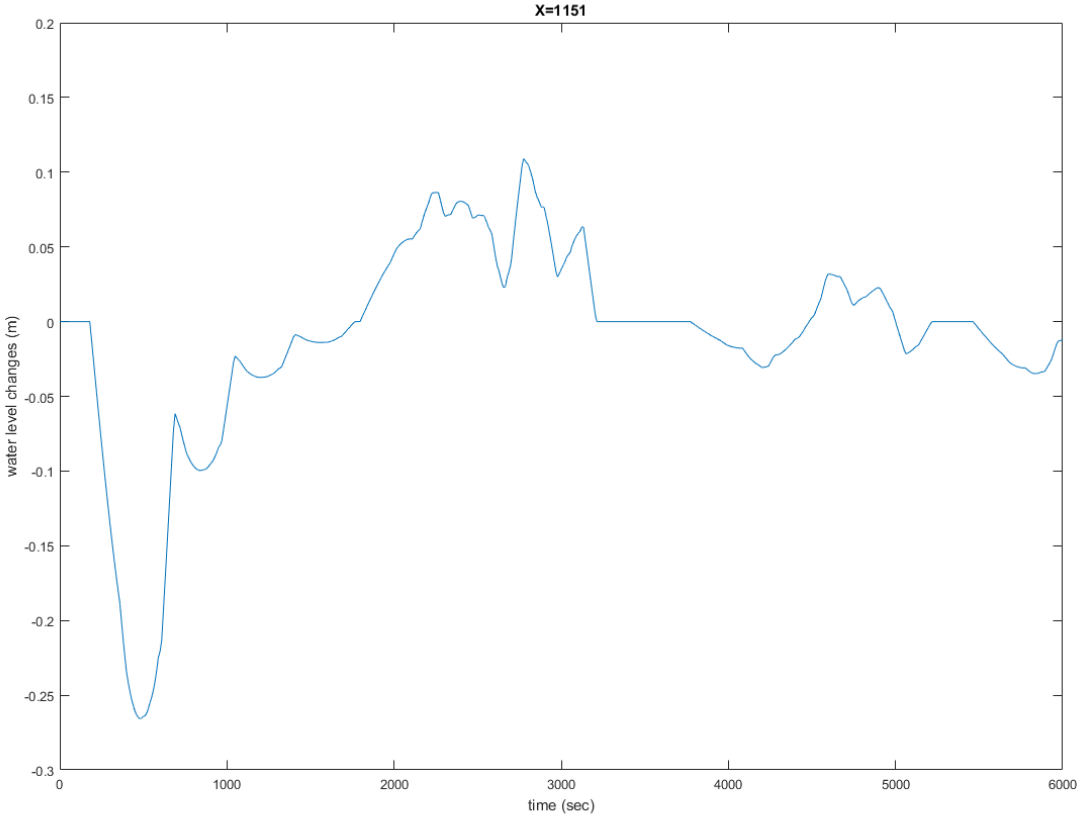

Figure F.12: Sc3: Water level changes in scenario with four culverts at location X1151

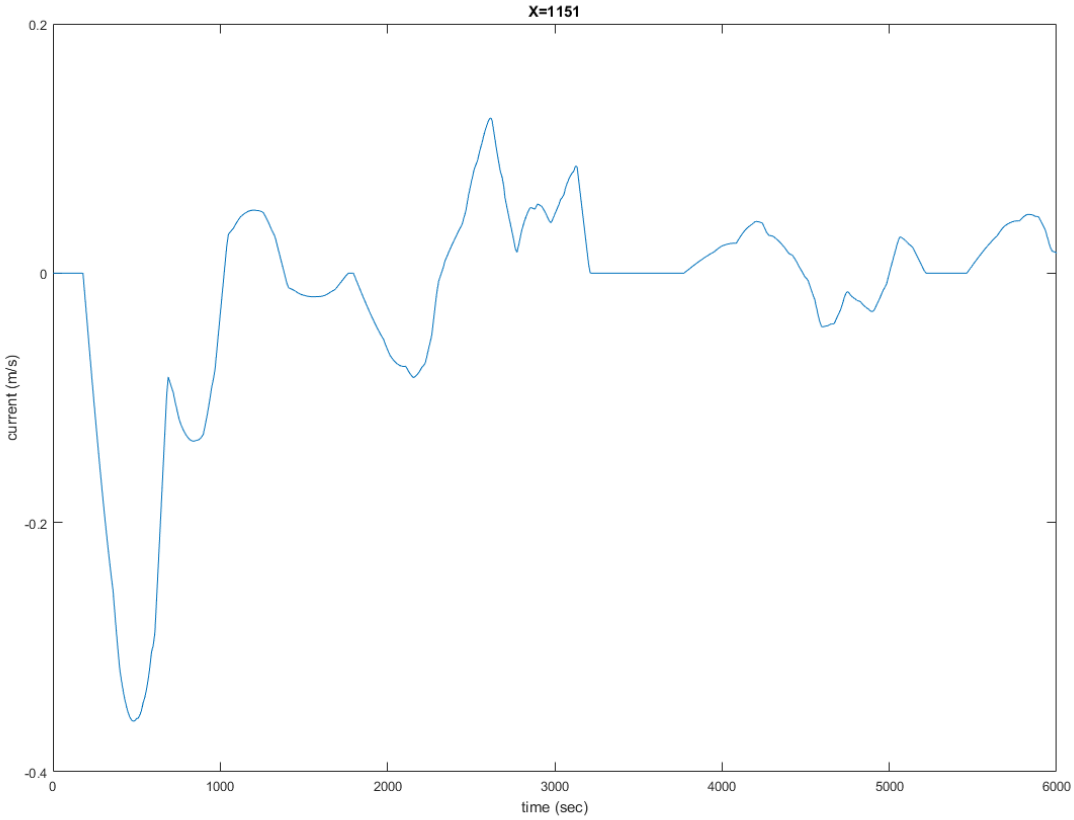

Figure F.13: Sc3: Four culverts at location X1151

LOCATION X4000

Location X4000 is on the narrow canal section between the lock basin and the wide port Stein section. There are no transition points between X4000 and X1151. Changes in currents between figures F.9, F.11 and F.13 and figures F.15, F.17 and F.19 must be due to interactions between waves. The next transition point is at X = 6000. Reflections from this location can be observed at the mid section between $t = 2000$ and $t = 4000$.
The negative extreme values at X = 4000 are practically the same as on location X = 1151, only scenario 2 is 2% smaller. The maximum currents due to positive water level changes are more spread out over time than on X = 1151, resulting in lower currents of respectively 29%, 51% and 36%. An overview of the extreme values of the water level changes and currents at location X4000 can be found in table F.3.

Table F.3: Extreme values at X_4000 in Scenario 1,2 and 3

	Sc1	Sc2	Sc3
z_{min} [m]	-0,235	-0,133	-0,266
z_{max} [m]	0,076	0,039	0,070
u_{min} [m/s]	-0,318	-0,180	-0,359
u_{max} [m/s]	0,103	0,053	0,095
$Downtime$ [min:sec]	08:51	09:46	07:43

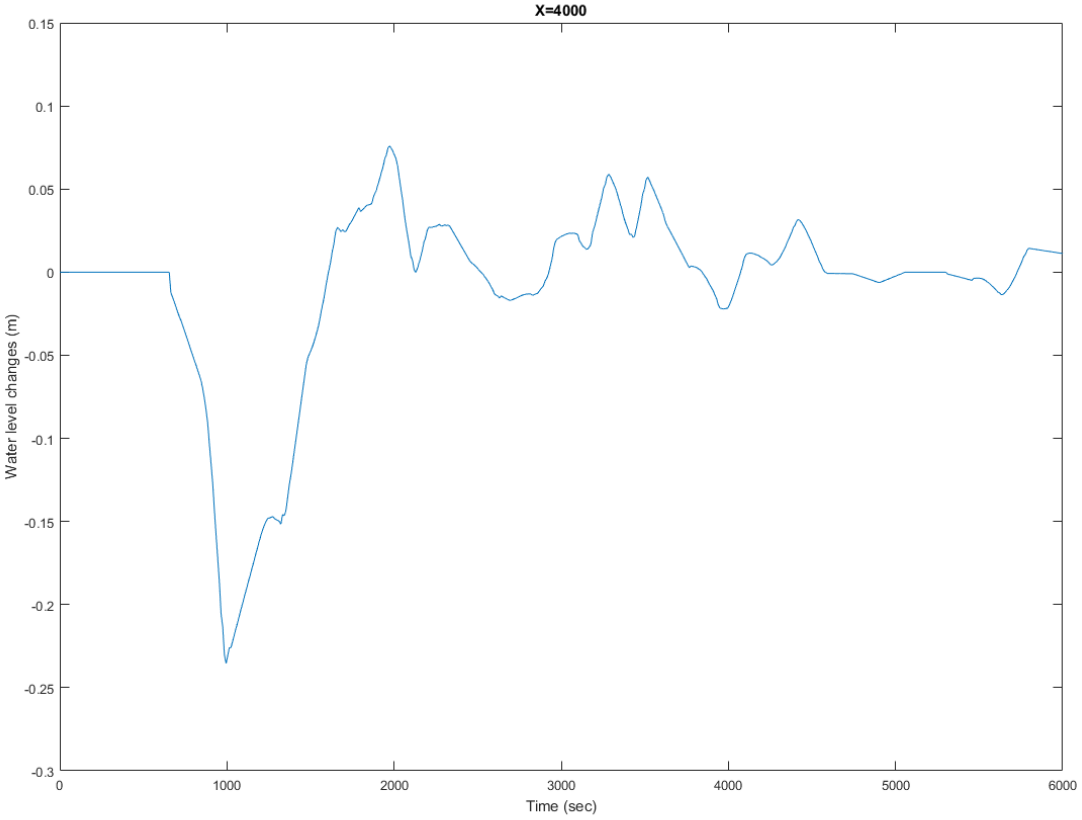

Figure F.14: Sc1: Water level changes in scenario with the original situation at location X4000

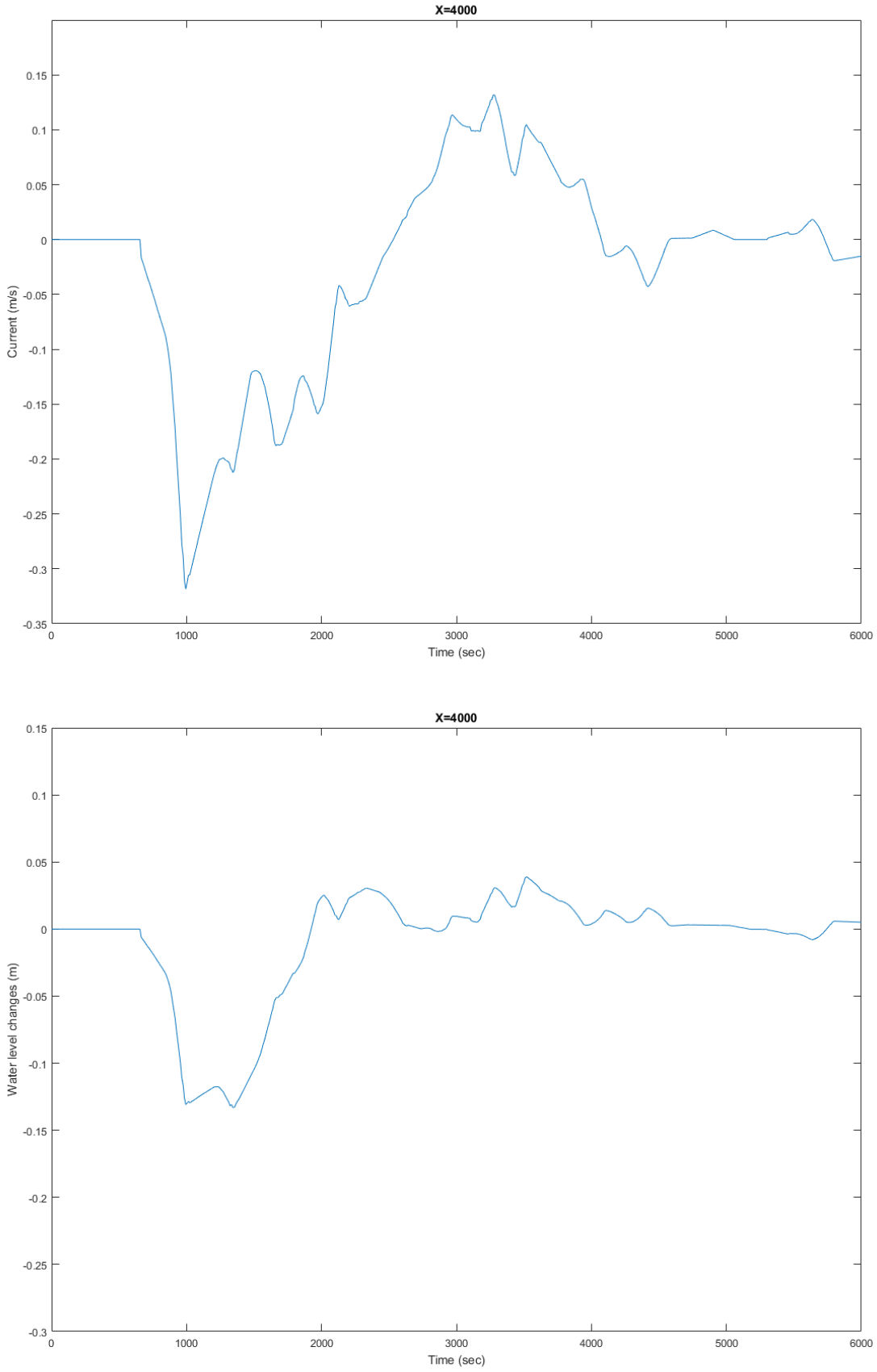

Figure F.16: Sc2: Water level changes in scenario with one culvert at location X4000

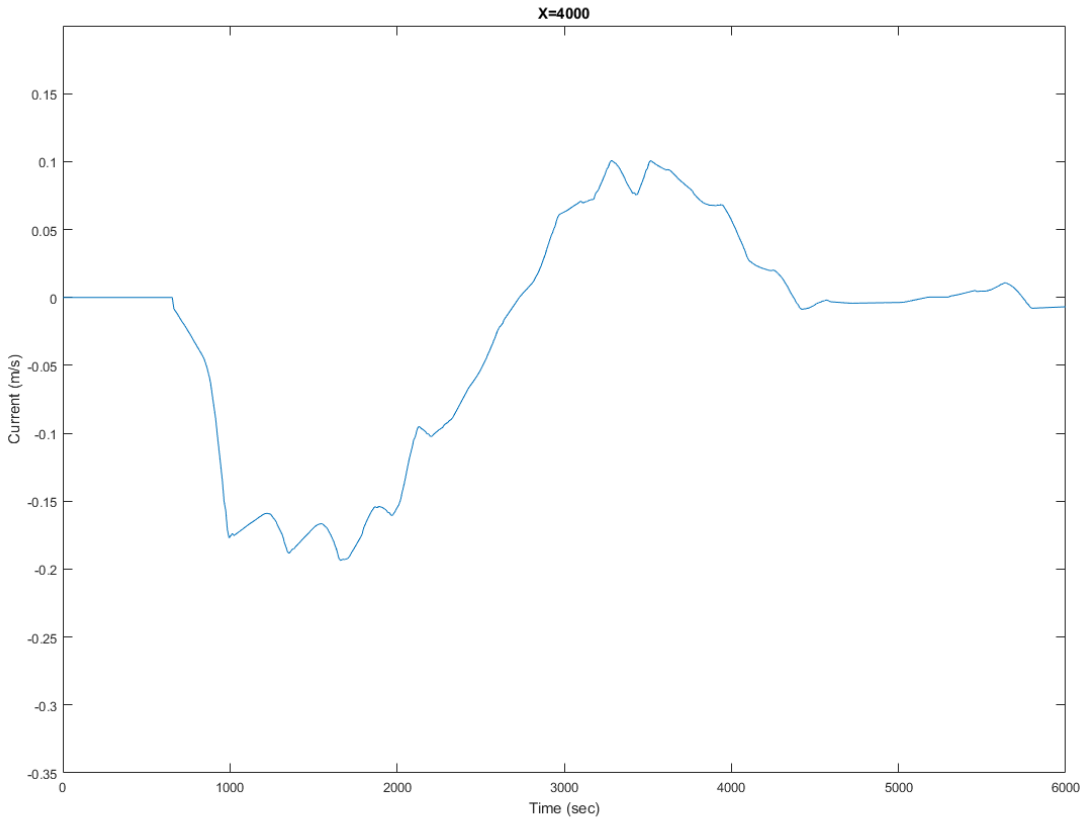

Figure F.17: Sc2: Currents in scenario with one culvert at location X4000

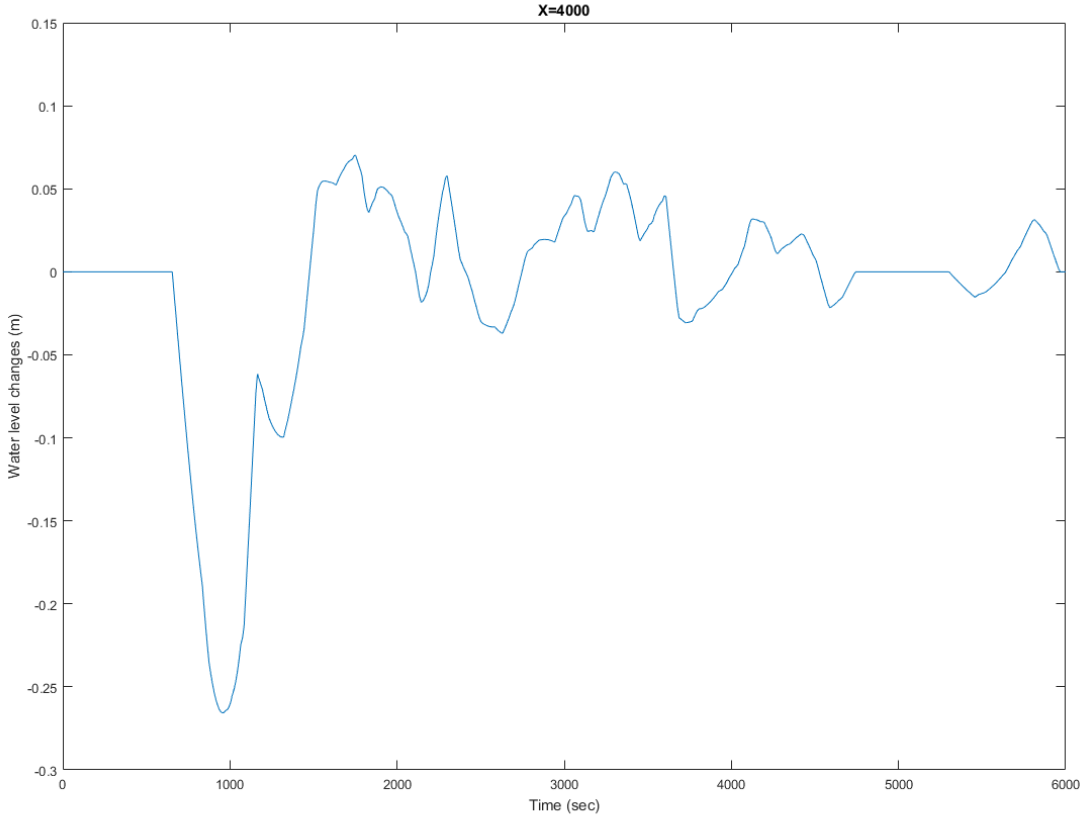

Figure F.18: Sc3: Water level changes in scenario with four culverts at location X4000

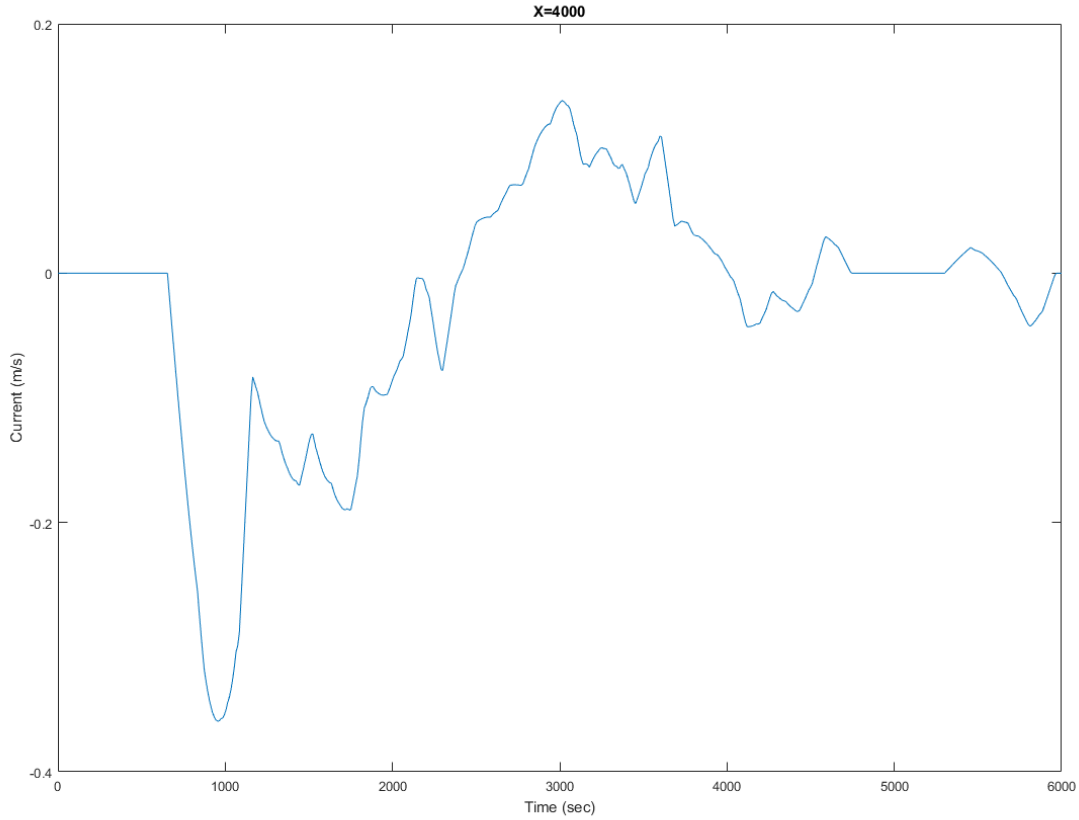

Figure F.19: Sc3: Currents in scenario four culverts at location X4000

LOCATION X5900

Location X5900 is located on the small canal section, before the widening to the wide port Stein section. The results of the model of the three scenarios are presented in figures F.21, F.23 and F.25.
The differences between the third and first scenario low, 6%. Difference between the second and first scenario is rather high, about 44%. This corresponds with the differences on the other locations on the narrow section. The highest negative current changes in all three scenarios are significantly lower at X5900 than at X4000, 28%, 29% and 32% lower. Location X5900 is situated just before the transition point at X6000. The positive reflection wave created by this transition point results in the decrease of the water level change at X5900 and its corresponding current. An overview of the extreme values of the water level changes and currents at location X5900 can be found in table F.4.

Table F.4: Extreme values at X_5900 in Scenario 1,2 and 3

	Sc1	Sc2	Sc3
z_{min} [m]	-0,170	-0,095	-0,180
z_{max} [m]	0,074	0,042	0,086
u_{min} [m/s]	-0,230	-0,129	-0,243
u_{max} [m/s]	0,100	0,057	0,117
$Downtime$ [min:sec]	04:30	00:00	05:25

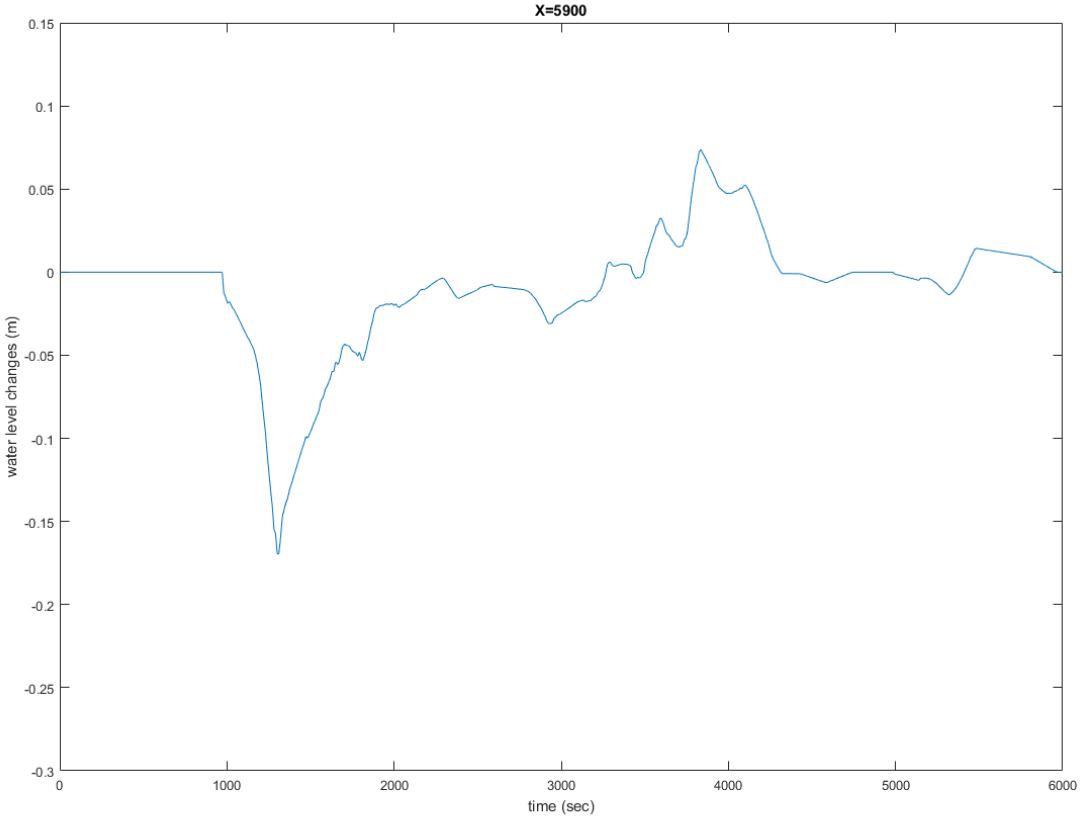

Figure F.20: Sc1: Water level changes in scenario with the original situation at location X5900

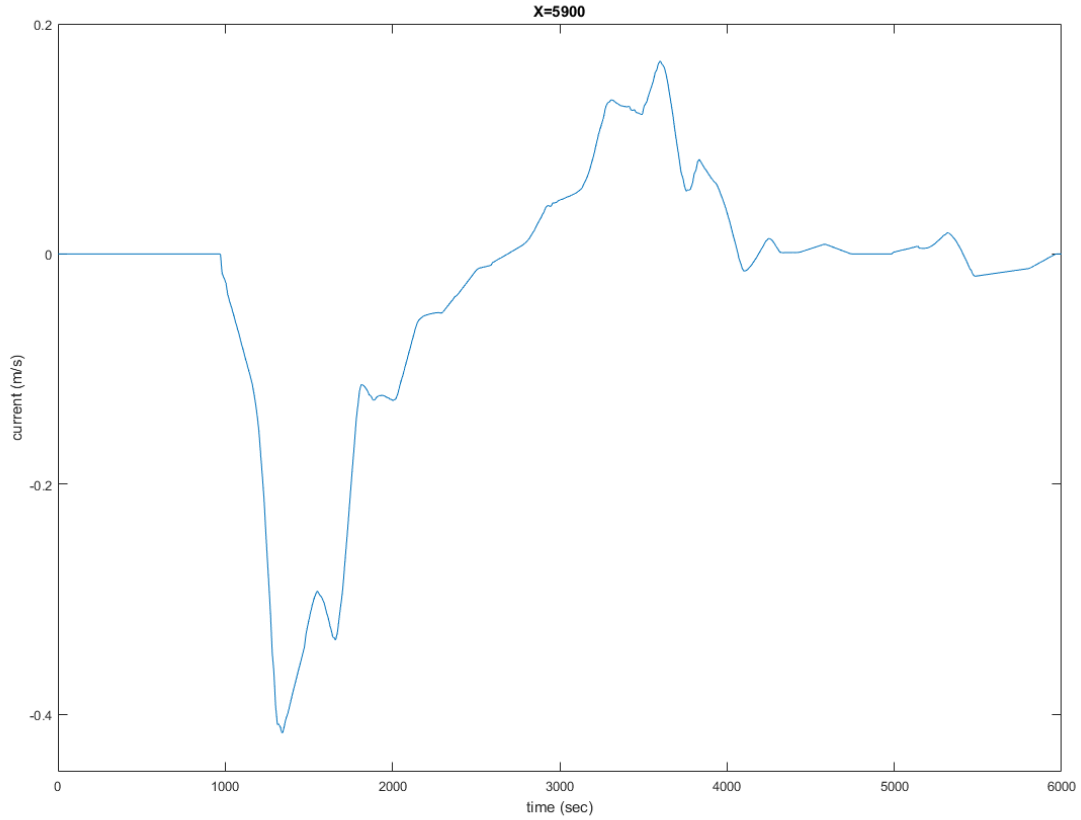

Figure F.21: Sc1: Currents in scenario with the original situation at location X5900

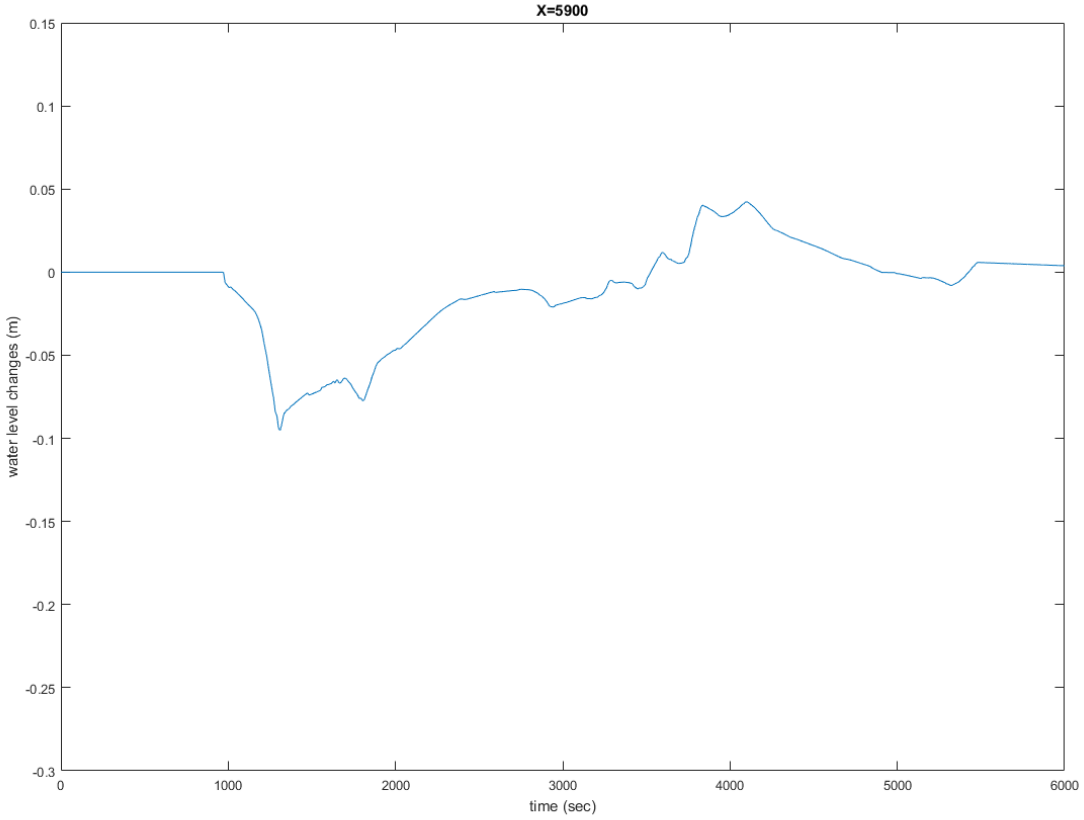

Figure F.22: Sc2: Water level changes in scenario with one culvert at location X5900

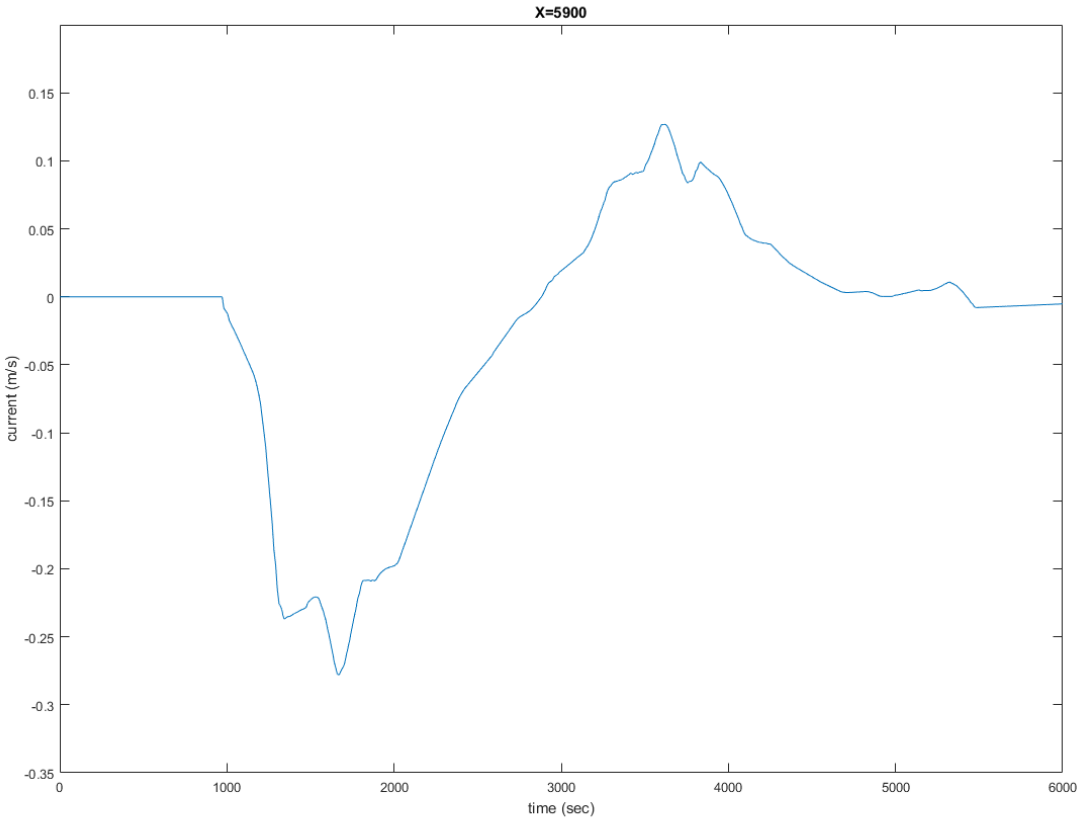

Figure F.23: Sc2: Currents in scenario with one culvert at location X5900

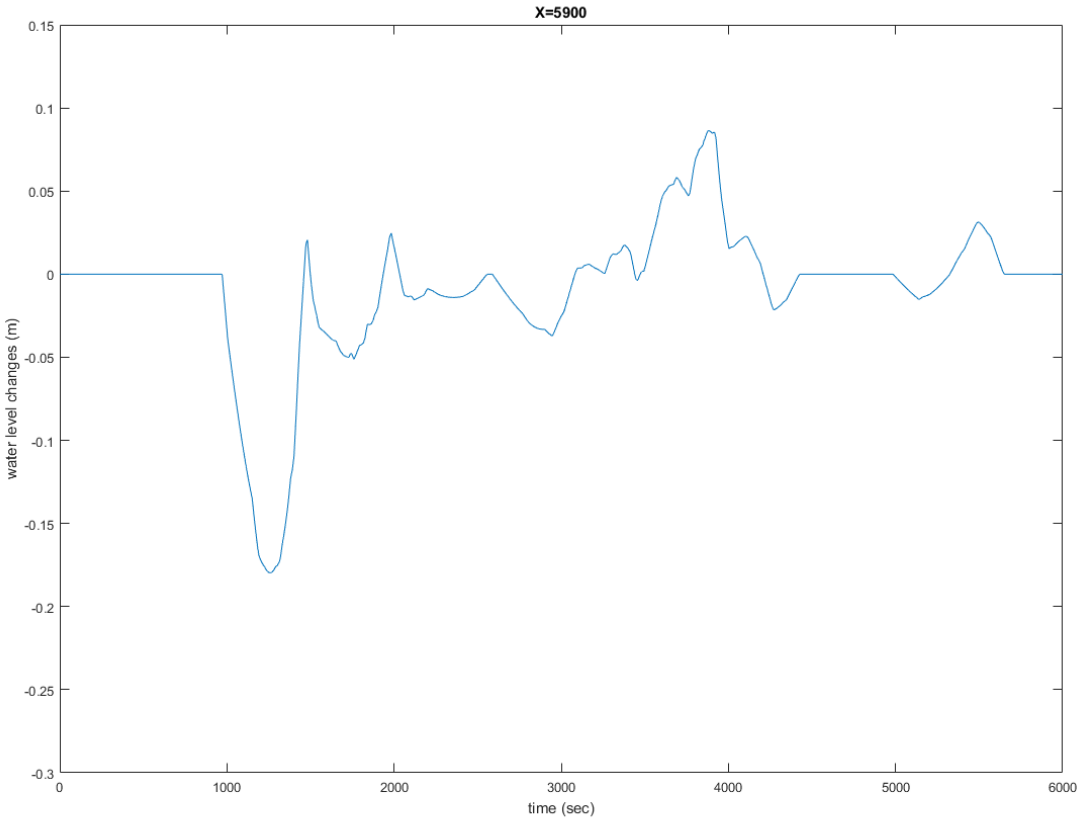

Figure F.24: Sc3: Water level changes in scenario with four culverts at location X5900

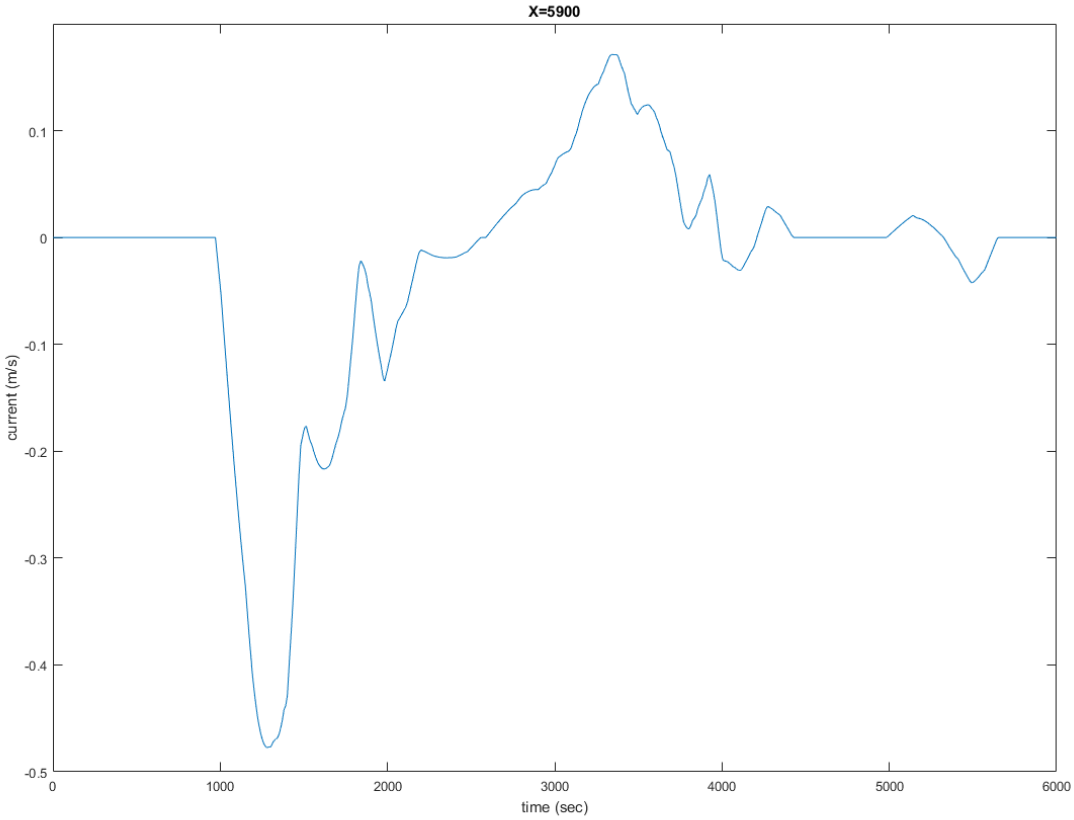

Figure F.25: Sc3: Currents in scenario with four culverts at location X5900

LOCATION X6001

Location X6001 is situated on the wide section of port Stein, right after the transition point of the narrow section of the canal and the wider section of the port of Stein. The results of the model can be found in figures F.27, F.29 and F.31. The primary wave is lower than at location X5900 in all three scenarios, 9%, 10% and 1% lower. This is a result of the wider cross section at location X6001. The extreme values of the current due to negative translation waves are 0.208, 0.116 and 0.240 m/s. The currents due to positive translation waves are lower than at location X5900 as well, 6%, 11% and 3% lower. The extreme values of the water level deviations and currents at location X6001 can be found in table F.5.

Table F.5: Extreme values at X_6001 in Scenario 1,2 and 3

	Sc1	Sc2	Sc3
z_{min} [m]	-0,154	-0,086	-0,177
z_{max} [m]	0,069	0,038	0,084
u_{min} [m/s]	-0,208	-0,116	-0,240
u_{max} [m/s]	0,094	0,051	0,113
$Donwtime$ [min:sec]	04:36	00:00	05:14

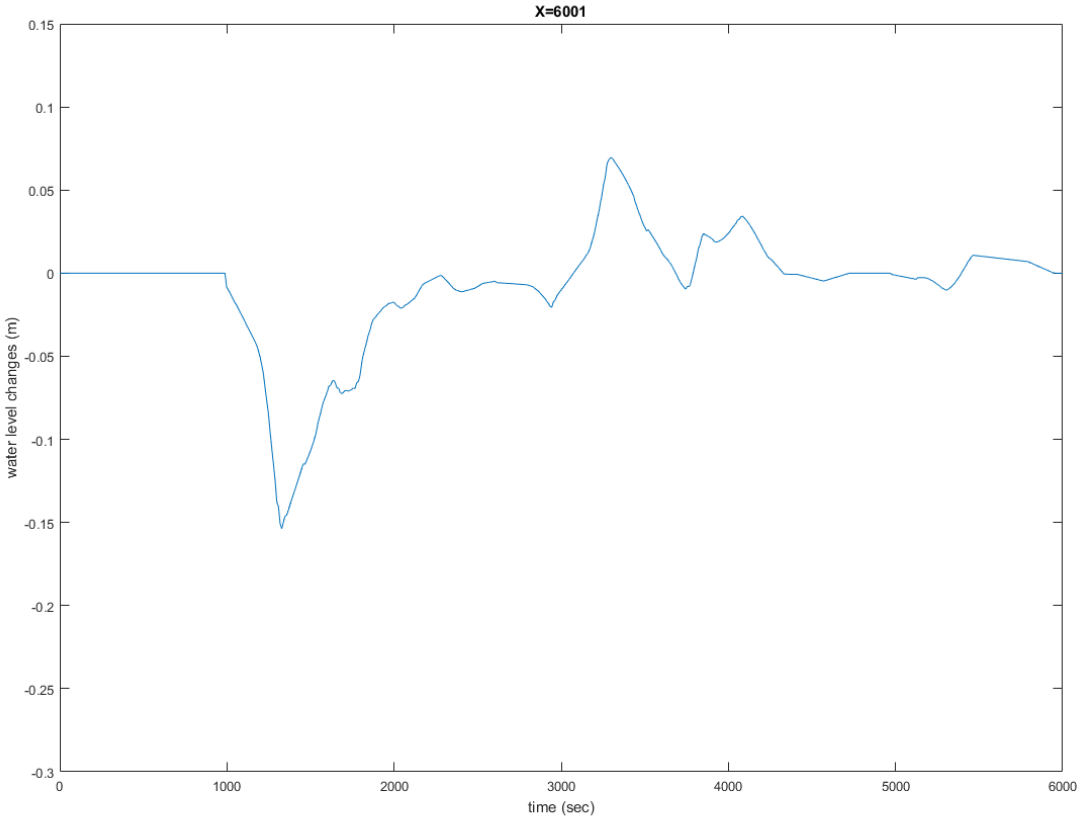

Figure F.26: Sc1: Water level changes in scenario with original situation at location X6001

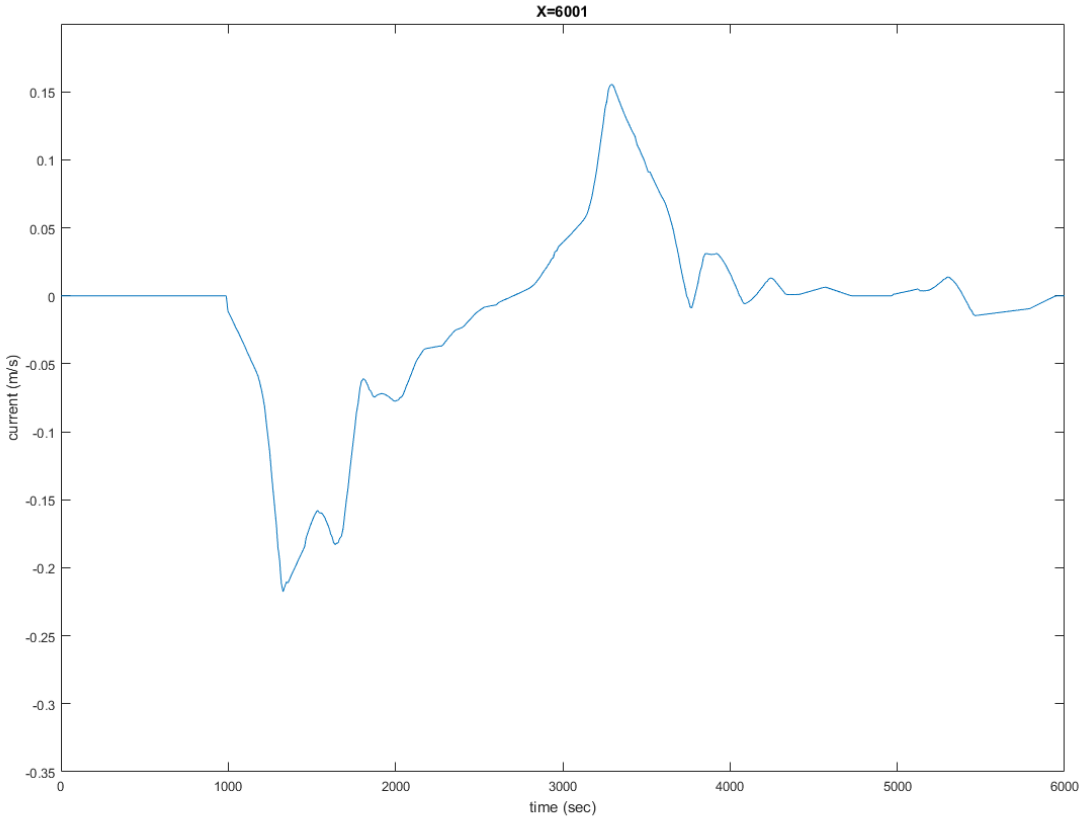

Figure F.27: Sc1: Currents in scenario with original situation at location X6001

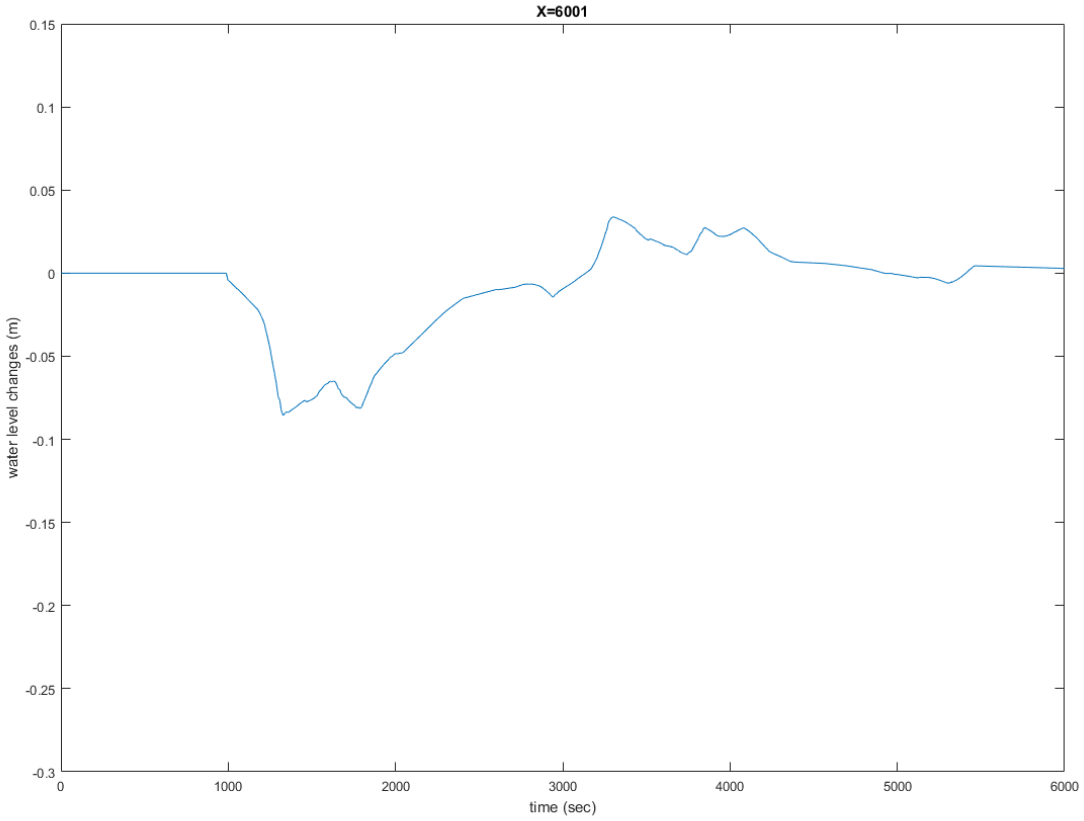

Figure F.28: Sc2: Water level changes in scenario with one culvert at location X6001

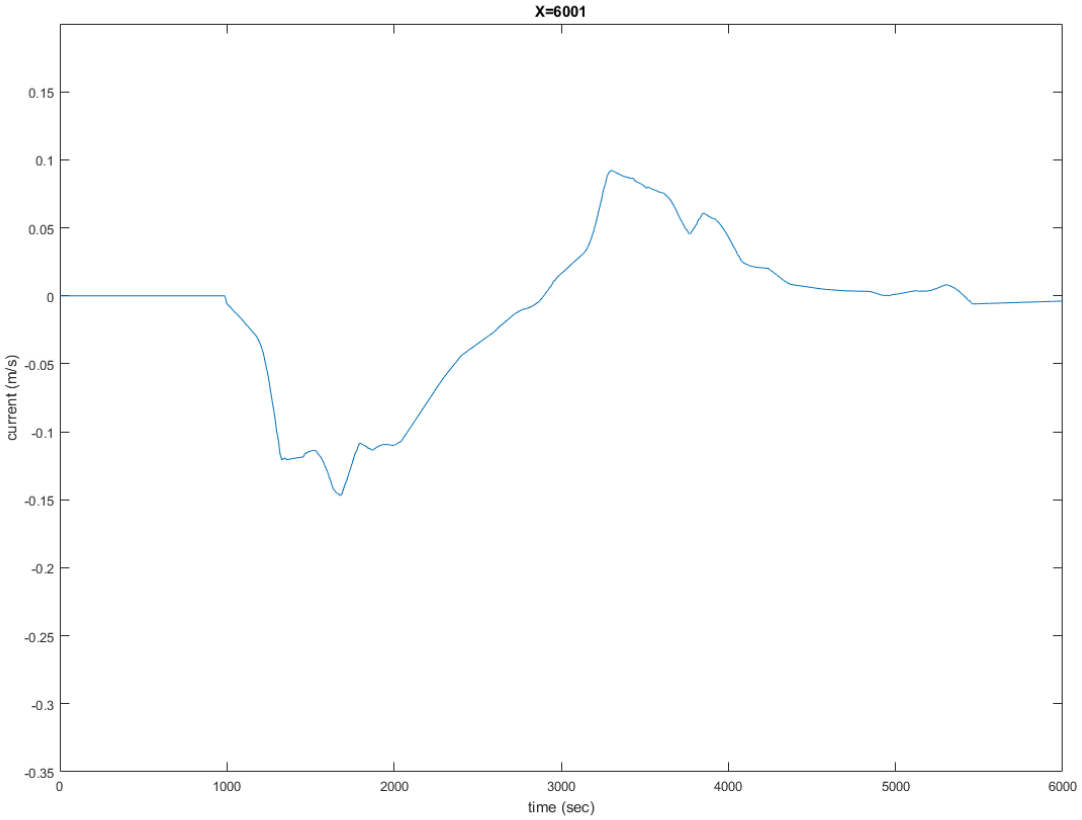

Figure F.29: Sc2: Currents in scenario with one culvert at location X6001

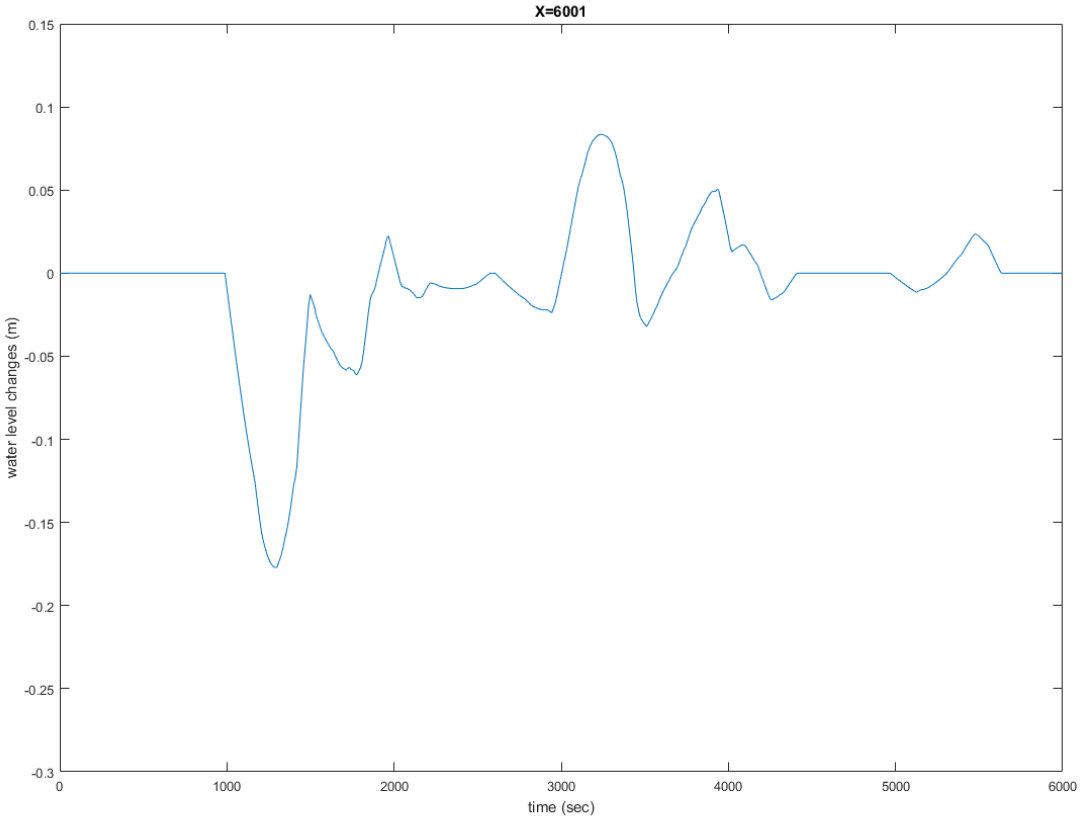

Figure F.30: Sc3: Water level changes in scenario with four culverts at location X6001

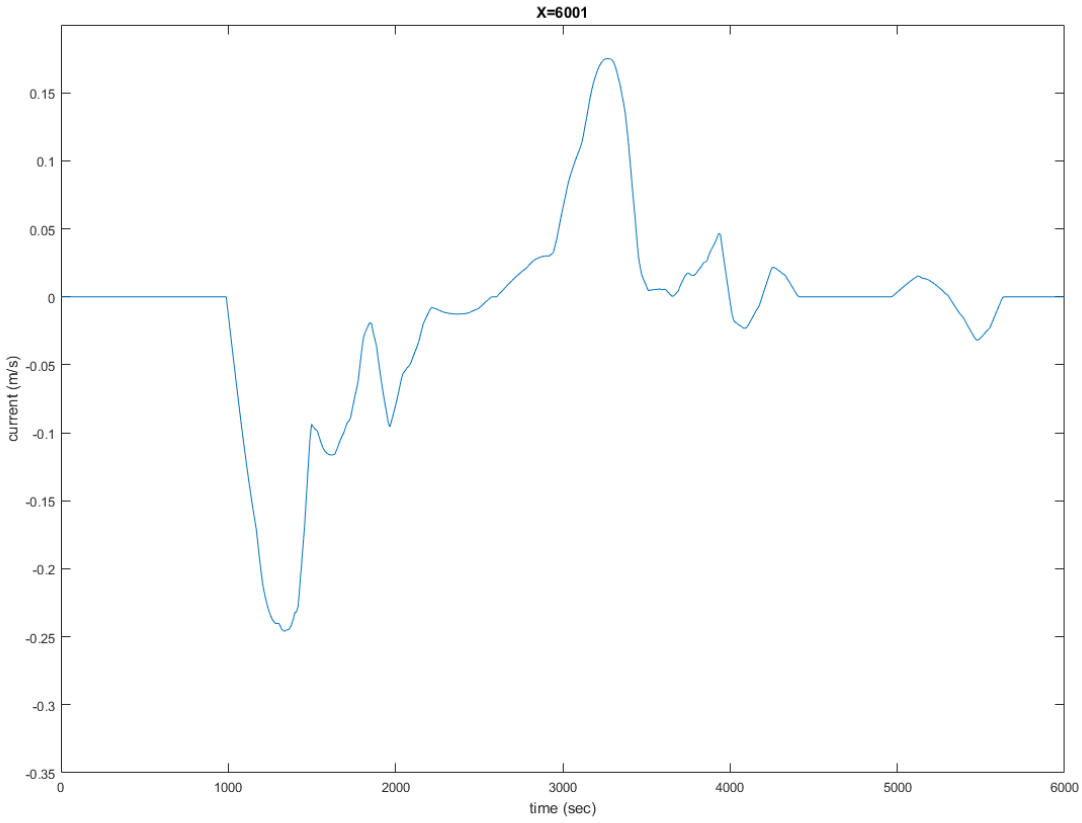

Figure F.31: Sc3: Currents in scenario with four culverts at location X6001

SCENARIO 4: FILLING MIDDLE AND EAST LOCK CHAMBER SIMULTANEOUSLY

Scenario 4 is analysed in this section. This scenario is a bit in between the two groups. The discharge of the fourth scenario is much larger than in the first three scenarios but it is still one wave. An overview of the extreme values and downtime in scenario 4 can be found in table F.6. The results are presented in figures F.33 till F.41.

Table F.6: Overview of extreme values and downtime of scenarios 1 and 4, at 5 locations

Scenario	Parameter	X_Born	X_1151	X_4000	X_5900	X_6001
Sc4	z_{min} [m/s]	-0,285	-0,389	-0,389	-0,274	-0,253
	z_{min} [m/s]	0,167	0,152	0,104	0,112	0,117
	u_{min} [m/s]	-0,385	-0,527	-0,527	-0,370	-0,343
	u_{max} [m/s]	0,226	0,206	0,141	0,152	0,158
	$Dtime$ [min:sec]	24:36	25:03	12:37	09:56	09:23

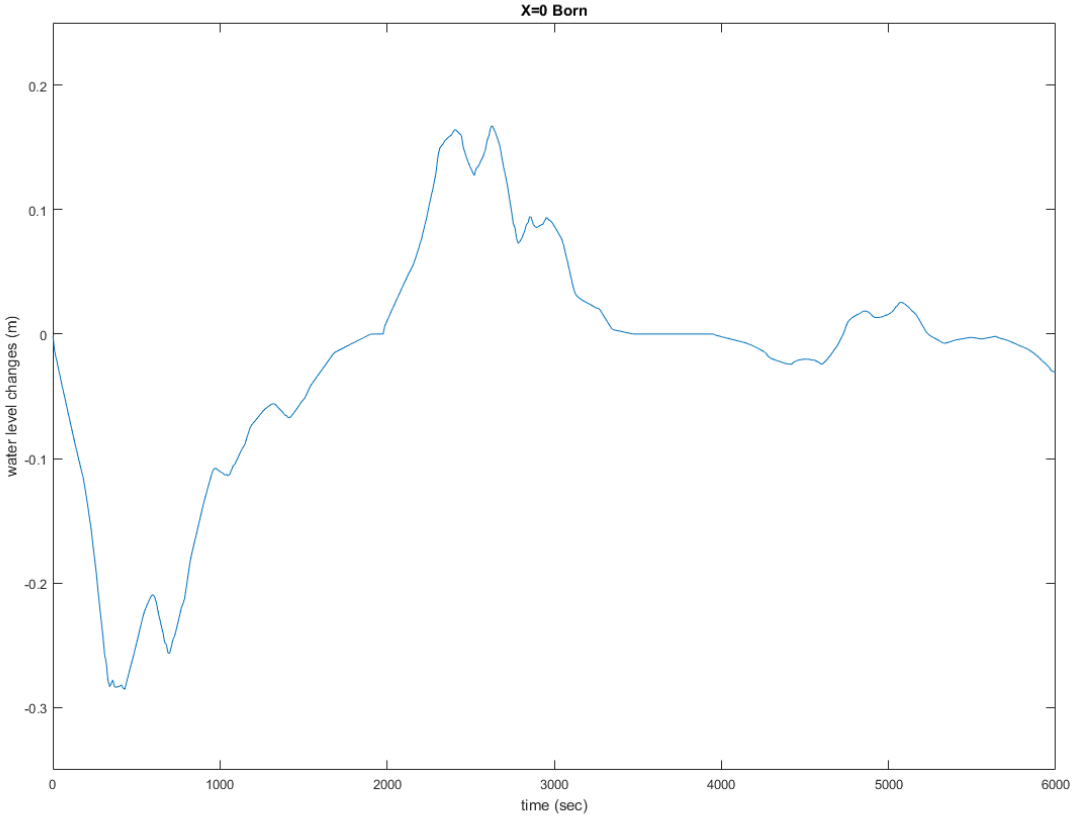

Figure F.32: Sc4: Water level changes due to 2 x 2 culverts simultaneously at location XBorn

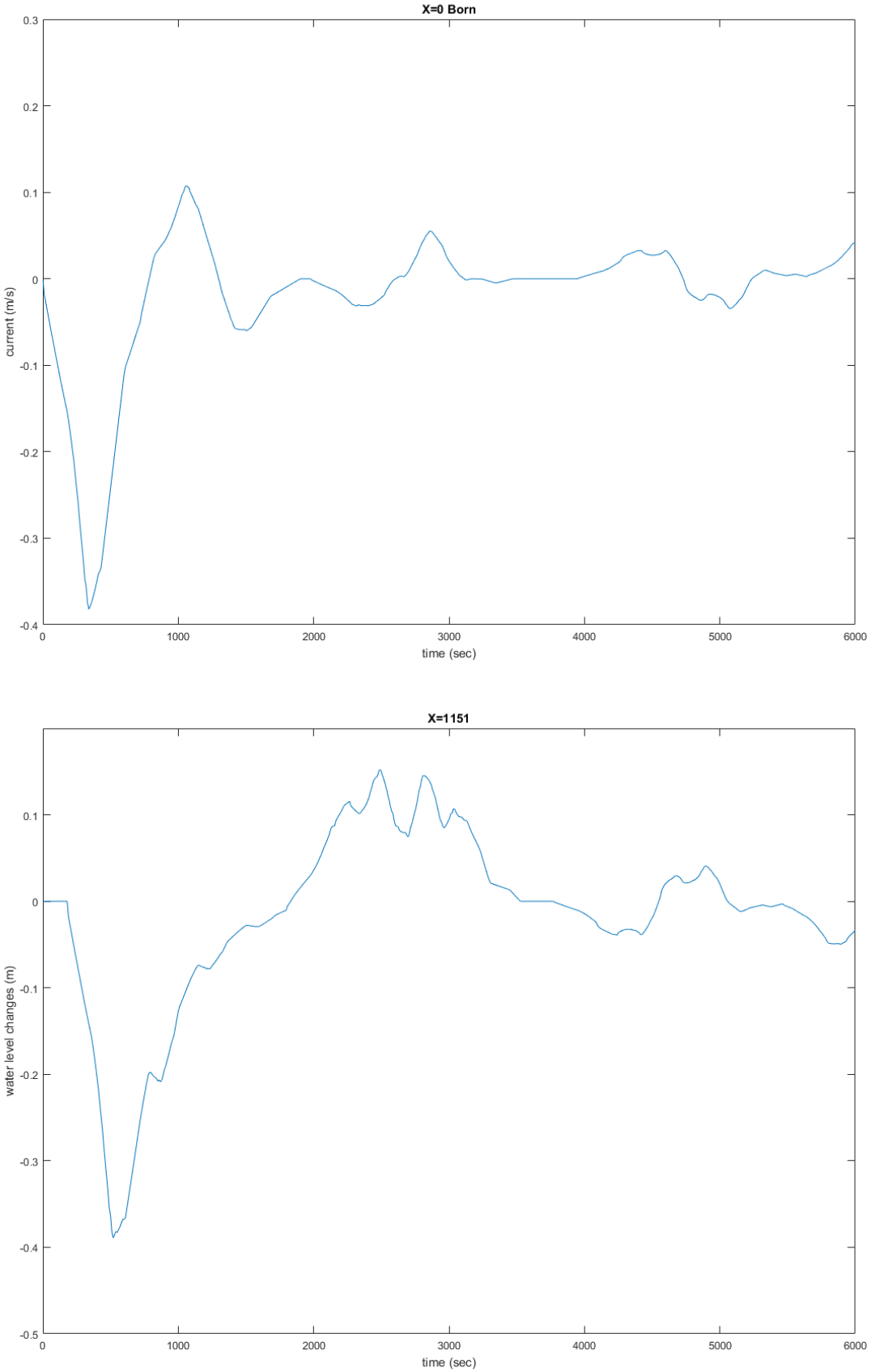

Figure F.34: Sc4: Water level changes due to 2 x 2 culverts simultaneously at location X1151

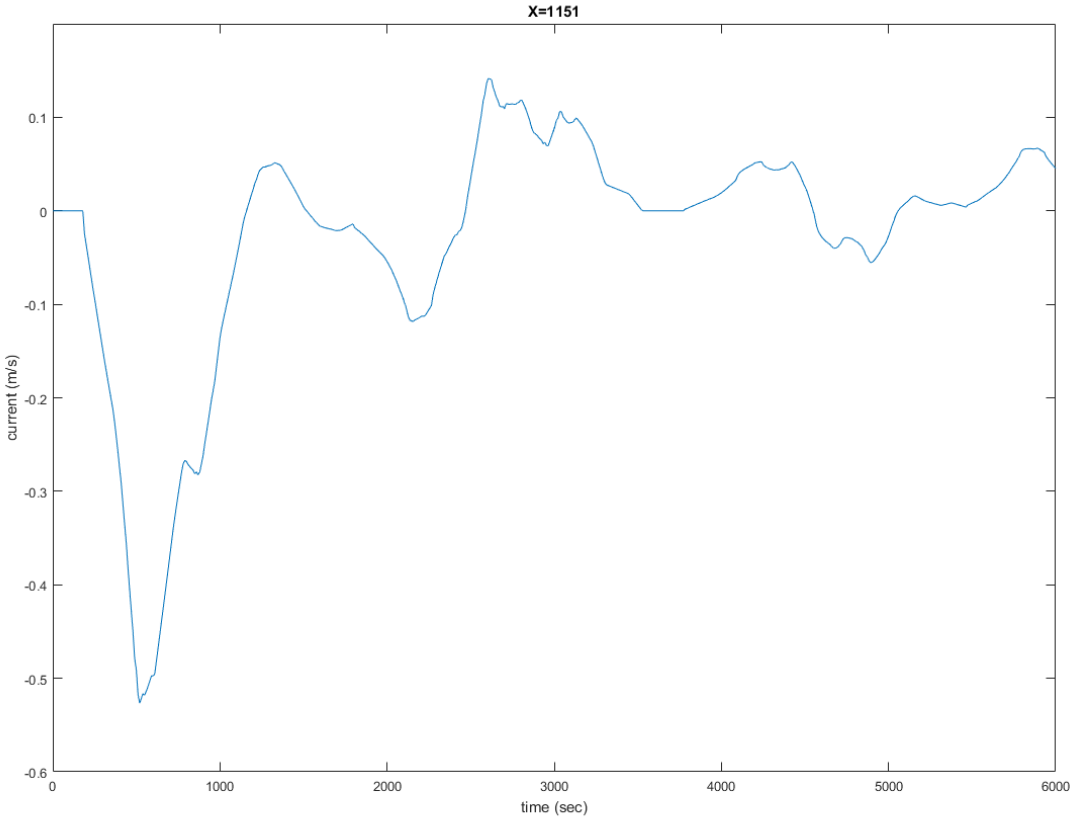

Figure F.35: Sc4: Currents due to 2 x 2 culverts simultaneously at location X1151

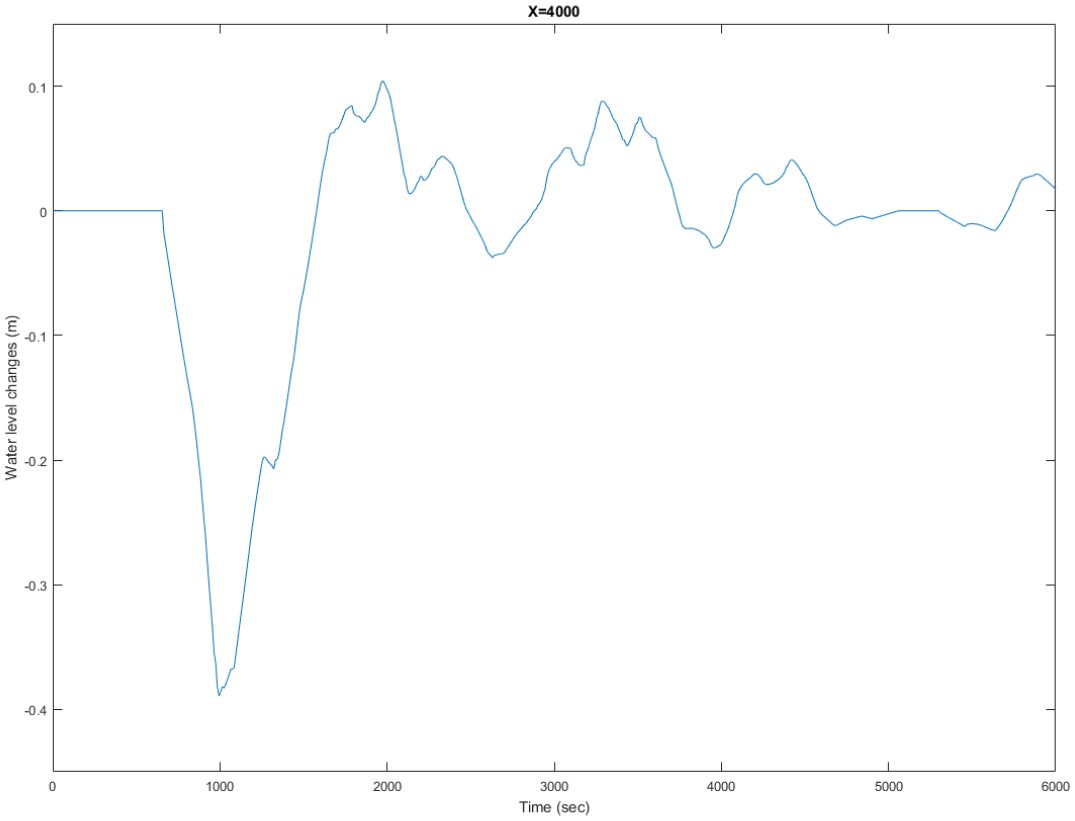

Figure F.36: Sc4: Water level changes due to 2 x 2 culverts simultaneously at location X4000

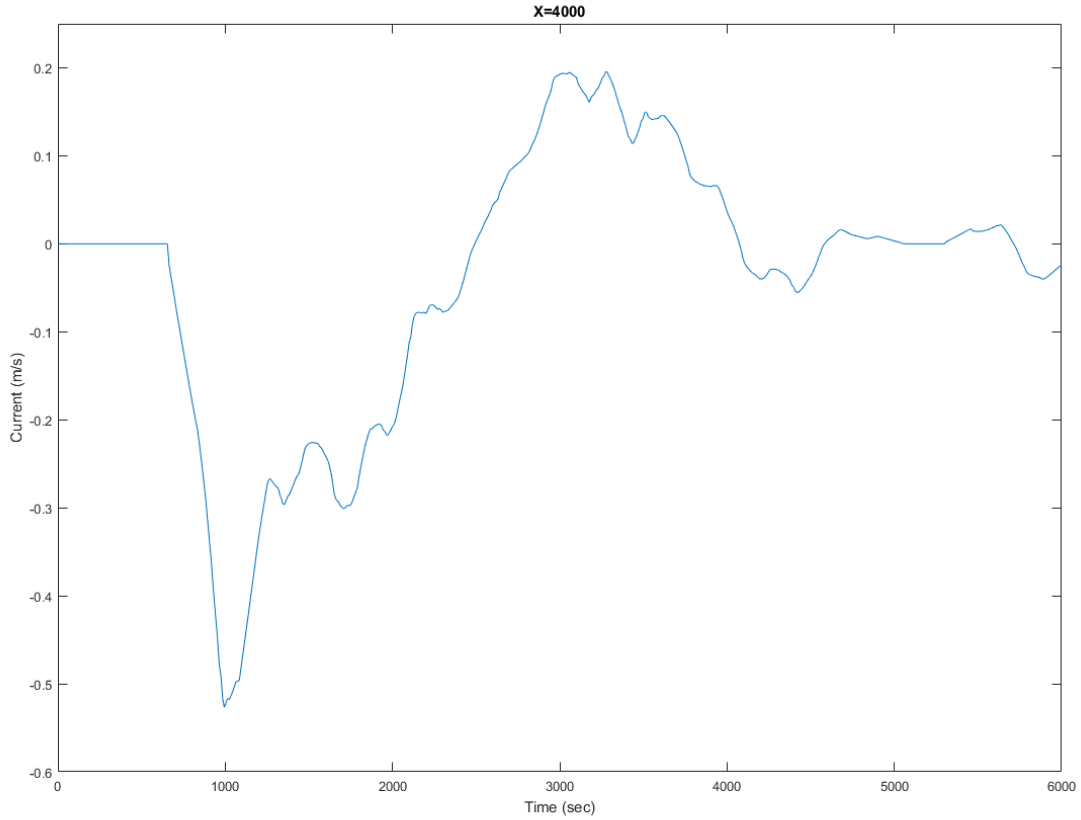

Figure F.37: Sc4: Currents due to 2 x 2 culverts simultaneously at location X4000

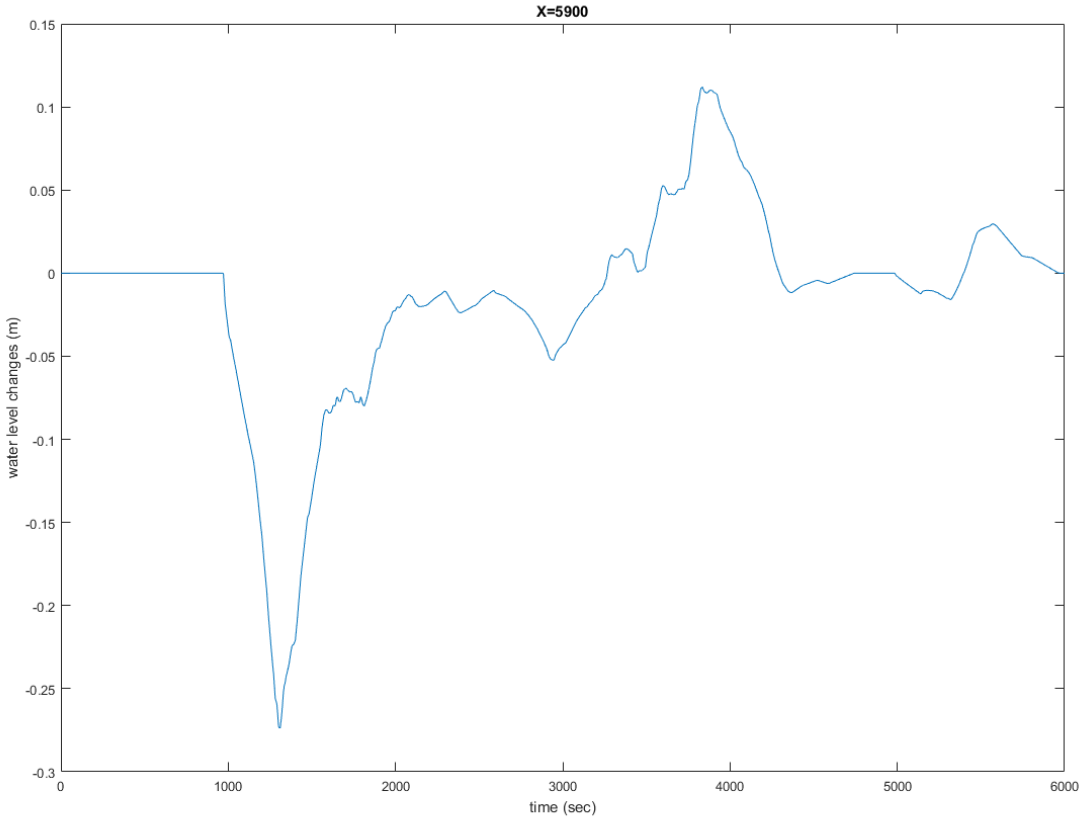

Figure F.38: Sc4: Water level changes due to 2 x 2 culverts simultaneously at location X5900

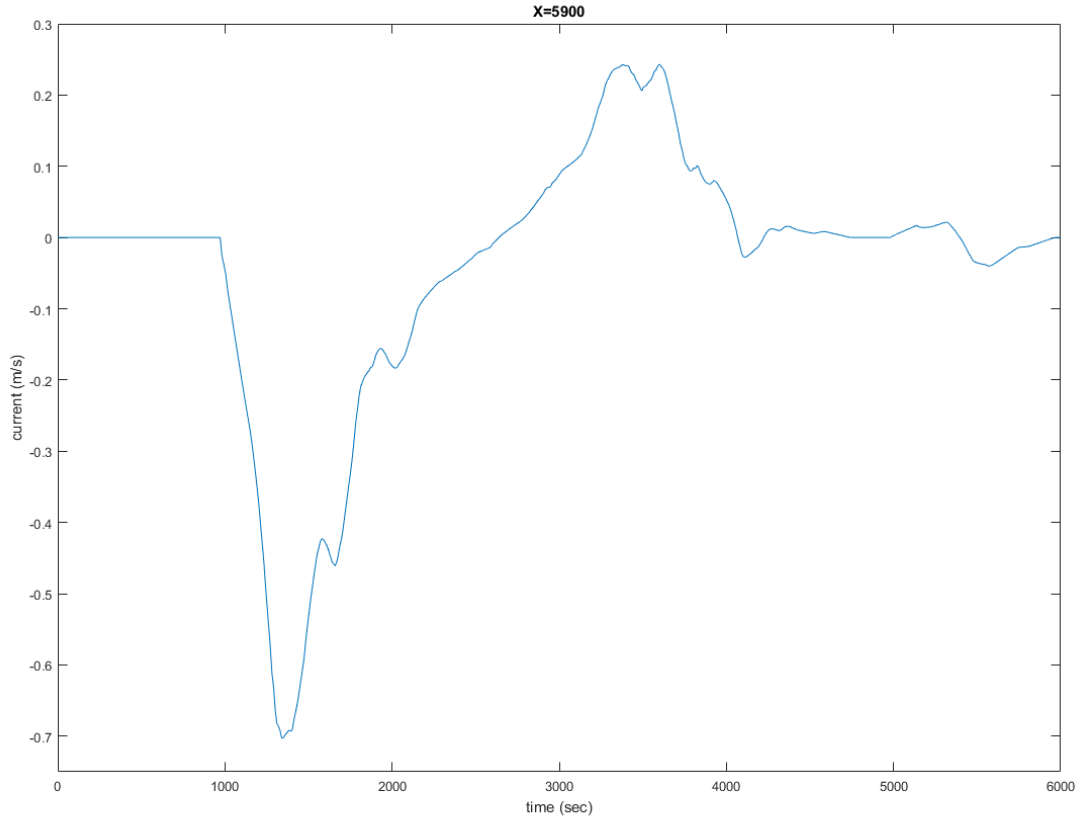

Figure F.39: Sc4: Currents due to 2 x 2 culverts simultaneously at location X5900

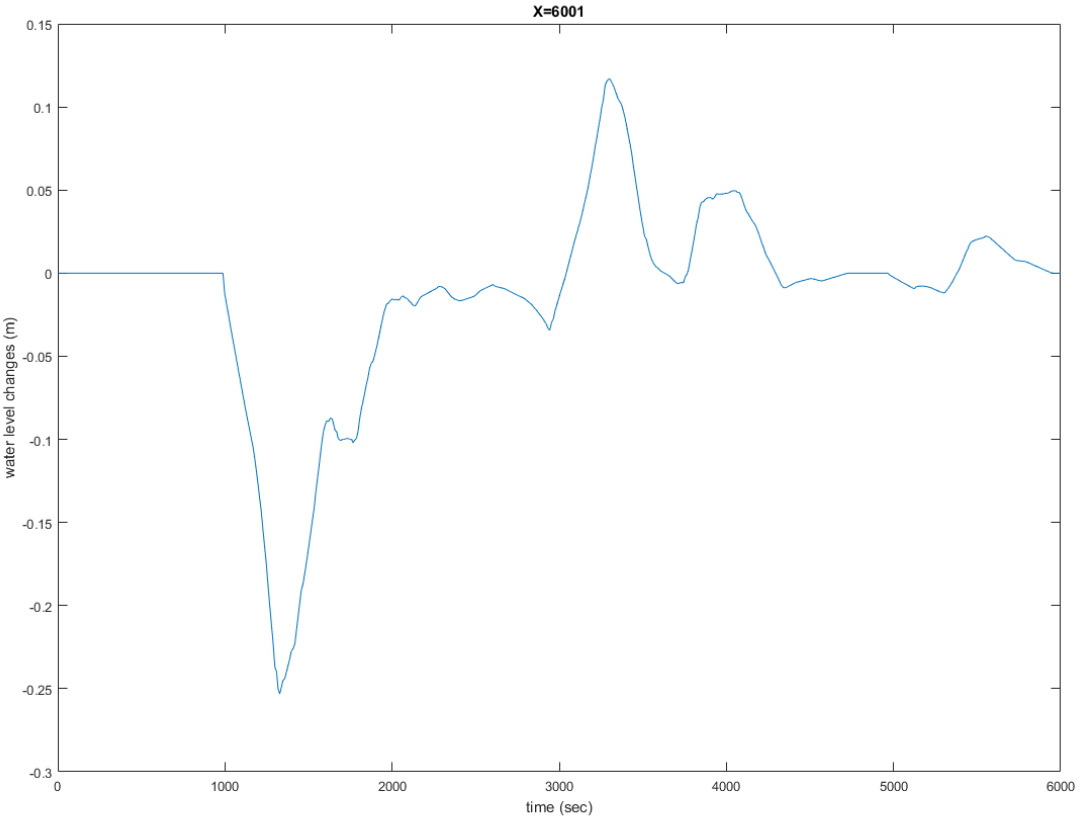

Figure F.40: Sc4: Water level changes due to 2 x 2 culverts simultaneously at location X6001

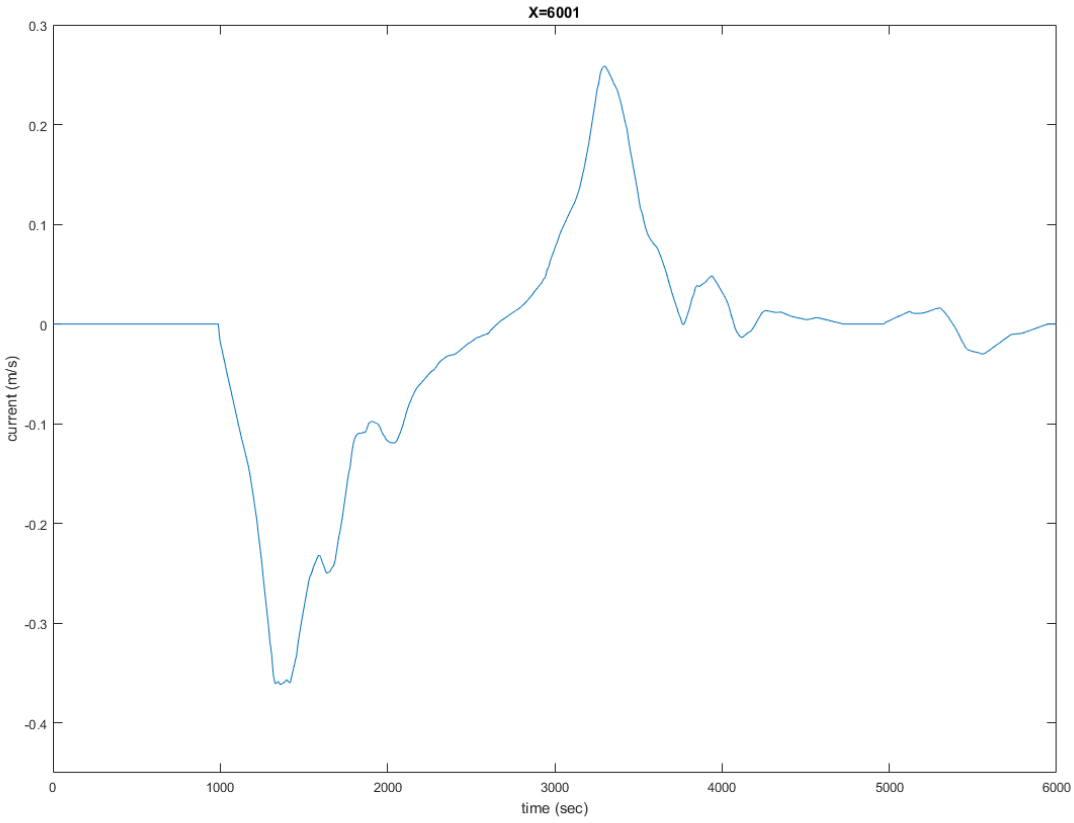

Figure F.41: Sc4: Currents due to 2 x 2 culverts simultaneously at location X6001

F.2. GROUP 2: DIFFERENT FILLING AND EMPTYING REGIMES

The influence of filling the lock chambers in different intervals is researched in this section. Changes is wave height due to interference of reflections of the primary wave with a second wave are investigated. In this case the primary waves are created by the Middle lock chamber, the second waves are a result of filling the East lock chamber. A distinction in discharge-time relation has been made as well. First, the original wave has been investigated, using 2 culverts. Second, the situation with one culvert is analysed.

F.2.1. FILLING AND EMPTYING REGIMES WITH NORMAL WAVE

In this section the effects of two sequential wave on the canal are modelled. To create realistic scenarios, the choice has been made to model the situation with first a wave created by the Middle lock chamber, followed by filling the East chamber. The alternative was modelling two times a wave by the Middle chamber, this is possible in the model but impossible in reality. The time between two waves is respectively 5 minutes, 10 minutes and 15 minutes. These correspond to scenarios 5, 6 and 7. In this section two culverts will be used as discharge-time relation, for both Middle as East lock chamber. The corresponding discharges are visualized in figure F.42.

Per location the three scenarios will be addressed and analysed. Changes in the primary wave, effects of reflections, extreme values and the to be expected downtime will shortly be addressed.

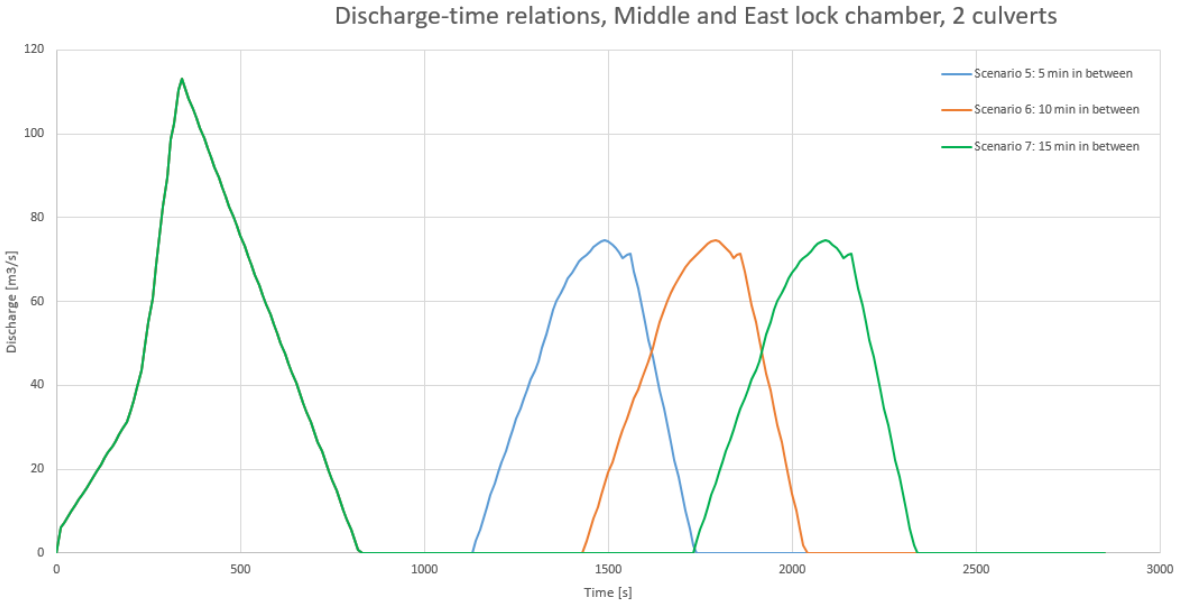

Figure F.42: Discharge-time relations with 2 culverts used at Middle and East chamber

LOCATION X=0 BORN

The primary waves have the same water level changes in scenarios 5, 6 and 7. At this time reflections have not been interfering jet between each other. The results of the model are presented in figures F.44, F.46 and F.48. The shape of the waves are about the same, the differences are the peaks coming later in scenario 6 and 7. This is a result of the longer time between the Middle wave and the East wave. The extreme values and downtime are presented in table F.7. The longer the time between the waves, the lesser the resulting downtime. The difference between 5 minutes or 15 minutes in between the waves result in 4 minutes less downtime. This is almost a quarter of the downtime.

Table F.7: Extreme values at X_Born in Scenario 5, 6 and 7

	Sc5	Sc6	Sc7
z_{min} [m]	-0,173	-0,173	-0,173
z_{max} [m]	0,096	0,086	0,076
u_{min} [m/s]	-0,234	-0,234	-0,234
u_{max} [m/s]	0,130	0,116	0,103
$Downtime$ [min:sec]	16:56	15:27	12:52

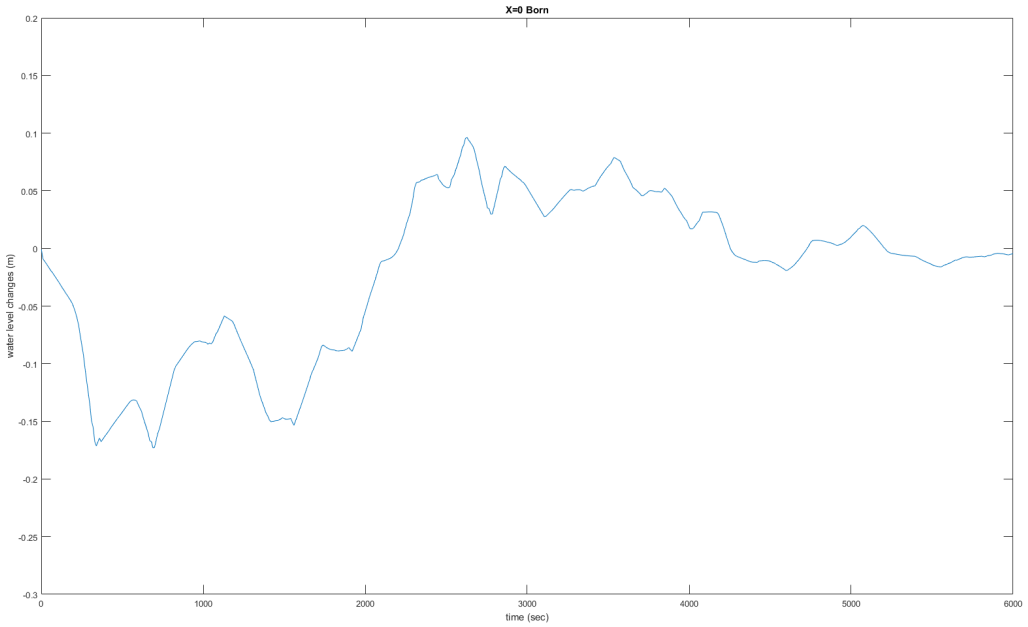

Figure F.43: Sc4: Water level changes in scenario with Middle and East chamber filled with 2 culverts, 5 minutes in between, at location XBorn

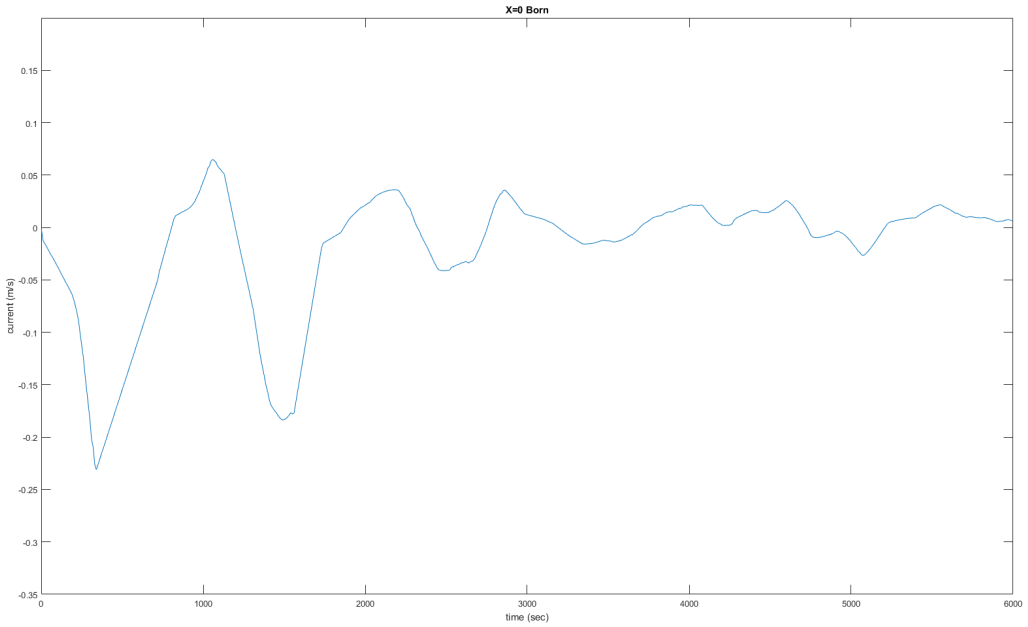

Figure F.44: Sc4: Currents in scenario with Middle and East chamber filled with 2 culverts, 5 minutes in between, at location XBorn

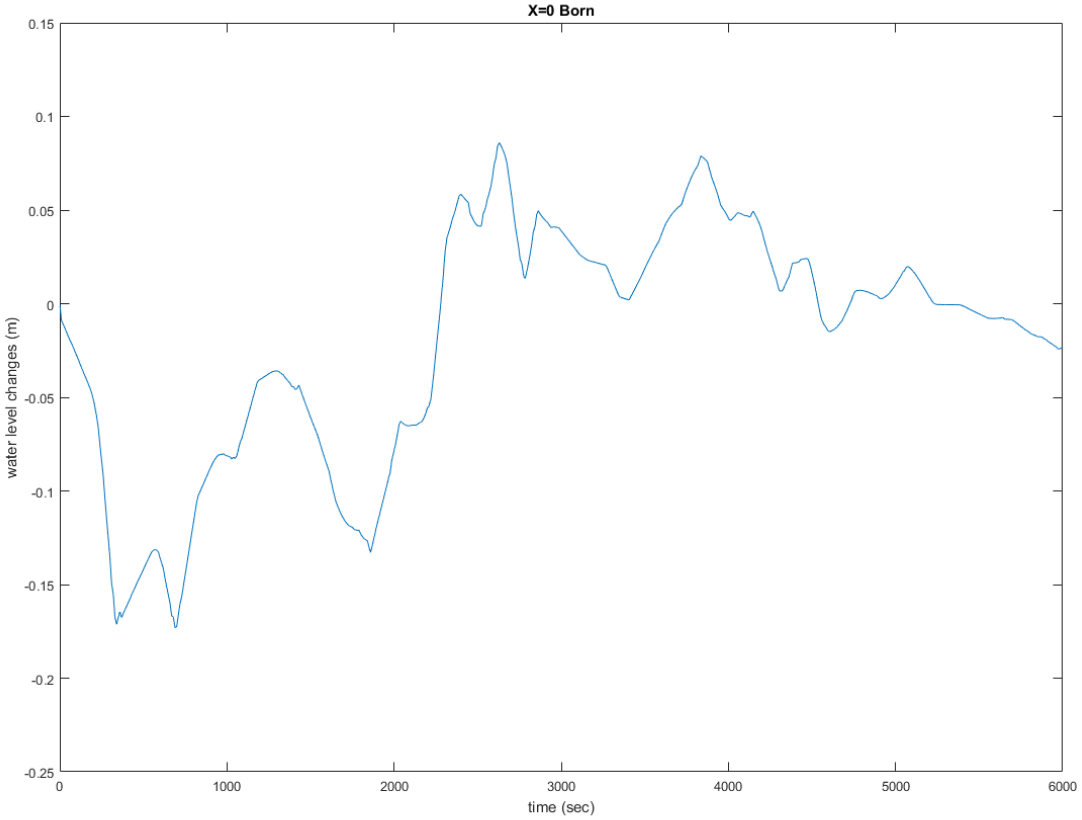

Figure F.45: Sc5: Water level changes in scenario with Middle and East chamber filled with 2 culverts, 10 minutes in between, at location XBorn

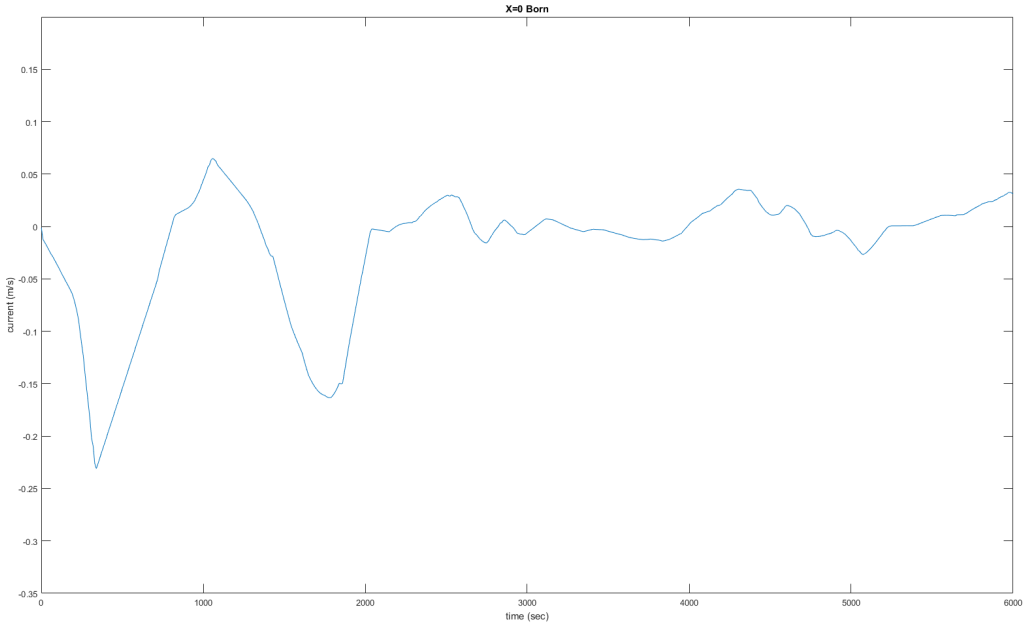

Figure F.46: Sc5: Currents in scenario with Middle and East chamber filled with 2 culverts, 10 minutes in between, at location XBorn

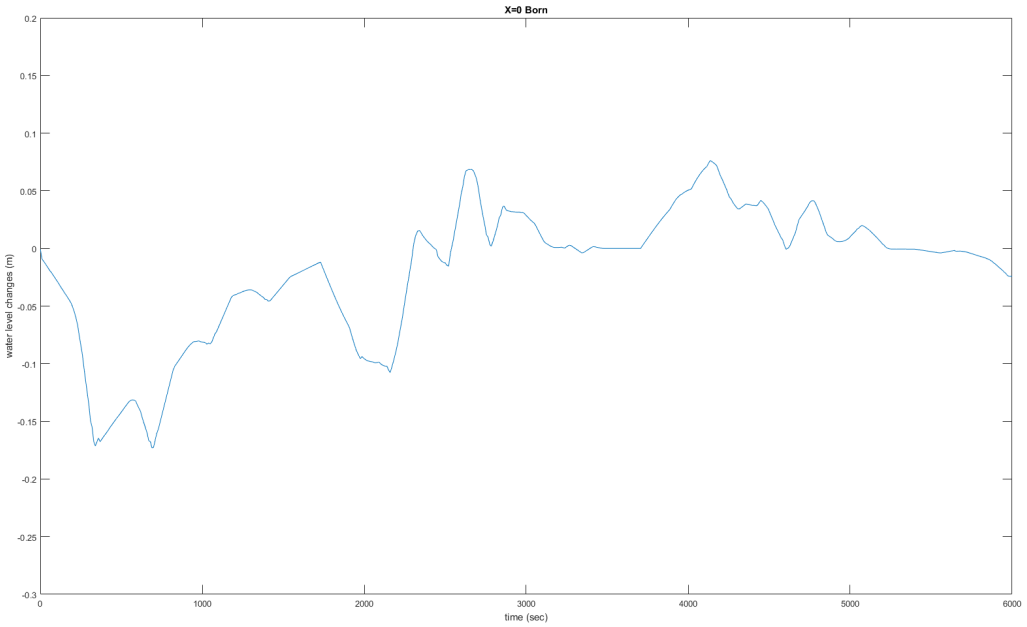

Figure F.47: Sc6: Water level changes in scenario with Middle and East chamber filled with 2 culverts, 15 minutes in between, at location XBorn

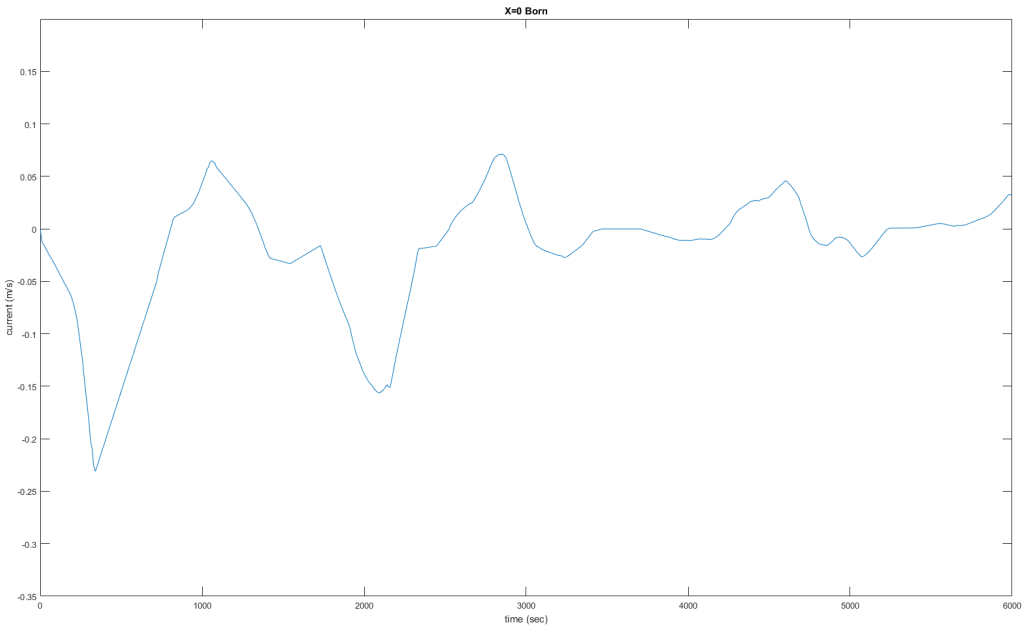

Figure F.48: Sc6: Currents in scenario with Middle and East chamber filled with 2 culverts, 15 minutes in between, at location XBorn

LOCATION X=1151

The primary waves of the first wave respond in the same way as they did in scenario 1, they increase with 36% compared to the primary wave at location Born. The primary waves of the second wave cannot be taken from the results from scenario 1. The second wave is created by the East lock chamber, not the Middle lock chamber as in scenario 1. Also, adaptation in the pattern can be observed due to interference with reflection waves. Because of the different time intervals between the first and second wave, the peaks and troughs later in the modelled time period differ from each other, as can be seen in figures F.50,F.52 and F.54. Downtime at this location is the highest in scenario 5 with almost 16 minutes, lowest in scenario 7 with 11 minutes. The rest of the extreme values can be found in table F.8.

Table F.8: Extreme values at X_1151 in Scenario 5, 6 and 7

	Sc5	Sc6	Sc7
z_{min} [m]	-0,235	-0,235	-0,235
z_{max} [m]	0,092	0,077	0,074
u_{min} [m/s]	-0,318	-0,318	-0,318
u_{max} [m/s]	0,125	0,104	0,100
$Downtime$ [min:sec]	15:50	14:23	10:59

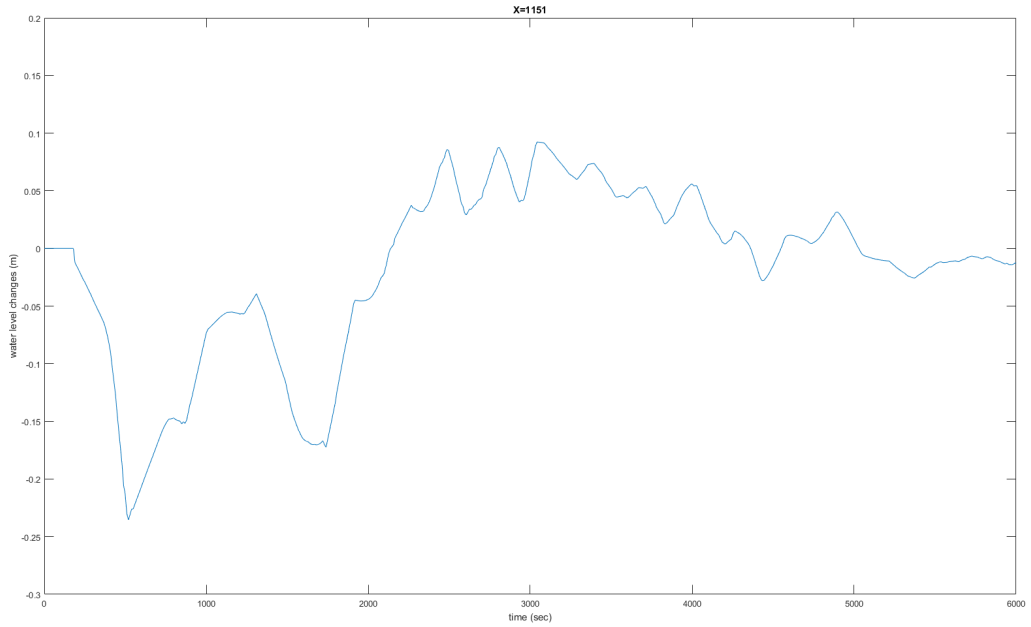

Figure F.49: Sc4: Water level changes in scenario with Middle and East chamber filled with 2 culverts, 5 minutes in between, at location X1151

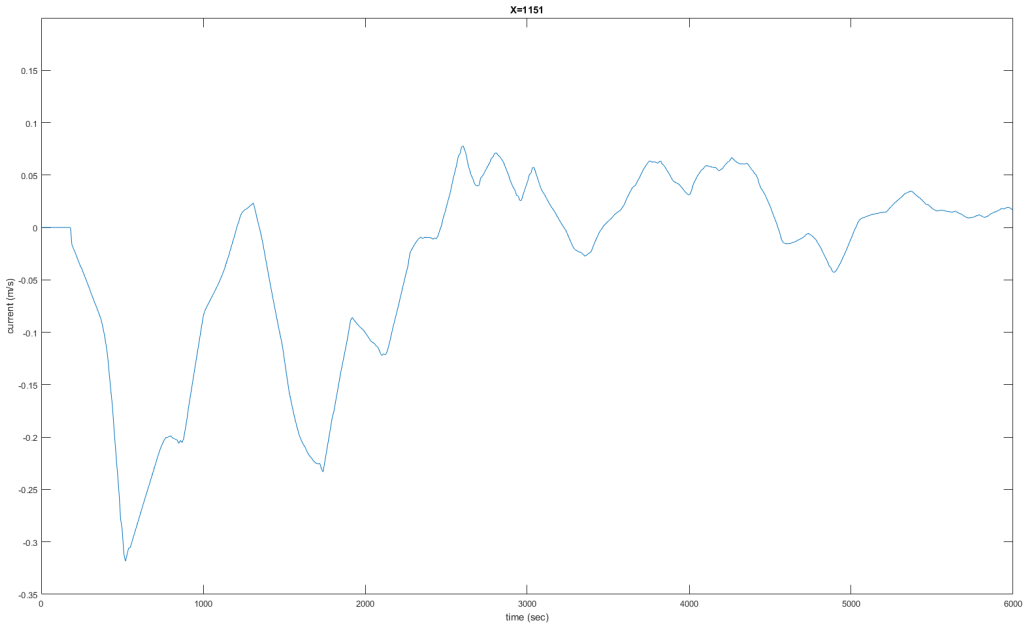

Figure F.50: Sc4: Currents in scenario with Middle and East chamber filled with 2 culverts, 5 minutes in between, at location X1151

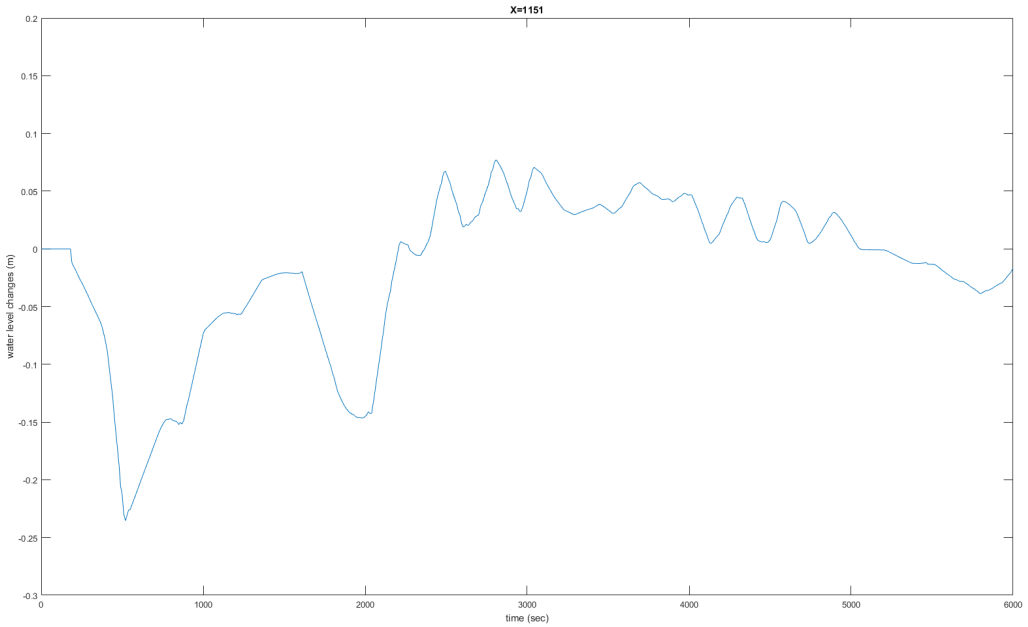

Figure F.51: Sc5: Water level changes in scenario with Middle and East chamber filled with 2 culverts, 10 minutes in between, at location X1151

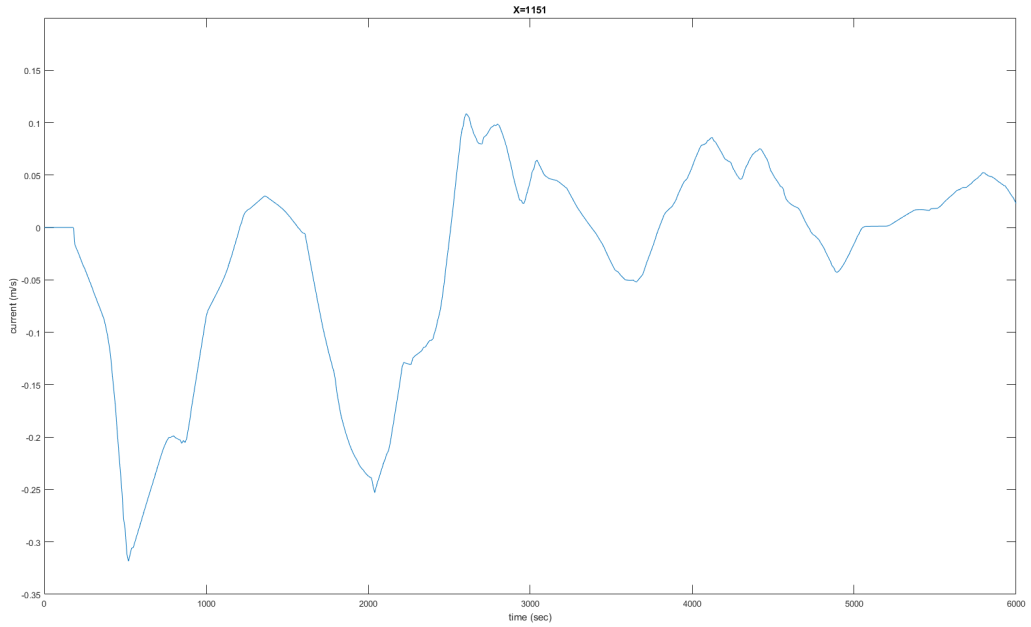

Figure F.52: Sc5: Currents in scenario with Middle and East chamber filled with 2 culverts, 10 minutes in between, at location X1151

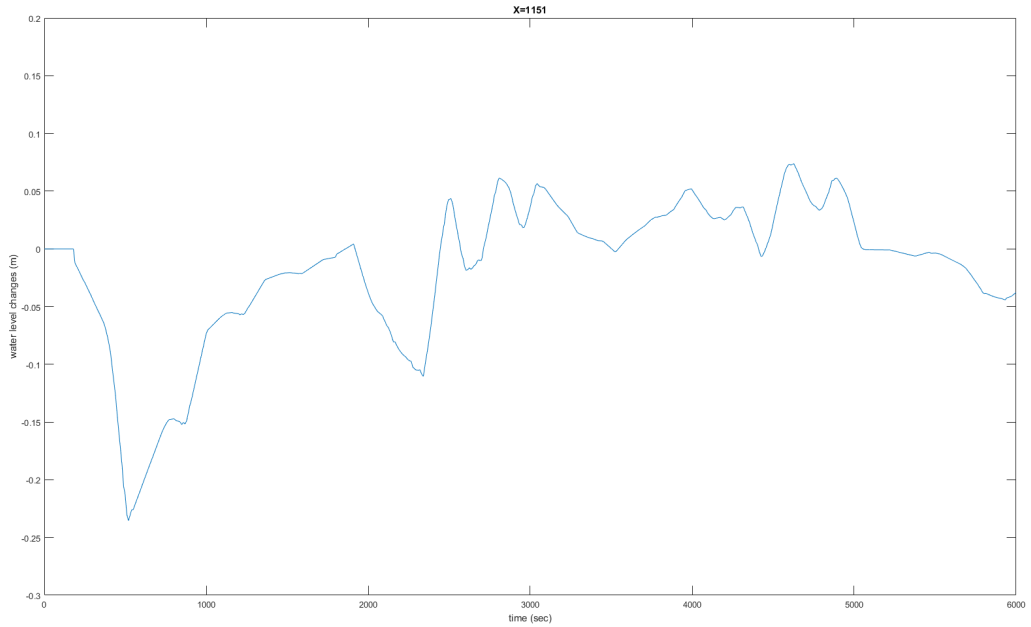

Figure F.53: Sc6: Water level changes in scenario with Middle and East chamber filled with 2 culverts, 15 minutes in between, at location X1151

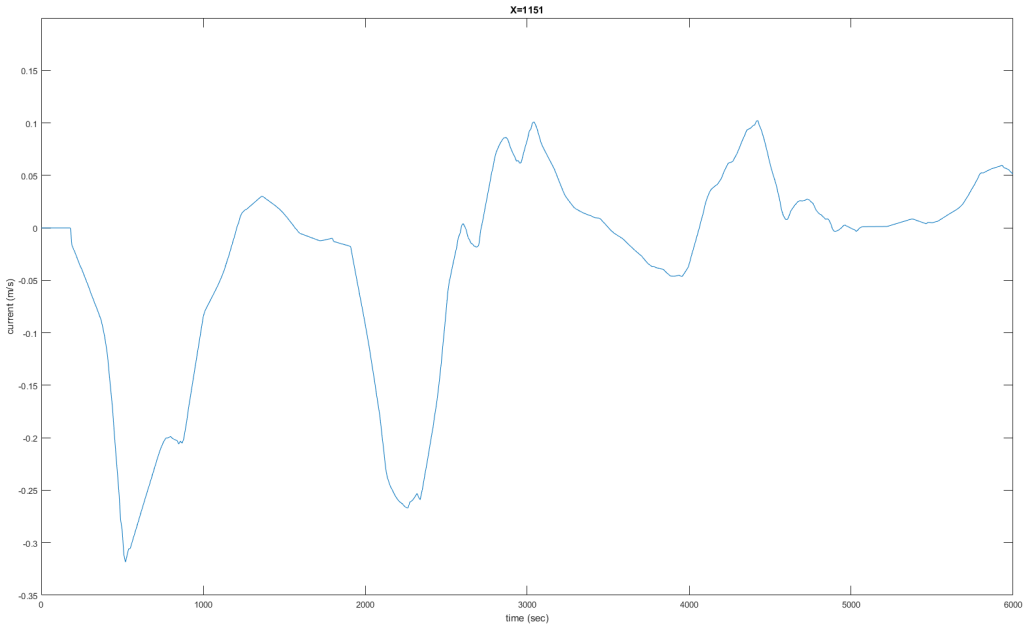

Figure F.54: Sc6: Currents in scenario with Middle and East chamber filled with 2 culverts, 15 minutes in between, at location X1151

LOCATION X=4000

As was seen at location X1151, the primary waves of the first wave react at location X4000 the same as in scenario 1 where one wave was implemented. The effects of interaction between reflections and the second wave are clearly visible. The second wave in scenario 5 is damped much more than the second wave in scenario 7. The current in scenario 5 is 0.2 m/s where the current in scenario 7 is 0.24 m/s, 20% higher. This is also visible in the downtime, 12:33 to 15:36 minutes between scenario 5 and 7. The extreme values of the water level change and currents can be found in table F.9.

Table F.9: Extreme values at X_4000 in Scenario 5, 6 and 7

	Sc5	Sc6	Sc7
z_{min} [m]	-0,235	-0,235	-0,235
z_{max} [m]	0,076	0,091	0,103
u_{min} [m/s]	-0,318	-0,318	-0,318
u_{max} [m/s]	0,103	0,123	0,139
$Downtime$ [min:sec]	12:33	14:18	15:36

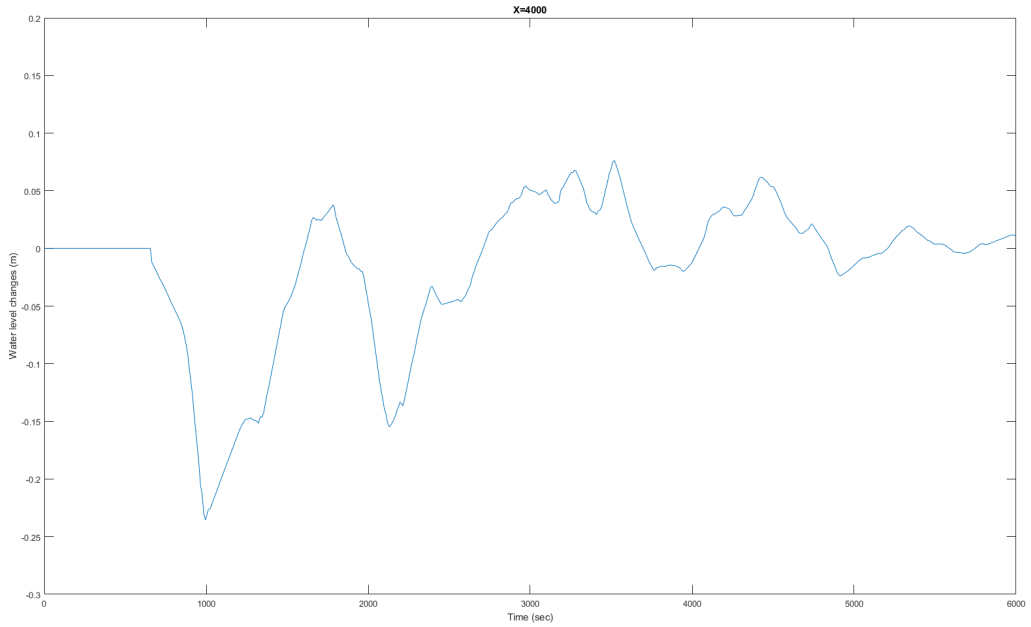

Figure F.55: Sc4: Water level changes in scenario with Middle and East chamber filled with 2 culverts, 5 minutes in between, at location X4000

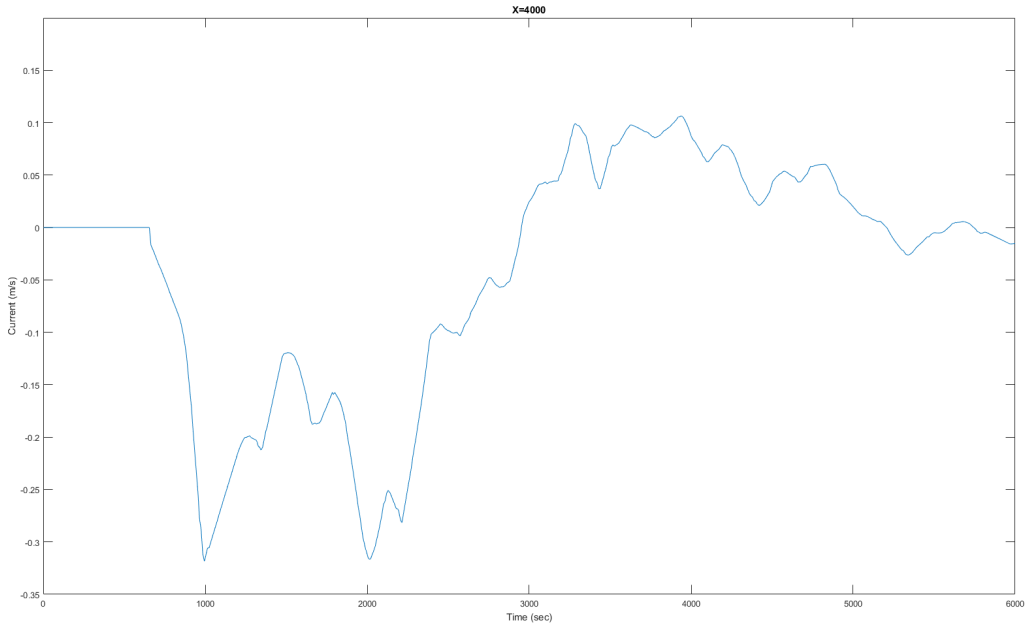

Figure F.56: Sc4: Currents in scenario with Middle and East chamber filled with 2 culverts, 5 minutes in between, at location X4000

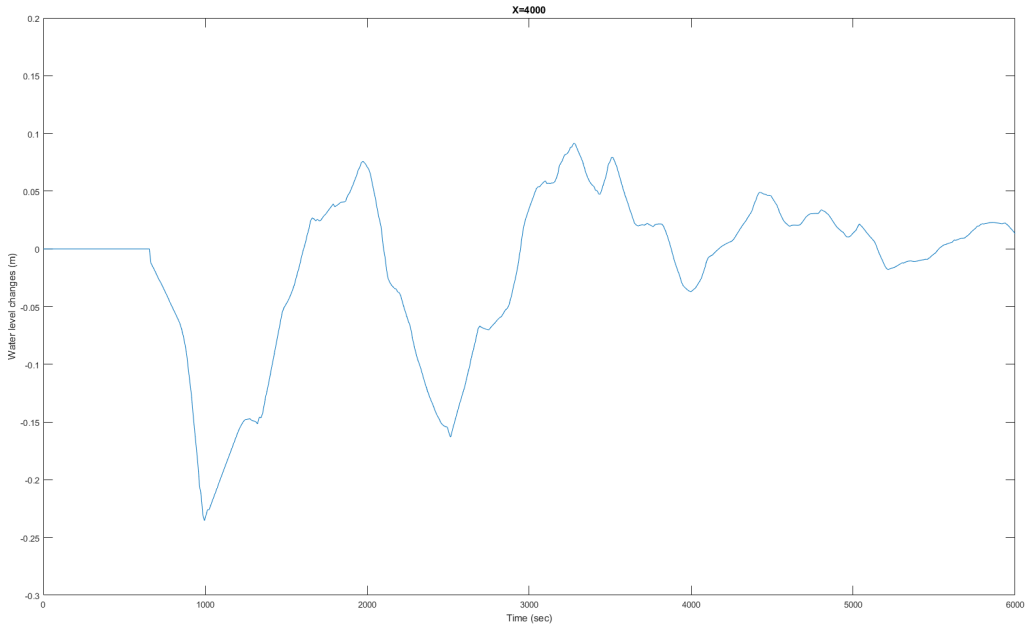

Figure F.57: Sc5: Water level changes in scenario with Middle and East chamber filled with 2 culverts, 10 minutes in between, at location X4000

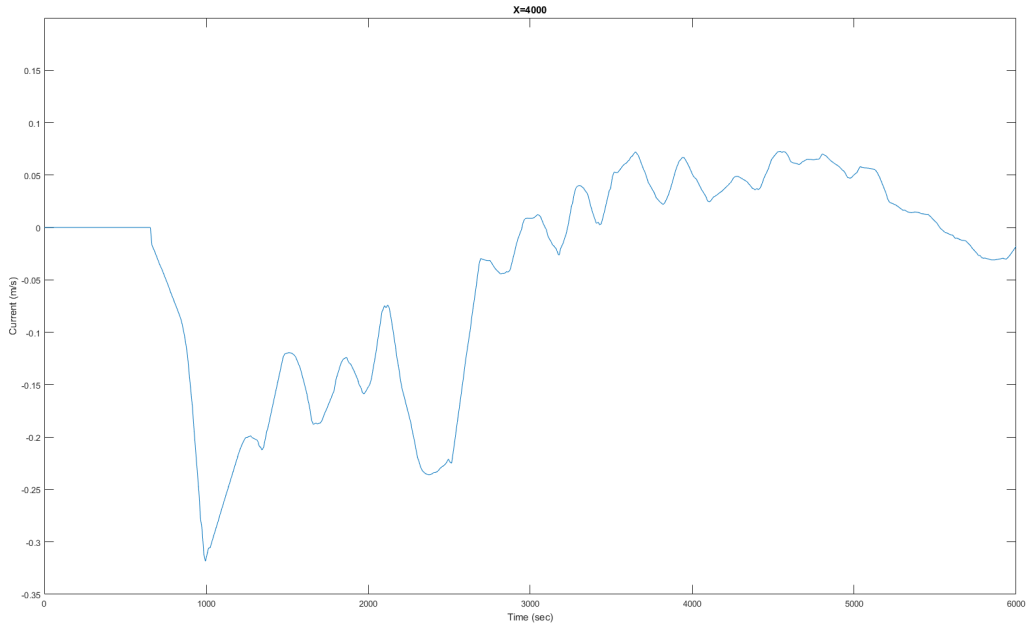

Figure F.58: Sc5: Currents in scenario with Middle and East chamber filled with 2 culverts, 10 minutes in between, at location X4000

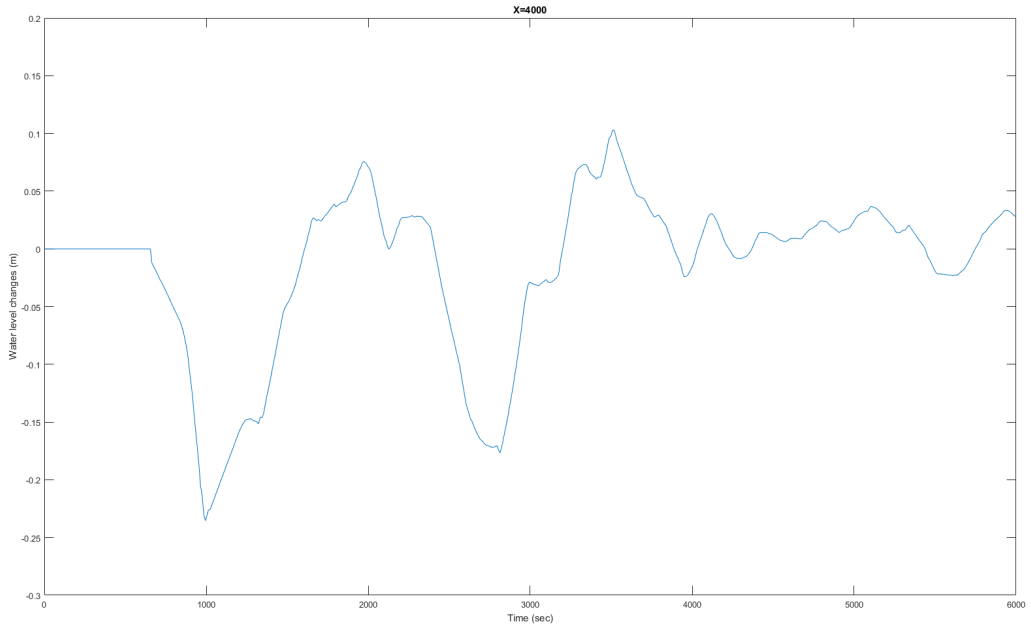

Figure F.59: Sc6: Water level changes in scenario with Middle and East chamber filled with 2 culverts, 15 minutes in between, at location X4000

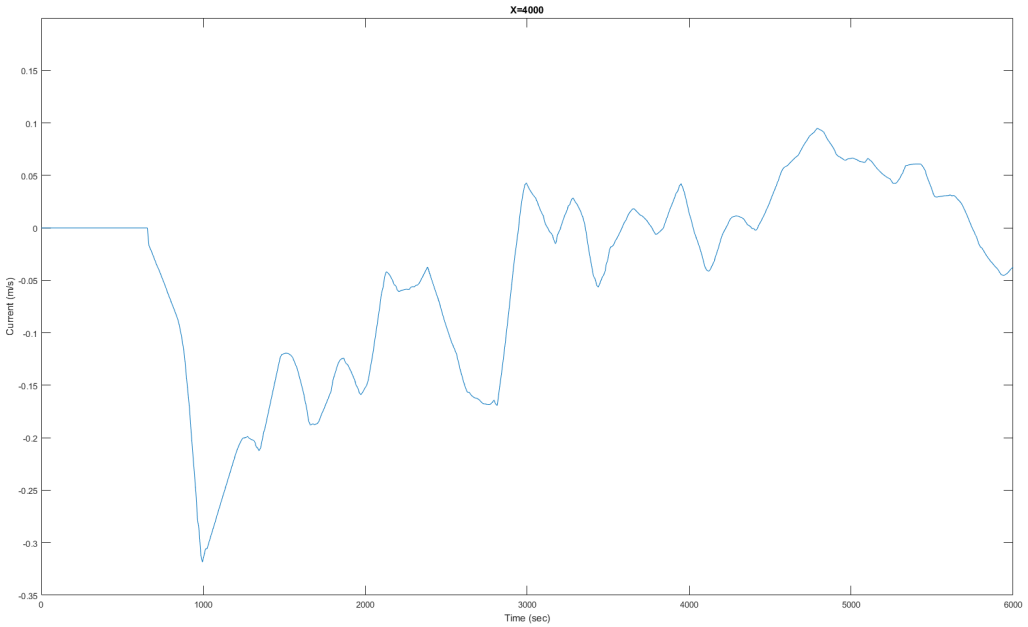

Figure F.60: Sc6: Currents in scenario with Middle and East chamber filled with 2 culverts, 15 minutes in between, at location X4000

LOCATION X=5900

The maximum current due to the primary wave is 0.23 m/s, this is 28% lower than at location X4000. An explanation for the lowering of the current and water level has been given in the previous chapter. The magnitudes of the currents are relatively low compared to locations X1151 or X4000. This is recognizable in the downtime as well. The downtime in scenarios 5, 6 and 7 are between 8 and 9 minutes, as can be seen in table F.10.

Table F.10: Extreme values at X_5900 in Scenario 5, 6 and 7

	Sc5	Sc6	Sc7
z_{min} [m]	-0,170	-0,170	-0,170
z_{max} [m]	0,066	0,066	0,075
u_{min} [m/s]	-0,230	-0,230	-0,230
u_{max} [m/s]	0,089	0,089	0,101
$Downtime$ [min:sec]	08:10	08:26	08:57

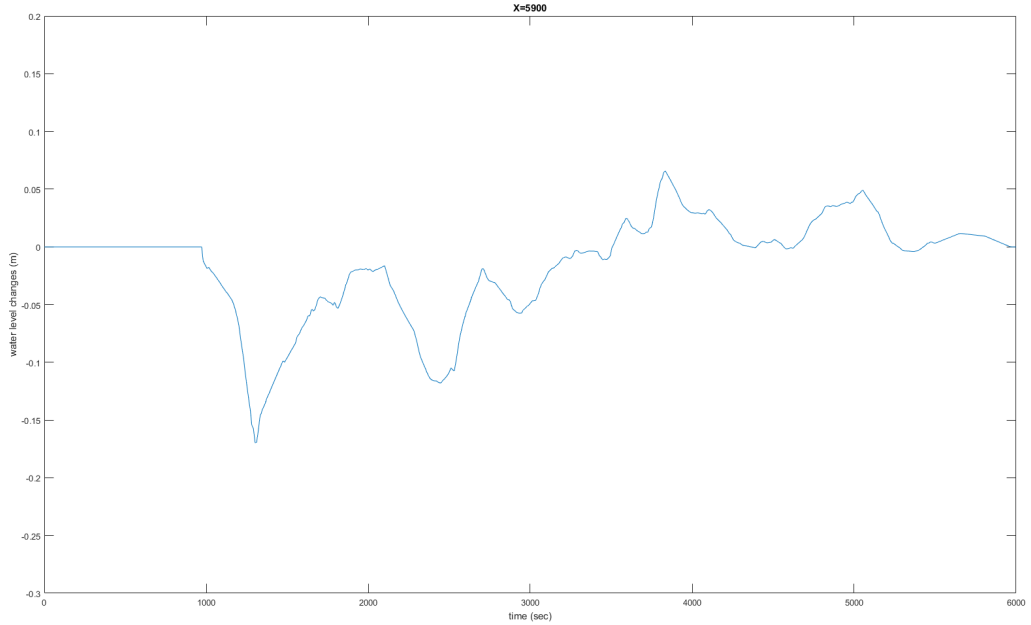

Figure F.61: Sc4: Water level changes in scenario with Middle and East chamber filled with 2 culverts, 5 minutes in between, at location X5900

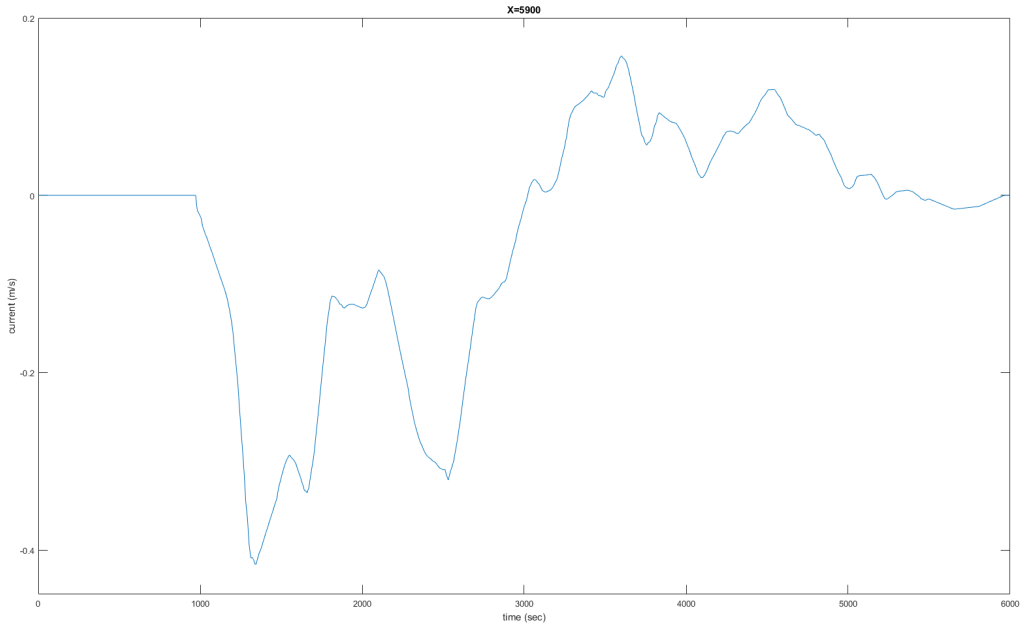

Figure F.62: Sc4: Currents in scenario with Middle and East chamber filled with 2 culverts, 5 minutes in between, at location X5900

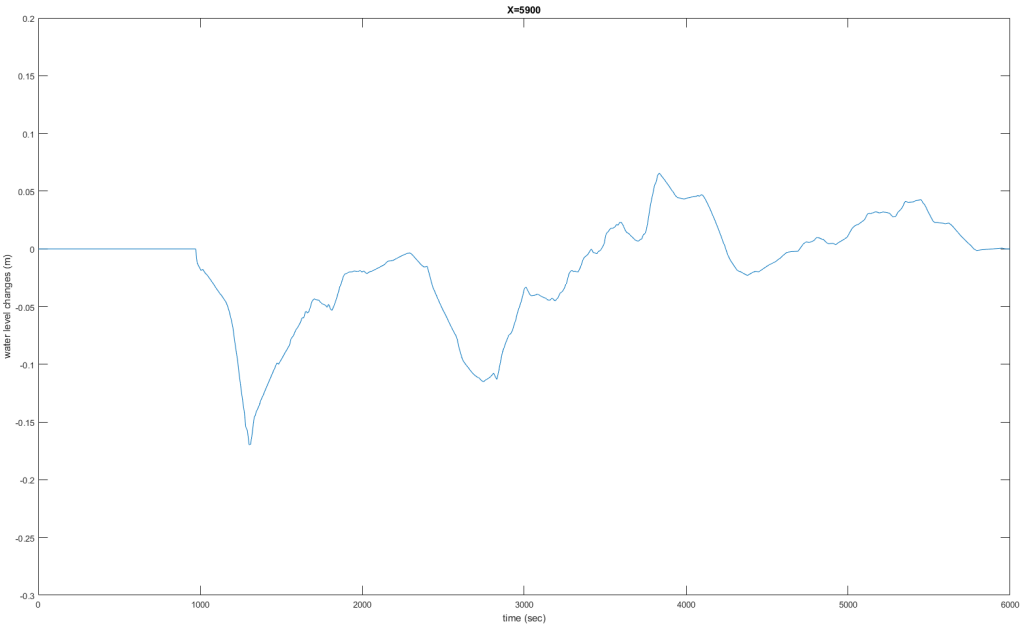

Figure F.63: Sc5: Water level changes in scenario with Middle and East chamber filled with 2 culverts, 10 minutes in between, at location X5900

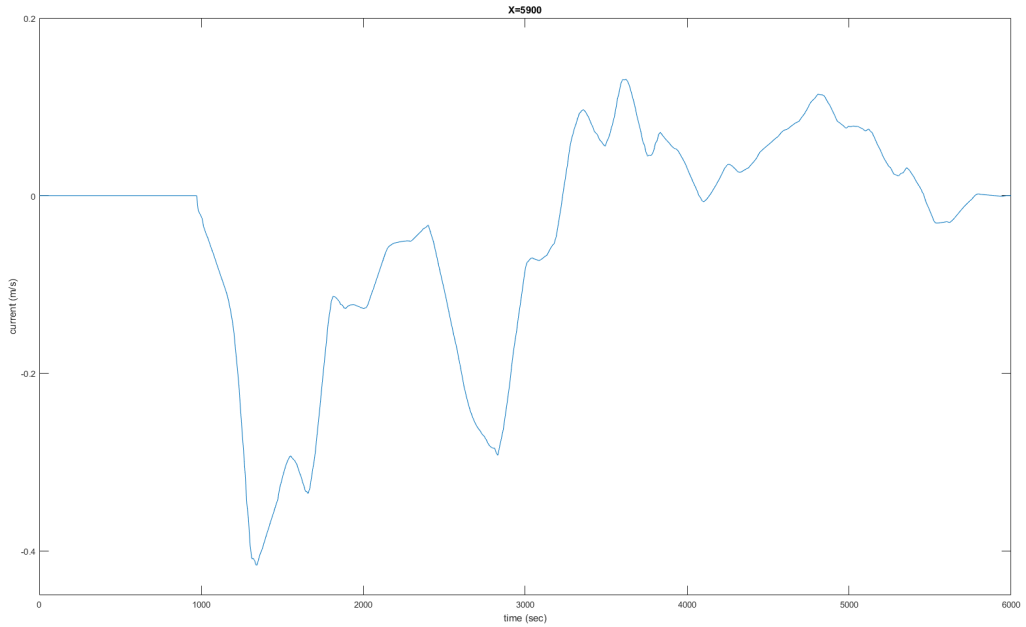

Figure F.64: Sc5: Currents in scenario with Middle and East chamber filled with 2 culverts, 10 minutes in between, at location X5900

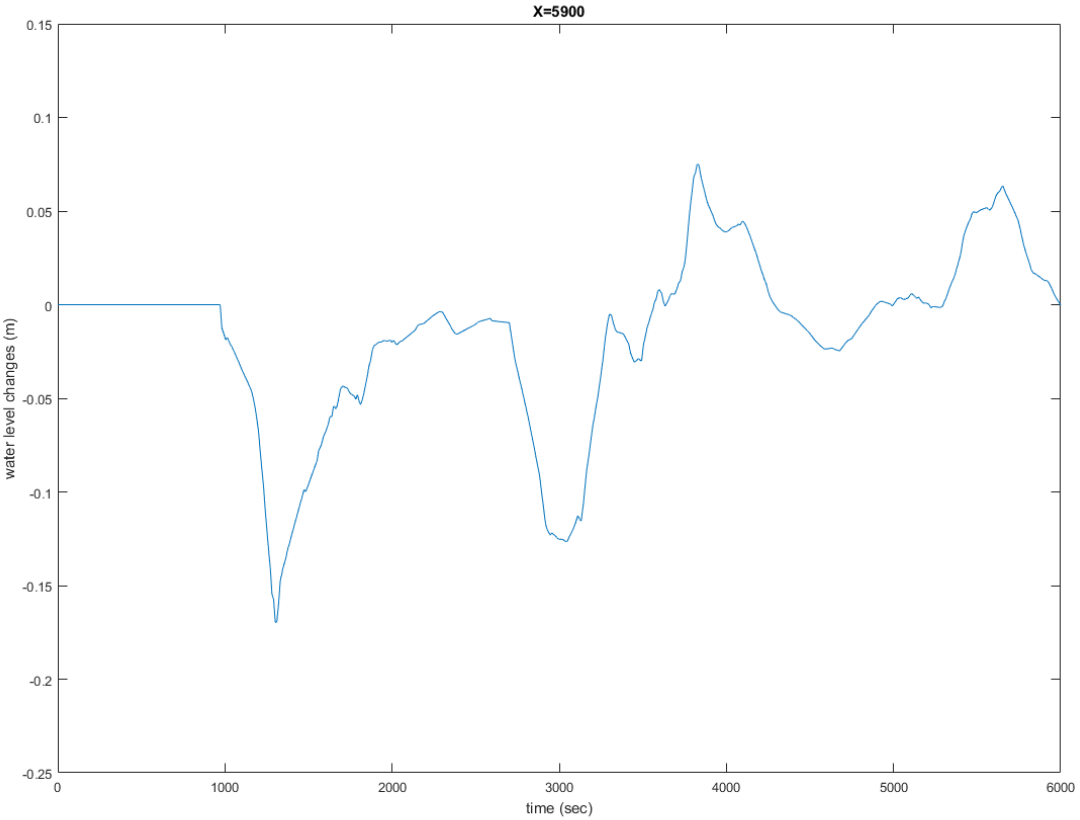

Figure F.65: Sc6: Water level changes in scenario with Middle and East chamber filled with 2 culverts, 15 minutes in between, at location X5900

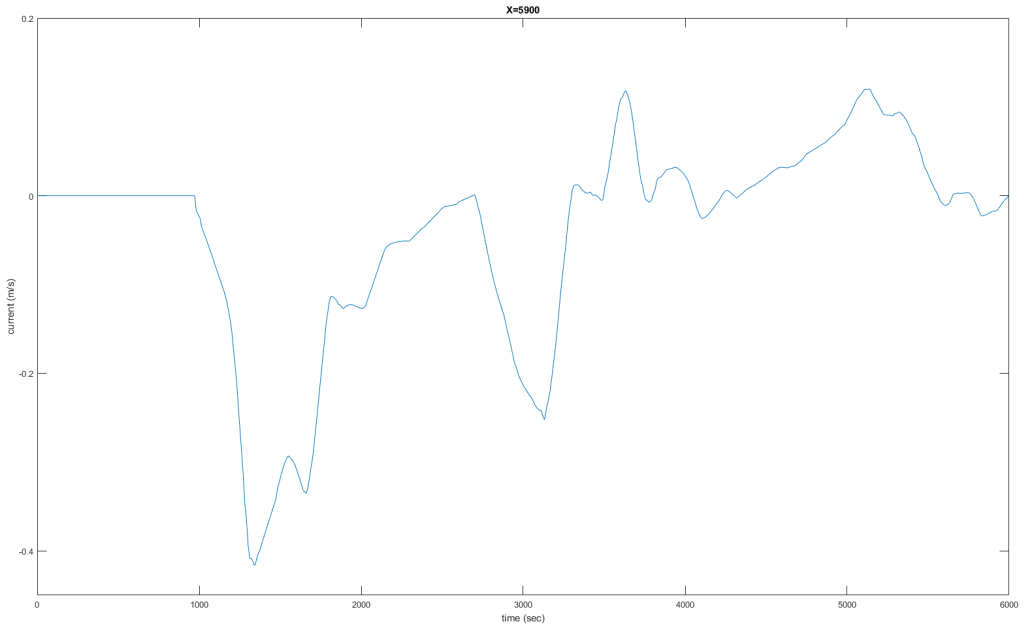

Figure F.66: Sc6: Currents in scenario with Middle and East chamber filled with 2 culverts, 15 minutes in between, at location X5900

LOCATION X=6001

Location X6001 is located in the wide section of the port of Stein, just after the transition point. The primary wave is lower at X6001 than at the section between X1151 and X5900 due to the widening of the canal. The water level changes and currents are lower over the whole time period. The downtime due to high currents is between 7 and 8 minutes, with the highest downtime in scenario 5. The values for the other parameters are given in table F.11.

Table F.11: Extreme values at X_6001 in Scenario 5, 6 and 7

	Sc5	Sc6	Sc7
z_{min} [m]	-0,154	-0,154	-0,154
z_{max} [m]	0,062	0,054	0,046
u_{min} [m/s]	-0,208	-0,208	-0,208
u_{max} [m/s]	0,084	0,073	0,062
$Downtime$ [min:sec]	07:56	07:54	07:18

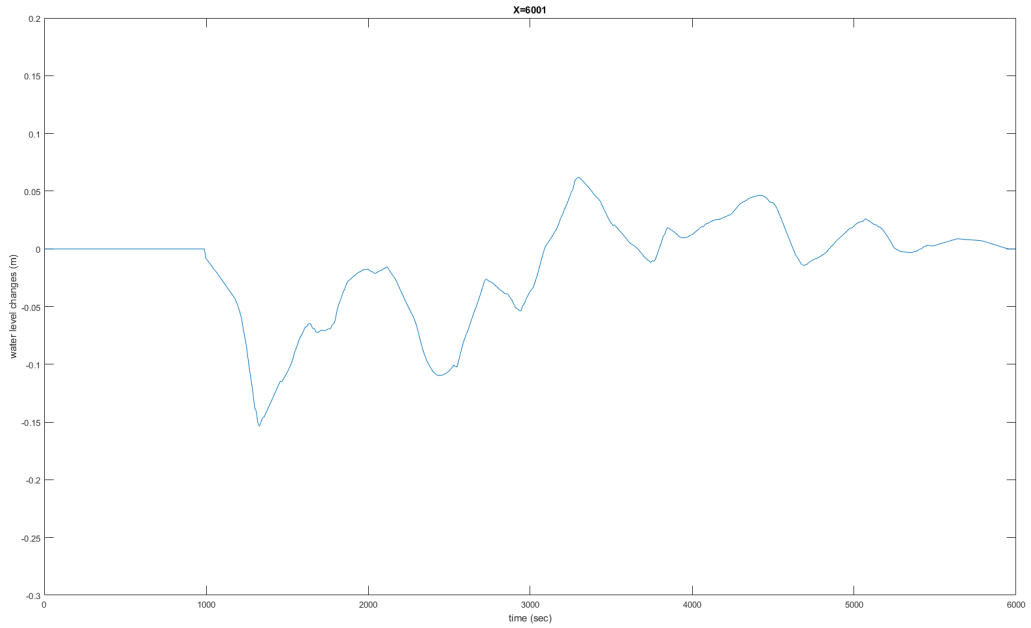

Figure F.67: Sc4: Water level changes in scenario with Middle and East chamber filled with 2 culverts, 5 minutes in between, at location X6001

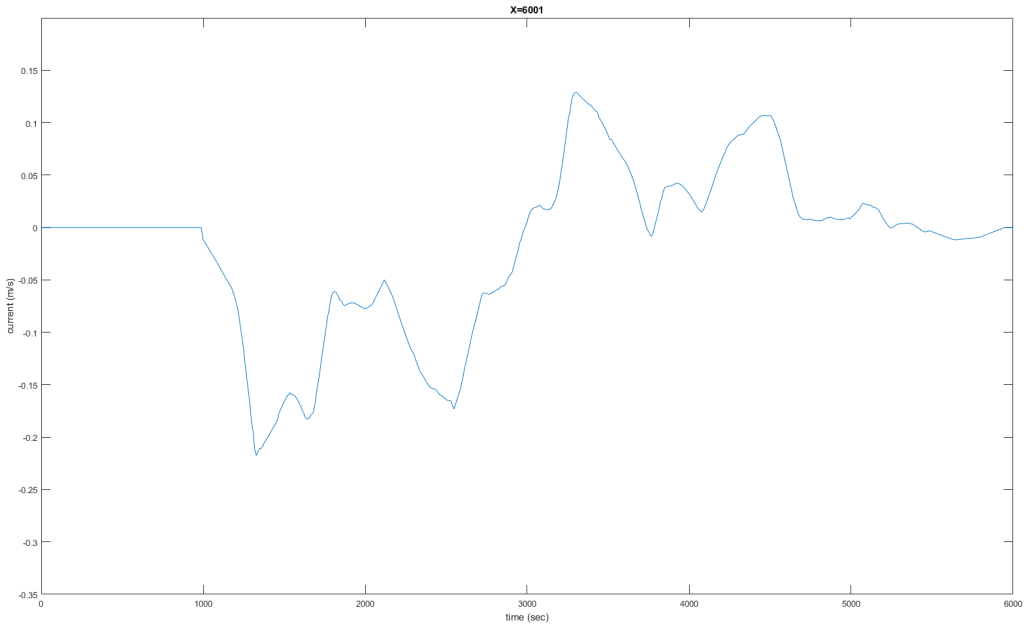

Figure F.68: Sc4: Currents in scenario with Middle and East chamber filled with 2 culverts, 5 minutes in between, at location X6001

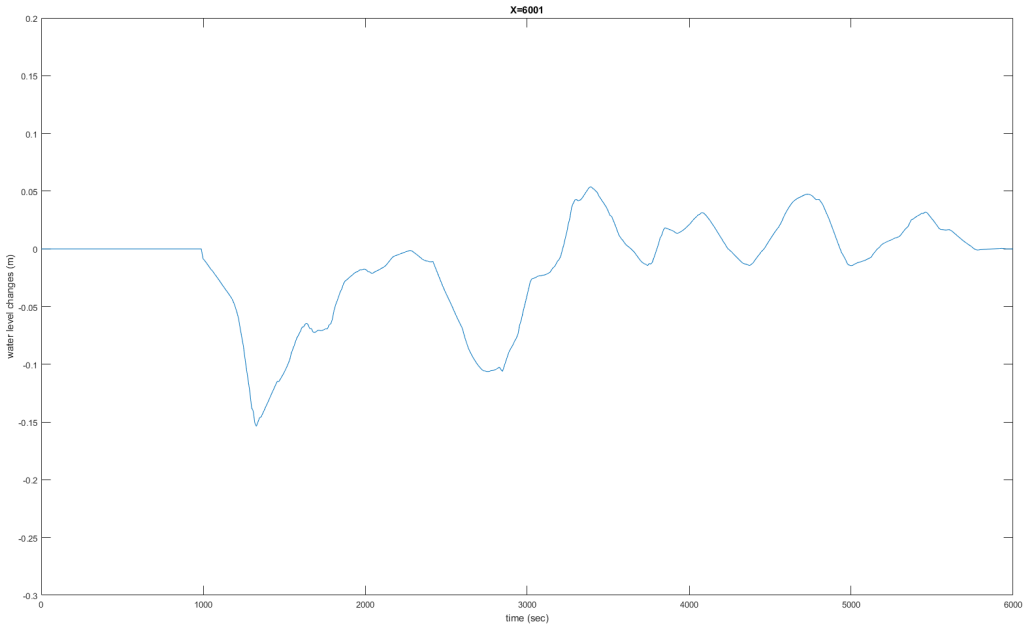

Figure F.69: Sc5: Water level changes in scenario with Middle and East chamber filled with 2 culverts, 10 minutes in between, at location X6001

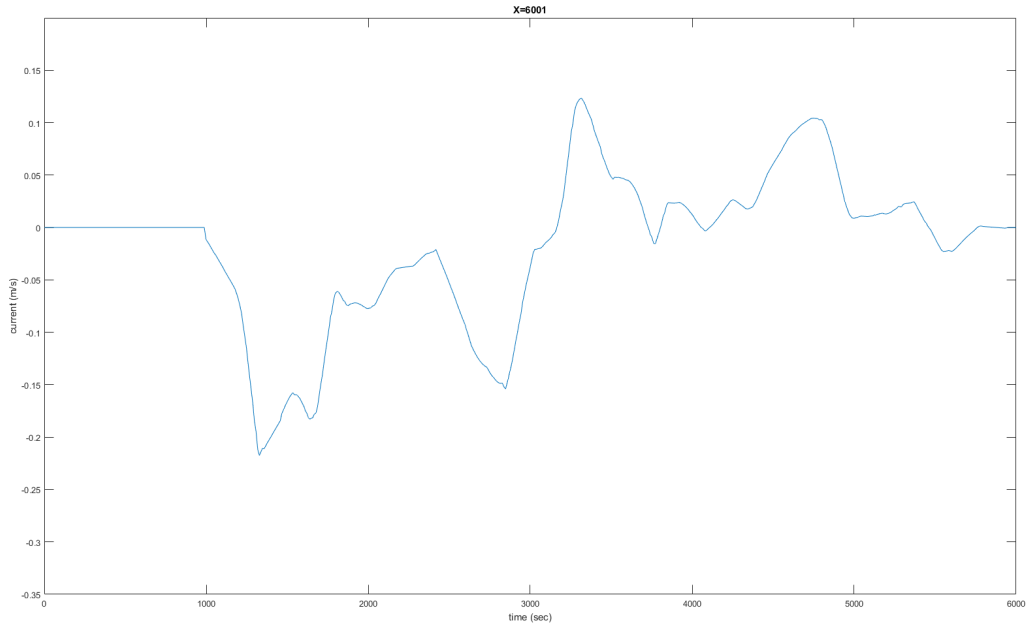

Figure F.70: Sc5: Currents in scenario with Middle and East chamber filled with 2 culverts, 10 minutes in between, at location X6001

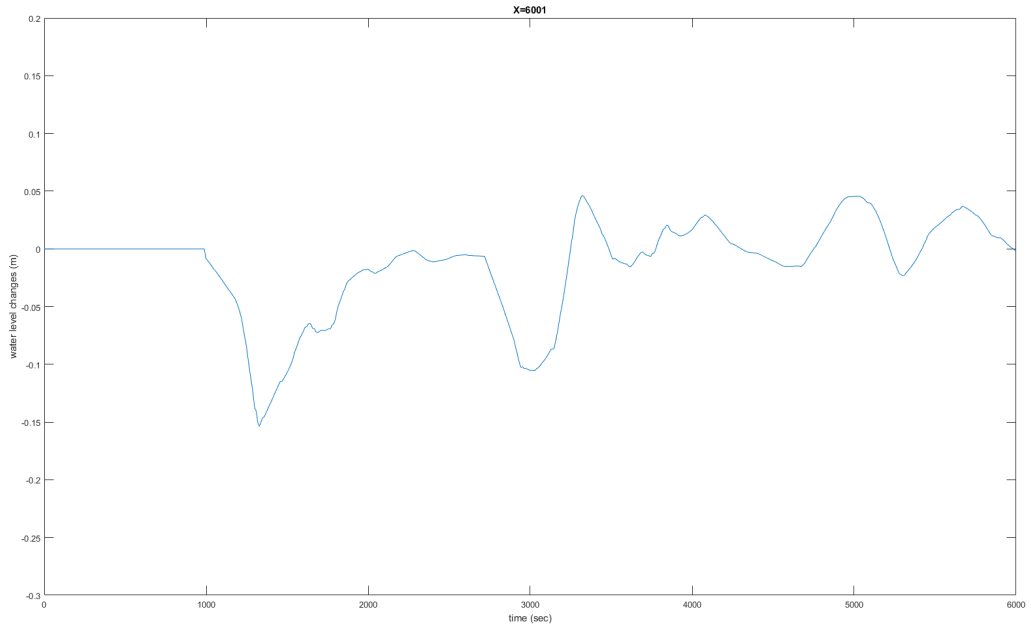

Figure F.71: Sc6: Water level changes in scenario with Middle and East chamber filled with 2 culverts, 15 minutes in between, at location X6001

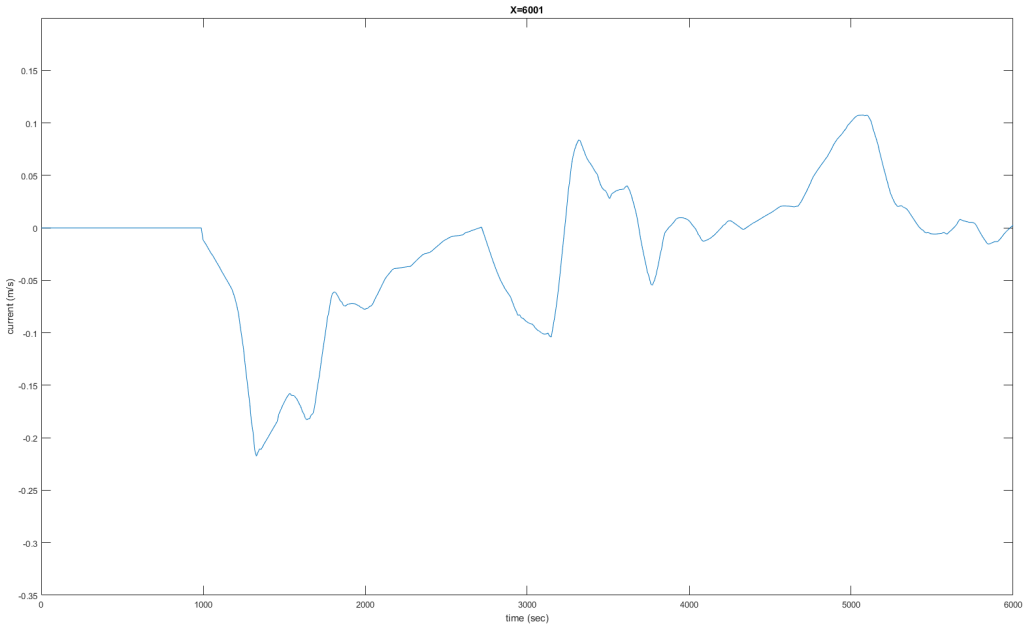

Figure F.72: Sc6: Currents in scenario with Middle and East chamber filled with 2 culverts, 15 minutes in between, at location X6001

F.2.2. FILLING AND EMPTYING REGIMES WITH LOW DISCHARGE WAVES

In this section the effects of two sequential wave on the canal are modelled as well. The same filling and emptying regime is modelled, first the Middle chamber, then the East chamber, filling with 5, then 10 and finally 15 minutes in between the waves. The difference is that in this section only one culvert is used to fill the lock chambers. The discharge-time relations are presented in figure F.73. The implementation of these relations correspond with scenarios 8,9 and 10. The scenarios will again be discussed per location.

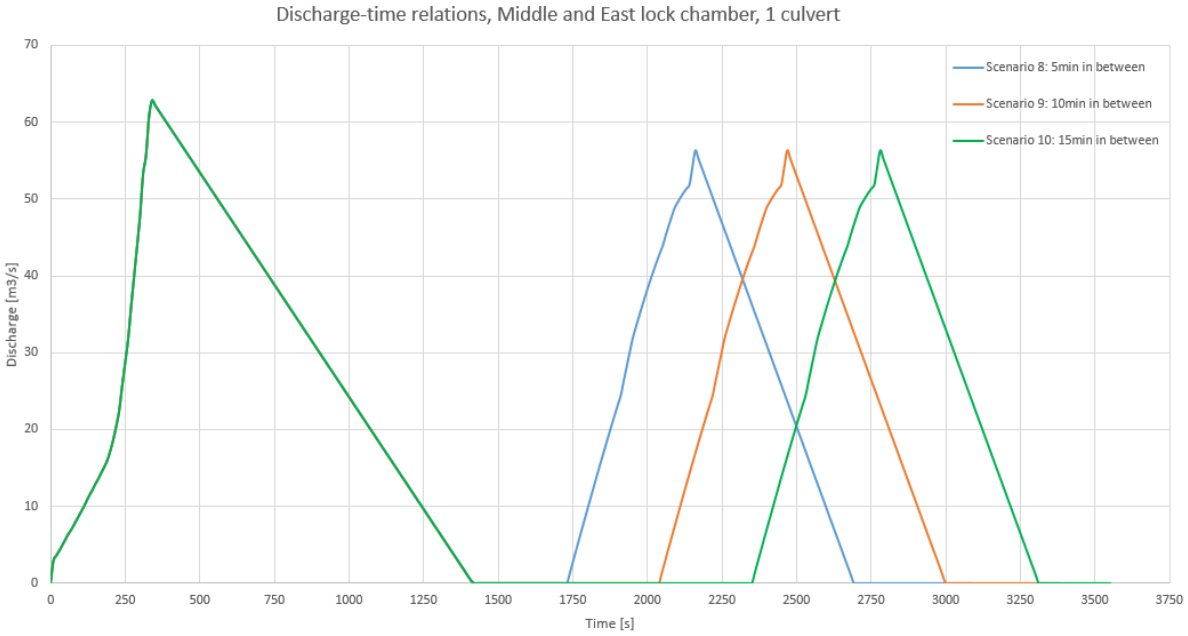

Figure F.73: Discharge-time relations with 1 culvert used at Middle and East chamber

LOCATION X=0 BORN

The primary wave of the first wave is in scenarios 8,9 and 10 the same. The water level changes have not been affected by interaction with the second wave, as can be seen in figures F.75, F.77 and F.79. The pattern of the wave after about t = 1500s differs between the scenarios. The second wave starts to interfere with the reflections of the first wave. Only 1 culvert is used in these scenarios, the wave height is relatively low. This results in lower currents and less downtimes than in the situation with 2 culverts. The downtime in scenarios 8,9 and 10 are about 9 minutes, in scenarios 5, 6 and 7 between 13 and almost 17 minutes. An overview of the maximum currents is given in table F.12.

Table F.12: Extreme values at X_Born in Scenario 8,9 and 10

	Sc8	Sc9	Sc10
z_{min} [m]	-0,135	-0,135	-0,135
z_{max} [m]	0,055	0,057	0,065
u_{min} [m/s]	-0,182	-0,182	-0,182
u_{max} [m/s]	0,074	0,077	0,088
$Downtime$ [min:sec]	09:07	09:07	09:07

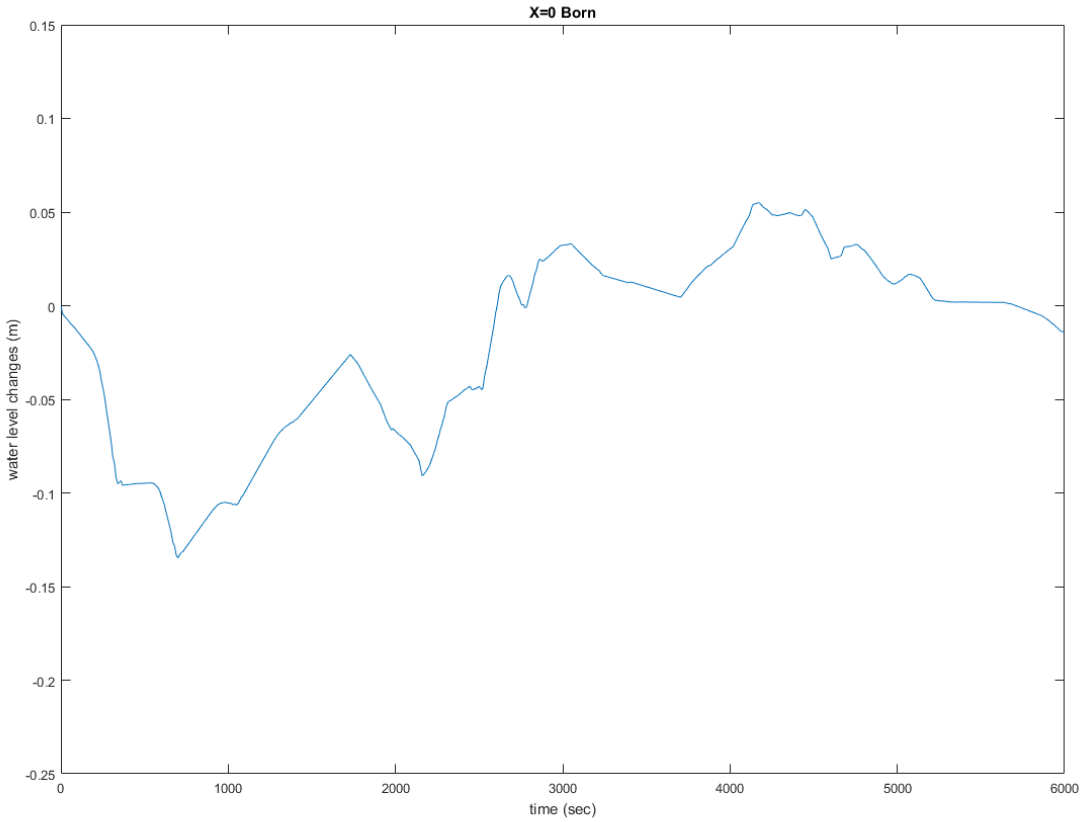

Figure F.74: Sc7: Water level changes in scenario with Middle and East chamber filled with 1 culverts, 5 minutes in between, at location XBorn

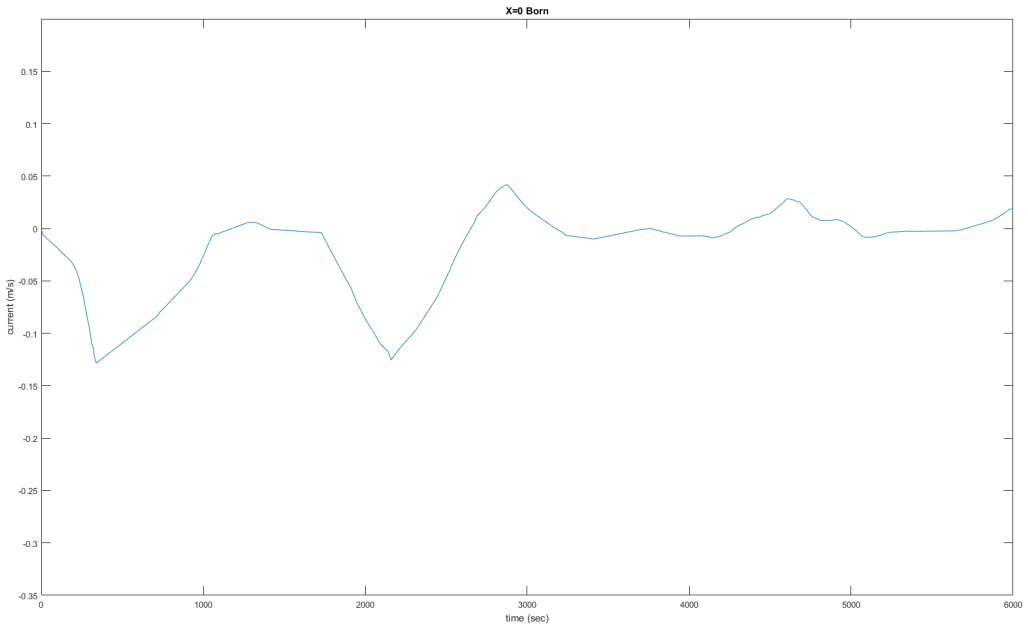

Figure F.75: Sc7: Currents in scenario with Middle and East chamber filled with 1 culverts, 5 minutes in between, at location XBorn

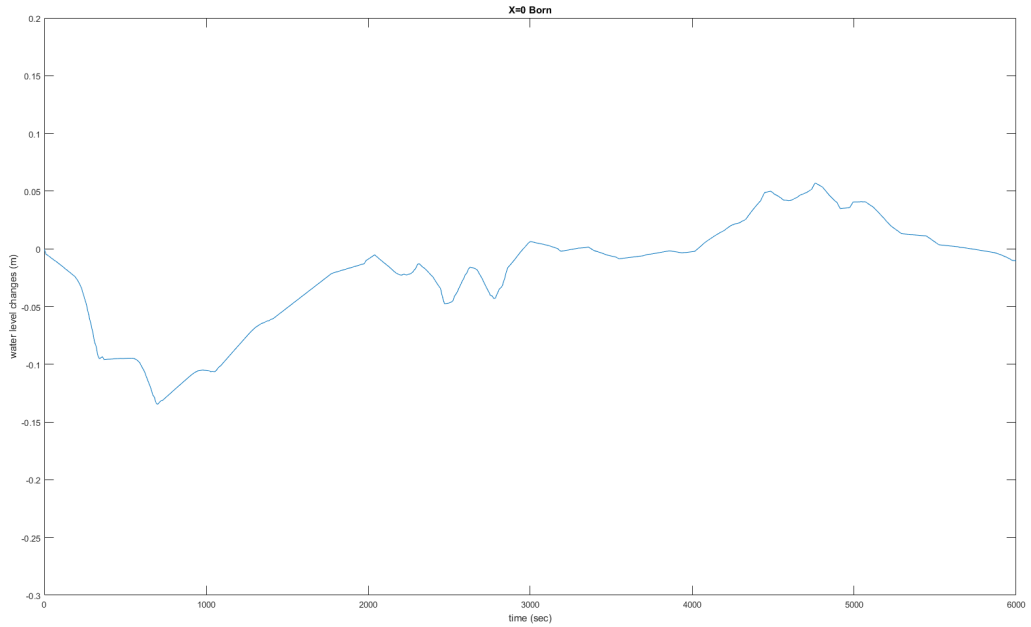

Figure F.76: Sc8: Water level changes in scenario with Middle and East chamber filled with 1 culverts, 10 minutes in between, at location XBorn

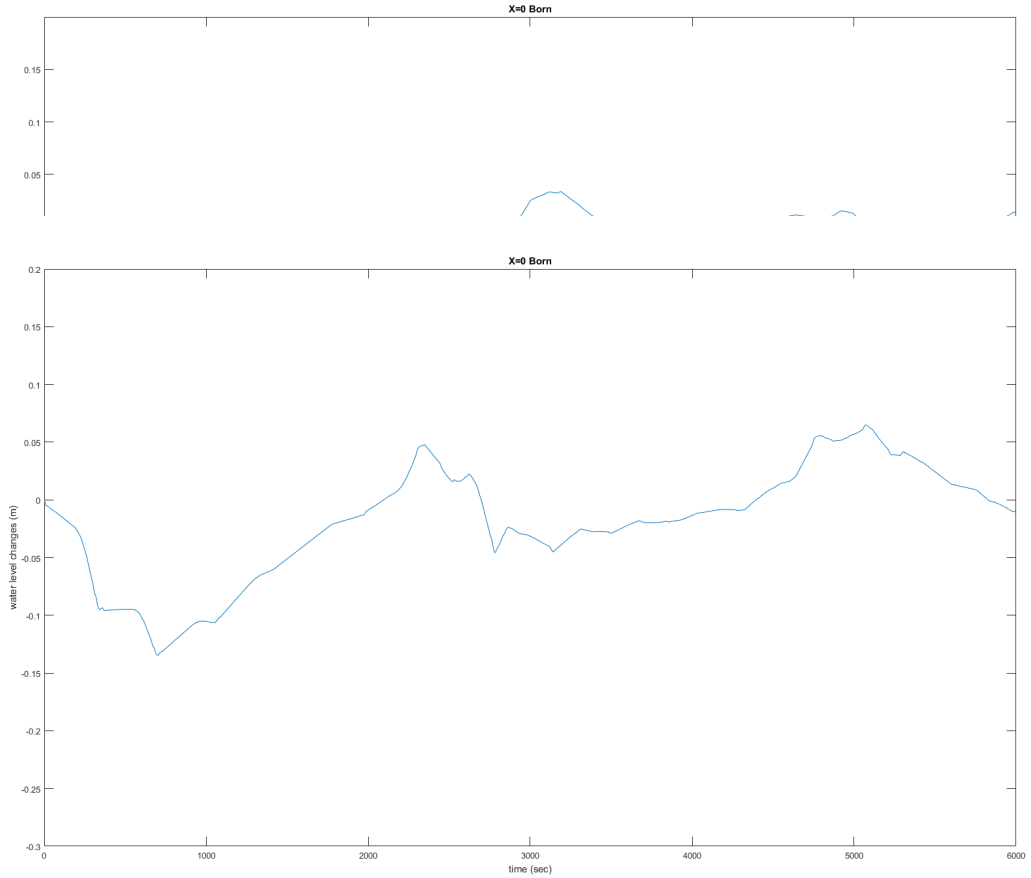

Figure F.78: Sc9: Water level changes in scenario with Middle and East chamber filled with 1 culverts, 15 minutes in between, at location XBorn

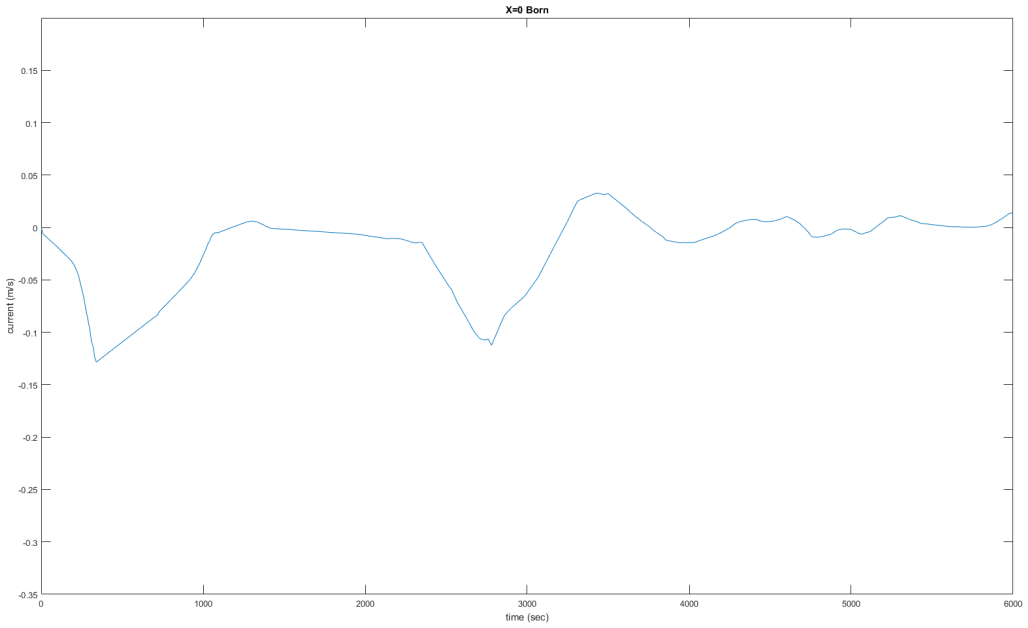

Figure F.79: Sc9: Currents in scenario with Middle and East chamber filled with 1 culverts, 15 minutes in between, at location XBorn

LOCATION X=1151

At location XBorn, the primary wave of the first wave was amplified by the first reflection of the first wave. At location X1151, these primary wave and reflection wave are more behind each other. The result is less amplification due to the transition point, only an increase of the current with 10%. The time interval of the current is longer, resulting in a longer downtime: more than 12 minutes. This is about one third longer than at location XBorn. The extreme values of the currents and water level changes are given in table F.13.

Table F.13: Extreme values at X_1151 in Scenario 8,9 and 10

	Sc8	Sc9	Sc10
z_{min} [m]	-0,136	-0,136	-0,136
z_{max} [m]	0,049	0,061	0,070
u_{min} [m/s]	-0,184	-0,184	-0,184
u_{max} [m/s]	0,067	0,082	0,095
$Downtime$ [min:sec]	12:19	12:19	12:19

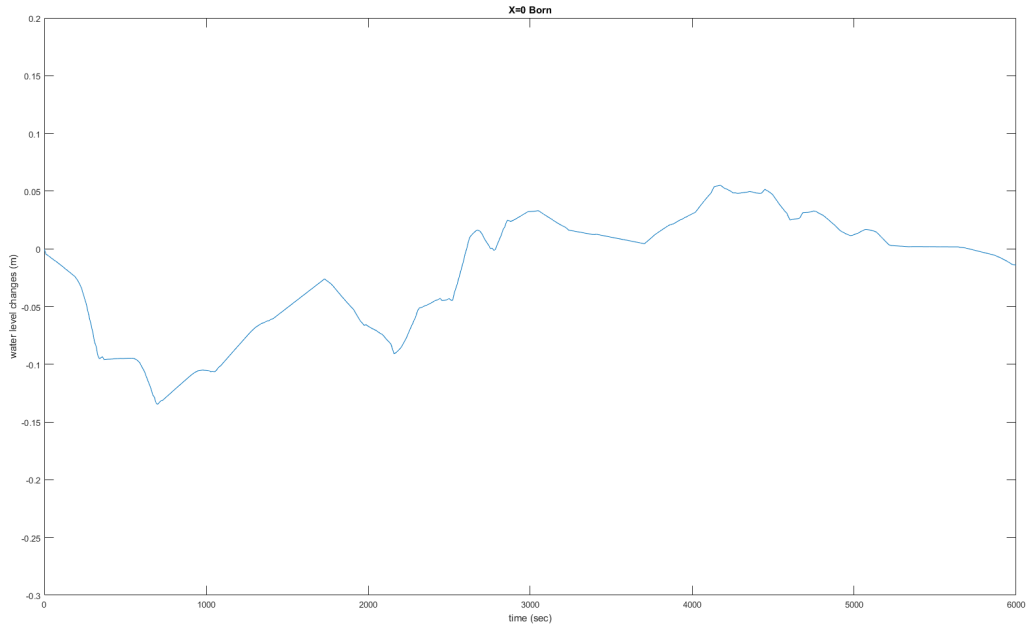

Figure F.80: Sc7: Water level changes in scenario with Middle and East chamber filled with 1 culverts, 5 minutes in between, at location X1151

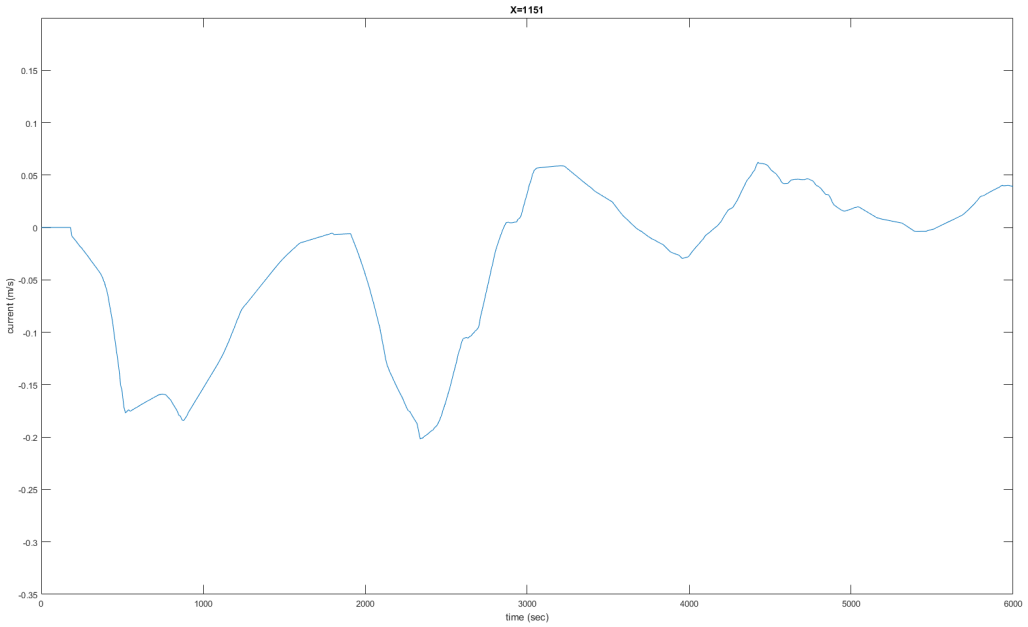

Figure F.81: Sc7: Currents in scenario with Middle and East chamber filled with 1 culverts, 5 minutes in between, at location X1151

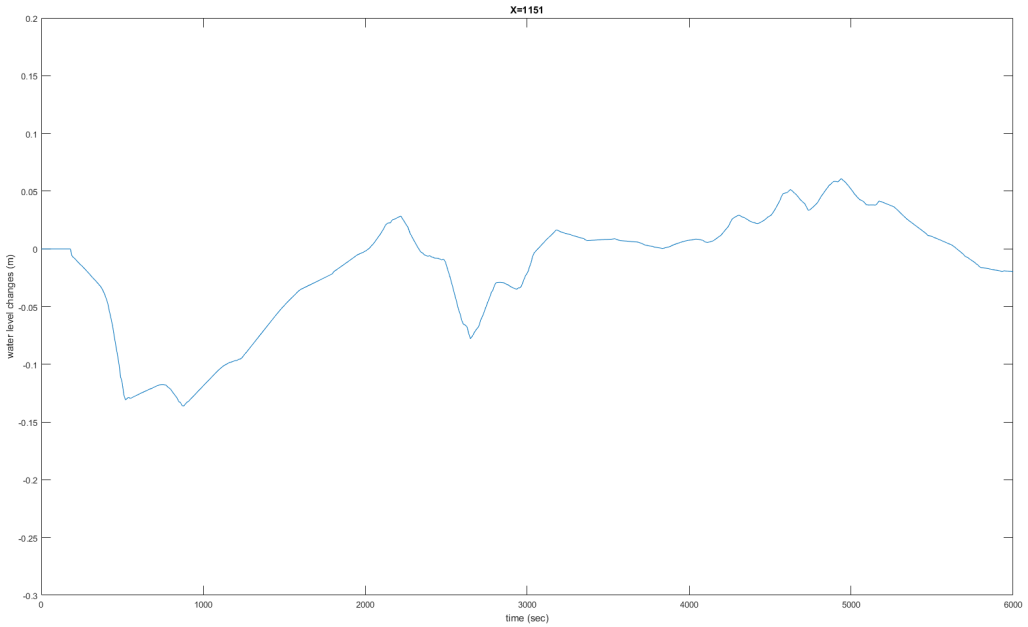

Figure F.82: Sc8: Water level changes in scenario with Middle and East chamber filled with 1 culverts, 10 minutes in between, at location X1151

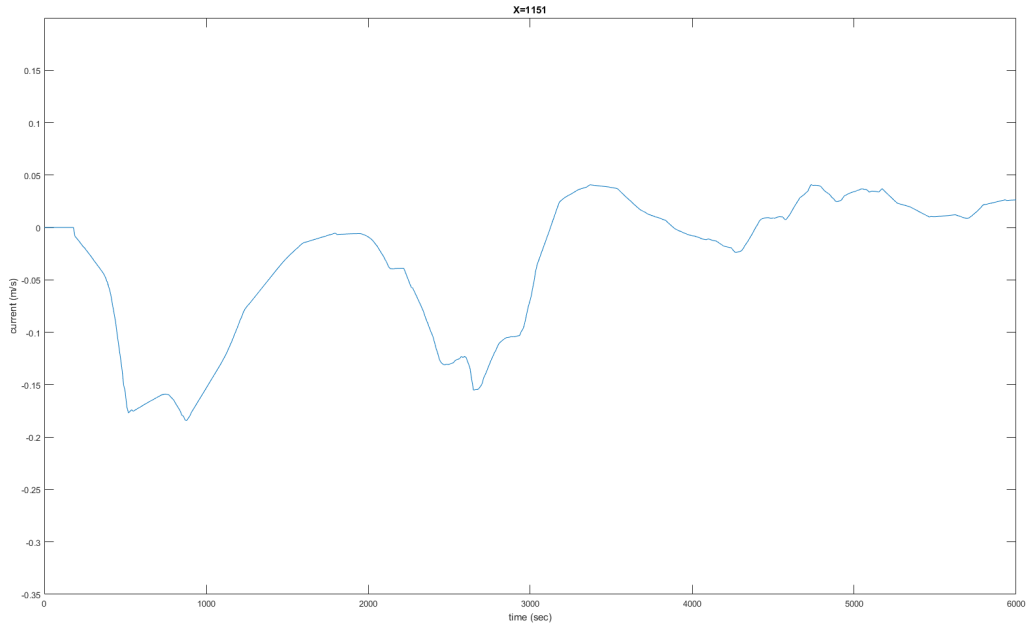

Figure F.83: Sc8: Currents in scenario with Middle and East chamber filled with 1 culverts, 10 minutes in between, at location X1151

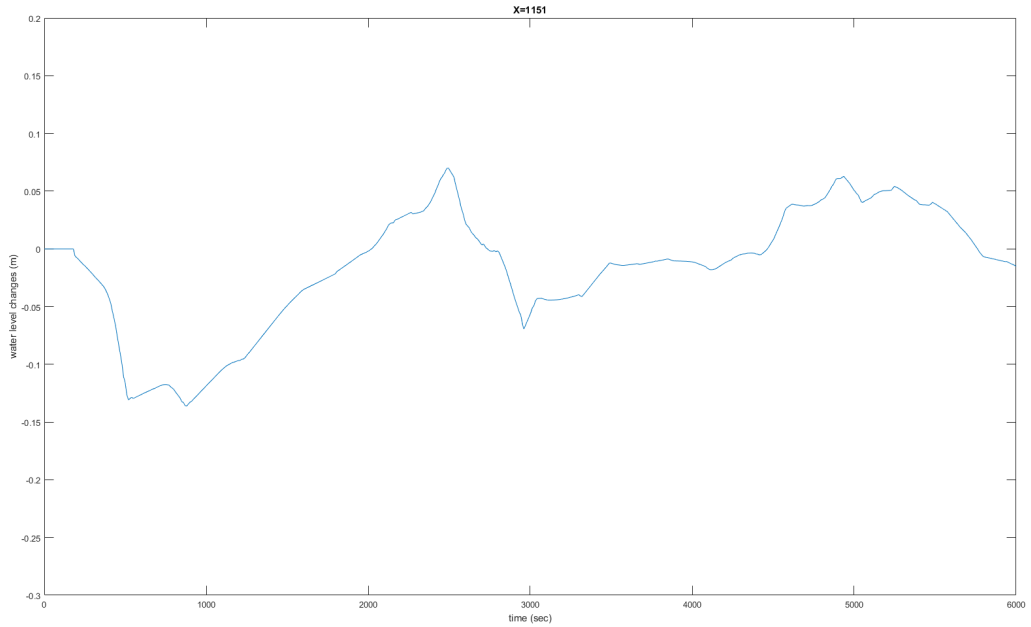

Figure F.84: Sc9: Water level changes in scenario with Middle and East chamber filled with 1 culverts, 15 minutes in between, at location X1151

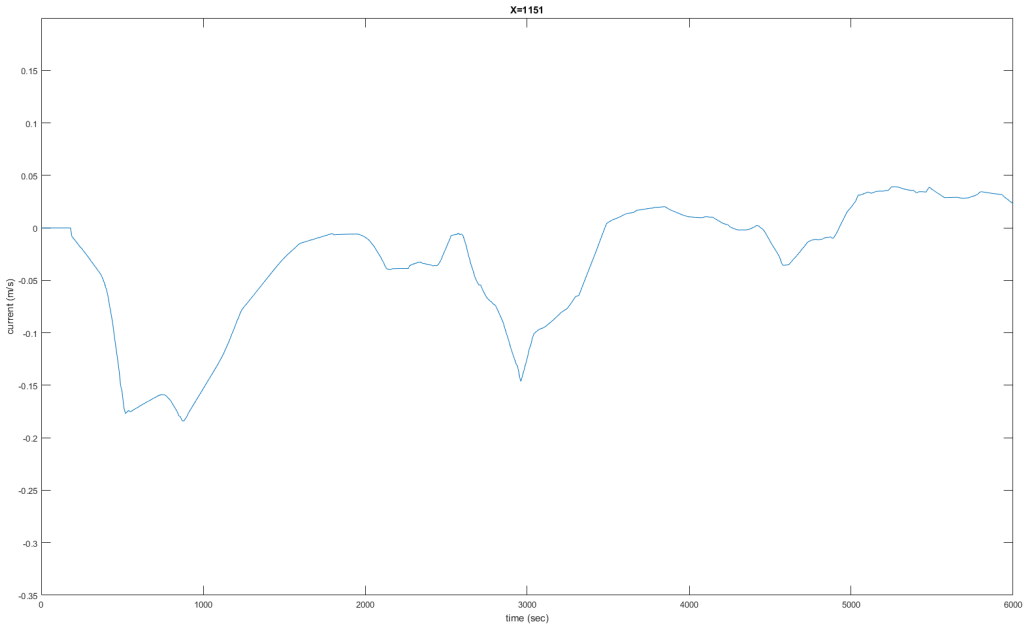

Figure F.85: Sc9: Currents in scenario with Middle and East chamber filled with 1 culverts, 15 minutes in between, at location X1151

LOCATION X=4000

The results of the model are presented in table F.14 and figures F.87, F.89 and F.91. The primary wave of the second wave is now more clearly visible. There are two troughs with high currents. This generates larger downtime, respectively 14, 12 and 11 minutes. Scenario 10 results in the least downtime. The second wave is more damped by the reflections of the first wave.

Table F.14: Extreme values at X_4000 in Scenario 8,9 and 10

	Sc8	Sc9	Sc10
z_{min} [m]	-0,133	-0,133	-0,133
z_{max} [m]	0,059	0,045	0,047
u_{min} [m/s]	-0,180	-0,180	-0,180
u_{max} [m/s]	0,080	0,061	0,063
$Downtime$ [min:sec]	14:16	12:20	10:43

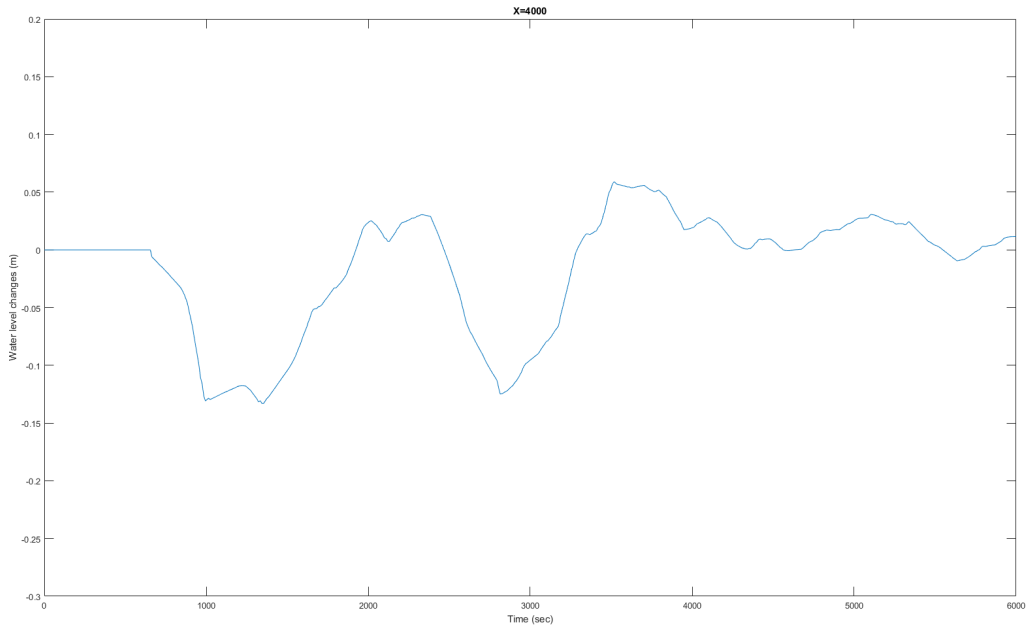

Figure F.86: Sc7: Water level changes in scenario with Middle and East chamber filled with 1 culverts, 5 minutes in between, at location X4000

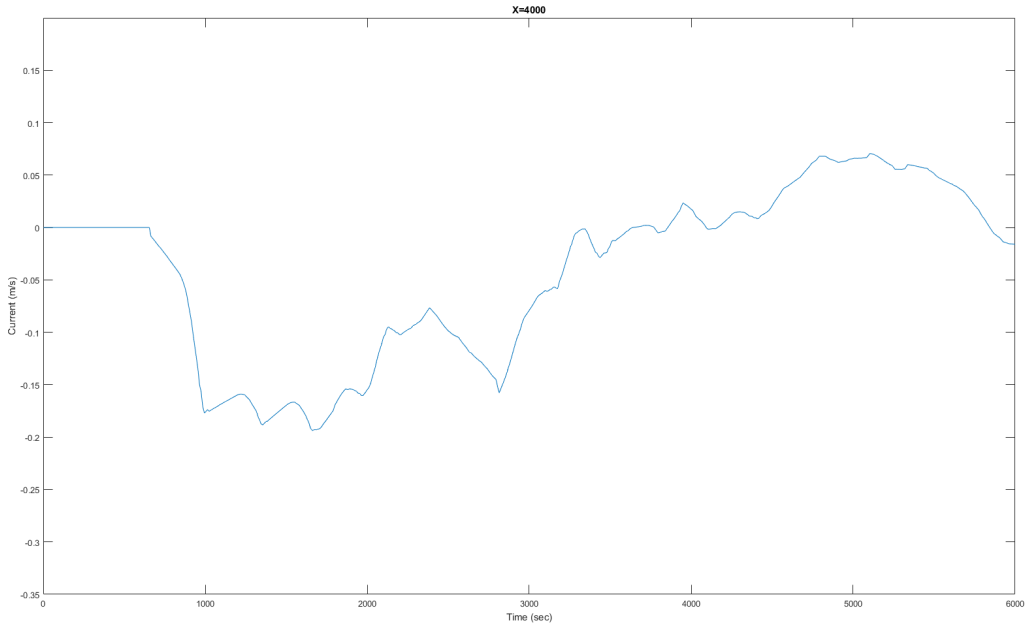

Figure F.87: Sc7: Currents in scenario with Middle and East chamber filled with 1 culverts, 5 minutes in between, at location X4000

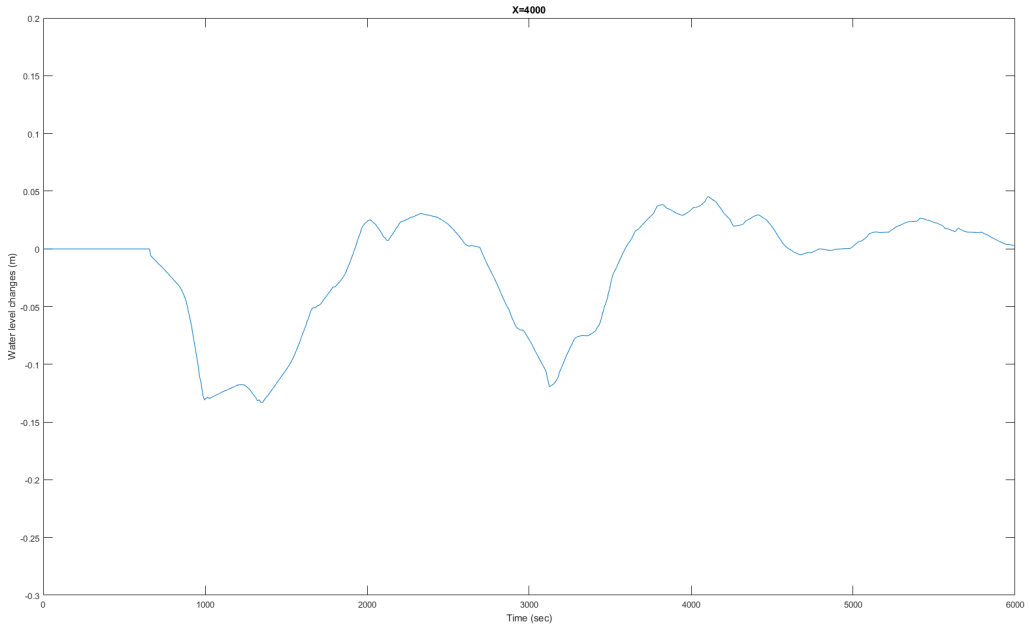

Figure F.88: Sc8: Water level changes in scenario with Middle and East chamber filled with 1 culverts, 10 minutes in between, at location X4000

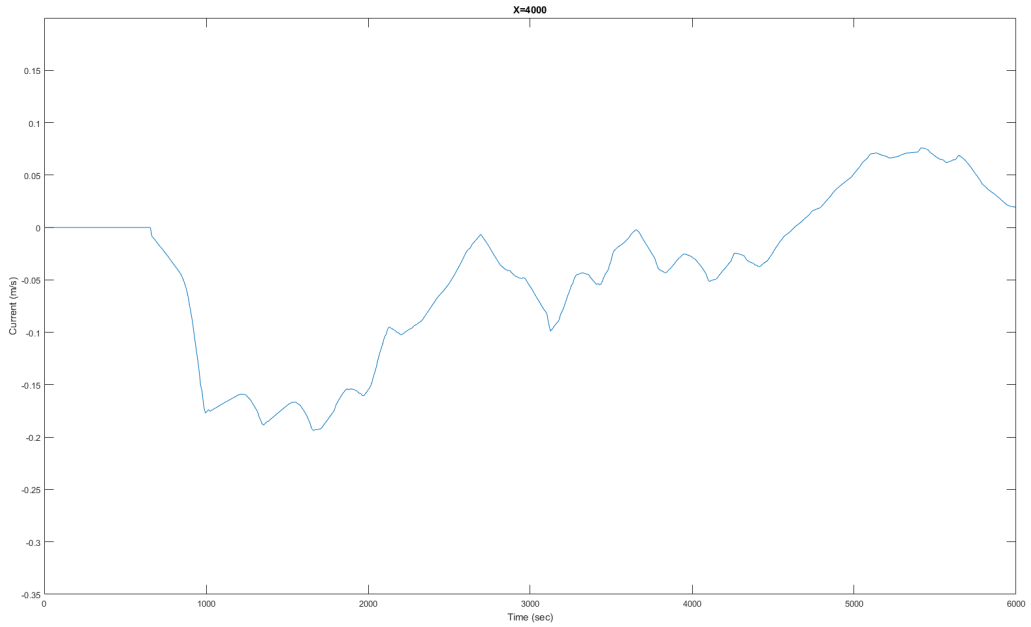

Figure F.89: Sc8: Currents in scenario with Middle and East chamber filled with 1 culverts, 10 minutes in between, at location X4000

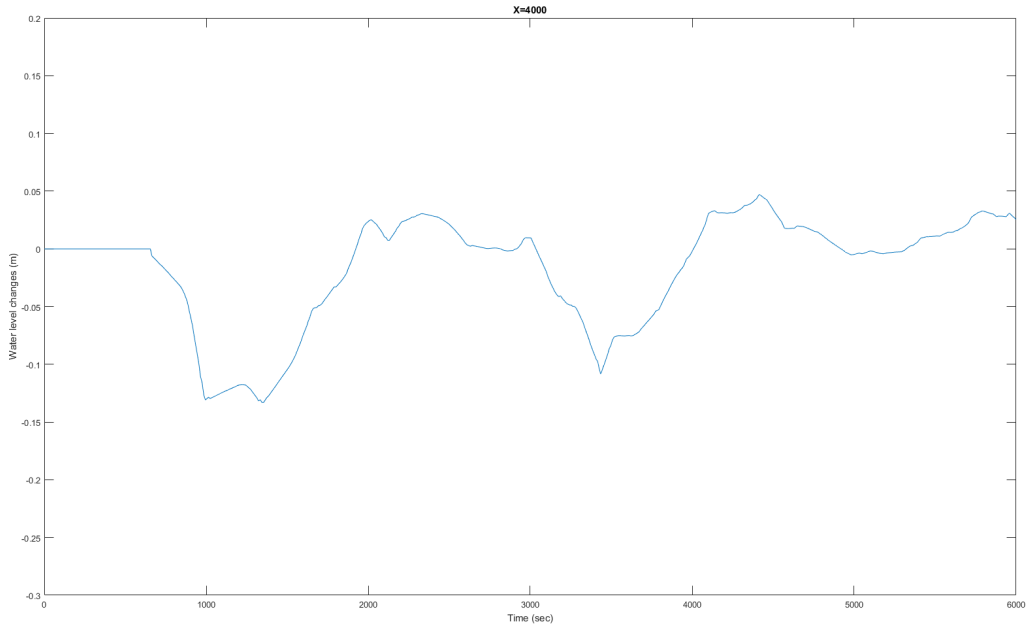

Figure F.90: Sc9: Water level changes in scenario with Middle and East chamber filled with 1 culverts, 15 minutes in between, at location X4000

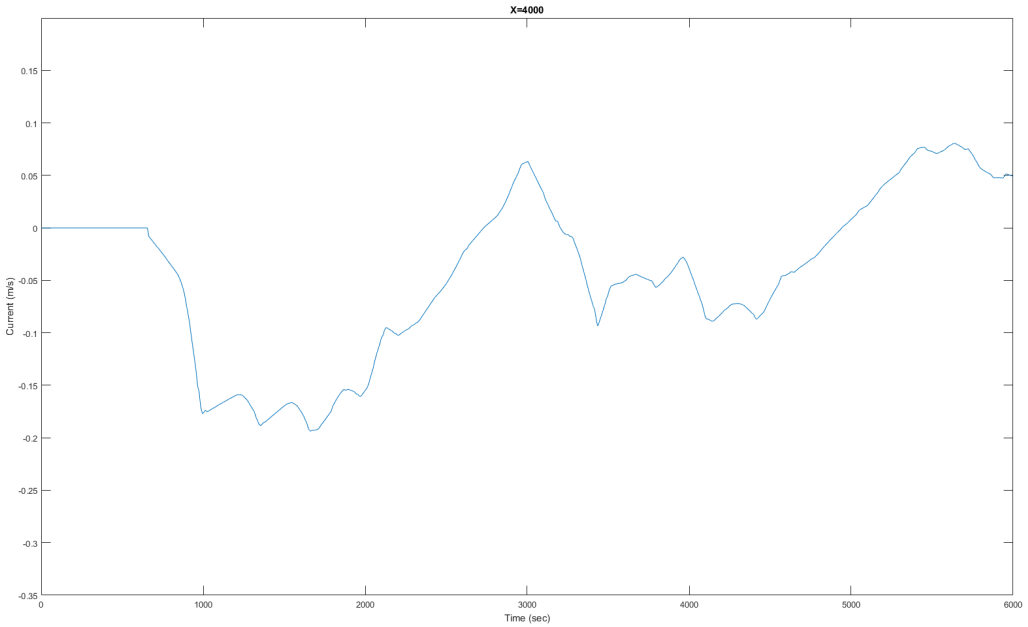

Figure F.91: Sc9: Currents in scenario with Middle and East chamber filled with 1 culverts, 15 minutes in between, at location X4000

LOCATION X=5900

As discussed in the previous sections, the primary wave is lower due to the reflection as a result of the transition point at X6000. The water level changes and currents decreased significantly, with 27%, 29% and 29%. As a result, the downtime is negligible: 7 seconds in scenario 8 and zero in scenarios 9 and 10. The results are presented in table F.15 and figures F.93, F.95 and F.97.

Table F.15: Extreme values at X_5900 in Scenario 8,9 and 10

	Sc8	Sc9	Sc10
z_{min} [m]	-0,097	-0,095	-0,095
z_{max} [m]	0,043	0,042	0,020
u_{min} [m/s]	-0,131	-0,129	-0,129
u_{max} [m/s]	0,058	0,057	0,027
$Downtime$ [min:sec]	00:07	00:00	00:00

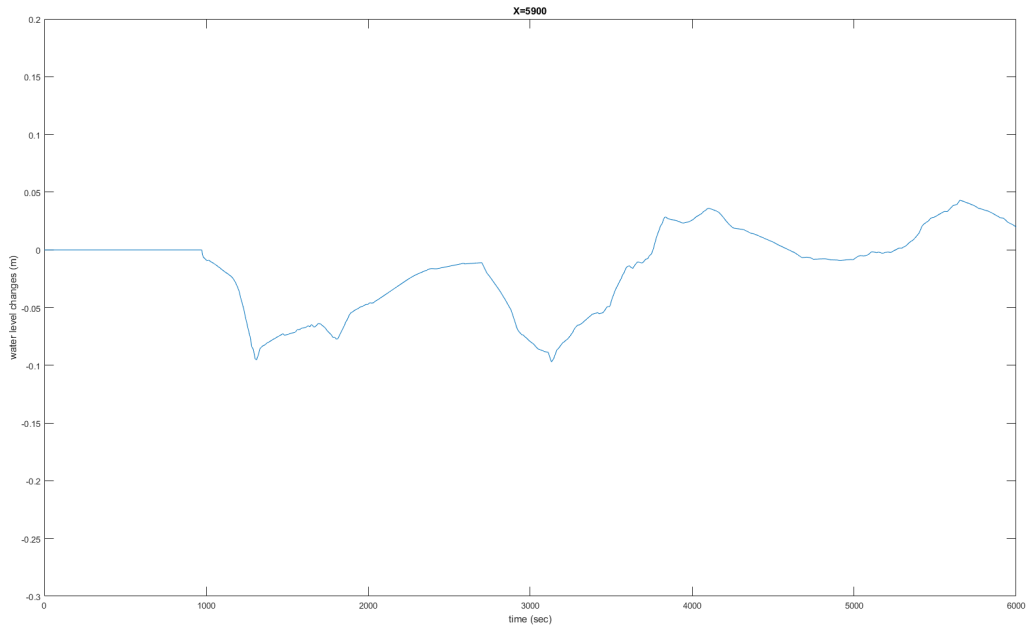

Figure F.92: Sc7: Water level changes in scenario with Middle and East chamber filled with 1 culverts, 5 minutes in between, at location X5900

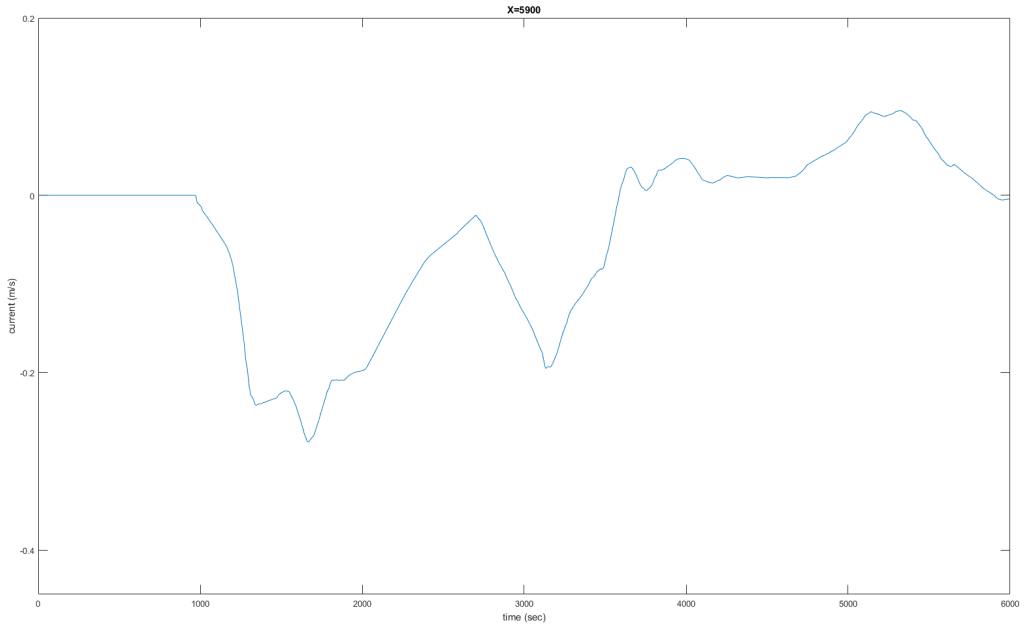

Figure F.93: Sc7: Currents in scenario with Middle and East chamber filled with 1 culverts, 5 minutes in between, at location X5900

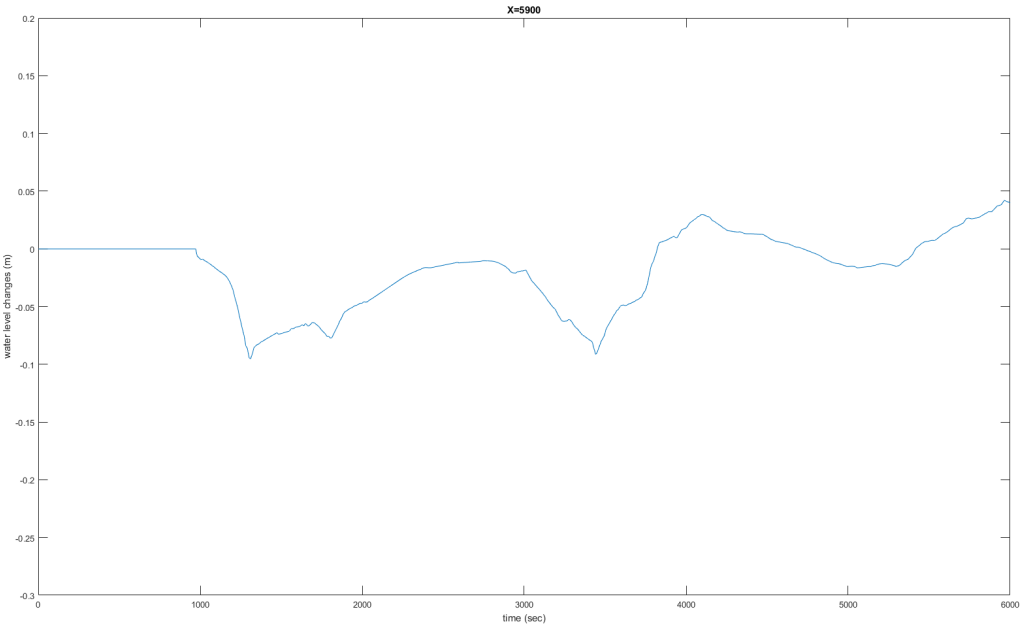

Figure F.94: Sc8: Water level changes in scenario with Middle and East chamber filled with 1 culverts, 10 minutes in between, at location X5900

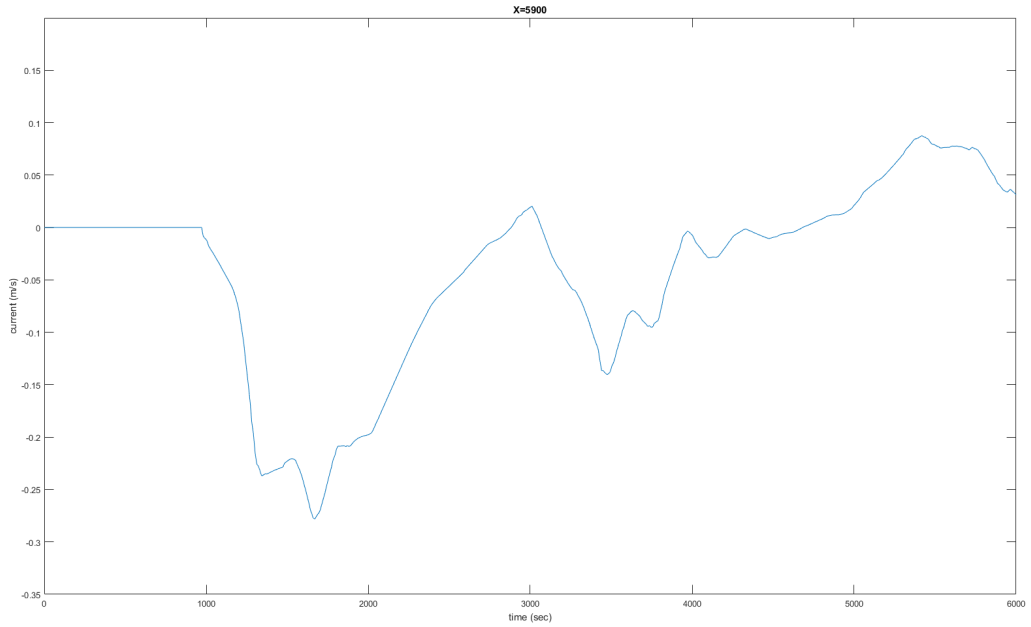

Figure F.95: Sc8: Currents in scenario with Middle and East chamber filled with 1 culverts, 10 minutes in between, at location X5900

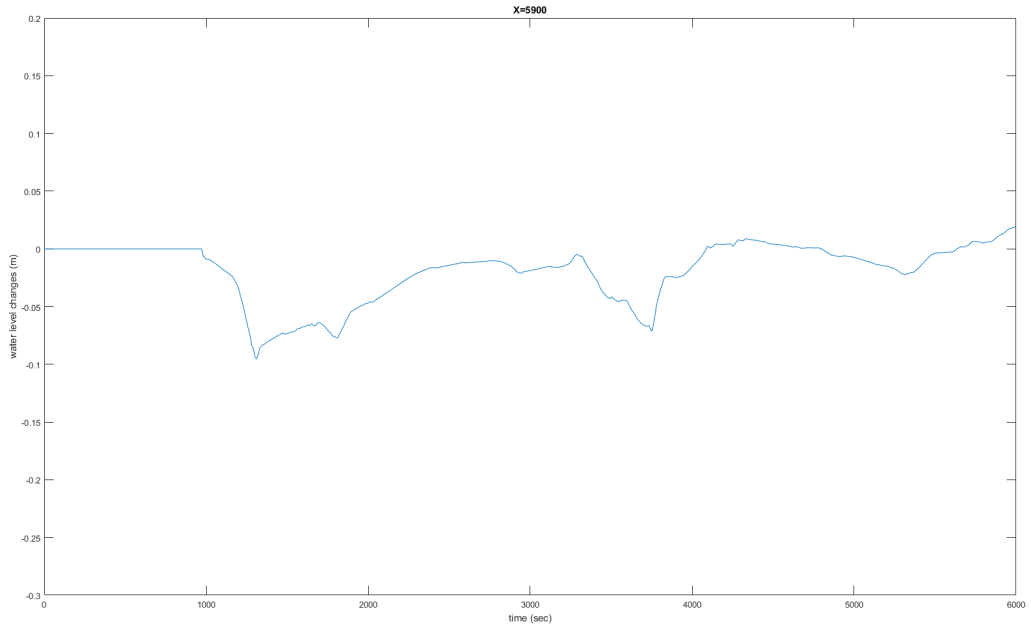

Figure F.96: Sc9: Water level changes in scenario with Middle and East chamber filled with 1 culverts, 15 minutes in between, at location X5900

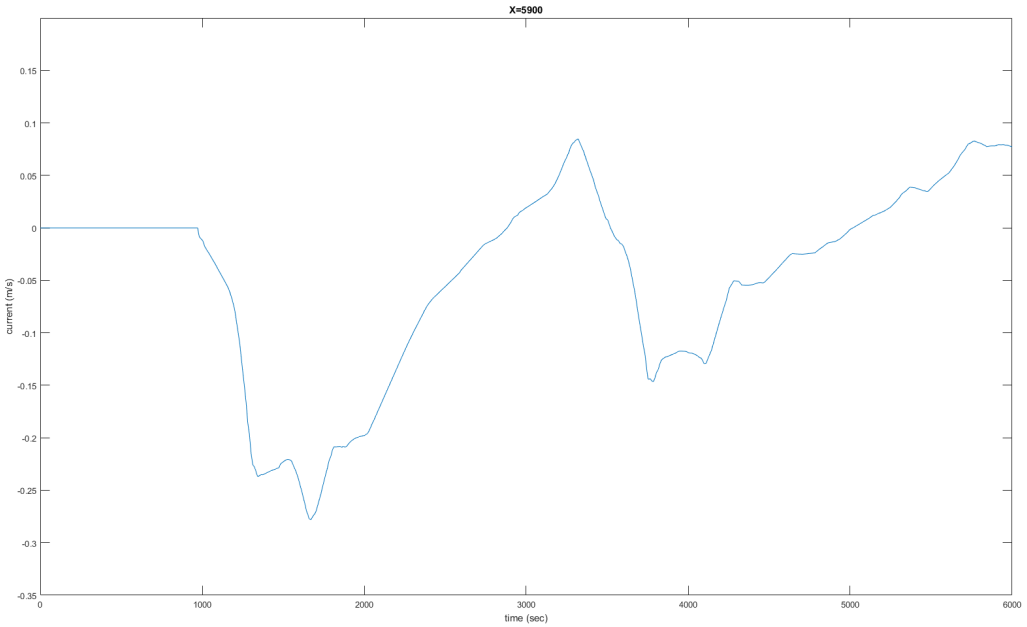

Figure F.97: Sc9: Currents in scenario with Middle and East chamber filled with 1 culverts, 15 minutes in between, at location X5900

LOCATION X=6001

The primary waves are in all three scenarios low, about 10% lower than at location X5900. No downtime is noted. The interactions with reflections can be seen at the peaks and troughs at different time sections. They do not result in very extreme situations. The results of the model of scenarios 8,9 and 10 are given in figures F.99, F.101 and F.103 and in table F.16.

Table F.16: Extreme values at X_6001 in Scenario 8,9 and 10

	Sc8	Sc9	Sc10
z_{min} [m]	-0,086	-0,086	-0,086
z_{max} [m]	0,028	0,033	0,034
u_{min} [m/s]	-0,116	-0,116	-0,116
u_{max} [m/s]	0,038	0,045	0,046
$Downtime$ [min:sec]	00:00	00:00	00:00

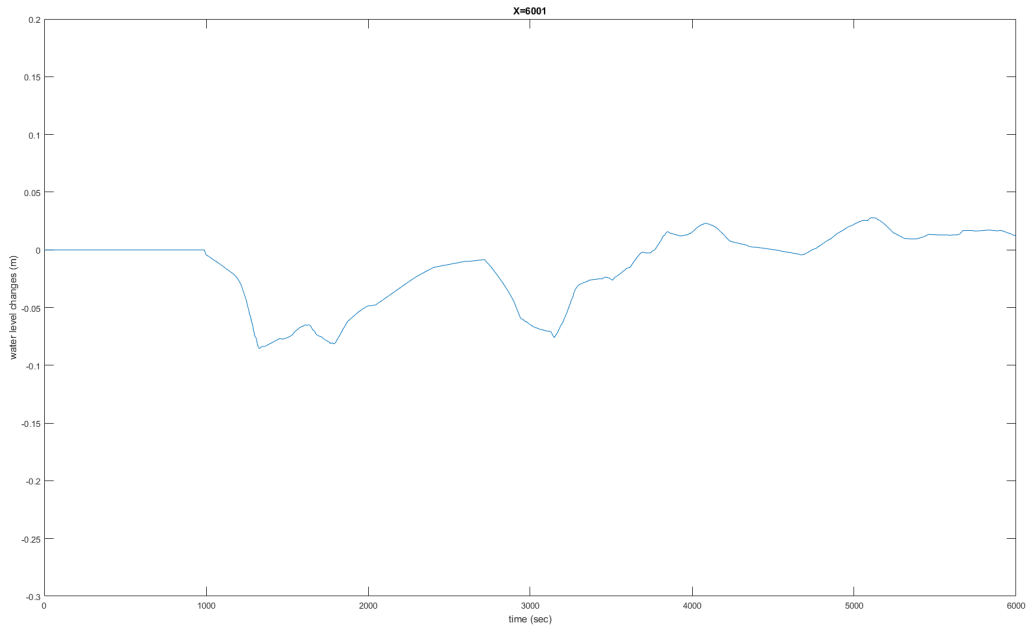

Figure F.98: Sc7: Water level changes in scenario with Middle and East chamber filled with 1 culverts, 5 minutes in between, at location X6001

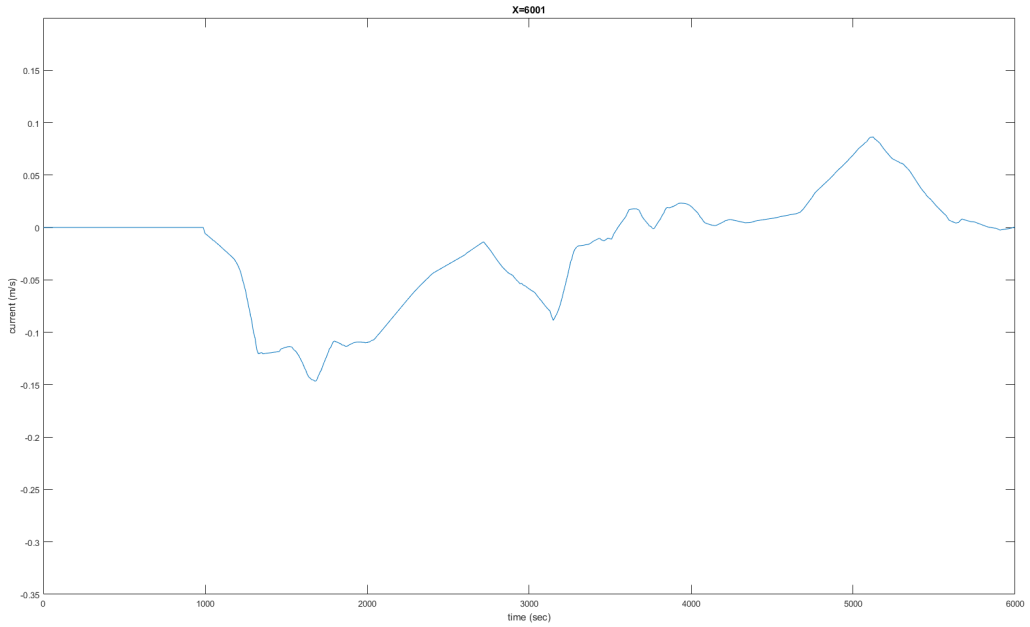

Figure F.99: Sc7: Currents in scenario with Middle and East chamber filled with 1 culverts, 5 minutes in between, at location X6001

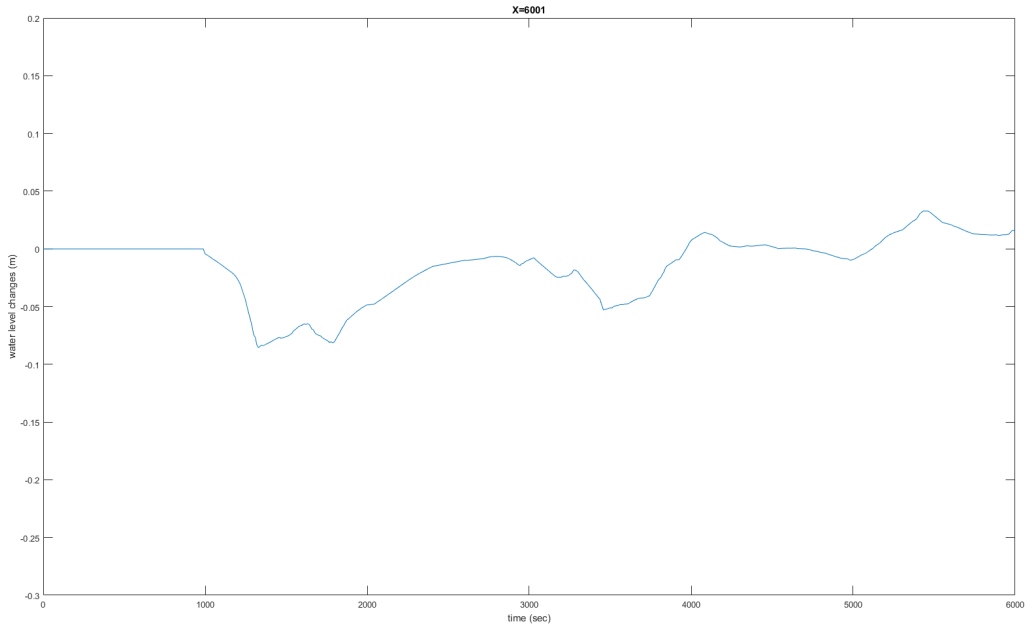

Figure F.100: Sc8: Water level changes in scenario with Middle and East chamber filled with 1 culverts, 10 minutes in between, at location X6001

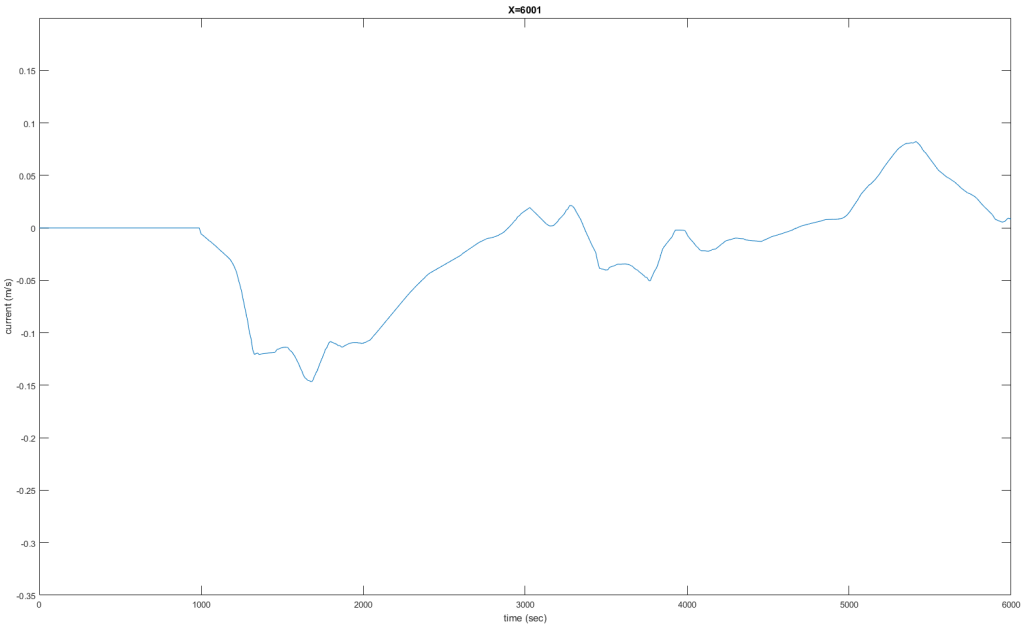

Figure F.101: Sc8: Currents in scenario with Middle and East chamber filled with 1 culverts, 10 minutes in between, at location X6001

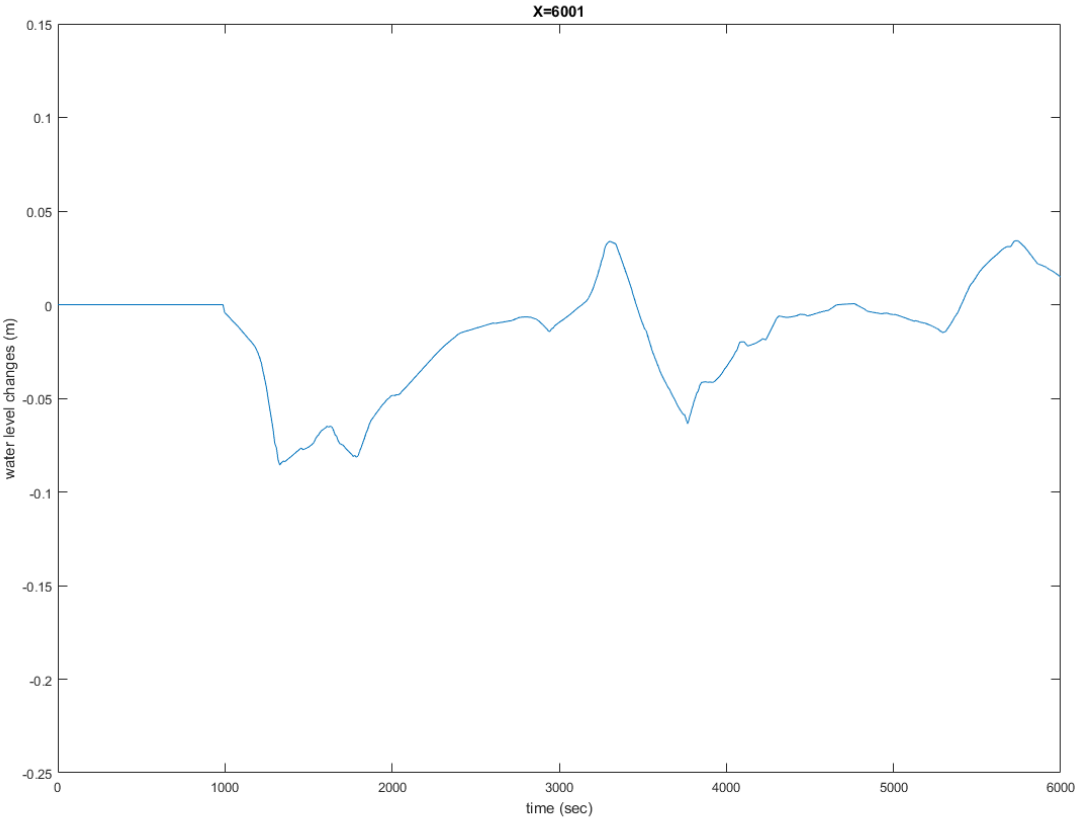

Figure F.102: Sc9: Water level changes in scenario with Middle and East chamber filled with 1 culverts, 15 minutes in between, at location X6001

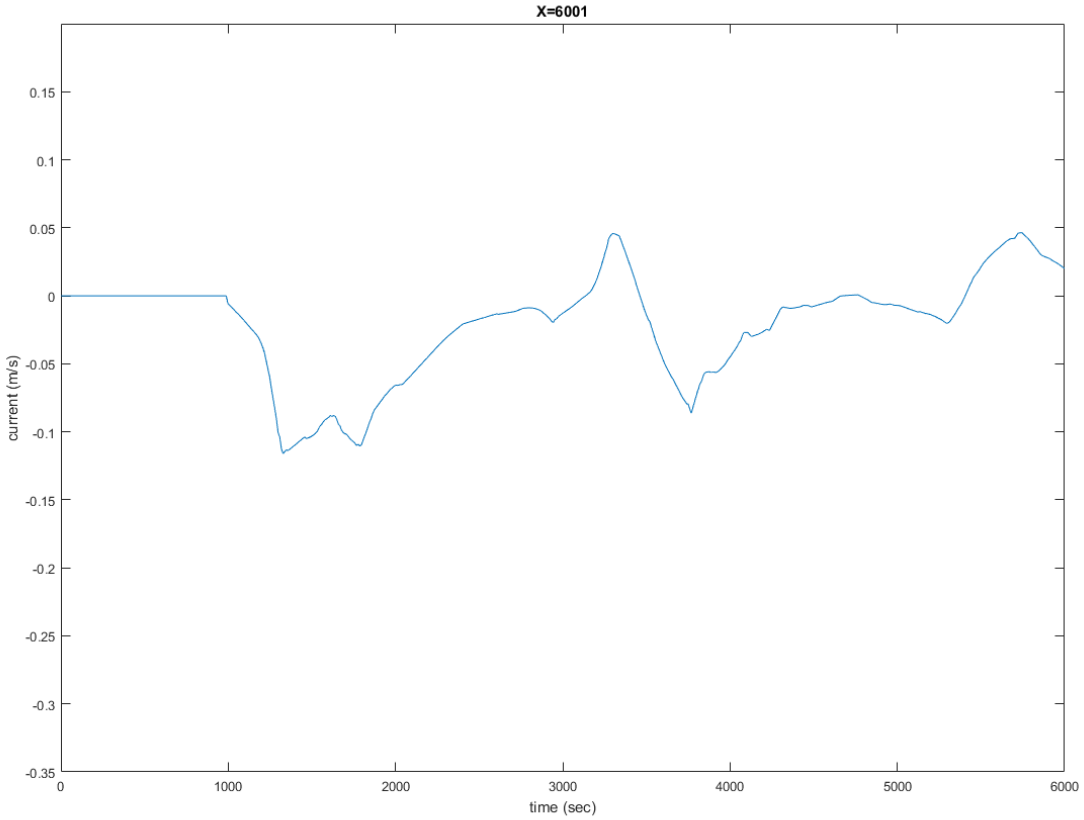

Figure F.103: Sc9: Currents in scenario with Middle and East chamber filled with 1 culverts, 15 minutes in between, at location X6001